



HAL
open science

**Contribution of capillary electrophoresis for the
therapeutic drug monitoring of patients treated by
targeted cancer therapy : application to tyrosine kinase
Inhibitors**
Omar Ahmed

► **To cite this version:**

Omar Ahmed. Contribution of capillary electrophoresis for the therapeutic drug monitoring of patients treated by targeted cancer therapy : application to tyrosine kinase Inhibitors. Human health and pathology. Université Montpellier, 2019. English. NNT : 2019MONTTS148 . tel-03204106

HAL Id: tel-03204106

<https://theses.hal.science/tel-03204106>

Submitted on 21 Apr 2021

HAL is a multi-disciplinary open access archive for the deposit and dissemination of scientific research documents, whether they are published or not. The documents may come from teaching and research institutions in France or abroad, or from public or private research centers.

L'archive ouverte pluridisciplinaire **HAL**, est destinée au dépôt et à la diffusion de documents scientifiques de niveau recherche, publiés ou non, émanant des établissements d'enseignement et de recherche français ou étrangers, des laboratoires publics ou privés.

THÈSE POUR OBTENIR LE GRADE DE DOCTEUR DE L'UNIVERSITÉ DE MONTPELLIER

En Chimie analytique

École doctorale Sciences Chimiques Balard

Unité de recherche Institut des Biomolécules Max Mousseron, UMR 5247
CNRS-UM-ENSCM, Université de Montpellier, France

Contribution of capillary electrophoresis for the therapeutic drug monitoring of patients treated by targeted cancer therapy: application to tyrosine kinase inhibitors

Présentée par **Omar S.AHMED**

Le 03 Décembre 2019

Sous la direction de Prof. **Catherine PERRIN**
et le co-encadrement de Dr. **Yoann LADNER**

Devant le jury composé de

Marianne Fillet, Professeur des Universités, Université de Liège

Anne Varenne, Professeur des Universités, Chimie ParisTech

Laurent Philibert, Praticien de Centres de Lutte Contre le Cancer, Institut
du Cancer de Montpellier (ICM)

Yoann Ladner, Dr, Université de Montpellier

Catherine Perrin, Professeur des Universités, Université de Montpellier

Rapporteur

Rapporteur

Guest invité

Co-encadrant de thèse

Directrice de thèse



UNIVERSITÉ
DE MONTPELLIER

Acknowledgement

I would like to express my deepest and sincere gratitude to my PhD director, Prof. Catherine PERRIN, for her enlightening guidance and inspiring instruction in the development and completion of this study. Pr. PERRIN stimulated my interest in the field of discourse analysis and improved my ability in writing. In the process of meeting and discussion, Pr. PERRIN not only provided prudent and pointed guidance but also gave me warm and sincere support to complete my PhD.

I would like to pass my infinite thanks to Dr. Yoann LADNER who was a friend more than a supervisor. Your comments, corrections, questions were the light for my studies. Without your help, I couldn't arrive to this day. And i am here at the end of my PhD because of your support and help.

Dr. Pavel Dubský, I would like to thank you not only for helping me to solve a problem concerning my research and to publish a paper with you. But the thanks start from the day you welcomed me in your laboratory in Prague without knowing me before. You supported me with your smile, gentleness, help, advice and science. You also showed me the beauty of Prague with your guidance. You are a true idol for me. To Michal Malý, your intelligence, your passion for science and your work added a huge value to my work which ended by a published paper. Wish you dear Michael a good end of your PhD and a successful future.

I would like to thank Prof. Jean-Jacques VASSEUR, the director of École doctorale Sciences Chimiques Balard and Mme Pascale DECOMBLE, Responsable administrative et financière Ecole doctorale in Montpellier for their support and encouragement during PhD.

My infinite thanks to Prof. Thierry Durand, directeur de recherche première classe CNRS for his non-stop help during my PhD.

I would like to thank Prof. Marianne Fillet and Prof. Anne Varenne for being members of the jury and examine my work.

Also, I would like to thank Dr Laurent Philibert for his help during my PhD to understand the cancer, TKIs and hallmarks of cancer.

I am appreciative of the members of the great group, F12, Gaëlle Causot, Jérôme Montels and the other members of the group, for their support and encouragement.

I would like to thank also Adrien Chouchou for the support and the help given to me.

I would like to thank also Charf-eddine and Samira who was like a family to me in France.

Also, I would like to thank also Ayman El Jundi, Meriem Dadouch, Nawel benbouguerra, Moussa and hajer for their fantastic support during my PhD.

I would like to pass my endless acknowledgments for the PhD grant given by Misr University for science and technology (MUST), 6th October City, Egypt. Also, my endless acknowledgments to Prof. Laila Abdel Fattah, Prof. Joseph Joachim and Prof. Emmanuel Cornillot the coordinators of the collaboration between MUST University and the University of Montpellier.

Also, I would like to thank Dr. Marie-dominique Blanchin for her support and help. Without your help I couldn't speak French.

My endless thanks to Amr AHMED for his help and his advice to finish writing the PhD manuscript.

My endless thanks also to Ahmed H.Elmenoufy for his help during my PhD.

To Taher Hatahet, great thanks to you my friend for the advices and the encouragement given to me to finish my PhD.

To my mother-in-law Dr. Afaf Yassin, thanks god that you are in my life.

To my father-in-law Mr. Abdel-fattah, you was like real father to me.

To my sisters-in-law Menna and Samaa, thank you both for the support given to me during PhD.

To my uncle Mohamed Omar, the father, the backbone in my life, I don't have any words to describe your support and the encouragement given to me. After the death of my Father, you was the one taking care of me. **(To the memory of my father died 05-5-2003)**

To Prof/ Adel Saad, I will always remember you in my life.

To Prof/ Mohamed F. El-Miligi, I am blessed to have you in my life, to have your name as a recommendation was an honor to me. God only knows my feeling towards you.

To my wife Alaa and to my two children Adam and Adham,
you are the secret of my life. Without you, I am nothing.

**To the memory of my
mother
died 31-10-2014**

Table of abbreviations

Abl	Abelson murine leukemia
ACN	Acetonitrile
ADCC	Antibody-dependent cellular cytotoxicity
ADME	Absorption, distribution, metabolism and excretion
ADP	Adenosine diphosphate
Akt, PKB, PDK1	Protein Kinase B
AFMC	Analyte focusing by micelle collapse
ALK	Anaplastic lymphoma kinase
ALL	Acute lymphocytic leukemia
APCs	Antigen presenting cells
ATP	Adenosine triphosphate
AUC	Area under the curve
Bax	Bcl-2-associated X
B.C.	Before Christ
Bcl-xL	B-cell lymphoma-extra-large
Bcl-2	B-cell lymphoma 2
BCR	Break point cluster region
B cells	Bursa of Fabricius cells
BGE	Background electrolyte
BTK	Bruton's tyrosine kinase
CARs	Chimeric antigen receptors
CCD	Contactless conductivity detector
CD4+	Cluster of differentiation 4+
CD8+	Cluster of differentiation 8+
CE	Capillary electrophoresis
CEC	Capillary electrochromatography
CGE	Capillary gel electrophoresis
CIEF	Capillary isoelectric focusing
C _{min}	Residual or trough concentration
C _{max}	Serum peak concentration

CMC	Critical micelle concentration
CML	Chronic myeloid leukemia
CTLs	Cytotoxic T lymphocytes
CYP3A4	Cytochrome P450 3A4
CZE	Capillary zone electrophoresis
DAD	Diode array detector
DLLME	Dispersive liquid-liquid microextraction
DMSO	Dimethylsulphoxide
DNA	Deoxyribonucleic acid
d-SPE	Dispersive solid phase extraction
EC	Electrophorèse capillaire
ECM	Extracellular matrix
ECZ	Electrophorèse capillaire de zone
EGF	Epidermal growth factor
EGFR	Epidermal growth factor receptor
EMT	Epithelial-to-mesenchymal transition
EOF	Electro-osmotic flow
ERK	Extracellular signal-regulated kinases
FASS	Field amplified sample stacking
FASI	Field amplified sample injection
FDA	Food and drug administration
FGF	Fibroblast growth factor
GC	Gas chromatography
GIST	Gastrointestinal stromal tumor
GTPases	Guanosine triphosphatases
HCC	Hepatocellular carcinomas
HER	Human epidermal growth factor receptor
HF	Hollow fiber
HGFR	Hepatocyte growth factor receptor
HGF	Hepatocyte growth factor
HIF-1	Hypoxia-inducible factor-1
HILIC	Hydrophilic interaction liquid chromatography

HLB	Hydrophilic lipophilic balance
ICM	Institute of cancer in Montpellier
IGFR	Insulin like growth factor receptor
IGF	Insulin like growth factor
INR	International normalized ratios
ITK	Inhibiteurs de la tyrosine kinase
IUPAC	International union of pure and applied chemistry
ITP	Isotachopheresis
JAK	Janus kinase
LC	Liquid chromatography
LE	Leading electrolyte
LIF	Laser induced fluorescence
LLE	Liquid-liquid extraction
LOD	Limit of detection
LOQ	Limit of quantification
LPME	Liquid phase microextraction
LVSS	Large volume sample stacking
mAb	Monoclonal antibody
MAP	Mitogen activated protein
Mcl-1	Induced myeloid leukemia cell differentiation protein
MDZ	Micellar dilution zone
MEC	Minimum effective concentration
MEKC	Micellar electrokinetic chromatography
MEPS	Microextraction by packed sorbent
m-RNA	Messenger ribonucleic acid
MS	Mass
MTC	Maximum toxic concentration
m-TOR	Mammalian target of rapamycin
NIH	National cancer institute
NK cells	Natural killer cells
NRTKs	Non-receptors tyrosine kinases
NS	Net survival

NSCLC	Non-small cell lung cancer
PBMC	Peripheral blood mononuclear cell
PD	Pharmacodynamic
PDGFR	Platelet-derived growth factor receptor
PDMS	Polydimethylsiloxane
PTFE	Polytetrafluoroethylene
PI3-kinases	Phosphoinositide 3-kinases
PIP ₃	Phosphatidylinositol (3,4,5)-trisphosphate
PK	Pharmacokinetic
PP	Protein precipitation
PKB	Protein kinase B
PS	Pseudo-stationary phase
PTEN	Phosphatase and tensin homolog
PTKs	Protein tyrosine kinases
q	Net charge of the analyte
QuEChERS	Quick, easy, cheap, effective, rugged and safe
RB	Retinoblastoma
RCC	Renal cell carcinoma
RSD	Relative standard deviation
RTKs	Receptors tyrosine kinase
SALLE	Salting-out liquid-liquid extraction
SARs	Structure activity relationships
SBSE	Stir bar sorptive extraction
SDME	Single drop microextraction
SEF	Sensitivity enhancement factor
SFKs	Src family of kinases
SLM	Supported liquid membrane
SPE	Solid phase extraction
SPME	Solid-phase microextraction
STP	Suivi thérapeutique personnalisée
SULLE	Sugaring-out assisted liquid-liquid extraction
t _{1/2}	Half life time

T _h cells	Helper T cells
TAMs	Tumor-associated macrophages
TCR	T cell receptor
t-ITP	Transient isotachoporesis
TGF- α	Transforming growth factor alpha
TGF- β	Transforming growth factor-beta
TKIs	Tyrosine kinase inhibitors
TP53	Tumor protein 53
TSP-1	Thrombospondin-1
UK	United Kingdom
UV	Ultraviolet
VEGF	Vascular endothelial growth factor

Table of Contents

General Introduction.....	1
Résumé de thèse.....	3
Chapter I.....	10
Tyrosine kinase inhibitors (TKIs)-mechanisms, uses, relevant problem and bioanalysis ..	10
Preface.....	11
1. Cancer	12
1.1. Defination of cancer.....	12
1.2. Cancer statistics	13
1.3. Hallmarks of Cancer	13
1.4. Cancer therapy.....	22
2. Targeted cancer therapy	23
2.1. Protein tyrosine kinases.....	25
2.2. Tyrosine kinase inhibitors	30
3. Overview of Therapeutic Drug Monitoring (TDM)	35
3.1. TDM and TKIs	36
4. Our project.....	44
4.1. Protocol used for the TDM of TKIs at the ICM.....	44
4.2. Selected TKIs for our project.....	45
5. Sample preparation	48
5.1. Protein precipitation (PP).....	49
5.2. Liquid-liquid extraction (LLE).....	49
5.3. Solid phase extraction (SPE).....	51
5.4. Dispersive solid-phase extraction (d-SPE).....	52
5.5. QuEChERS.....	53
5.6. Microextraction techniques.....	54
6. Capillary electrophoresis (CE)	61
6.1. Introduction to CE	61
6.2. CZE theory	61
6.3. Analytical parameters and CE instrumentation	64
6.4. Hydrodynamic injection	65
6.5. Electrokinetic injection	66
6.6. Capillary zone electrophoresis (CZE) and other modes	67

6.7. Detection in CE.....	68
6.8. Stacking phenomenon in CE	70
6.9. TDM and CE.....	76
General conclusion of the chapter	81
References	82
Chapter II.....	125
Influence of salt and acetonitrile in the sample on CE analysis of TKIs.....	125
Preface.....	126
Section I	127
I.1 Materials and methods of sections II and IV.....	127
I.2 Preliminary results	129
References of section I	131
Section II	133
<i>Paper 1: Influence of salt and acetonitrile on the capillary electrophoresis analysis of imatinib in plasma samples</i>	<i>133</i>
Section III (Supplementary results)	150
Section IV	169
IV.1 Application of the developed CE-UV methodology (section II) to human plasma spiked with the four TKIs.....	169
References of section IV	170
General conclusion of the chapter	171
Chapter III	172
Salting-out assisted liquid-liquid extraction (SALLE) as an extraction technique: Application to the CZE analysis of TKIs	172
Preface.....	173
Section I	174
I.1 Salting-out effect & SALLE	174
I.2 Clinical and bioanalytical applications of SALLE.....	176
I.3 Preliminary results.....	180
References of section I	183
Section II (published paper)	190
<i>Paper 2: Coupling of salting-out assisted liquid-liquid extraction with on-line stacking for the analysis of tyrosine kinase inhibitors in human plasma by capillary zone electrophoresis</i>	<i>190</i>

Section III	210
III.1 Comparison of both methodologies developed in chapter II and chapter III for the extraction and quantification of the four TKIs:.....	210
Section IV	213
IV.1 Experimental:	213
IV.2 Results and discussion	215
General conclusion of the chapter	218
Chapter IV	219
Automation of the SALLE-CE methodology	219
Preface.....	220
Section I	221
I.1 Literature review on automation of sample extraction and analysis.....	221
References of section I	230
Section II	236
<i>Paper 3: A fully automated on-line salting-out assisted liquid-liquid extraction capillary electrophoresis methodology: Application to tyrosine kinase inhibitors in human plasma.....</i>	<i>236</i>
Supplementary results.....	257
General conclusion of the chapter	259
Chapter V	260
Application of SALLE for the direct extraction of TKIs from blood	260
Preface.....	261
<i>Ppaer 4: Direct salting-out assisted liquid-liquid extraction (SALLE) from human blood: application for the analysis of tyrosine kinase inhibitors</i>	<i>262</i>
General conclusion of the chapter	283
General conclusion and perspectives.....	284
Résumé un page en Anglais et en Français.....	286

Table of figures

Résumé de thèse

Figure 1: Facteurs causant la variabilité interindividuelle de la concentration plasmatique des ITK.....4

Figure 2: structures moléculaires des inhibiteurs de la tyrosine kinase étudiés (ITK). (1) le mésylate d'imatinib, (2) le chlorhydrate d'erlotinib, (3) le sorafénib et (4) le ditosylate de lapatinib.....5

Figure 3: Électrophérogrammes obtenus à partir (A) de blanc (sans l'imatinib) et (B) d'un échantillon de mésylate d'imatinib dans le plasma humain. Conditions d'analyse : capillaire en silice 50 µm i.d., longueur totale : 30 cm, longueur effective 20 cm. BGE : acide citrique - tampon acide ε-aminocaproïque I 150 mM pH 2,0. Température : 25 ° C. Tension : 15 kV. Volume d'injection de l'échantillon : 156 nl (correspondant à 40% de la longueur du capillaire jusqu'à la fenêtre du détecteur). Détection : 254 nm.6

Figure 4 : Électrophérogrammes (A) d'un échantillon blanc de plasma (sans ITK) et solutions de plasma humain dopés avec les 4 ITK en utilisant la méthodologie SALLE (B) sans, (C) avec évaporation de l'extrait organique. Conditions analytiques : silice capillaire 50 µm i.d., longueur totale : 30 cm, longueur effective : 20 cm. BGE : acide citrique - tampon acide ε-aminocaproïque I 150 mM pH 2,0. Température : 25 ° C. Tension de séparation : 15 kV. Volume d'injection de l'échantillon : 313 nl (correspondant à 80% du volume capillaire jusqu'à la fenêtre du détecteur). Détection : 254 nm.....8

Chapter I

Figure 1: Schema showing the linguistic journey to the origin of the word "cancer".....12

Figure 2: Cancer and cardiovascular diseases are the leading causes of death in France in 2014 ^[5].....13

Figure 3: The hallmarks of cancer ^[9,10]14

Figure 4: Cell proliferation by the activation of EGFR.....15

Figure 5: Therapeutic targeting of the hallmarks of cancer ^[10]24

Figure 6: RTK Families. RTKs contain 20 subfamilies, shown here schematically with the family members listed beneath each receptor. Structural domains in the extracellular regions, identified by structure determination or sequence analysis, are marked according to the key. The intracellular domains are shown as red rectangles ^[78]27

Figure 7: Domain organization of the major families of NRTKs. NRTKs are subdivided into nine main families, based on their similarities in domain structure. The catalytic (SH1, kinase), p-Tyr binding (SH2), and protein-protein interaction (SH3) domains share a high degree of homology ^[81]28

Figure 8: Back in-time journey showing the discovery of TKIs and the FDA approval until now.....30

Figure 9: Factors causing inter-individual variability of TKIs plasmatic concentration.....33

Figure 10: Variation of plasma concentration of a drug at multiple doses given at regular time bases...36

Figure 11: Protocol used at the ICM for the extraction of TKIs.....45

Figure 12: SALLE concept.....	51
Figure 13: Schema of dispersion methodology by dispersive solid phase extraction.....	53
Figure 14: Commercially available Quechers kits.....	54
Figure 15: Classification of different microextraction techniques ^[300] . LPME: liquid phase micro extraction, SPME: solid phase microextraction, SDME: single drop microextraction, FNME: fiber-packed needle microextraction, MEPS: microextraction by packed syringe, HF-LPME: hollow fiber liquid phase microextraction, DLLME: dispersive liquid-liquid microextraction.....	55
Figure 16: Various modes of SDME including direct immersion SDME, headspace SDME and three-phase SDME ^[305]	56
Figure 17: (A) Schematic representation of flat membrane-based liquid-phase microextraction ^[309] . (B) Schematic representation of HF-LPME system ^[310]	57
Figure 18: The DLLME procedure ^[312]	58
Figure 19: Schematic overview of the micro-extraction by packed sorbent (MEPS) syringe ^[316]	59
Figure 20: Schematic of SBSE ^[324]	60
Figure 21: Schema showing electro-osmotic mobility, electrophoretic mobility and apparent mobility of cations, anions and neutral substances.....	62
Figure 22: Schema showing electro-osmotic mobility, electrophoretic mobility and apparent mobility of cations, anions and neutral substances.....	63
Figure 23: Differential solute migration superimposed on electro-osmotic flow in capillary zone electrophoresis ^[338]	63
Figure 24: (A) Schematic diagram of the basic instrumentation for CE. The sample and the electrolyte solution are switched when making injections. (B) Cross section of a capillary column for capillary electrophoresis.....	64
Figure 25: Methods of sample injection. (A), (B) and (c) represent hydrodynamic injection while, (D) represent electrokinetic injection. (A) hydrodynamic injection by applying pressure at the inlet. (B) hydrodynamic injection by vacuum at the outlet. (C) hydrodynamic injection by elevating the injection reservoir relative to the exit reservoir. (D) electrokinetic injection.....	65
Figure 26: Techniques for increasing the path length of the capillary. (A) Bubble cell and (B) Z-shape cell.....	69
Figure 27: The mechanism of FASS.....	71
Figure 28: The mechanism of LVSS.....	72
Figure 29: Mechanism of sweeping.....	73
Figure 30: Mechanism of pH mediated stacking.....	74
Figure 31: Mechanism of ITP.....	75

Chapter II

Section I

Figure 1: Analysis of imatinib mesylate and propranolol hydrochloride at the concentration of 5 and 20 µg/mL respectively at different I of the BGE 50, 100, 150 and 200 mM. Both compounds were prepared in (a) 100 % water (b) 1.0% NaCl (m/v) in water and (c) 2.0% NaCl (m/v) in water. Analysis conditions: silica capillary 50 µm i.d., total length 50 cm, effective length 40 cm. BGE: citric acid – ε-aminocaproic acid at pH 4.0. Temperature: 25°C. Separation voltage: 15 kV. Sample injection volume: 120 nL (corresponding to 15% of the capillary volume till the detector window). Detection: 254 nm.....**130**

Figure 2: Effect of increasing I of the BGE on the form of peak of imatinib in the presence of 1.0% salt (m/v).....**131**

Section II

Figure 1: (A) Molecular structure of imatinib mesylate. (B) analysis of imatinib mesylate in 100% water at two different pH of the BGE. Analysis conditions: silica capillary: 50 µm i.d., total length: 50 cm. BGE: citric acid – ε-aminocaproic acid buffer IS 50 at pH 4.0 and at pH 2.0. Temperature: 25°C. Separation voltage: 15 kV. Sample injection volume: 60 nl (corresponding to 7.5% of the capillary length till the detector window). Detection: 254 nm.....**140**

Figure 2: Analysis of imatinib mesylate at two different IS and pH of the BGE. Analysis conditions: silica capillary: 50 µm i.d., total length: 50 cm. BGE: citric acid – ε-aminocaproic acid buffer (A) IS 50 mM pH 4.0, (B) IS 150 mM pH 4, (C) IS 50 mM pH pH 2.0 (D) IS 150 mM pH 2.0. Temperature: 25°C. Separation voltage: 15 kV. Sample injection volume: 60 nl (corresponding to 7.5% of the capillary length till the detector window). Detection: 254 nm.....**141**

Figure 3: Simulation results of imatinib peak development in buffers of pH 4 and various IS values (in mM). See Experimental for simulation conditions. Time-frames at 2 min (120 s); the time is relevant to simulation conditions and do not correspond to experimental time. A) concentration profiles, Na and imatinib have separate y axes. B) trends of two measures, imatinib peak baseline (BLS) width and its separation from Na rear boundary, with IS. x-axis goes from higher IS values to lower IS values.....**143**

Figure 4: Simulation results of imatinib peak development in buffers of pH 2 and various IS values (in mM). See Experimental for simulation conditions. Time-frames at 2 min (120 s); the time is relevant to simulation conditions and do not correspond to experimental time. A) profiles of imatinib. Arrows indicate stacked zones of imatinib that belongs to the same IS profile. B) profiles of the BGE co-ion, ε-aminocaproic acid (more to the left), and the sample co-ion, Na (more to the right).....**144**

Figure 5: Electropherograms of imatinib mesylate obtained after adding ACN solvent with a total capillary length of 50 cm. Analysis conditions: BGE: citric acid – ε-aminocaproic acid buffer IS 150 mM (A) pH 4.0 and (B) pH 2.0. Temperature: 25°C. Separation voltage: 15 kV. Sample injection volume corresponding to 7.5 % of the capillary length till the detector window. Detection: 254 nm.....**146**

Figure 6: Analysis of imatinib samples in 50/50 ACN/1.0% NaCl m/v water v/v. (A) Effect of sample injected volumes (57, 148, 295 nL corresponding to 7.5, 20 and 40% of the capillary length till the

detector window) on the analysis of imatinib mesylate. Analysis conditions: silica capillary 50 μm i.d., total length: 50 cm. BGE: citric acid – ϵ -aminocaproic acid buffer I 150 mM pH 2.0. Temperature: 25°C. Separation voltage: 15 kV. Sample injection volumes are expressed in percentage corresponding to the capillary length filled with the sample till the detector window. Detection: 254 nm. (B) Effect of injected sample volume (57 to 295 nL corresponding to 2.5 to 40% of the capillary length till the detector window) on imatinib peak height in different solubilizing medium (100% water, 1.0% NaCl m/v in water and 50/50 ACN/1.0% NaCl m/v water v/v).....**147**

Figure 7: Electropherograms of the imatinib mesylate obtained from (A) blank sample (no imatinib) and (B) human plasma sample. Analysis conditions: silica capillary 50 μm i.d., total length: 30 cm. BGE: citric acid – ϵ -aminocaproic acid buffer IS 150 mM pH 2.0. Temperature: 25°C. Separation voltage: 15 kV. Sample injection volume: 156 nl (corresponding to 40% of the capillary length till the detector window). Detection: 254 nm.....**148**

Section III (Supplementary results)

Figure S 1: Simulation time-frames at pH 4.0, I 75 mM. Legend and units provided in section 1.1. Description of panels follows in the text. Horizontal dashed lines signify individual boundaries. Arrows (flags) points to the direction of boundary movement. Scales of x and y axes may differ for different panels.....**152**

Figure S 2 (two pages): Comparison between I 75 mM (left) and I 150 mM (right) at pH 4.0. Legend and units provided in section 1.1. Description of panels follows in the text. Horizontal dashed lines signify individual boundaries. Scales of x and y axes may differ for different panels but are kept the same for each pair of left and right panels. Time frames for I 75 mM are the same as in Figure S1.....**156**

Figure S 3 (two pages): Comparison between pH 4.0 (left) and pH 2.0 (right) at I 75 mM. Legend and units provided in section 1.1. Description of panels follows in the text. Horizontal dashed lines signify individual boundaries. Scales of x and y axes may differ for every panel as well as within every pair of left and right panels. Time-frames for I 75 mM are the same as in Figure S 1.....**162**

Figure S 4 (two pages): Comparison between I 75mM (left) and I 150 mM (right) at pH 4.0. Legend and units provided in section 1.1. Description of panels follows in the text. Horizontal dashed lines signify individual boundaries. Scales of x and y axes are the same throughout the entire figure (except for x-axis, panel H). Time-frames for I 75 mM are the same as in Figure S 3.....**166**

Section IV

Figure 1: Electropherogram of 4 TKIs obtained from (A) standard and (B) human plasma samples. Analysis conditions: silica capillary 50 μm i.d., total length 30 cm, effective length 20 cm. BGE: citric acid – 6-aminocaproic acid buffer I 150 mM pH 2.0. Temperature: 25 °C. Separation voltage: 15 kV. Sample injection volume: 156 nl (corresponding to 40% of the capillary volume till the detector window). Detection: 254 nm.....**169**

Chapter III

Section I

Figure 1: Concept of SALLE.....**175**

Figure 2: Testing different mixture of ACN/water (v/v) at different concentration of salt (m/v).....181

Figure 3: picture of a mixture of 50/50 (v/v) ACN/water and 10 % (m/v) of NaCl salt. Methyl red indicator solution was added and was mainly solubilized in organic phase.....182

Section II

Figure 1: Molecular structures of the studied Tyrosine Kinase Inhibitors (TKIs). (1) imatinib mesylate, (2) erlotinib hydrochloride, (3) sorafenib and (4) lapatinib ditosylate.....198

Figure 2: Analysis of imatinib mesylate, lapatinib ditosylate, erlotinib hydrochloride and sorafenib in (a) lower (mostly aqueous) phase and (b) upper (mostly ACN) phase obtained by SALLE methodology. Analysis conditions: silica capillary 50 μm i.d., total length 50 cm, effective length 40 cm. BGE: citric acid – ϵ -aminocaproic acid buffer I 150 mM pH 2.0. Temperature: 25°C. Separation voltage: 15 kV. Sample injection volume: 60 nl (corresponding to 7.5% of the capillary volume till the detector window). Detection: 254 nm.....199

Figure 3: Electropherogram of 4 TKIs obtained by SALLE methodology with a total capillary length of (A) 50 cm (effective length 40 cm) and (B) 30 cm (effective length 20 cm). Analysis conditions: BGE: citric acid – ϵ -aminocaproic acid buffer I 150 mM pH 2.0. Temperature: 25°C. Separation voltage: 15 kV. Sample injection volume till the detector window: 7.5 %. Detection: 254 nm.....200

Figure 4: Effect of sample injected volume (7.5, 15 and 80 % of effective capillary volume) on the separation of TKIs. Analysis conditions: silica capillary 50 μm i.d., total length 30 cm, effective length 20 cm. BGE: citric acid – ϵ -aminocaproic acid buffer I 150 mM pH 2.0. Temperature: 25°C. Separation voltage: 15 kV. Sample injection volumes are expressed in percentage of injected volume till the detector window. Detection: 254 nm.....201

Figure 5: Effect of injected sample volume (from 7.5 to 80 % of effective capillary volume) on the analyte corrected peak areas. Analysis conditions: silica capillary 50 μm i.d., total length 30 cm, effective length 20 cm. BGE: citric acid – ϵ -aminocaproic acid buffer I 150 mM pH 2.0. Temperature: 25°C. Separation voltage: 15 kV. Sample injection volumes are expressed in percentage of injected volume till the detector window. Detection: 254 nm.....202

Figure 6: Electropherogram of 4 TKIs obtained from standard and human plasma samples using SALLE methodology. Analysis conditions: silica capillary 50 μm i.d., total length 30 cm, effective length 20 cm. BGE: citric acid – ϵ -aminocaproic acid buffer I 150 mM pH 2.0. Temperature: 25°C. Separation voltage: 15 kV. Sample injection volume: 30 nl (corresponding to 7.5% of the capillary volume till the detector window). Detection: 254 nm.....203

Figure 7: Electropherograms of (A) blank sample (no TKIs) and of the 4 TKIs obtained from human plasma samples using SALLE methodology (B) without, (C) with the evaporation of the organic extract. Analysis conditions: silica capillary 50 μm i.d., total length 30, effective length 20 cm. BGE: citric acid – ϵ -aminocaproic acid buffer I 150 mM pH 2.0. Temperature: 25°C. Separation voltage: 15 kV. Sample injection volume: 313 nl (corresponding to 80% of the capillary volume till the detector window). Detection: 254 nm.....204

Section III

Figure 1: Electropherograms by method I and method II of the 4 TKIs obtained from human plasma samples. Analysis conditions: silica capillary i.d. 50 μ m, total length 30 cm, effective length 20 cm. BGE: citric acid—amino caproic acid buffer I 150 mM pH 2.0. Temperature: 25°C. Separation voltage: 15 kV. Sample injection volume for method I was 156 nl (corresponding to 40% of the capillary volume till the detector window). For method II was 313nl (corresponding to 80% of the capillary volume till the detector window). Detection: 254nm.....**211**

Section IV

Figure 1: (A) effect of injected sample volume (from 7.5–80 % of effective capillary volume) on the analyte corrected peak areas. Analysis conditions: silica capillary 50 m i.d., total length 30 cm, effective length 20 cm. BGE: citric acid/6-aminocaproic acid buffer I 150 mM pH 2.0. Temperature: 25 °C. Separation voltage: 15 kV. Sample injection volumes are expressed in percentage of injected volume till the detector window. Detection: 254 nm. (B) zoom in on the curve of imatinib mesylate.....**213**

Figure 2: Electropherograms of imatinib mesylate obtained by SALLE methodology with a total capillary length of 50 cm (effective length 40 cm). Analysis conditions, BGE: citric acid/6-aminocaproic acid buffer I 150 mM pH (A) 2.0 and (B) 4.0. Temperature: 25°C. Separation voltage: 15 kV. Sample injection volume: 7.5% of the capillary effective length. [imatinib] = 5.0 μ g/mL. Detection: 254 nm.....**215**

Figure 3: Effect of sample injected volume (7.5, 20, 40 and 50% of effective capillary volume) on imatinib analysis. Analysis conditions: silica capillary 50 m i.d., total length 50 cm, effective length 40 cm. BGE: citric acid/6-aminocaproic acid buffer I 150 mM, pH 4.0. Temperature: 25 °C. Separation voltage: 15 kV. Sample injection volumes are expressed in percentage of injected volume of the capillary effective length. Detection: 254 nm.....**216**

Figure 4: Effect of injected sample volume from (A) 2.5 to 40% and from (B) 2.5 to 20% of the capillary effective length on imatinib corrected peak areas. Analysis conditions: silica capillary 50 μ m i.d., total length 50 cm, effective length 40 cm. BGE: citric acid/6-aminocaproic acid buffer I 150 mM pH 4.0. Temperature: 25 °C. Separation voltage: 15 kV. Sample injection volumes are expressed in percentage of injected volume till the detector window. Detection: 254 nm.....**217**

Chapter IV

Section I

Figure 1: Schema of FIA.....**222**

Figure 2: Hardware of SIA.....**223**

Figure 3: Schema of SWIA.....**224**

Figure 4: Typical LLE flow analysis system manifold using FIA.....**225**

Figure 5: Typical solid phase extraction flow analysis system manifold using FIA.....**226**

Figure 6: Different interfaces used to couple FIA, SIA and SWIA with CE.....**227**

Figure 7: Some commercially available robots used for sample preparation.....	228
Figure 8: Schema representation of the developed system for in-syringe analysis ^[47]	230

Section II

Figure 1: A-SALLE-CE-UV procedure. Step (1) delivering of appropriate micro-volumes of solutions (ACN and NaCl stock solution) from outlet side to the inlet side (sample vial) by hydrodynamic injection in inverse mode. Followed by mixing by air bubbles injected from an empty vial (hydrodynamic injection in inverse mode). Step (2) after mixing, separation into 2 phases (upper mostly organic phase from bulk mostly aqueous phase) occurred. Step (3) hydrodynamic injection of the upper mostly organic phase (hydrodynamic injection, forward mode). Step (4) Separation and detection of the three TKIs by CE-UV.....**243**

Figure 2: Molecular structures of (1) lapatinib ditosylate, (2) erlotinib hydrochloride and (3) sorafenib.....**244**

Figure 3: Electropherogram of the 3 TKIs obtained from blank sample (no TKIs) and human plasma samples using A-SALLE-CE-UV procedure. Analysis conditions: silica capillary 50 μm i.d., total length 31 cm, effective length 21 cm. BGE: citric acid – ϵ -aminocaproic acid buffer IS 150 mM pH 2.0. Temperature: 25°C. Separation voltage: 15 kV. Sample injection volume: 39 nl (corresponding to 10% of the capillary effective length). Detection: 254 nm.....**245**

Figure 4: Effect of increasing the hydrodynamic pressure during 6 minutes on the volume obtained of (A) ACN and (B) NaCl. Effect of increasing the time at 60 psi on the volume obtained of (C) ACN and (D) NaCl.....**247**

Figure 5: Analysis of lapatinib ditosylate, erlotinib hydrochloride and sorafenib after injecting upper phase (mostly ACN) obtained by A-SALLE-CE-UV methodology. Analysis conditions: silica capillary 50 μm i.d., total length 31 cm, effective length 21 cm. BGE: citric acid – ϵ -aminocaproic acid buffer IS 150 mM pH 2.0. Temperature: 25°C. Separation voltage: 15 kV. Sample injection volume: 287 nl (corresponding to 70% of the capillary effective length). Detection: 254 nm.....**249**

Figure 6: Effect of the type of salting-out agent on (A) the corrected peak area and (B) the number of theoretical plates (N) of the 3 TKIs.....**250**

Figure 7: Electropherograms of the 3 TKIs obtained from blank plasma sample (no TKIs) and human plasma samples spiked with the three TKIs using A-SALLE-CE-UV procedure. Analysis conditions: silica capillary 50 μm i.d., total length 31 cm, effective length 21 cm. BGE: citric acid – ϵ -aminocaproic acid buffer IS 150 mM pH 2.0. Temperature: 25°C. Separation voltage: 15 kV. Sample injection volume: 287 nl (corresponding to 70% of the capillary effective length). Detection: 254 nm.....**251**

Supplementary results

Figure 1: Schema of adjusting an eppendorf (Thermoscientific, Pittsburgh, USA) of 600 μL to be placed in a plastic CE vial.....**257**

Figure 2: Two phases separation after applying A-SALLE procedure visually verified by the addition of 2 μ L methyl red indicator.....257

Chapter V

Figure 1: Structures of the four selected TKIs. (1) imatinib mesylate, (2) lapatinib ditosylate, (3) erlotinib hydrochloride and (4) sorafenib.....271

Figure 2: SALLE procedure of TKIs from human plasma and blood.....272

Figure 3: electropherograms of (A.a) imatinib mesylate, (B.a) lapatinib ditosylate, erlotinib hydrochloride and sorafenib, final concentration of 5.0 μ g/ml at pH (A) 4.0 and pH (B) 2.0 of the BGE. (A.b) and (B.b) represent the electropherograms obtained for blank standard samples (no TKIs). Analysis conditions: silica capillary 50 μ m i.d., total length 30 cm, effective length 20 cm. BGE: citric acid – ϵ -aminocaproic acid buffer I 150 mM. Temperature: 25°C. Separation voltage: 15 kV. Sample injection volume: (A) 78.31 nl (corresponding to 20% of the capillary volume till the detector window) and (B) 313 nl (corresponding to 80% of the capillary volume till the detector window). Detection: 254 nm.....273

Figure 4: electropherograms of (A.a) and (A.c) imatinib mesylate, (B.a) and (B.c) lapatinib ditosylate, erlotinib hydrochloride and sorafenib, final concentration of 5.0 μ g/ml at pH (A) 4.0 and pH (B) 2.0 of the BGE in (A.a) plasma and (A.c) blood samples. (A.b), (A.d), (B.b) and (B.d) represent the electropherograms obtained for blood and plasma blank samples. Analysis conditions: as in figure 3.....274

Figure 5: chromatograms of SALLE upper phase extract of TKIs standard solutions at concentration of 5.0 μ g/ml. (A.a) analysis of imatinib mesylate standard solution using C18 column 100 mm*2.1 mm*5.0 μ m, isocratic elution using ACN/phosphate buffer 5.0 mM at pH 7.0, 70/30 (v/v), flow rate 1.5 ml/min and detection at 256 nm. (B.a) analysis of the three others TKIs (erlotinib hydrochloride, sorafenib and lapatinib ditosylate) extracted also by SALLE using Altima phenyl column 250 mm*4.6 mm*5.0 μ m, gradient elution using ACN/ammonium acetate (20 mM), flow rate 2.0 ml/min and detection at 256 nm. (A.b) and (B.b) represent the chromatograms obtained for blank standard samples (no TKIs) under the same conditions as standard solutions.....275

Figure 6: chromatograms of blank (no TKIs), blood and plasma samples spiked with TKIs (5.0 μ g/ml). (A.a) and (A.c) represent analysis of imatinib in plasma and blood samples respectively. (B.a) and (B.c) represent analysis of the three others TKIs in also in plasma and blood samples respectively. (A.b), (A.d), (B.b) and (B.d) represent the chromatograms obtained for blood and plasma blank samples. Analysis conditions: as in figure 5.....276

Table of tables

Chapter I

Table 1: Classification of cancer immunotherapy ^[74]	25
Table 2: TKIs, their targets and their therapeutic indications.....	31
Table 3: LC-UV and LC-DAD methods for the quantitation of TKIs.....	37
Table 4: LC-MS and LC-MS/MS methods for the quantitation of TKIs.....	40
Table 5: Chemical structures, physicochemical properties and trade names of the selected TKIs.....	47
Table 6: Summary of the CE modes and their applications.....	68
Table 7: Application of CE in bioanalysis.....	78

Chapter II

Section II

Table 1: Summary of the quantitative results achieved on plasma samples with injected sample volume equal to 40% of the capillary volume till detector window.....	148
---	------------

Chapter III

Section I

Table 1: Most recent applications of SALLE in different fields.....	175
Table 2: Clinical and bioanalytical applications of SALLE.....	177
Table 3: Salting-out data for the phase-separation by sodium chloride ^[16]	181

Section II

Table 1: Summary of SALLE-CE-UV quantitative results achieved on plasma samples with injected sample volume equal to 80 % of the capillary volume till detector window.....	205
--	------------

Section III

Table 1: Comparison between method I based on PP by ACN and method II based on SALLE for the analysis of imatinib mesylate.....	211
--	------------

Chapter IV

Section II

Table 1: Summary of A-SALLE-CE-UV quantitative results achieved on plasma samples with injected sample volume equal to 70 % of the capillary effective length.....	252
---	------------

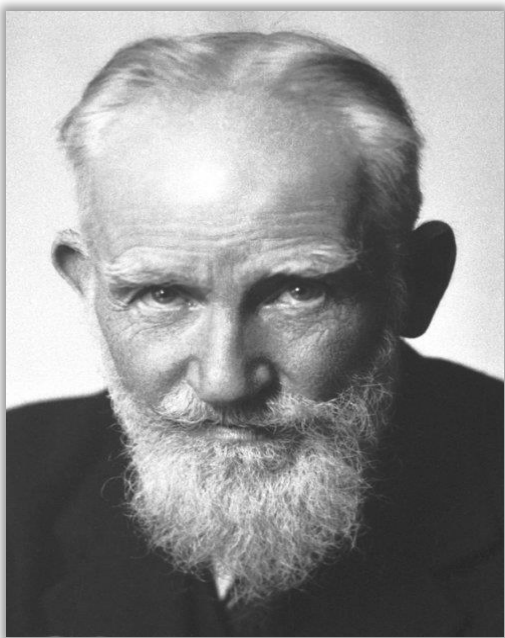
Supplementary results

Table 1: The detailed steps of the A-SALLE-CE-UV methodology.....	258
--	------------

Chapter V

Table 1: Mobile phase composition.....**268**

Table 2: Summary of SALLE-LC-UV and SALLE-CE-UV quantitative results achieved on blood samples.....**277**



Bernard Shaw

“Science is always wrong. It never solves a problem without creating ten more.”

General introduction

Cancer is a major burden of disease worldwide. Each year, tens of millions of people are diagnosed with cancer around the world, and more than half of the patients eventually die from it [1]. There are many types of cancer treatment depending on the type and the stage of cancer. Targeted cancer therapies are considered as the next generation of evolutionary cancer therapies with less toxicity and more specificity towards cancer [2].

Tyrosine kinase inhibitors (TKIs) are a class of targeted therapy used in the treatment of many types of malignant diseases. TKIs have many advantages including ease of administration by oral route and ability to target multiple cellular survival pathways [3]. In clinical practice, oncologists spend long time to adapt the dose of TKIs for every patient to increase the efficacy of treatment and to minimize as much as possible associated adverse side effects. Indeed, the inter-patients pharmacokinetic variability of TKIs is reported in several studies and was related to genetics, drug-drug interactions, poor adherence, concomitant food intake or drug food interaction, different ethnic group, renal and/or hepatic functions and environment factors [4].

Therapeutic drug monitoring (TDM) of TKIs was suggested in many studies as a tool to improve the efficacy and safety profile of the treatment [5]. Routine TDM of TKIs requires to develop analytical methodologies to measure their concentration. At the institute of cancer in Montpellier (ICM) in France, the protocol used for the analysis of TKIs from patients' plasma is a multistep (12 steps) extraction-HPLC-UV protocol. This time consuming protocol doesn't allow the doctor to take a decision concerning the dose of TKIs during the time of medical consultation with the patient. Moreover, this could adversely affects patients' quality of life in terms of having frequently to go to the hospital to finish his/her consultation and to have the correct dose of TKIs. These constraints besides, the adverse effects associated with TKIs therapy, contribute to emotional distress among cancer patients.

This work developed in this PhD consisted in studying the contribution of CE, more specifically capillary zone electrophoresis (CZE), as an analytical technique for the TDM of patients treated by TKIs. The objective was to develop generic CZE methodology that can be used for the TDM of different TKIs. Four TKIs were chosen for this project namely imatinib mesylate, erlotinib hydrochloride, lapatinib ditosylate and sorafenib. All the above contexts are the subject of the first chapter of this manuscript.

In the second chapter, the factors affecting the analysis of TKIs in plasma samples by CZE are discussed. These factors are related to the high content of salt and biological proteins in plasma. A special program called Simul, which displays the dynamics of separation process inside the CE capillary was used to

General introduction

understand the behavior of TKIs in high saline aqueous matrix such as human plasma. The treatment of human plasma sample has been also studied in chapter, this step being a major source of errors and usually time-consuming. At the end of the chapter, a simple, sensitive, specific and cost-effective CE-UV methodology was proposed for the analysis of human plasma samples spiked with imatinib in the context of TDM.

In the third chapter, an extraction method based on salting-out liquid-liquid extraction (SALLE) was tested for the extraction of the all four TKIs from human plasma. This method has the advantages to eliminate biological proteins, salts and to extract TKIs from plasma. This SALLE method was coupled to CE-UV for the separation of TKIs in an easy operational procedure, with low consumption of organic solvent and environmental benignity. A comparison between the analytical performance of SALLE method and the method developed in chapter II was also discussed.

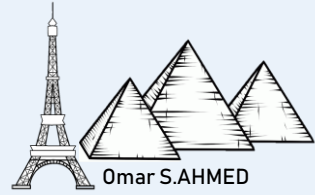
In the fourth chapter, a fully automated analytical methodology combining SALLE and CE for the analysis of TKIs in plasma samples was evaluated. This automated methodology combines the advantages of manual SALLE-CE-UV methodology in a simple and easy way without any modifications to the commercially available CE instrument. A comparison between the analytical performances of manual and automated SALLE methodology was established.

Finally, in the last chapter, the developed SALLE methodology was applied for the direct extraction of TKIs from blood. The SALLE technique was coupled to liquid chromatography (LC) with UV detection as CE-UV. Both methodologies (SALLE-CE-UV and SALLE-LC-UV) were compared in terms of their analytical performances to be considered as a valuable tool in the TDM for the fast extraction and the direct analysis of TKIs after whole blood sample collection.

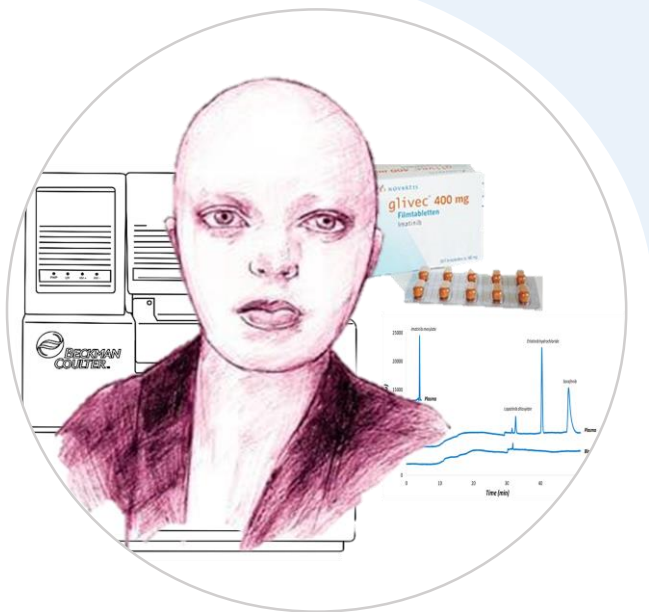
Reference

- [1] X. Ma, H. Yu, Cancer Issue: Global Burden of Cancer, *Yale J. Biol. Med.* 79 (2006) 85–94.
- [2] V.V. Padma, An overview of targeted cancer therapy, *Biomed.* 5 (2015) 1–6.
- [3] T. Kuo, G.A. Fisher, Current status of small-molecule tyrosine kinase inhibitors targeting epidermal growth factor receptor in colorectal cancer, *Clin. Colorectal Cancer.* 5 (2005) 62-70.
- [4] H.J. Klümpen, C.F. Samer, R.H.J. Mathijssen, J.H.M. Schellens, H. Gurney, Moving towards dose individualization of tyrosine kinase inhibitors, *Cancer Treat. Rev.* 37 (2011) 251–260.
- [5] T. Terada, S. Noda, K.I. Inui, Management of dose variability and side effects for individualized cancer pharmacotherapy with tyrosine kinase inhibitors, *Pharmacol. Ther.* 152 (2015) 125–134.

Résumé de thèse



Apport de l'électrophorèse capillaire pour le Suivi Thérapeutique Personnalisé de patients traités par thérapie ciblée: Application aux Inhibiteurs de Tyrosine Kinase



Résumé de thèse

L'objectif de ce travail a consisté à étudier l'apport de l'électrophorèse capillaire (EC), plus spécifiquement l'électrophorèse capillaire de zone (ECZ), en tant que technique analytique pour les patients traités par les inhibiteurs de la tyrosine kinase (ITK). La première partie du chapitre I donne un aperçu de l'importance des ITK, de leur problème et de la nécessité de quantifier leur concentration plasmatique à intervalles réguliers en appliquant le suivi thérapeutique personnalisée (STP). Les ITK sont des médicaments qui bloquent l'action d'une enzyme, la tyrosine kinase. Cette enzyme participe au processus de signalisation qui se déroule dans les cellules une fois que les facteurs de croissance se sont fixés aux récepteurs présents sur les cellules. La tyrosine kinase joue un rôle dans la communication, le développement, la division et la croissance des cellules [1]. Les ITK sont utilisés dans le cadre de la thérapie ciblée contre le cancer et repose sur une inhibition du facteur de croissance. Ils peuvent être utilisés pour empêcher la croissance d'une tumeur. En outre, la prise par voie orale facilite le traitement pour les patients. La variabilité pharmacocinétique des ITK entre patients est rapportée dans plusieurs études [2] et serait liée à de nombreux facteurs, tels que le régime alimentaire, la consommation ou non de tabac, d'alcool ou médicaments. Les facteurs responsables de la variabilité inter-individuelle de la concentration plasmatique des ITK qui affecte l'efficacité du traitement sont mentionnés à la Fig. 1.

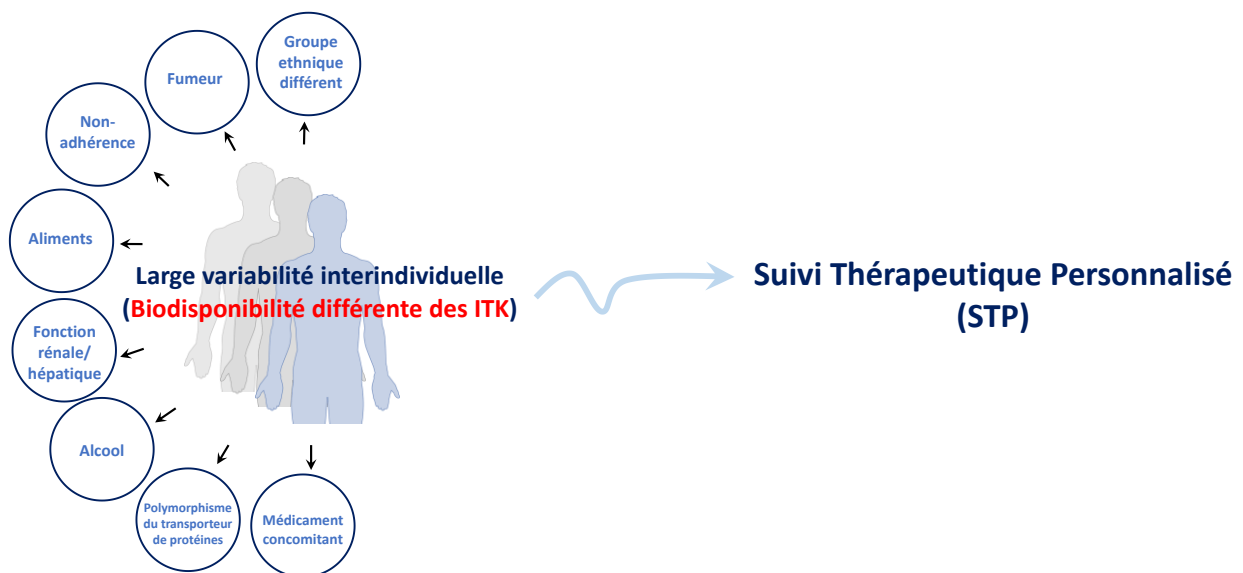


Figure 1: Facteurs causant la variabilité interindividuelle de la concentration plasmatique des ITK

Le STP est la pratique clinique consistant à mesurer des médicaments spécifiques ou leurs métabolites à des intervalles de temps spécifiés afin de maintenir une concentration constante dans la circulation

sanguine du patient, optimisant ainsi le dosage pour chaque patient. Le STP des ITK nécessite de développer des méthodes analytiques pour mesurer les concentrations plasmatiques des ITK.

L'objectif de ce projet a été de développer une méthode d'analyse générique utilisant l'EC et pouvant être utilisée pour le STP de différents ITK. Quatre ITK ont été choisis pour ce projet : le mésylate d'imatinib, le chlorhydrate d'erlotinib, le sorafénib et le ditosylate de lapatinib (Fig. 2).

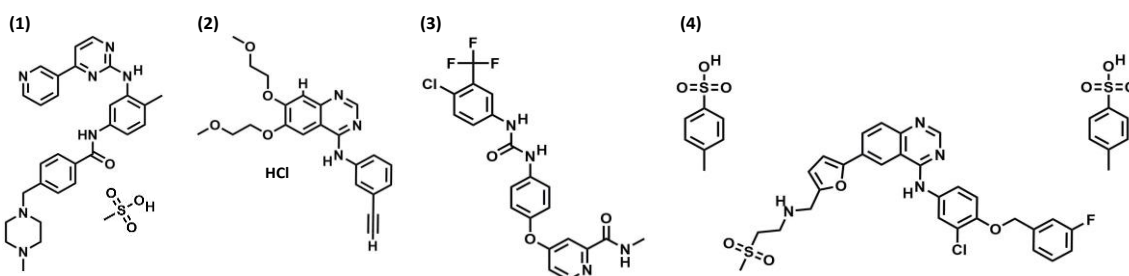


Figure 2: structures moléculaires des inhibiteurs de la tyrosine kinase étudiés (ITK). (1) le mésylate d'imatinib, (2) le chlorhydrate d'erlotinib, (3) le sorafénib et (4) le ditosylate de lapatinib.

Une revue détaillée des différentes méthodes de préparation des échantillons utilisées pour extraire les analytes au sein de matrices biologiques, en particulier le plasma humain, est décrite et discutée. Cette étude bibliographique montre que la précipitation biologique de protéines à l'aide de solvants tels que l'acétonitrile (ACN) est la méthode la plus courante, la plus simple et la plus facile à appliquer. Elle permet d'obtenir des taux de recouvrement élevés des ITK dans le plasma.

Le chapitre II décrit une méthodologie analytique simple, sensible, spécifique et peu coûteuse qui a été développée durant ce projet pour l'analyse d'échantillons de plasma dopés à l'imatinib par ECZ-UV. Plusieurs conditions d'analyse comme la force ionique (I) et le pH de l'électrolyte de fond (BGE) composé d'acide citrique et d'acide ϵ -amino caproïque ont été testés. L'effet de la présence de présence de chlorure de sodium (NaCl), naturellement présent dans des échantillons de plasma à une concentration proche de 1,0% (m/v), sur le comportement électrophorétique de l'imatinib a été étudié. Des simulations informatiques réalisées avec le logiciel Simul (groupe ECHMET, université de Prague, République-Tchèque) ont été utilisées pour aider à l'interprétation des résultats expérimentaux et ainsi comprendre le comportement électrophorétique de l'imatinib dans un capillaire en présence de NaCl. Lors de tests à différents pH (2 et 4) et différentes force ionique I de BGE (de 50 à 150 mM), différentes formes ont été observées expérimentalement pour le pic d'imatinib et ont pu être corrélées avec la simulation informatique. Ces expériences ont prouvé que la déformation du pic d'imatinib était une conséquence de la présence de sel (ion sodium) dans l'échantillon, qui conduit à des mobilités de l'imatinib différentes

dans la zone d'échantillon en fonction du pH et de la force ionique du BGE. L'ajout d'ACN dans l'échantillon de plasma pour précipiter les protéines a permis d'améliorer la symétrie du pic à pH 2, permettant d'analyser l'imatinib dans des échantillons de plasma grâce à cette procédure simplifiée. Les Fig. 3A et 3B montrent les électrophérogrammes obtenus pour le plasma blanc (sans imatinib) et le plasma dopé à l'imatinib après précipitation des protéines par l'acétonitrile. Aucun pic interférent n'a été observé, ce qui démontre la spécificité de la méthode proposée. Le volume maximum d'échantillon injecté sans déformation du pic était de 156 nL (correspondant à 40% du volume capillaire jusqu'à la fenêtre du détecteur) et était similaire à celle obtenue avec une solution échantillon d'imatinib standard seul. Ce résultat indique que les performances de pré-concentration en ligne sont similaires pour les deux solutions injectées (étalon et échantillon plasmatique) et confirme la robustesse de la méthode proposée pour l'analyse de l'imatinib dans des échantillons de plasma.

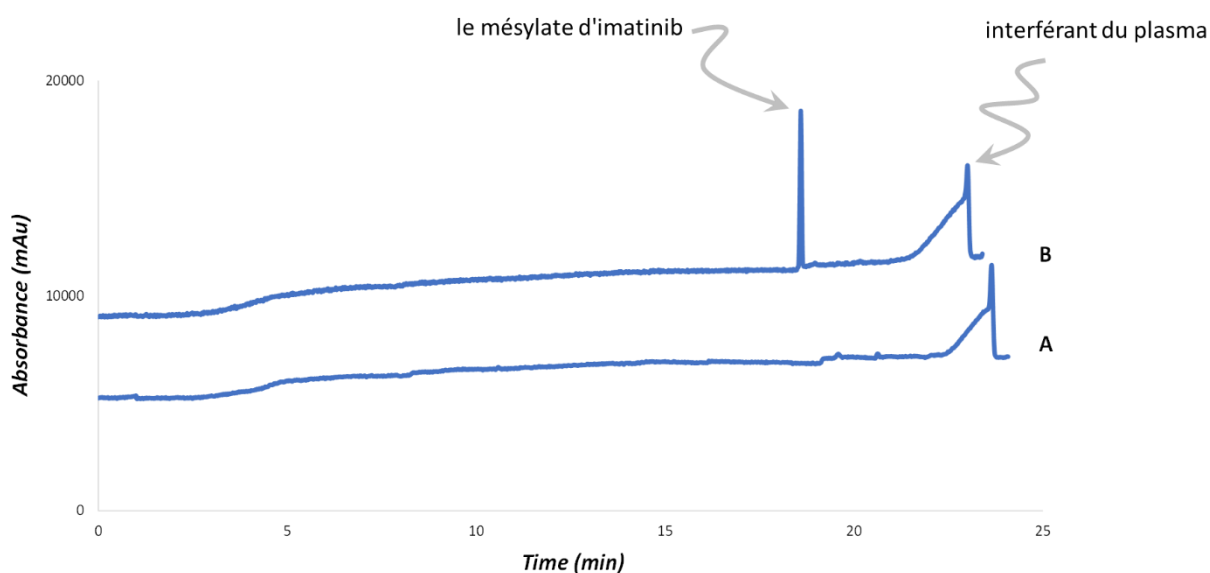


Figure 3: Électrophérogrammes obtenus à partir (A) de blanc (sans l'imatinib) et (B) d'un échantillon de mésylate d'imatinib dans le plasma humain. Conditions d'analyse : capillaire en silice 50 μm *i.d.*, longueur totale : 30 cm, longueur effective 20 cm. BGE : acide citrique - tampon acide ϵ -aminocaproïque / 150 mM pH 2,0. Température : 25 ° C. Tension : 15 kV. Volume d'injection de l'échantillon : 156 nL (correspondant à 40% de la longueur du capillaire jusqu'à la fenêtre du détecteur). Détection : 254 nm.

Les limite de détection (LOD) et limite de quantification (LOQ) à 48 et 191 ng/mL, respectivement ont été obtenues à partir du surnageant des échantillons de plasma après précipitation avec l'ACN. Celles-ci sont beaucoup plus faibles que la concentration plasmatique moyenne d'imatinib observée chez des patients traités par le mésylate d'imatinib (environ 1000 ng/ml). Une bonne linéarité a été obtenue dans la gamme de concentration de 191 à 5000 ng/mL ($r^2 > 0,997$). Des écarts types relatifs inférieurs à 1,68% et à 2,60% ($n = 6$) pour les temps de migration et les aires corrigées, respectivement, ont été observés à la limite de

quantification. La même méthodologie a été appliquée pour les trois autres ITK (le chlorhydrate d'erlotinib, le sorafénib et le ditosylate de lapatinib). Bien que les formes de pics obtenues soient symétriques, les performances de la méthode en termes de LOQ et de résolution des pics, notamment dans le cas du lapatinib, n'étaient pas suffisantes par rapport à la concentration plasmatique du lapatinib (environ 1740 ng/mL). Une autre stratégie pour extraire et concentrer les quatre ITK a été développée par la suite.

Dans le chapitre III, le couplage d'une méthode d'extraction, salting-out liquid-liquid extraction (SALLE), à l'analyse par CZE a été développée pour surmonter les limitations rencontrées avec la méthode développée précédemment. La méthode SALLE est une méthode d'extraction liquide-liquide dans laquelle l'addition de sels (par exemple NaCl) dans une solution d'échantillon composée d'un mélange miscible d'eau et un solvant organique (tel que ACN ou acétone) induit la séparation en deux phases (la phase organique et la phase aqueuse).

La méthode SALLE a permis d'extraire les 4 ITK d'intérêt dans la phase organique, ici l'ACN, avec des rendements d'extraction variant entre 60 et 100%. La phase organique contenant les molécules extraites a ensuite pu être analysée avec une séparation des ITKs en moins de 30 minutes par l'ECZ-UV. La pré-concentration en ligne des ITKs dans le capillaire a pu être développée grâce à la présence d'ACN dans l'échantillon et a permis de détecter les ITKs à des concentrations allant jusqu'à 200 µg/mL. La méthode SALLE-EC-UV a ensuite été appliquée à l'analyse des 4 ITKs dans le plasma humain et a donné des résultats similaires à ceux obtenus avec des solutions étalons. La Fig. 4 montre les électrophérogrammes obtenus à partir de plasma pour un volume d'échantillon injecté de 313 nL (correspondant à 80% du volume capillaire jusqu'à la fenêtre du détecteur). La Fig. 4A montre l'injection d'un échantillon blanc (sans ITK). La Fig. 4B montre l'électrophérogramme obtenu à partir de plasma dopé avec les 4 ITK. Aucun pic interférant au temps de la migration des analytes n'a été détecté, démontrant la spécificité de la méthode. En comparant les résultats obtenus avec la solution étalon, les profils électrophorétiques obtenus pour les 4 ITK, et particulièrement pour le sorafénib, sont très différents en termes de temps de migration, de formes de pic et de résolution. Cela peut être lié à un effet de la matrice entre les échantillons de plasma et les solutions étalons, notamment en ce qui concerne la teneur en sel. La Fig. 4C montre l'électrophérogramme d'un plasma dopé avec les quatre ITK après évaporation de la phase organique obtenue après la méthode SALLE et reconstitué dans de l'ACN. Une grande amélioration en termes de temps de migration, de formes des pics et de résolutions des 4 ITK a été observée, se rapprochant du profil obtenu avec la solution étalon. L'augmentation du signal observée après l'évaporation de

l'échantillon (Fig. 4C) peut être attribuée à l'élimination partielle des sels résiduels. Les limites de quantification de l'imatinib mésylate, du lapatinib ditosylate, du chlorhydrate d'erlotinib et du sorafenib ont été déterminées à 380, 900, 62 et 350 ng /mL, respectivement. Ces valeurs de LOQ sont bien inférieures aux concentrations plasmatiques moyennes observées chez les patients traités par les ITK. Des écarts-types relatifs (RSD) inférieurs à 1,24 et 2,84% sur les temps de migration et les aires corrigées, respectivement, ont été observés à la limite de quantification montrant la bonne répétabilité de la méthode basée sur l'utilisation de l'EC.

La méthode SALLE-CE-UV développée ici offre un certain nombre d'avantages, notamment une grande capacité de séparation entre les analytes, une procédure opérationnelle simple, une faible consommation de solvant organique, un faible impact environnemental et une forte tolérance à des matrices fortement salines.

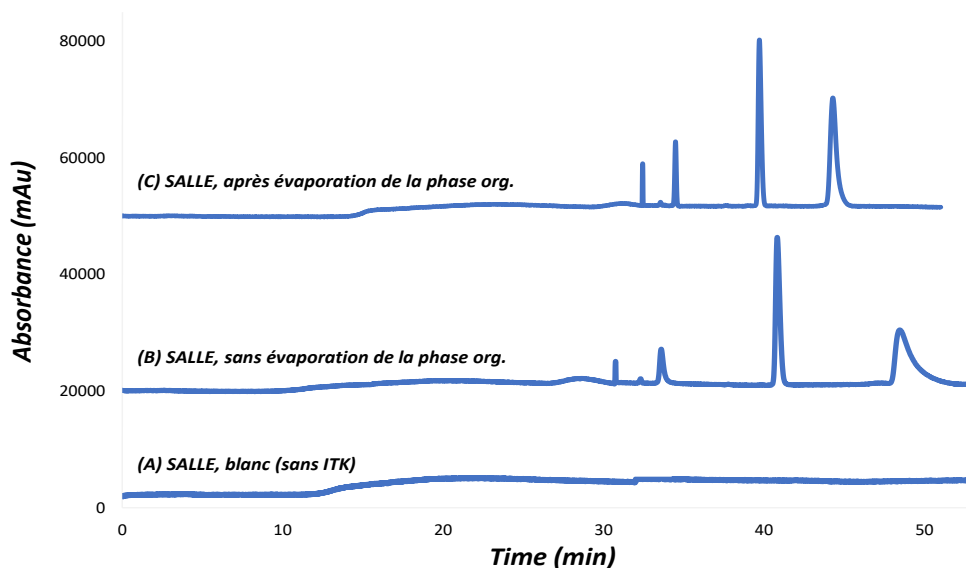


Figure 4 : Électrophérogrammes (A) d'un échantillon blanc de plasma (sans ITK) et solutions de plasma humain dopés avec les 4 ITK en utilisant la méthodologie SALLE (B) sans, (C) avec évaporation de l'extrait organique. Conditions analytiques : silice capillaire 50 μm i.d., longueur totale : 30 cm, longueur effective : 20 cm. BGE : acide citrique - tampon acide ϵ -aminocaproïque / 150 mM pH 2,0. Température : 25 ° C. Tension de séparation : 15 kV. Volume d'injection de l'échantillon : 313 nl (correspondant à 80% du volume capillaire jusqu'à la fenêtre du détecteur). Détection : 254 nm.

Dans le chapitre IV, la méthode de SALLE-EC-UV présentée au chapitre précédent a été entièrement automatisée. Cette méthode, appelée A-SALLE-EC-UV, permet le dessalage, la précipitation des protéines, l'extraction liquide-liquide automatisée, la pré-concentration en ligne et la séparation électrophorétique

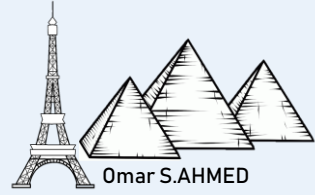
des analytes dans les échantillons de plasma de manière totalement intégrée. Cette méthodologie a été réalisée sans aucune modification au niveau de l'instrument commercial d'électrophorèse capillaire. Cette nouvelle approche, A-SALLE-EC-UV, a été appliquée pour l'analyse de 3 des ITK précédemment étudiés dans des échantillons de plasma. Cette méthode a été validée en termes de linéarité, LOQ, LOD et répétabilité. Ainsi, il peut être considéré comme un moyen rapide, simple, peu coûteux, pratique et bien adapté à un possible STP d'ITK.

Dans le dernier chapitre, des échantillons de sang de patients ont été traités par la technique SALLE, méthode décrite dans le chapitre III, pour l'extraction et la quantification d'ITK. Les échantillons obtenus ont ensuite pu être analysés par CE-UV ou chromatographie liquide-UV. Ces méthodes analytiques, SALLE-CE-UV et SALLE-LC-UV offrent de nombreux avantages en combinant une procédure d'extraction plus rapide à partir d'échantillons de sang et une grande efficacité de la séparation. Les performances des deux méthodologies ont été évaluées en termes de LOQ, LOD, spécificité, répétabilité, temps total d'analyse et de coût.

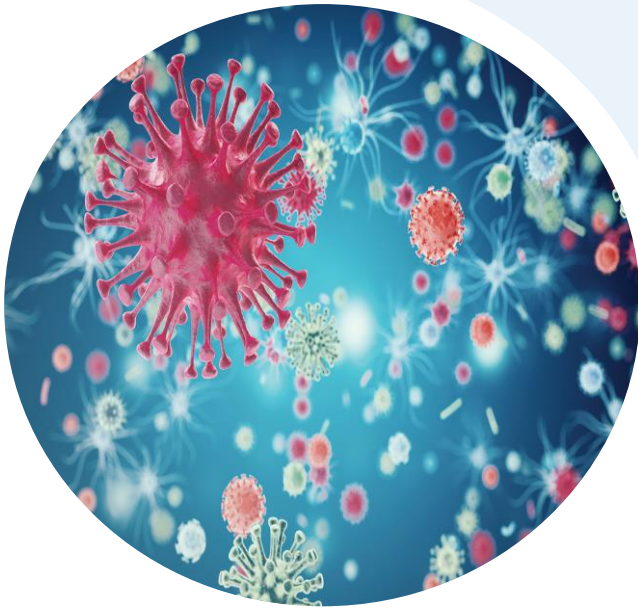
References

- [1] C. Natoli, B. Perrucci, F. Perrotti, L. Falchi, S. Iacobelli, Consorzio Interuniversitario Nazionale per Bio-Oncologia (CINBO), Tyrosine kinase inhibitors, *Curr. Cancer Drug Targets*. 10 (2010) 462–83.
- [2] H.J. Klümpen, C.F. Samer, R.H.J. Mathijssen, J.H.M. Schellens, H. Gurney, Moving towards dose individualization of tyrosine kinase inhibitors, *Cancer Treat. Rev.* 37 (2011) 251–260.

Chapter I



Tyrosine kinase inhibitors (TKIs)-mechanisms, uses, relevant problems and bioanalysis



Preface

In this chapter, an introduction about cancer disease and the hallmarks causing this disease are discussed. In addition, a state-of-the-art on the importance of TKIs in targeted cancer therapy, their mechanisms of action, their use and associated issues will be presented. Also, the significance to measure the plasmatic concentrations of ITK on a regular basis to adapt their doses, i.e. Therapeutic Drug Monitoring (TDM) will be discussed. Eventually, an overview about the extraction methods used for the analysis of drugs from biological matrices is given. In addition, the importance of capillary electrophoresis (CE) technique for the bioanalysis of as an alternative technique to liquid chromatography (LC) is discussed.

1. Cancer

1.1. Definition of cancer

According to the national cancer institute [1], cancer is a term for diseases in which abnormal cells divide without control and can invade nearby tissues. Cancer cells can also spread to other parts of the body through the blood and lymph nodes systems. Edwin smith papyrus, possibly attributable to Imhotep (the Egyptian physician-architect), described the first documented case of breast cancer. The case was deemed incurable if the disease was “cool to touch, bulging and spread all over the breast”. Yet it was more than 2000 years later – around 400 BC that the Greek physician Hippocrates first named a mass of cancerous cells “*karkinos*”, the Greek word for “crab” (Fig. 1) [2]. This was because the finger-like spreading projections from a cancer called to his mind the shape of a crab.

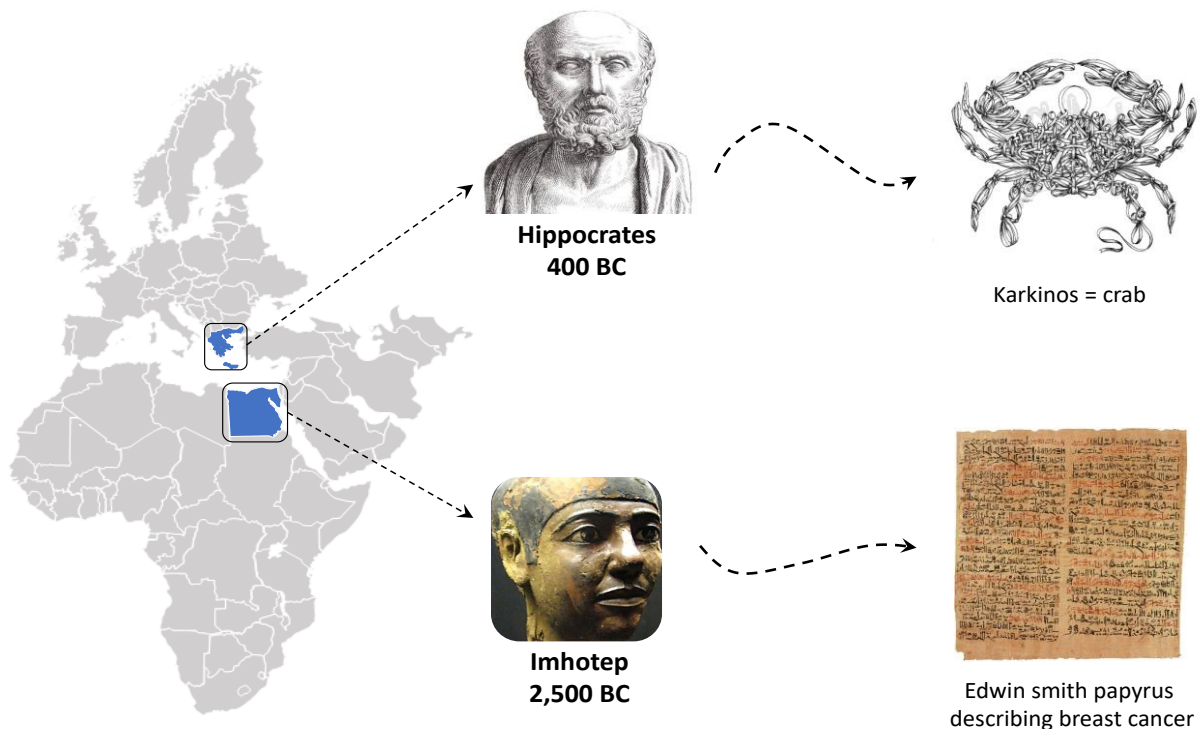


Figure 1: Schema showing the linguistic journey to the origin of the word "cancer"

According to the cancer research center in the United Kingdom (UK) [3], there are more than 200 types of cancer, characterized by abnormal cell growth. Many cancers are in the form of solid tumors, which are masses of tissue while, other types such as leukemia, generally do not form solid tumors. Cancerous tumors are malignant as they can spread into, or invade nearby tissues. In addition, as these tumors grow, some cancer cells can break off and travel to distant places in the body through the blood or the lymph system and form new tumors far from the original tumor.

1.2. Cancer statistics

Cancer is responsible for more than one-fourth of deaths worldwide [4]. In France, cancer accounted for 28.5% of all deaths in 2014, followed by cardiovascular diseases (25%) [5]. Statistics presented gender differences as shown in Fig 2. 33% of all deaths among men were related to cancer. This proportion was lower among women with 24% of the total number of deaths compared to 27% for cardiovascular diseases. Occurrence of cancer is mainly correlated to the high rate of cigarette smoking and to the high consumption of alcohol, which are considered as risk factors for developing cancer [6,7].

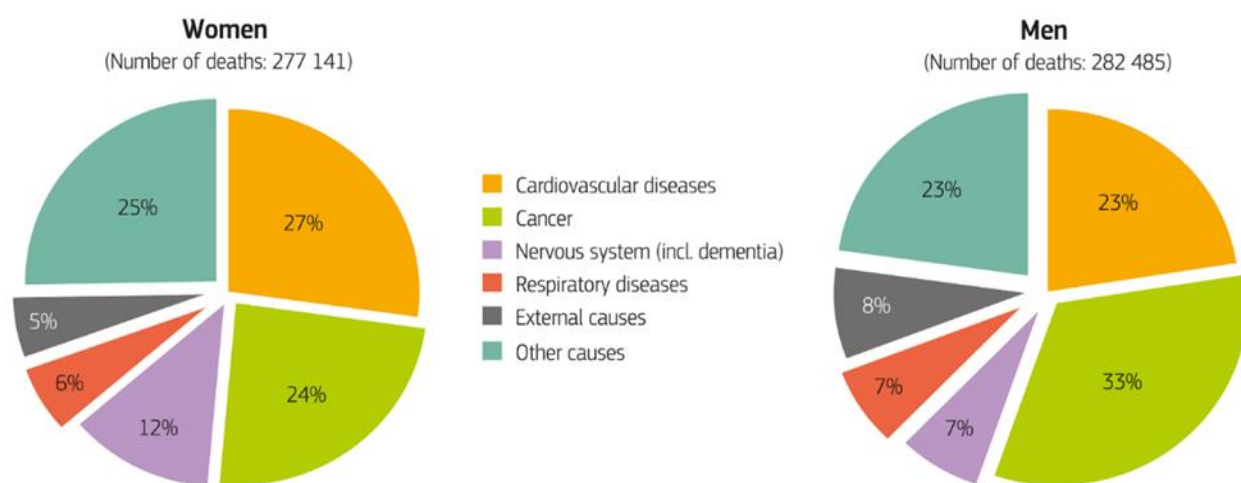


Figure 2: Cancer and cardiovascular diseases are the leading causes of death in France in 2014 [5]

The number of new cases of cancer in 2018 in France was estimated at nearly to 455,618 for both sexes. Between 2007 and 2016, the number of new cases of cancer was estimated at 356,109 per year, an increase by nearly 22% was observed in 2018. Two main factors contribute to such increase: 1/an ageing population and 2/delayed effect from the increase of women smokers [8]. The rate of lung cancer among women has increased by 5% every year since 1990 and now 45% of all cancers among women in France are lung cancer. All of these numbers show the devastating effect of cancer disease. In order to rationalize the complexity of cancer, we have to understand the hallmarks of cancer that will help to further understand the strategies used for the treatment of cancer.

1.3. Hallmarks of Cancer

The hallmarks of cancer are a list of properties that cancerous cells all have in common. These properties are gained through mutations to genes that produce proteins responsible for cell division and cell survival. In 2000, D. Hanahan [9] published a very well-known article describing the hallmarks of cancer. They were

comprised into six shared biological capabilities acquired during the multistep development of human tumors. This was later updated by D. Hanahan in 2011 [10] by adding four more hallmarks. These hallmarks govern the transformation of normal cells to cancer (malignant or tumor) cells. Herein, the ten hallmarks described in 2011, will be discussed (Fig. 3).

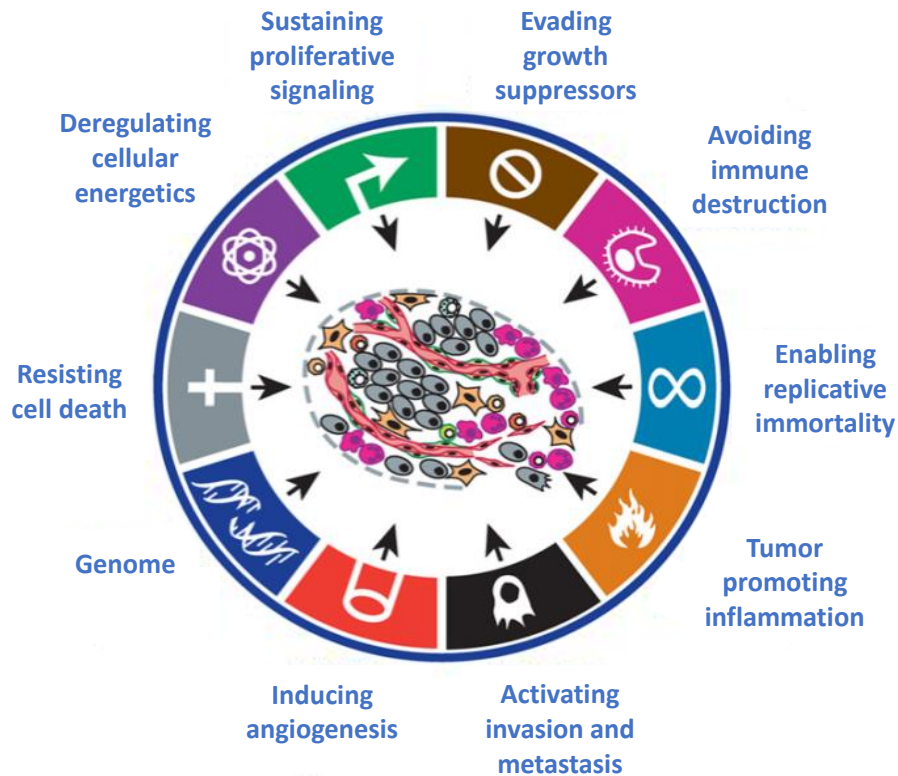


Figure 3: The hallmarks of cancer [9,10]

1.3.1. Sustaining proliferative signaling (Self-sufficiency in growth signals)

Cancer cells stimulate their own growth, which means they become self-sufficient in growth signals, and no longer depend on external signals. The most obvious characteristic of cancer cells is the ability to maintain chronic proliferation (expanding). Normal tissues tightly control cell division and cell progression. Growth promoting signals such as epidermal growth factor (EGF) binds to its receptor (epidermal growth factor receptor (EGFR)). This will cause the receptor to dimerize to activate the release of growth factor proteins (intracellular signaling). These proteins are responsible for activating the cell division for adjacent cells. Growth factors proteins bind to growth factor receptor typically containing intracellular tyrosine kinase domains in the cell membrane. This binding causes a signal transduction cascade inside the cells (a

number of interactions of transmitter proteins inside the cells) leading at final to cell division and cell proliferation as shown in Fig 4.

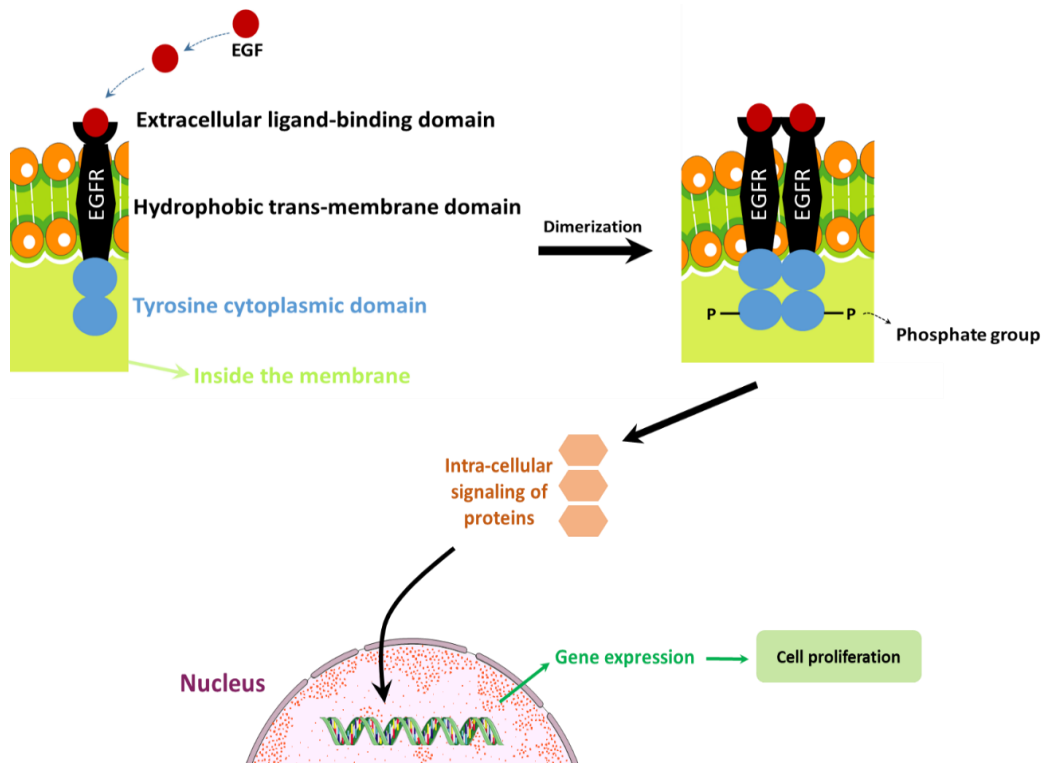


Figure 4: Cell proliferation by the activation of EGFR

Cancer cells are able to escape the constraint that normally regulate cell proliferation and have the ability to maintain proliferative signaling by several ways: 1/ production of growth factor ligands, 2/ signals sending to stimulate normal cells, 3/ over-expression of receptor proteins, 4/ somatic mutation in the human DNA sequencing, 5/ having defects in the negative-feedback mechanisms and 6/ triggering cell senescence.

Production of growth factor ligands by cancer cells and growth modulatory substances to which they can respond via the expression of cognate receptors to these ligands, result in autocrine proliferative stimulation [11]. Also, cancer cells send signals to stimulate normal cells within the supporting tumor-associated stroma. These stimulated normal cells reciprocate by supplying cancer cells with various growth factors [12,13]. In addition, the over-expression of receptor proteins displayed at the cancer cell surface, rendering such cells hyper-responsive to otherwise-limiting amounts of growth factor ligand [14,15]. Somatic mutations which activate additional downstream signaling pathways by somatic

mutation in the human DNA sequencing, are another way of cancer cells to maintain proliferative signaling. [16]. Other mutation which presents in the catalytic subunit of phosphoinositide 3-kinase (PI3-kinase) isoforms, are being detected in an array of tumor types. This mutation serves to hyper-activate the PI3- kinase signaling pathway, including its key Akt/protein kinase B (PKB) signal transducer (downstream activation) [17,18]. Another way for cancer cell to sustain proliferation, is to have defects in the negative-feedback mechanisms that weaken normal proliferative signaling.

An example of this type is the regulation that involves the Ras oncoprotein (responsible for transmitting signals inside the cells, belongs to a class of protein called small GTPase). The oncogenic mutations affecting Ras genes compromise Ras GTPase activity, which operates as an intrinsic negative-feedback mechanism to ensure that active signal transmission is temporary. In mutation, cells are undergoing a permanent form of growth arrest known as *senescence*, an intrinsic tumor suppressor program. This gives the ability to cancer cells to induce activation of high levels of sustained MAP kinase and PI3 kinase signaling [19].

Another example of this type, involves the phosphatase and tensin homolog (PTEN), which counteracts PI3-kinase by degrading its product, phosphatidylinositol (3,4,5) trisphosphate (PIP3). Loss-of-function mutations in PTEN amplify PI3K signaling and promote tumorigenesis [17,18].

A last example of this type is the mammalian target of rapamycin (mTOR) kinase, a coordinator of cell growth and metabolism that lies both upstream and downstream of the PI3K pathway. In the circuitry of some cancer cells, mTOR activation results, via negative feedback, in the inhibition of PI3K signaling. Thus, when mTOR is pharmacologically inhibited in such cancer cells (such as by the drug rapamycin), the associated loss of negative feedback results in increased activity of PI3K and its effector Akt/PKB, thereby blunting the antiproliferative effects of mTOR inhibition [20,21].

The last way where cancer cells can sustain proliferative signaling is by triggering cell senescence. Cell senescence is a permanent form of growth arrest. Accordingly, some cancer cells may accommodate to high levels of oncogenic signaling by deactivating their senescence which was recently described in details by S. Lee [22] in 2019. He showed that many conventional chemotherapeutic agents, but possibly many other anticancer drugs as well, act to some extent via the induction of senescence in cancer cells reversing tumor cell proliferation.

1.3.2. Evading Growth Suppressors

Cancer cells must also avoid cell mechanisms, which manage cell proliferation. Many of these mechanisms (programs) depend on actions of tumor suppressor genes. Cancer cells in order to proliferate have to outsmart these powerful mechanisms by tumor suppressor genes. A tumor suppressor gene, or anti-oncogene, is a gene that inhibits cell growth and cell proliferation. When this gene mutates, weakening its function, the cell can progress to cancer cell. The two tumor suppressors which govern cell fate including cell growth are the retinoblastoma (RB)-associated proteins [23] and tumor protein 53 (TP53) proteins [24].

Cancer cells with defects in RB pathway have persistent cell proliferation (non-stop way). On the other hand, approximately 50% of all human tumors carry a protein 53 (P53) mutation, and at least 52 over nearly 100 different types of tumor have P53 mutations senescence showing the importance of TP53 as a gate guard for cell proliferation. Moreover, mutant P53 gene may have a role in the development of basal and squamous cell carcinomas, two types of skin cancer [25].

Another way for cancer cells to avoid growth suppressors is through the corruption of the transforming growth factor beta (TGF- β) pathway which is best known for its antiproliferative effects [26–28]. In many late-stage tumors, TGF- β is found instead to activate a cellular program, termed the epithelial-to-mesenchymal transition (EMT). In this process, the cells lose their epithelial characteristics, including their polarity and specialized cell-cell contacts, and acquire a migratory behavior, allowing them to move away from their epithelial cell community and to integrate into surrounding tissue, even at remote locations (see work of J. Xu [29]).

1.3.3. Resisting cell death

Apoptosis (programmed cell death) is considered as a line of defense against cancer progression and many strategies based cancer treatment aims to activate apoptosis [30,31]. The mechanism behind apoptosis is based on both upstream regulators and downstream effectors components [30]. The upstream regulators are divided into two major circuits, 1/ the extrinsic apoptotic program, (e.g. Fas receptor or also called death receptor) and 2/ the intrinsic program. Apoptosis is controlled by counterbalancing of the Bcl-2 family of regulatory proteins (apoptosis regulator proteins) [30]. B-cell lymphoma-extra-large (Bcl-xL), Bcl-2-like protein 2 (Bcl-w), induced myeloid leukemia cell differentiation (Mcl-1) are inhibitors of

apoptosis, acting in large part by binding to and thereby suppressing two proapoptotic triggering proteins (Bax and Bak). An example of the cancer way to avoid apoptosis is the deoxyribonucleic acid (DNA) mutation to TP53 tumor suppressor [32]. Signaling imbalances resulting from excessive levels of oncogene signaling and DNA damage associated with cancer cells, weaken apoptosis. Alternatively, tumors may increase expression of antiapoptotic regulators (Bcl-2, Bcl-xL, as mentioned above) or expression of survival signals (insulin-like growth factor 1/2 (Igf1/2)). The latter is a survival factor [33] that initiates a signaling cascade that starts by tyrosine phosphorylation of substrates leading to the activation of serine kinases. Serine kinases modulate the activity of members of the Bcl-2 family, which regulates the apoptotic machinery in most cells.

Another example, the signaling pathway involving the PI3- kinase, AKT, and mTOR kinases, which is stimulated by survival signals to block apoptosis, similarly inhibits autophagy (another line of defense like apoptosis). when survival signals are insufficient, the PI3K signaling pathway is down regulated, with the result that autophagy and/or apoptosis may be induced [34].

1.3.4. Enabling Replicative Immortality

There is a circumventing counting mechanism at the end of the linear chromosome that shut off cell division when a preset is reached. Cancer short-circuits this counting mechanisms by the induction of enzyme expressed in stem cells called telomerase. Telomerase is a cellular reverse transcriptase (molecular motor) that adds new DNA onto what is called telomeres. Telomeres is a guanine-rich tandem DNA repeats (caps) at the chromosomal end. It maintains chromosomal stability and cellular replication causes their loss [35]. Telomeres are controlled by the presence of telomerase enzyme. Progressive telomere shortening from cell division (replicative aging) provides a barrier for tumor progression. While telomerase does not drive the oncogenic process, it is permissive and required for the sustain growth of most advanced cancers. Cancer cells have evolved the ability to overcome senescence by using mechanisms capable of maintaining telomere lengths (such as expressing telomerase), which enables cancer cells to divide indefinitely [36]. Since telomerase is not expressed in most normal human cells, this has led to the development of targeted telomerase cancer therapeutic approach [37].

1.3.5. *Inducing Angiogenesis*

The growing mass of cancer cells like normal cells needs oxygen, nutrients and glucose to feed up their growth and to get rid of waste products. Angiogenesis is the physiological process through which new blood vessels form pre-existing vessels, formed in the earlier stage of vasculogenesis. Angiogenesis continues the growth of the vasculature by processes of sprouting and splitting. As a normal physiologic process, angiogenesis is turned on, but only temporarily. In contrast, during tumor progression, an angiogenesis is almost permanent, causing continually sprouting new vessels that help sustain expanding neoplastic growths [38]. There are angiogenic regulators (signaling proteins) that bind to stimulatory or inhibitory cell surface receptors displayed by vascular endothelial cells to control angiogenesis process. The well-known inducers and inhibitors of angiogenesis are vascular endothelial growth factor-A (VEGF-A) and thrombospondin-1 (TSP-1), respectively. The VEGF-A gene [39] is a member of the platelet-derived growth factor (PDGF)/VEGF growth factor family which induces proliferation and migration of vascular endothelial cells, and blood vessels. It is essential for both physiological and pathological angiogenesis (cancer progression). Several VEGF inhibitors have been approved by the food and drug administration (FDA) for the treatment of advanced cancer. Moreover, members of the fibroblast growth factor (FGF) family [40] have been implicated in sustaining tumor angiogenesis when their expression is chronically up regulated.

1.3.6. *Activating Invasion and Metastasis*

This hallmark is specifically responsible for symptomatic and lethal types of cancer. Invading cancer cells which are very aggressive, grow by migrating and invading into normal cells. These normal cells could be local (at the same site) or throughout the body organs. This kind of cancer is called invasive metastasis. The associated cancer cells typically develop alterations in their shape as well as in their attachment to other cells and to the extracellular matrix (ECM). Loss of E-cadherin by cancer cells is one of the most known alteration. E-cadherin (epithelial adhesion molecule) is thought to enable metastasis by disrupting intercellular contacts, an early step in metastatic dissemination [41].

The process of metastasis depends on its interactions with the homeostatic factors that promote tumor-cell growth, survival, angiogenesis and invasion [42]. Also, contributions of stromal cells (bone marrow cells) to invasion and metastasis has been verified. There is clinical and experimental evidence that macrophages promote cancer initiation and malignant progression. Experimental model of metastatic

breast cancer, tumor-associated macrophages (TAMs) supply epidermal growth factor (EGF) to breast cancer cells [43].

1.3.7. Deregulating cellular energetics

Cancer cells become dynamic and flexible in the way of using nutrients to fuel their cell growth. Alternative energy resources are tapped to provide fuel and biomaterials for chronic cancer cell proliferation such as up-regulation of glycolysis, resulting in increased glucose consumption [44]. Cancer cells shift their energy production by limiting their energy metabolism largely to glycolysis (in the cytosol), leading to what is called aerobic glycolysis. This metabolic reprogramming has been shown to be associated with activated oncogenes (e.g. RAS) and mutant tumor suppressors (e.g., TP53) [45,46].

Recent molecular studies of cancer have revealed that, in addition to the contributions of oncogenes and tumor suppressor genes to the growth of cancer cells, some of these genes directly affect cellular energy metabolism [47]. The products of these genes alter the expression of transcription factors that regulate genes that encode metabolic enzymes.

Hypoxia, a non-physiological level of oxygen tension, plays an important role in cancer progression. Hypoxia interferes with cancer cell metabolism by inducing cell quiescence. It stimulates a complex cell signaling network in cancer cells, including the hypoxia-inducible factor-1 (HIF-1) pathway and perhaps other transcription factors. This simulation might plays a central role in promoting the survival of cancer cells in adverse tumor microenvironments [48,49].

1.3.8. Avoiding immune destruction

In many cases, the immune system of the body detects cancer cells and seeks to resist or eradicate them. Both innate and adaptive immune systems play important roles in anticancer immune response [50]. The innate immune cells can release signals which are essential to stimulate responses from both T cells (T killer and T helper) and B cells [51]. Adaptive immune system mainly consists of B cells, T killer (CD8+ cytotoxic T lymphocytes), the corner stone of immune response fighting cancer, as well as T helper (CD4+ T_H1 helper cells) [52]. Antigen presenting cells (APCs) is the link between the innate and the adaptive immune system by identifying foreign antigens and presenting to T cells. Lethal tumors adapt themselves to avoid such attack.

During the early stages of tumor development, malignant cells can be poor stimulators, present poor targets or become resistant to the innate immune response, while at later stages, progressively growing tumors impair the adaptive immune response by causing alterations in T-cell signal transduction and function [53]. Deficiencies to the immune system could lead to the development of carcinogen-induced tumors. In particular, deficiencies in the development or function of CD8⁺ cytotoxic T lymphocytes, CD4⁺ T_H1 helper cells, or natural killer (NK) cells each led to demonstrable increases in tumor incidence proved experimentally on mice [54].

Recently, there is an evidence of the existence of antitumor immune responses in some forms of human cancer [55]. For example, patients with colon and ovarian tumors that are heavily infiltrated with cytotoxic T lymphocytes (CTLs) and NK cells have a better prognosis than those that lack such abundant killer lymphocytes. More recently, data obtained from research in both mouse and human models with cancer provided a proof that immune system can sometimes collectively function as extrinsic tumor-suppressor mechanisms [54].

1.3.9. Genome instability and mutation

The above mentioned hallmarks depend largely on alterations in the genomes of cancer cells. Failure of the genome maintenance systems that protect the genome DNA from being corrupted, rearranged or damaged. The result is mutation that convey on cancer cell.

Epigenetic mechanisms such as DNA methylation and histone modifications could lead to inactivation of tumor suppressor genes [56]. Other mutations involve affecting the DNA-maintenance machinery, often referred to as the “caretakers” of the genome (behave much like tumor suppressor genes). These mutations (defects) in these caretaker genes includes those whose products are involved in 1/ detecting DNA damage and activating the repair machinery, 2/ directly repairing damaged DNA, and 3/ inactivating or intercepting mutagenic molecules before they have damaged the DNA [57]. Also, the loss of telomeric DNA in many tumors is considered as a genomic instability as previously explained in point 1.2.4.

1.3.10. Tumor-promoting inflammation

Tumors are wounds that do not heal [58]. Recent research showed that immune cells that help in wound healing, helps cancer to be more and more aggressive by enhancing tumorigenesis and progression [59]. Inflammation caused by immune system can contribute to multiple hallmark capabilities by supplying

bioactive molecules to the tumor microenvironment. These molecules include growth factors that sustain proliferative signaling, and survival factors that limit cell death. Also, proangiogenic factors and extracellular matrix-modifying enzymes that facilitate angiogenesis, invasion, and metastasis, and inductive signals that lead to activation of EMT (see point 1.2.2) and other hallmark-facilitating programs [60,61].

1.3.11. Conclusion about the hallmarks of cancer:

The complexity of cancer could be explained by ten common traits ("hallmarks") that govern the transformation of normal cells into cancer cells. The acquisitions of these hallmarks capabilities by neoplastic cells are sufficient to generate aggressive and lethal types of cancer. Knowledge of these hallmarks has led to the development of modern therapeutics that targets one or more of these hallmarks.

1.4. Cancer therapy

Cancer therapy is related to 1/ the treatment of cancer, 2/ the relief of the symptoms associated with cancer, such as pain and 3/ relief of the adverse effects caused by the treatment. The types of cancer treatment depend on the type and the stage of cancer. Some patients will have only one treatment, others will have a combination of treatments.

Surgery is an option of cancer therapy based on removing the tumor tissues, reducing the risk of cancer spread and often increasing the effectiveness of other forms of treatment. The latter is based on placing a constant venous infusion with portable pump to deliver chemotherapeutic agents [62]. This helps to heal a significant proportion of highly localized solid cancers, which are accessible to surgeon. Many types of surgery existed for different purposes including: 1/ diagnostic surgery (biopsies) to remove a space of suspicious cells to study, 2/ staging surgery to find out the size of the tumor and if or where the cancer has spread, 3/ curative surgery to remove the tumor and some of the nearby healthy tissue, 4/ palliative surgery is used to improve the quality of life of cancer patient (e.g. stop bleeding) and finally 5/ debulking surgery is used to remove most of the cancer tumor when it is impossible to remove the entire tumor to prevent spreading to the nearby tissues or cells. Although surgery of primary or even metastatic tumors can save or extend life, it has long been acknowledged that it may precipitate, accelerate tumor recurrence or metastasis [63].

Radiotherapy or radiation therapy, on the other hand, is a treatment that involves exposing patients to high radiation energy (X-rays, electrons) to destroy cancer cells. Radiotherapy may be used before surgery to shrink the cancer or after surgery to kill any cancer cells that remain in the area after the operation. Approximately 50% of all cancer patients receive radiation therapy during their course of illness besides other treatment modalities (e.g. chemotherapy) [64]. Radiotherapy is very effective but it should be targeted specifically to cancer cells to avoid damaging normal surrounding tissues (secondary effect). That is the reason why radiotherapy cannot be used in all types of cancers (e.g. invasive cancers).

Chemotherapy is a cancer treatment that uses anticancer drugs frequently called chemotherapeutic agents [65]. There are more than 100 different chemotherapy drugs. As previously mentioned with surgery, chemotherapy may be given with a curative or palliative purpose. Nitrogen mustards alkylating agents were the first chemotherapeutic agents to be used for the treatment of cancer and it was discovered in 1942 [66]. This valuable class of alkylating agent exerts its biological activity by binding to DNA, cross-linking two strands, preventing DNA replication and ultimate cell death. However, the lack of selectivity to cancer cells restricts the wide usage of nitrogen mustard agents to achieve further clinical significance [67].

Another example of chemotherapeutic agents are the so-called antimetabolites. The antimetabolites [68] do not directly attack the DNA bases like nitrogen mustards but rather interfere with synthesis of DNA precursors leading to cancer cell death. Like most chemotherapeutic agents, antimetabolites have toxic effect on normal cells. This toxicity gave birth to a unique group of cancer therapy, called targeted cancer therapy. Recently targeted cancer therapy has gain importance due to its specificity towards cancer cells while sparing toxicity to off-target cells.

2. Targeted cancer therapy

Mechanism-based targeted cancer therapies were considered as the next generation of evolutionary cancer therapies. Targeted therapeutics can be classified according to their effects on one or more hallmark capabilities as shown into 10 categories corresponding to the 10 hallmarks of cancer (Fig 5).

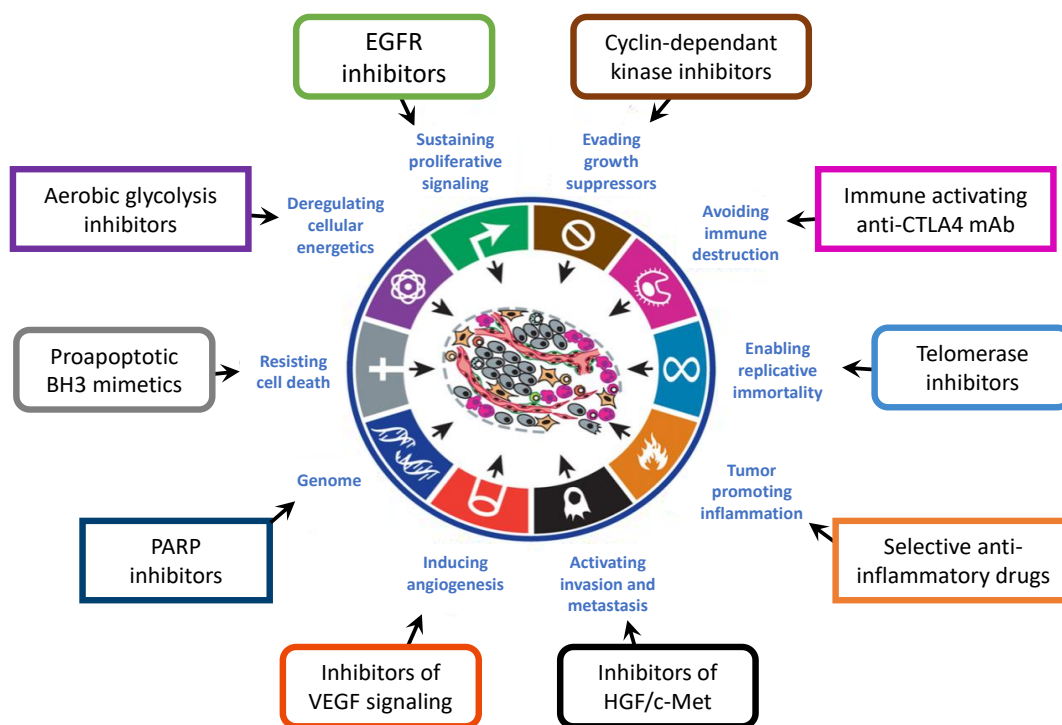


Figure 5: Therapeutic targeting of the hallmarks of cancer [10]

Each hallmark-targeting cancer drug was developed and directed toward specific targets that are involved in one way or another in enabling particular capabilities. An example of targeted cancer therapy is to target the telomerase enzyme. As mentioned in point 1.3.4, telomerase does not drive the oncogenic process, it is permissive and required for the sustain growth of most advanced cancers. Currently there are many drugs designed to inhibit telomerase enzyme. Imetelstat (GRN163L) has been one of the most widely developed and is arguably the most successful [69].

As also mentioned before, Inflammation is closely linked to cancer (see point 1.2.10). Anti-inflammatory agents such as non-steroidal anti-inflammatory drugs (NSAIDs) have anti-colon cancer effects [70,71]. Other clinical trials have indicated that long-term use of aspirin decreases the incidence of colorectal, esophageal, breast, lung and bladder cancers [72].

Another example is the role played by the immune system in both host-protecting and cancer-promoting mechanisms. Cancer immunotherapy, a type of cancer targeted therapy, is the treatment that uses your body own immune system to help fighting cancer. Recently, cancer immunotherapy field is growing tremendously, such as using cancer vaccinations, T-cell therapy and immune checkpoint blockade therapy [73]. Immunotherapies may be subdivided into passive and active based on their ability to engage the

host immune system against cancer. Passive immunotherapy is the administration of monoclonal antibodies (mAbs), lymphocytes or cytokines, which boost existing the immune system to fight against cancer. An example, mAbs that block the interaction of cytotoxic T lymphocyte-associated antigen (CTLA-4) with its ligands can enhance immune responses, including anti-tumor immunity [74]. Active immunotherapy aims to stimulate self-immune system to attack tumor cells via vaccination, non-specific immunomodulation, or targeting specific antigen receptors [75].

The classification of cancer immunotherapy is shown in [Table 1](#).

Table 1: Classification of cancer immunotherapy [73]

Passive immunotherapy		Active immunotherapy	
<i>Immuno-modulating antibodies</i>	<i>Adoptive immunotherapy</i>	<i>Specific</i>	<i>Non-specific</i>
- Immune checkpoints inhibitors	- Tumor-infiltrating lymphocytes	- Vaccines	-Immune adjuvants
- Immune co-stimulatory antibodies	- TCR gene-modified lymphocytes		- Cytokines
	- Chimeric antigen receptors (CARs)		

One of the most important target frequently associated in many hallmarks, is the abnormal activation of protein phosphorylation. In turn, kinase signaling pathways were involved in the proliferation, survival, motility, metabolism, angiogenesis, and evasion of tumor cells. Currently, there are multiple examples of small molecule kinase inhibitors with both selectivity and suitable pharmaceutical properties that have produced meaningful clinical benefits. In the next point, we will discuss small molecule kinase inhibitors which are concerned in this project.

2.1. Protein tyrosine kinases

2.1.1. Human protein kinases

Human protein kinase family consists of 518 members discovered by Manning in 2002 [76]. These enzymes are classified as protein-serine/threonine kinases (385 members), protein-tyrosine kinases (90 members), and protein tyrosine kinase-like enzyme (43 members). Protein-tyrosine kinases which are concerned in this project are discussed below.

2.1.2. *Protein tyrosine kinases*

The protein-tyrosine kinases include receptor tyrosine kinases (RTKs, 58 members) and non-receptor tyrosine kinases (NRTKs, 32 members). A small group of enzymes including mitogen-activated protein kinase (MEK1/2), which catalyze the phosphorylation of both threonine and tyrosine residues within the activation segment of target protein are classified as dual specificity kinases. Protein tyrosine kinases are important mediators of the signaling cascade taking place inside the cell. They are considered as determinant step in many biological processes like growth, differentiation, metabolism and apoptosis (programmed cell death) in response to external and internal stimuli. Tyrosine kinases are classified as mentioned before into RTKs and NRTKs. Humans have 58 known RTKs, which fall into 20 subfamilies. All RTKs [77] have a similar molecular architecture, with ligand binding domains in the extracellular region, a single trans-membrane helix, and a cytoplasmic region that contains the protein tyrosine kinase domain plus additional carboxy (C-) terminal and juxtamembrane regulatory regions as shown in [Fig 6](#).

Generally, growth factor binds to RTKs inducing what is called dimerization [78] taking into consideration that insulin receptor and IGF1 receptor are normally dimers ([Fig 6](#), red dotted rectangular) [79]. Their activation is done by structural changes stimulating signaling cascade inside the cell.

On the other hand, NRTKs are subdivided into 9 main families and 32 sub-families ([Fig 7](#)), based on their similarities in domain structure with a high degree of homology (sequence similarities) in the catalytic Src Homology 1 (SH1), p-tyrosine binding Src Homology 2 (SH2), and protein–protein interaction Src Homology 3 (SH3) domains [80].

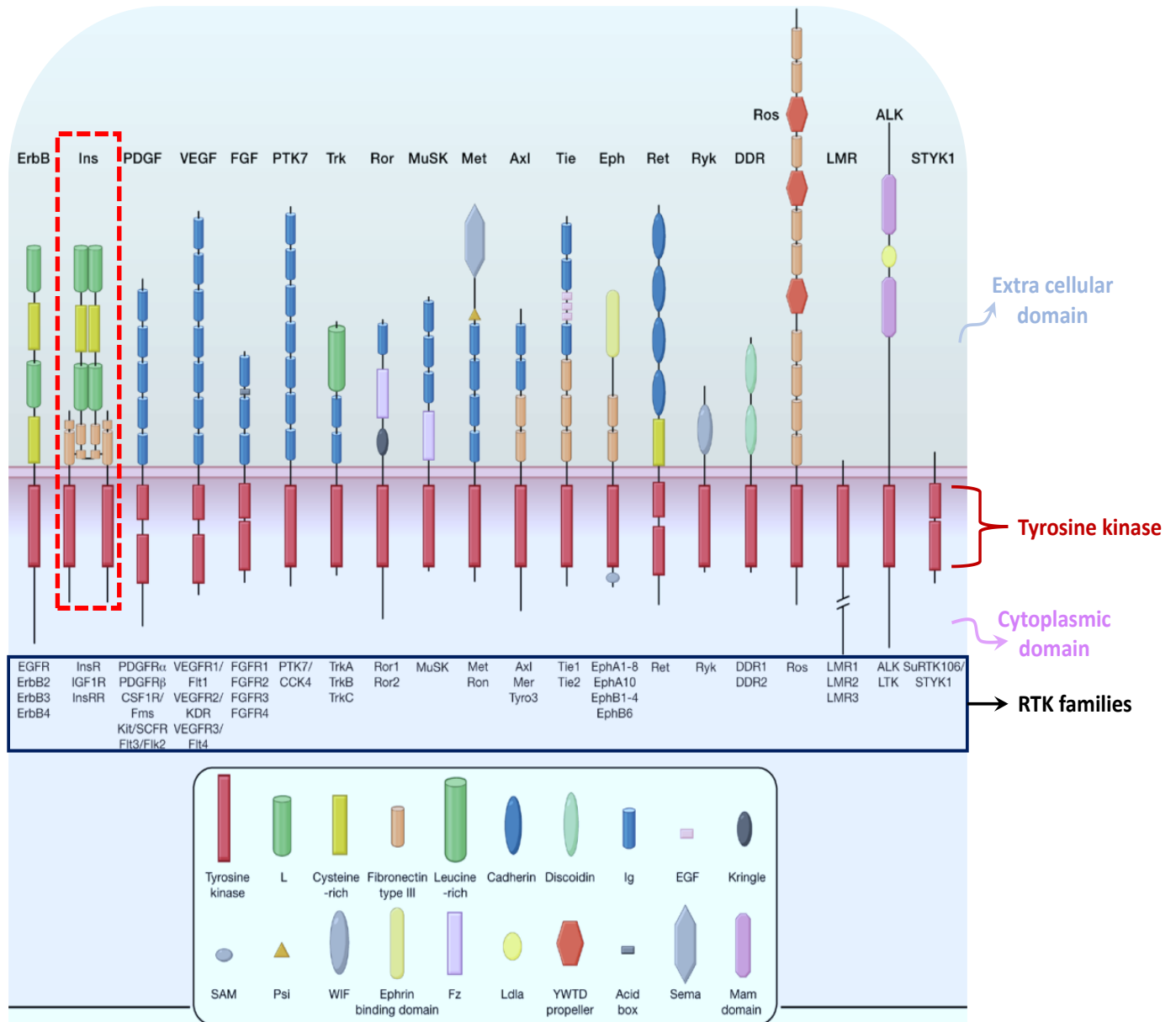


Figure 6: RTK Families. RTKs contain 20 subfamilies, shown here schematically with the family members listed beneath each receptor. Structural domains in the extracellular regions, identified by structure determination or sequence analysis, are marked according to the key. The intracellular domains are shown as red rectangles [77].

The tyrosine kinase domain spans approximately 300 residues and consists of an N terminal lobe comprising a 5 stranded β sheet and one α helix, while the C terminal domain is a large cytoplasmic domain that is mainly α helical. ATP binds in the cleft in between the two lobes and the tyrosine containing sequence of the protein substrate interacts with the residues of the C terminal lobe. The activation mechanism of NRTKs is more complex than RTKs, involving heterologous protein-protein interaction to enable trans-phosphorylation. Due to the presence of cellular inhibition proteins, lipids and through

intramolecular auto-inhibition, NRTKs are maintained in an inactivated state. Through intracellular activation signals, they are recruited to trans-membrane receptors and phosphorylated by other kinases. Both RTKs and NRTKs activities are tightly regulated in normal cells.

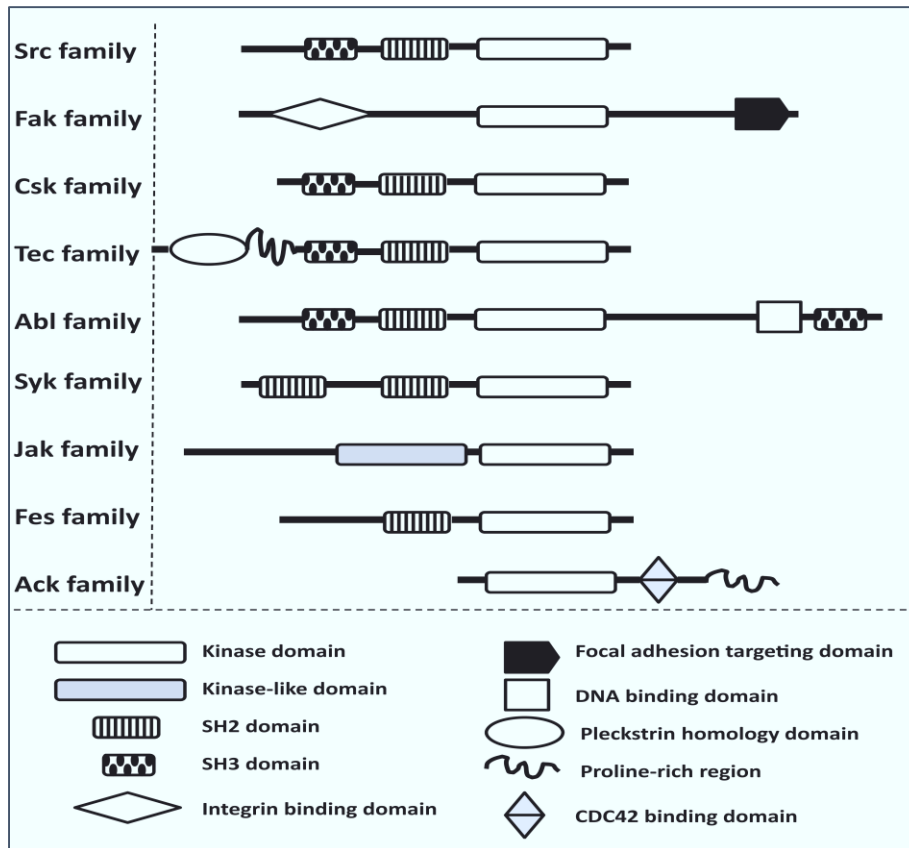


Figure 7: Domain organization of the major families of NRTKs. NRTKs are subdivided into nine main families, based on their similarities in domain structure. The catalytic (SH1, kinase), p-Tyr binding (SH2), and protein-protein interaction (SH3) domains share a high degree of homology [80].

Abnormal activation of tyrosine kinases due to enhanced expression, mutation or stimulation leading to abnormal downstream oncogenic signaling will lead to the development of cancer. Main examples of the oncogenic activation of tyrosine kinases are presented hereafter.

2.1.3. Oncogenic activation of tyrosine kinases (main examples)

2.1.3.1. BCR-ABL and human leukemia

Abelson murine leukemia (Abl) viral oncogene homolog [81] is a human protein which is encoded by the Abl gene located on chromosome 9. BCR-Abl is a mutant protein resulting from the reciprocal translocation of the Abl tyrosine kinase gene on chromosome 9 to the break point cluster region (BCR)

region of chromosome 22. This chromosomal anomaly results in Philadelphia chromosome which is responsible for the permanent tyrosine kinase activity of BCR-Abl leading to the proliferation of leukemic cells causing chronic myelogenous leukemia (CML).

2.1.3.2. Tel-Abl and human leukemia

Tel-Abl tyrosine kinase over-phosphorylation is another type of mutated fusion proteins. It is due to the reciprocal translocation of TEL gene on with ABL. It expresses a chimeric Tel-Abl protein that contains the same portion of the Abl tyrosine kinase fused to Tel [82]. Tel, which is a putative transcription factor, is fused in-frame with exon-2 of the ABL proto-oncogene, producing a fusion protein product with elevated tyrosine kinase activity. This is the cause of what is called acute lymphocytic leukemia (ALL).

2.1.3.3. EGFR over-expression

The over-expression of EGFR (a RTK) and its primary ligand EGF is very relative to many human cancers including non-small cell lung cancer (NSCLC) [83], primary urinary bladder cancer [84] and breast cancer [85]. Transforming growth factor alpha (TGF α), another ligand of EGFR, is also involved in lung cancer [86].

2.1.3.4. PDGFR over-expression

Concurrent expression of platelet-derived growth factor receptor (PDGFR) type α , a RTK in breast cancer, is associated with tumorigenesis [87]. Concurrent expression of PDGFR and its cognate ligand PDGF-A and PDGF-B has been observed in gliomas (i.e. type of brain tumor) [88].

2.1.3.5. Insulin-like growth factor receptor (IGFR) over-expression

IGFR is a receptor trans-membrane tyrosine kinases which are activated by binding to ligands insulin-like growth factor 1 (IGF-I) and insulin-like growth factor 2 (IGF-II). Elevated IGF-I autophosphorylation and kinase activity has been reported in breast cancer [89]. High circulating levels of IGF-I are associated with an increased risk of prostate cancer [90].

2.2. Tyrosine kinase inhibitors

As previously discussed, protein tyrosine kinases have been found to play a crucial role in various hallmarks of cancer. Growth factor receptors, often carrying tyrosine kinase activities in their cytoplasmic

domains, are overexpressed in many and many types of cancer. This makes tyrosine kinases as perfect anticancer targets, providing more opportunities for drug discovery and drug development. Tyrosine kinase inhibitors (TKIs) are a class of targeted therapy used in the treatment of many types of malignant diseases [91]. TKIs compete with adenosine triphosphate (ATP) at its binding site especially on RTKs. As a result, inhibition of tyrosine kinases, which are involved in several pathways, including tumor cell growth, differentiation and proliferation, will lead to the inhibition of cancer proliferation and progression. Unlike chemotherapy, these anti-cancer drugs target molecular abnormalities (mutations) in the tumor cells. They block the chronic activation of signaling pathways caused by tyrosine kinases by attaching themselves to the active protein site i.e. in NRTKs or cell membrane tyrosine kinase i.e. in RTKs. Imatinib, the first TKIs (also known as “Gleevec” or “Glivec”), was invented in the late 1990s by biochemist Nicholas Lyndon followed by several TKIs as shown in Fig 8.

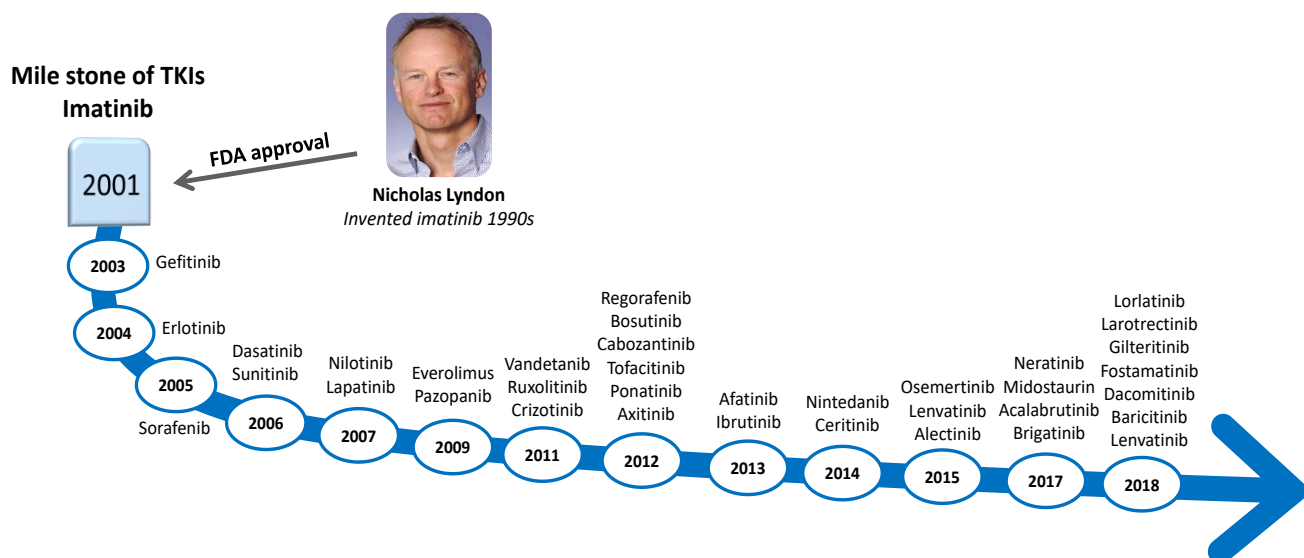


Figure 8: Back in-time journey showing the discovery of TKIs and the FDA approval until now

The first clinical trial of imatinib took place in 1998 and the drug received FDA approval in May 2001. Imatinib was a breakthrough in the targeted cancer therapy and was mainly used to treat chronic myeloid leukemia (CML) [92]. This was followed by the development of many TKIs. Until now, FDA has approved 37 orally effective TKIs in March, 2018 [80]. The majority (27 TKIs) inhibit RTKs and 10 TKIs inhibit NRTKs. Table 2 indicates 37 tyrosine kinase inhibitors, their primary targets (as many of them are multi-targets, for example; sunitinib [93]) and their therapeutic use. In general, TKIs compete with ATP on the binding site of tyrosine kinase with ATP, inhibiting tyrosine kinase phosphorylation and thereby cancer cell proliferation. It has high selectivity and small adverse reaction [94].

Table 2: TKIs, their targets and their therapeutic indications

TKIs (Trade name)	Primary targets	Therapeutic indication(s)
Acalabrutinib (Calquence®)	Bruton's tyrosine kinase (BTK)	Mantle cell lymphomas [95]
Afatinib (Tovok®)	EGFR	Non-small cell lung carcinoma (NSCLC) [96]
Alectinib (Alecensa®)	Anaplastic lymphoma kinase (ALK)	ALK-positive NSCLC [97]
Axitinib (Inlyta®)	VEGFR	Advanced renal cell carcinomas (RCC) [98]
Baricitinib (Olumiant®)	Janus kinase (JAK1/2/3) and Tyk	Rheumatoid arthritis [99]
Bosutinib (Bosulif®)	BCR-ABI	CML [100]
Brigatinib (Alunbrig®)	ALK	ALK-positive NSCLC [101]
Cabozantinib (Cometriq®)	RET	Advanced medullary thyroid cancers [102]
Ceritinib (Zykadia®)	ALK	ALK-positive NSCLC resistant to crizotinib [103]
Crizotinib (Xalkori®)	ALK	ALK-positive NSCLC [104]
Dacomitinib (Visimpro®)	EGFR	EGFR-mutant NSCLC [105]
Dasatinib (Sprycell®)	BCR-Abl	CML [106]
Erlotinib (Tarceva®)	EGFR	Pancreatic cancer [107], NSCLC [108]
Everolimus (Afinitor®)	FKBP12/mTOR	HER2-negative breast cancers [109], pancreatic neuroendocrine tumors [110], renal cell carcinomas [111], subependymal giant cell astrocytomas [112]
Fostamatinib (Tavalisse®)	Syk	Chronic immune thrombocytopenia [113]
Gefitinib (Iressa®)	EGFR	NSCLC [114]
Gilteritinib (Xospata®)	FMS-like tyrosine kinase 3 (Flt3)	Acute myelogenous leukemias [115]
Ibrutinib (Imbruvica®)	BTK	CML [116], mantle cell lymphomas [117] and marginal zone lymphomas [118]
Imatinib (Gleevec®)	BCR-ABI	CML [92], ALL [119], dermatofibrosarcoma protuberans [120], hypereosinophilic syndrome [121], GIST [122], myelodysplastic/myeloproliferative disease [123]
Lapatinib (Tykerb®)	EGFR	HER2-positive breast cancers [124]

Larotrectinib (Vitrakvi®)	Neurotrophic receptor tyrosine kinase (NTRK)	Solid tumors with NTRK fusion proteins [125]
Lenvatinib (Lenvima®)	VEGFR, RET	Differentiated thyroid cancers and ARCC [126]
Lorlatinib (Lorbrena®)	ALK	ALK-positive NSCLC [127]
Midostaurin (Rydapt®)	Flt3	Acute myelogenous leukemias [128] and mastocytosis (mast cell leukemias) [129]
Neratinib (Nerlynx®)	ErbB2	HER2-positive breast cancers [130]
Nilotinib (Tasigna®)	BCR-Abl	Philadelphia chromosome-positive CML [131]
Nintedanib (Vargatef®)	FGFR	Idiopathic pulmonary fibrosis [132]
Osimertinib (Tagrisso®)	EGFR	NSCLC [133]
Pazopanib (Votrient®)	VEGFR	RCC [134], soft tissue sarcomas [135]
Ponatinib (Iclusig®)	BCR-Abl	Philadelphia chromosome-positive CML or ALL [136]
Regorafenib (Tafinlar®)	VEGFR	Colorectal cancers [137]
Ruxolitinib (Jakafi®)	JAK (1/2/3) and Tyk	Myelofibrosis [138], polycythemia vera [139]
Sorafenib (Nexavar®)	VEGFR	Hepatocellular carcinomas (HCC) [140], RCC [141], thyroid cancer [142]
Spebrutinib	BTK	Rheumatoid arthritis, lymphoma and leukemia lymphocytic chronic B-Cell [143]
Sunitinib (Sutent®)	VEGFR	GIST [144], pancreatic neuroendocrine tumors [145] and RCC [146]
Tofacitinib (Tasocitinib®)	JAK3	Rheumatoid arthritis [147]
Vandetanib (Zactima®)	VEGFR	Medullary thyroid cancers [148]

(Name®): commercially available trade name

2.2.1. Inter-individual variability of TKIs

In clinical practice, oncologists spend long time to adapt the dose of TKIs for every patient to increase the efficacy of treatment and to minimize as much as possible associated adverse side effects. The inter-

patients pharmacokinetic variability of TKIs is reported in several studies and was related to genetics, drug-drug interactions, poor adherence, concomitant food intake or drug food interaction, different ethnic group, renal and/or hepatic functions and environment factors [149]. TKIs are orally given on a daily basis at fixed doses, and such fixed dosing may cause much larger variation between individuals in terms of clinical efficacy and toxicity which was related to trough TKIs concentration [150]. The Factors causing inter-individual variability of TKIs plasmatic concentration affecting the effectiveness of treatment are mentioned in Fig. 9.

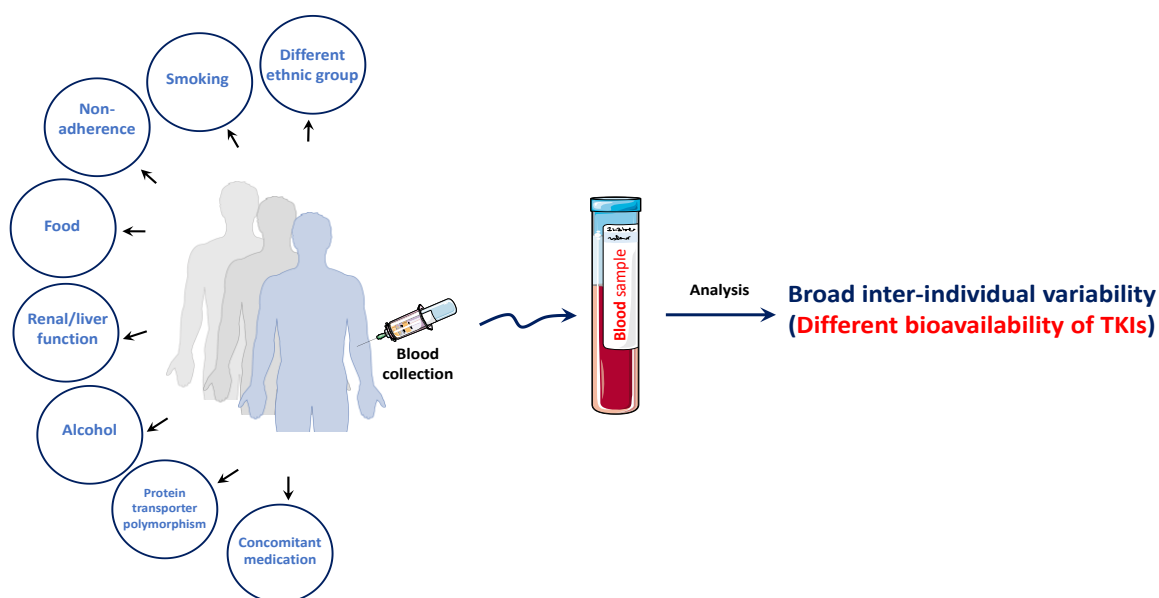


Figure 9: Factors causing inter-individual variability of TKIs plasmatic concentration

TKIs are absorbed from the intestine by what is called intestinal influx, which is mediated by drug transporters. ATP binding cassette membrane transporters, including ABCB1 and ABCG2, are expressed in normal tissues including the small intestine [151] and are responsible for regulating the oral absorption, biliary and urinary secretion, and penetration of blood brain barrier for several drugs including TKIs. It was found that, these transporters have an important role in preventing the intestinal absorption of TKIs (example; erlotinib [152]) and are responsible for TKIs brain accumulation (example; sorafenib [153]) or increasing exposure to TKIs due to transporter protein polymorphism (example; sunitinib in RCC patients [154]). Furthermore, genetic polymorphisms of ABCG2 was associated with higher exposure and toxicity of gefitinib [155] and erlotinib [156]. Patients with RCC may experience severe adverse events after the early use of sunitinib, such as facial acne, hypothyroidism and thrombocytopenia, due to ABCG2 polymorphism [157].

Different ethnic group could be another factor affecting the bioavailability of TKIs. It was found that the probability of successful treatment with imatinib was correlated with the ABCG2 polymorphism within the Asian population [158]. Moreover, relationships between sunitinib clearance and ABCG2 polymorphism were confirmed in Japanese [159] and Korean metastatic RCC patients [160]. Interestingly, ABCG2 polymorphism appears to be more common in Asians than non-Asians and is very rare in sub-Saharan African and Caucasian populations [161]. There is good evidence that people of east Asian ancestry have significantly higher response rates and superior survival outcomes to gefitinib [162], lapatinib [163] and regorafenib [164], when compared to non-east Asian patients.

Concomitant medications also affect the bioavailability of TKIs. The co-administration of TKIs with CYP3A4 inducers or inhibitors have been verified to greatly affect the bioavailability of TKIs [165]. Histamine H₂-receptor antagonist (H₂ blockers) [166] and proton pump inhibitors [167] can greatly affect the exposure to TKIs affecting the efficacy of treatment. Food on the other hand, affects directly the gastric pH which in turns, affects TKIs bioavailability and absorption. Concomitant administration of erlotinib and warfarin resulted in an increase in international normalized ratios (INR) values in a 47-year-old man with advanced lung cancer [168].

Food can strongly increase the exposure of patient to pazopanib and lapatinib leading to serious side effects [169]. High-fat meal leads to reduction of sorafenib bioavailability by 29% compared with its fasting bioavailability [170]. Likewise, grapefruit or grapefruit juice are CYP inhibitors and may increase erlotinib plasma concentrations. Heavy smoking (CYP inducer) is also considered as another factor affecting the bioavailability of TKIs. The pharmacokinetic profile of erlotinib was found to be significantly changed by smoking [171].

Patient non-adherence or non-compliance can be considered as one of the most important factors leading to therapeutic failure. In general, orally administrated therapy can potentially be given for a long period especially in the case of TKIs. The rise in the use of TKIs has brought the problem of patient non-adherence to the front. For example, patients treated by imatinib may stop their treatment after the appearance of adverse effects in the case of CML disease [172]. Therefore, poor adherence may be the predominant reason for the inability to obtain adequate responses [173,174]. The variability in drug exposure to TKIs may be also related to alcohol consumption and renal/liver functions [149].

Consequently, different strategies have to be followed to achieve correct dosing of TKIs. These strategies include dose individualization of TKIs, such as phenotype-guided dosing [175], genotype-guided dosing [176], toxicity-adjusted dosing [177] and therapeutic drug monitoring (TDM). The latter is a very promising strategy and recent evidences indicate that certain pharmacokinetic determining parameters, including trough plasma concentration, are correlated with clinical outcomes for many TKIs.

3. Overview of Therapeutic Drug Monitoring (TDM)

TDM is the clinical practice of measuring specific drugs at designated intervals to maintain a constant concentration in a patient's bloodstream at the active range, thereby optimizing individual dosage regimens [178]. The aim of TDM is to use appropriate concentrations of difficult-to-manage medications (narrow therapeutic index or medications with great inter-individual variability) to optimize clinical outcomes of patients. This includes 1/ enhancing bioavailability, 2/ reduce toxicity, 3/ prediction of tolerability and resistance to treatment, 4/ identification of drug-drug interactions [179,180] and 5/ facilitate diagnosis and consultation. TDM consists of several steps including sampling, measurement and interpretation of the drug blood concentration. In addition, TDM is used when there is a risk of patient non-adherence or when the dose of the drug can't be correlated to the appearance of adverse or side effects. TDM permits to quantify the actual drug concentration in patients' plasma or serum.

Generally, the steady state of any drug is assumed to be reached in 4–5 half-lives ($t_{1/2}$). A drug steady state occurs when the amount of drug administered (in a given time period) is equal to the amount of drug eliminated. For this reason, in practice, samples are collected from patients about 4 to 5 $t_{1/2}$ after starting therapy [181]. TDM is also the clinical assessment of a drug's pharmacokinetic properties. To study the pharmacokinetics of a drug, several parameters have to be defined. These parameters include the residual concentration serum peak and area under the curve (AUC). The residual or trough concentration (C_{min}) refers to the drug concentration measured just before the administration of the next dose. The serum peak drug concentration (C_{max}), is the maximum concentration of the drug reached in the body, in a steady state. This is achieved by the accumulation of the drug in the body until an equilibrium is reached, in which the concentration peak no longer increases (Fig. 10) [182,183]. AUC is the definite integral in a plot of drug concentration in blood plasma against time that helps to guide the dosage of this drug. The therapeutic index of a drug is the ratio between minimum effective concentrations (MEC) to the minimum toxic concentration (MTC). Its importance is to achieve therapeutic benefits of drugs without any side or toxic effects. Drugs concentration should always be in the therapeutic window. On the other hand, the time

between two successive C_{\min} could refer to the duration of action of the drug. The time of the collection of the sample is very important as the drug concentration changes during the dosing interval. The least variable point in the dosing interval is just before the next dose is given (C_{\min}). C_{\min} is what is usually measured for TDM [184].

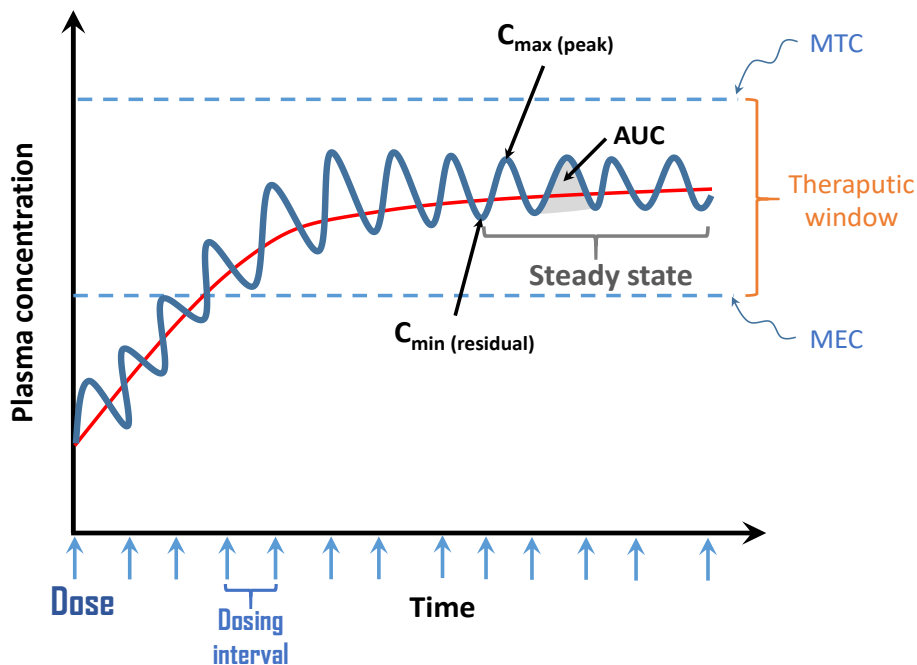


Figure 10: Variation of plasma concentration of a drug at multiple doses given at regular time bases.

3.1. TDM and TKIs

TDM of TKIs was suggested in many studies as a tool to improve the efficacy and safety profile of the treatment [185]. Plasma is the main biological matrix for TKIs. More rarely, other biological matrices, such as patients' urine and liver microsomes, are used [143,186]. The results of these studies differ significantly in 1/the use of different protocols for the preparation of the samples from different biological matrices and 2/the analytical technique used to measure TKIs.

At first, sample preparation is very important to 1/ eliminate the matrix effect interfering with the analysis, 2/ isolate and concentrate target compounds and 3/ maintain consistency of the analytical results. [Table 3](#) and [table 4](#) shows examples of methodologies used to extract and to quantify TKIs using liquid chromatography (LC) coupled to UV detection or photodiode array detection (DAD) ([table 3](#)) and to mass detection (MS or MS/MS, [table 4](#)). Sample preparation techniques used are most often based on protein

precipitation (PP), liquid-liquid extraction (LLE) and solid phase extraction (SPE). The principle of these techniques will be recalled in [part 5](#) of this chapter.

On the other hand, routine TDM of TKIs requires to develop analytical methods to measure their concentration. [Table 3](#) resumes LC-UV methods used to quantify TKIs. UV detection is the simplest, cost effective and most available technique in laboratories compared to other detection techniques making UV detection a competitor to MS detection. Although the low sensitivity associated compared to MS (nearly by 10x), most of the methods published for TKIs quantification by LC-UV or LC coupled to photodiode array detection (DAD) demonstrated sufficient sensitivity to measure TKIs in plasma (see LOQ values in [table 3](#)).

Table 3: LC-UV and LC-DAD methods for the quantitation of TKIs

LC-UV or LC-DAD				
TKIs	Extraction	Matrix	LOQ (ng/mL)	Ref
Imatinib	PP by methanol	Human plasma	30	[187]
Imatinib, its' metabolite (CGP-74588)	LLE by tertiary-butyl methyl ether followed by evaporation/reconstitution in the mobile phase	Human plasma	10	[188]
Nilotinib, imatinib, its' metabolite (CGP-74588)	SPE followed by evaporation and reconstitution in the mobile phase	Human plasma	50	[189]
Imatinib, dasatinib, and nilotinib	PP by ACN followed by SPE(C18), after elution by methanol then evaporation/reconstitution in the mobile phase	Human plasma	50	[190]

Imatinib and its metabolite (CGP74588)	LLE by hexane/ethyl acetate (30:70, v/v) then evaporation/reconstitution in the mobile phase	Human plasma	62.5	[191]
Imatinib, dasatinib	SPE (C18)	Human plasma	10	[192]
Erlotinib, gefitinib	LLE by ethyl acetate followed by evaporation/reconstitution in the mobile phase	Human plasma	20-80	[193]
Vemurafenib, erlotinib	PP by ACN followed by evaporation/reconstitution in mobile phase	Human plasma	1250-5000	[194]
Sorafenib	PP by ACN followed by LLE by ethyl acetate then evaporation/reconstitution in mobile phase	Human plasma	500	[195]
Bosutinib, pazopanib, dasatinib	LLE by 1-chlorbutane followed by evaporation/reconstitution in the mobile phase	Human plasma	20	[196]
Lapatinib	PP by ACN followed by evaporation/reconstitution in mobile phase	Human plasma	200	[197]
Sorafenib	LLE by diethyl ether followed by evaporation/reconstitution in the mobile phase	Human plasma	100	[198]
Lapatinib, erlotinib	PP by ACN followed by evaporation/reconstitution in mobile phase	Human plasma	125	[199]

Sunitinib	LLE by ethyl acetate followed by evaporation/reconstitution in mobile phase	Human plasma	20	[200]
Sunitinib, its metabolite (SU12662)	LLE by tertiary butyl methyl ether followed by evaporation/reconstitution in mobile phase	Human plasma	5.0	[201]

Most of TDM methods published recently, relied on using LC coupled to MS detection as shown in [Table 4](#). The hyphenation of LC with MS provides a valuable highly sensitive and selective analytical methodology for clinical practice [202]. The LOQ values for TKIs in most published LC-MS/MS methodologies range from 1 ng/mL to 1000 ng/mL compared to 30-5000 ng/mL for most of the LC-UV methods. However, the high selectivity of LC-MS and/or LC-MS/MS has been questioned recently especially for clinical practice such as TDM. This could be attributed to the effect observed when analyzing biological matrices (e.g. plasma, serum, etc). This effect concerned the ionization pattern of analytes themselves.

Although the high sensitivity and high selectivity of these analytical methodologies, the total analysis time was relatively long, particularly because of the necessary time dedicated to sample preparation. Besides, the high cost associated when using MS detection.

Table 4: LC-MS and LC-MS/MS methods for the quantitation of TKIs

LC-MS or LC-MS/MS				
TKIs	Extraction	Matrix	LOQ (ng/mL)	Ref
Imatinib, its' metabolite (N-desmethyl imatinib)	PP by semi-automated 96 well plate format	Human plasma	4.0	[203]
Imatinib, its' metabolite (N-desmethyl imatinib)	PP by ACN followed by evaporation/reconstitution in the mobile phase	Human plasma	30	[204]
Imatinib	PP by ACN followed by filtration of the supernatant	Human plasma	1.8	[205]
Imatinib, N-desmethylinatinib, dasatinib, nilotinib, erlotinib, gefitinib, lapatinib, sorafenib, sunitinib	PP by ACN	Human plasma or serum	< 10	[206]
Dasatinib, erlotinib, gefitinib, imatinib, lapatinib, nilotinib, sorafenib and sunitinib	PP by ACN followed by dilution of the supernatant with the mobile phase	Human plasma	20	[207]
Erlotinib, gefitinib, and imatinib	LLE by hexane/ethyl acetate followed by evaporation then, reconstitution in the mobile phase	Human plasma	5.0	[208]
Imatinib, its metabolite (N-desmethyl imatinib), nilotinib, lapatinib, erlotinib, sorafenib,	SPE	Human plasma	10	[209]

dasatinib, axitinib, gefitinib and sunitinib				
Imatinib, its metabolite (N-desmethyl imatinib), sunitinib, its metabolite (N-desethyl sunitinib), nilotinib, dasatinib, pazopanib and regorafenib	PP by methanol then dilution of the supernatant with water	Human plasma	100	[210]
Imatinib, nilotinib, dasatinib, sunitinib, sorafenib and lapatinib	PP by ACN	Human plasma	1.0	[211]
Imatinib, nilotinib and dasatinib	LLE by 0.1% formic acid in methanol	Dried blood spot	50	[212]
Erlotinib , its metabolite (O-desmethyl erlotinib)	LLE by hexane/ethyl acetate	Human plasma	10	[213]
Sorafenib, its active metabolite (sorafenib N-oxide)	PP by ACN/methanol	Human plasma	50	[214]
Regorafenib, sorafenib	PP by ACN followed by dilution with the mobile phase	Human plasma	50-80	[215]
Sorafenib	PP by ACN	Human plasma	7.3	[216]
Lapatinib	SPE	Human plasma	15	[217]
Lapatinib	LLE by methyl-tertiary butyl ether	Human plasma	5.0	[218]
Dasatinib and lapatinib	LLE by methyl-tertiary butyl ether:ACN (3:1, v/v):1.0 M ammonium formate (pH 3.5) (8:1, v/v) mixture	Cell samples	15-31 pg	[219]
Imatinib, dasatinib, ibrutinib, ponatinib, trametinib, sunitinib, cobimetinib, dabrafenib, erlotinib,	PP by ACN	Human plasma	0.75-250	[220]

lapatinib, nilotinib, bosutinib, sorafenib, and vemurafenib				
Dasatinib, imatinib	LLE by butyl acetate/butanol	Human plasma	3.0	[221]
Imatinib, dasatinib, nilotinib	LLE by methanol/water (70:30, v/v)	Peripheral blood mononuclear cell (PBMC)	5.0	[222]
Nilotinib	PP by ACN followed by evaporation/reconstitution in the mobile phase	Human serum and human serum	5.0	[223]
Imatinib, sorafenib, tofacitinib, afatinib, cabozantinib	LLE by diethyl ether followed by evaporation/reconstitution in mobile phase	Human plasma	2.5-5.0	[224]
Afatinib, axitinib, bosutinib, crizotinib, dabrafenib, dasatinib, erlotinib, gefitinib, imatinib, lapatinib, nilotinib, ponatinib, regorafenib, regorafenib M2, regorafenib M5, ruxolitinib, sorafenib, sunitinib, vandetanib	SPE (microelution 96-well plates)	Human plasma	0.1-25	[225]
Dasatinib, erlotinib, gefitinib, imatinib, lapatinib, nilotinib, pazopanib, sorafenib, sunitinib, and vemurafenib, N-desethyl sunitinib	PP by ACN	Human plasma	5-500	[226]
Afatinib, axitinib, dabrafenib, dasatinib, erlotinib, gefitinib, ibrutinib, imatinib, lapatinib, nilotinib, pazopanib, ruxolitinib,	PP by 1.0% formic acid in methanol	Human plasma	5-50	[227]

sorafenib, sunitinib, vandetanib and vemurafenib				
Imatinib, its' metabolite (CGP74588)	PP by methanol followed by evaporation/reconstitution in the mobile phase	Human plasma	20	[228]
Vandetanib	PP by ACN	Human plasma, rat liver microsomes	7.52	[229]
Erlotinib, its' metabolite (didesmethyl erlotinib)	PP by methanol	Human plasma	25	[230]
Erlotinib	Incubation in methanol for 18 h followed by evaporation/reconstitution in ammonium carbonate	Human scalp hair	0.4 ng/mg hair	[231]
Sunitinib	PP by ACN followed by evaporation/reconstitution in ammonium formate	Human plasma Cancer cells	0.1	[232]
Pazopanib	PP by methanol	Human plasma	1000	[233]
Dabrafenib, trametinib, vemurafenib, cobimetinib, pazopanib, regorafenib, regorafenib N-oxide, N-desmethyl- regorafenib-N-oxide	PP by methanol	Human plasma	1.0-200	[234]

4. Our project

According to all the above context, this work developed in this PhD consisted of studying the contribution of CE, more specifically capillary zone electrophoresis (CZE), as an analytical technique for patients treated by TKIs. The objective is to develop generic analytical methodologies using CE that can be used for the TDM of different TKIs.

Indeed, CE which is a separation technique based on physicochemical principles orthogonal to HPLC, could help to resolve some issues mentioned previously in the TDM of TKIs. On the other hand, CE is a miniaturized technique that only requires small volumes of samples and solvents which represents a very important parameter in terms of cost and environmental benignity.

The treatment of the biological sample (i.e. human plasma) has been thoroughly studied in this work, this step being a major source of errors and usually time-consuming as previously mentioned. Our focus was concentrated on new techniques for sample pretreatment, which are faster and easily automated compared to traditional LLE or SPE. The detection of TKIs was performed by UV detection. Although the lower sensitivity than MS, UV detection is well adapted to plasma concentrations of TKIs and has the advantages of being simpler to operate and also much less expensive compared to MS.

Four important medications in the management of patients, imatinib (Gleevec®), sorafenib (Nexavar®), erlotinib (Tarceva®) and lapatinib (Tyverb®) were studied. Imatinib for example was the first TKIs and is used till now for the treatment of CML. In turn, erlotinib is one of the basic molecules in the treatment of lung cancer (NSCLC). Lapatinib is used in the advanced phase of breast cancer. Sorafenib is one of the basic molecules in the treatment of liver cancer. At final, this work should demonstrate the potential of CE in as an alternative/complementary technique to LC for the TDM of TKIs. This work was carried out in collaboration with the institute of cancer in Montpellier (ICM) with Dr. Laurent Philibert. In the following points, we will discuss the protocol used in the ICM for the extraction of TKIs, physicochemical properties of the four selected TKIs, their therapeutic use in details including their doses and their side effects.

4.1. Protocol used for the TDM of TKIs at the ICM

The protocol used at the ICM for the extraction of TKIs from patients' plasma consisted of more than 12 steps as shown in Fig. 11. These steps start with the addition of an internal standard (glafenine) then, passing the sample through several sample pretreatment steps including alkalization with NaOH, mixing,

evaporation, reconstitution with the mobile phase, until finally injecting the reconstituted solution to HPLC coupled to UV detection. Although the high sensitivity and high selectivity of this analytical methodology, it takes a total analysis time of more than 1 hour per sample. This doesn't allow the doctor or general practitioner to take a decision concerning the dose of TKIs during the time of medical consultation with the patient. Moreover, this could adversely affect patients' quality of life in terms of having frequently to go to the hospital to finish his/her consultation and to have the correct dose of TKIs. These constraints besides, the adverse effects associated with TKIs therapy, contribute to emotional distress among cancer patients.

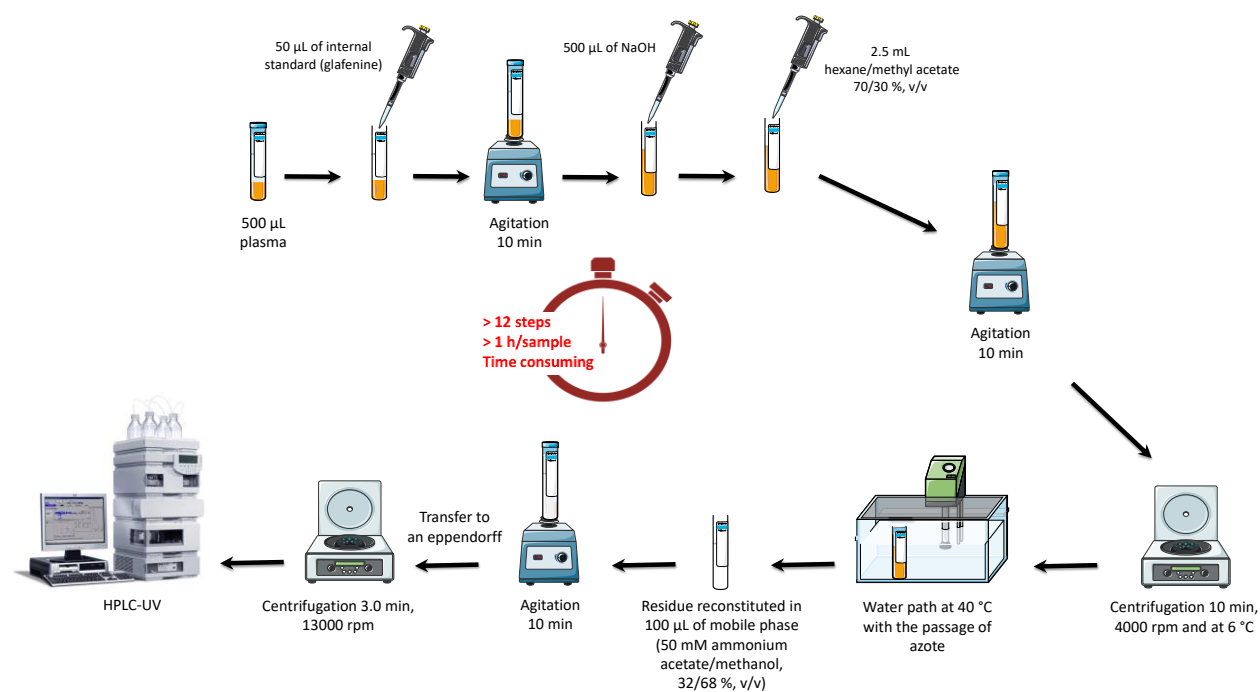


Figure 11: Protocol used at the ICM for the extraction of TKIs

4.2. Selected TKIs for our project

As mentioned before, imatinib mesylate, lapatinib ditosylate, erlotinib hydrochloride and sorafenib were chosen for our project. Imatinib is a 2-amino-4-pyrido-pyrimidine derivative that was the first FDA-approved TKIs for the first-line treatment of CML, GIST, dermatofibrosarcoma protuberans, myelodysplastic/myeloproliferative diseases with PDGFR gene-rearrangements, chronic eosinophilia leukemias, hypereosinophilic syndrome, and as a second-line treatment for aggressive systemic mastocytosis and ALL [92,119,121–123]. The standard dose of imatinib for the treatment of CML and GIST is 400 mg/day [235,236] based on body surface area calculations. The effective plasma threshold for trough imatinib levels (C_{\min}) was demonstrated to be around 1000 to 1110 ng/mL [235]. The adverse

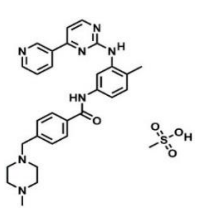
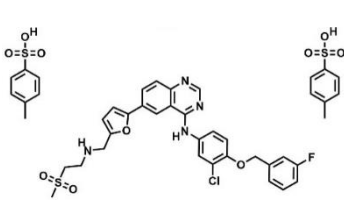
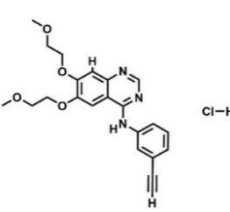
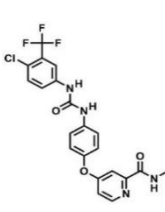
effects associated with imatinib use are variable from a patient to another. Some patients may experience rashes, others suffer from infraorbital edema. Other more serious effects include bone pain, optic effects, sensorineural hearing loss and impaired cardiac function (especially in elderly patients or patients treated on long term) [237]. Imatinib bioavailability is about 98%. Its $t_{1/2}$ is about 20 hours, it could be administered once daily [238]. Imatinib is metabolized by the cytochrome P450 specifically, the isoenzyme CYP3A4. N-desmethyl metabolite (CGP74588), which is the primary imatinib metabolite, has the same biological properties and represents 20% of imatinib plasma levels in patients treated with this drug [239]. For this reason, most of the above-mentioned methodologies dose imatinib with its metabolite.

On the other hand, erlotinib is an anilino-quinazoline derivative which is an effective EGFR antagonist that is used in the treatment of NSCLC and pancreatic cancer [107,108]. Rash, diarrhea, nausea, vomiting and fatigue are all associated adverse effects with erlotinib based on its dose. The approved daily dose of erlotinib (150 mg) and C_{min} was demonstrated to be 1200 ng/mL [240,241]. Erlotinib is metabolized by CYP3A4, CYP1A2, and CYP3A5. In clinical studies trough plasma concentrations of erlotinib and its metabolite O-desmethyl erlotinib seemed to correlate with treatment success and appearance of adverse effects [242,243]. For this reason, it is important to dose erlotinib with its metabolite [213].

Sorafenib is a pyridine-2-carboxamide derivative that is used in the treatment of RCC, HCC, and differentiated thyroid cancers [140–142]. The standard dose of sorafenib for the treatment of CML and HCC is 400-800 mg/day [244]. Most of sorafenib adverse effects are considered mild to moderate and manageable to varying degrees including diarrhea, fatigue, hand-foot skin reaction and hypertension however, cardiovascular events in some patients might lead to death [245]. The main circulating metabolite of sorafenib in the plasma is sorafenib N-oxide and it is produced through oxidation of sorafenib by CYP3A4 with similar activity to sorafenib [246]. So, it is important also to quantify both sorafenib and its metabolite [214].

Finally, lapatinib is an anilino-quinazoline derivative like erlotinib which, is used in the treatment of EGFR/HER2-positive breast cancer [124]. The recommended dose of lapatinib is 1250 mg once daily [247]. The plasma level of lapatinib for the was 1740 ng/ml [248]. The most common side effects associated with lapatinib use are diarrhea and rash, which are mostly mild to moderate in severity. Cardiac toxicity is rarely seen with lapatinib [249]. Lapatinib is extensively metabolized by cytochrome P450 to yield an O-debenzylated metabolite, which can undergo further oxidation to a reactive quinone imine which has a hepatotoxicity [250]. The structures of the four TKIs and their physicochemical properties including pKa, solubility, molecular weight and their active metabolites are given in [Table 5](#).

Table 5: Chemical structures, physicochemical properties and trade names of the selected TKIs

	Imatinib mesylate	Lapatinib ditosylate	Erlotinib hydrochloride	Sorafenib
Structure				
Trade name	Gleevec®	Tykerb®	Tarceva®	NEXAVAR®
IUPAC name	Methane sulfonic acid;4-[[4-methylpiperazin-1-yl)methyl]-N-[4-methyl-3-[(4-pyridin-3-yl)pyrimidin-2-yl)amino]phenyl]benzamide	<i>N</i> -[3-chloro-4-[(3-fluorophenyl)methoxy]phenyl]-6-[5-[(2-methyl sulfonyl ethylamino)methyl]furan-2-yl]quinazolin-4-amine;4-methylbenzenesulfonic acid	<i>N</i> -(3-ethynylphenyl)-6,7-bis(2-methoxyethoxy)quinazolin-4-amine	4-[4-[[4-chloro-3-(trifluoromethyl)phenyl]carbamoylamino]phenoxy]- <i>N</i> -methylpyridin-2-carboxamide
Molecular weight (g/mol)	493.6	925.5	393.4	464.8
Solubility	Soluble in water, soluble to very soluble in dimethyl sulfoxide (DMSO),	soluble in dimethyl sulfoxide (DMSO), sparingly soluble in water	Very slightly soluble in water, soluble in dimethyl sulfoxide	Insoluble in water, soluble in dimethyl

	methanol, and ethanol		(DMSO), methanol, and ethanol	sulfoxide (DMSO), methanol, and ethanol
Metabolites	N-desmethyl imatinib (CGP 74588) [251]	O-debenzylated metabolite, which can undergo further oxidation to a reactive quinone imine [250]	O-demethylation of the side chains and conjugation of the oxidative metabolites with glucuronic acid (M3, M8, and M18) and sulfuric acid (M9) [252]	Sorafenib N-oxide [214]
pKa	8.07, 3.73, 2.56, 1.52	7.2	2.66	5.18

From this table, we could conclude that the four selected TKIs are basic in nature according to their pKa, sparingly soluble to insoluble in water except for imatinib and they have all active metabolites.

In the following two main points, we will discuss sample preparation techniques as a main objective of this project is to simplify the sample preparation protocol of TKIs. In addition, CE technique in general will be discussed including general theory, different modes, etc. Finally, the application of CE in clinical practice, more specifically in TDM.

5. Sample preparation

Sample preparation is a crucial step in analytical chemistry, especially when dealing with complicated matrices encountered in biological samples. The complexity of biological samples (e.g. blood, plasma, serum, saliva, urine, feces, etc) is due to the presence of many endogenous compounds (e.g. proteins, salts, etc) that could adversely affect the analytical performance of the analytical method (specificity, repeatability, recovery, etc) and the quality of results obtained. Besides, the need to enrich analytes of interest which may be found in trace amount in biological matrices. There might be several steps in the sample preparation protocol itself such as extraction (e.g. SPE, LLE), filtration, dilution, evaporation,

reconstitution, etc). These steps depend on the complexity of the sample itself and the requirements of the technique used for analysis [253].

In the next lines, different extraction techniques will be discussed and their application in biological matrices. Protein precipitation (PP), liquid-liquid extraction (LLE) and solid phase extraction (SPE) are extensively used for the treatment of biological samples such as plasma [254].

5.1. Protein precipitation (PP)

PP is a fast and simple method of sample preparation that consists of adding either a water-miscible organic solvent (e.g. acetonitrile (ACN)), an inorganic acid (e.g. trichloroacetic acid, 10%), metal ions (e.g. zinc sulphate) or even salts (e.g. ammonium chloride) to the biological matrix (usually in a 3:1 or 4:1 ratio, v/v). After addition, centrifugation or filtration are operated to remove precipitated proteins [255,256]. Polson C. [255] assumed that ACN and zinc sulphate are the most efficient agent in terms of PP from human plasma with a protein precipitation efficiency (%) between 96.8 to 99.9 and 88.7 to 94.6% respectively.

PP is commonly used for fast sample clean-up and disrupting protein–drug binding. However, disadvantages of PP are also encountered. These disadvantages include: 1/the dilution of the sample (usually by a factor of four or five) and 2/ lack of selectivity due to matrix components which are not completely removed that may cause interferences with the analytical results obtained [256]. PP has been extensively used in the case of TKIs (tables 3 and 4). The fact that TKIs have a high binding affinity to biological proteins makes sense to use PP [257]. For example, erlotinib was found to be extensively bounded to plasma proteins (about 95%) [258]. Sorafenib was also highly bounded to protein with a higher affinity towards albumin [259]. It is therefore necessary to disrupt the protein–TKIs binding to be able to quantify the total amount of TKIs present in plasma samples. Nearly 52% of techniques mentioned in table 3 and 4, were based on PP. ACN is the most used protein precipitant due to its PP efficiency and compatibility with different analytical techniques. The supernatant is then either directly analyzed [199,203,205–207,210,214–216,226,229,260] or evaporation/reconstitution/dilution steps are needed to make the extract compatible with HPLC [194,195,197,204,213,223,232]. In some cases, PP is followed by LLE or SPE in order to achieve higher enrichment and cleaner extract [195,222].

5.2. Liquid-liquid extraction (LLE)

LLE is a separation process which deals with the transfer of a solute from one solvent to another. The two solvents are immiscible. Frequently, one of the solvents is water or an aqueous mixture and the other is

a non-polar organic liquid. LLE comprises a step of mixing followed by a step of phase separation. It is important to consider both steps in the selection of solvents and modes of operation [261].

Usually, the extract (organic phase) obtained by LLE is evaporated to dryness and the residue is reconstituted in a small volume of a suitable solvent i.e. mobile phase in case of LC to ensure higher enrichment [208,224]. The volume of reconstitution solvent is normally in the range 50 to 500 μ L to avoid dilution of the sample. Thus, when the amount of sample is limited to, e.g., 1 mL, the maximum enrichment factor (EF) obtained is in the range 2–20x (with 100% extraction efficiency) [262]. This is frequently the case with biological samples (especially for plasma), whereas substantially higher analyte enrichments (>20) may be obtained in cases where large sample volumes are available (e.g. urine sample for example). Some drawbacks are listed concerning the use of LLE such as: 1/ the need to use large volume of high purity expensive organic solvents which are non-friendly to the environment, 2/ the difficulty of handling with large sample volume, 3/ the low selectivity and sometimes 4/ the low enrichment factor of analytes obtained which requires further optimization of the preparation protocol.

Although these drawbacks, LLE is still considered as an attractive technique in bioanalysis. It has been widely used for the preparation of biological samples as they are aqueous in nature [263–266]. LLE was used for the extraction of both acidic and basic drugs from biological samples [263,267,268]. For example, D. Remane [263] has developed a simple extraction procedure for establishing a LC-MS/MS method for quantification of 136 analytes from different drug classes in human plasma. Many published works were based on using LLE then, injecting the extract to LC coupled to MS detection. Other examples dealt with the use of LC coupled to UV detection. R.L. Oostendorp developed a LC-UV method for the determination of imatinib mesylate and its main metabolite in human plasma [188]. Plasma samples spiked with imatinib and its metabolite was treated with tert-butyl methylether. Then, the organic phase was evaporated/reconstituted in the mobile phase prior to analysis. Also, many other examples concerning the use of LC coupled to UV or MS detection for the determination of TKIs are mentioned in [table 3](#) and [4, part 3.1](#). Nearly 32% of the extraction methods mentioned in both tables, are based on LLE with methyl tertiary butyl ether or hexane/ethyl acetate or diethyl ether solvents as the extracting solvents [218,219].

Salting-out assisted liquid–liquid extraction (SALLE) is another type of LLE. SALLE is based on adding salt (e.g. NaCl) into a sample solution composed of a miscible mixture of water and an organic solvent (such as ACN or acetone). The presence of a high concentration of salt induces a two phases separation (upper mostly organic phase from lower bulk aqueous phase) [262] as shown in [Fig. 12](#).

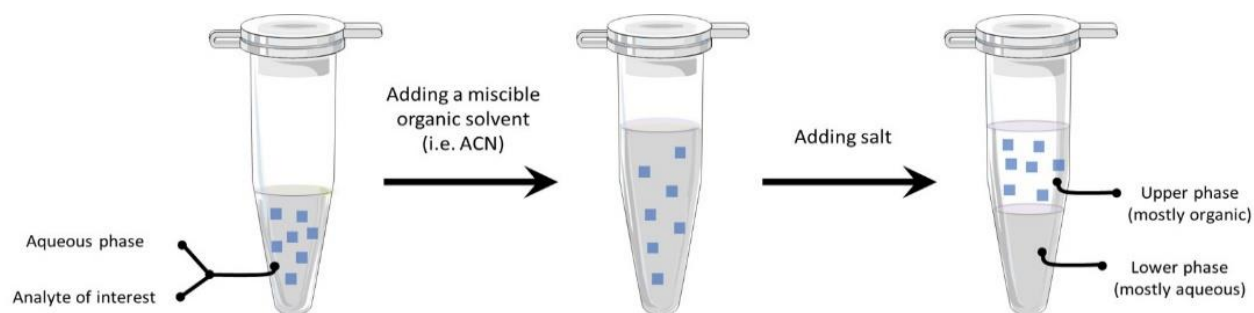


Figure 12: SALLE concept

SALLE appears to be well suited for the determination of drugs in biological samples as it allows deproteinization and extraction of analytes in the same procedure. Some applications of SALLE coupled to chromatographic systems were developed for the determination of molecules of interest in environmental and biological samples [269,270]. D. Liu [269] developed an SALLE procedure to treat plasma samples that were further analyzed using LC-MS to quantify intact oxytocin in human and rat plasmas. Isopropanol was used as the organic solvent protein precipitant and potassium hydrogen phosphate as the salting out agent. A. Gure [270] proposed SALLE for the extraction of residues of nine sulfonylurea herbicides in environmental water and banana juice samples.

5.3. Solid phase extraction (SPE)

SPE is a sample pretreatment technique in which analytes are dissolved or suspended in a liquid and are further separated according to their affinity to a solid matrix usually called sorbent (or stationary phase). SPE is not only used to remove the matrix interferences but, also to achieve a concentration of the analytes of interest. The sorbent used in SPE is usually filled in a packed syringe-shaped cartridge, but other forms come such as flat disks and μ SPE are also used. The nature and amount of the sorbent, loaded sample volume (with enough recovery), composition and volume of the washing and elution solutions (without loss of the analytes) are the effective parameters in SPE performance [271,272]. There are many types of SPE including normal phase SPE [271–273], reversed phase SPE [274], or ion exchange SPE. As shown in table 3 and 4, part 3.1, SPE was used for the extraction of TKIs from human plasma. A. Davies [189] used a cyanopropyl bonded phase cartridge to remove the contaminating plasma proteins and to extract TKIs prior to analysis by LC-MS/MS. M. Miura [192] on the other hand, used an Oasis hydrophilic lipophilic balance (HLB) extraction cartridge to extract imatinib from plasma. This was followed by an evaporation of the eluate and reconstitution in the mobile phase prior to analysis by LC-UV.

The advantages of SPE include good analyte recovery, adequate selectivity, reduced use of organic solvents, and easy automation [275]. Besides, the diverse use of SPE for different objectives which include purification [276], trace enrichment [277] and desalting [278]. Disadvantages of SPE include the relatively high cost of cartridges and the need to switch from one mode to another depending on the nature of the analyte of interest. In addition, biological samples such as plasma and blood can adversely affect the sorbent physical properties after handling few samples.

5.4. Dispersive solid-phase extraction (d-SPE)

Dispersive solid phase extraction (d-SPE) is based on the addition of a solid sorbent, usually silica or polymer based, directly into the sample solution [279,280]. The dispersion process increases the contact area between the sorbent and the analyte. The sorbents are chemically modified to modulate their affinities towards the analytes. These modifications ensure the selectivity for the analytes of interest, which allows the maximal retention, minimizing the interferences in the analytical matrix [279]. After the dispersion, the sorbent is isolated by a centrifugation or a filtration process. The analytes or interferences adsorbed on the surface of the sorbent can be easily eluted or eliminated with the addition of adequate organic solvents as shown in [Fig. 13](#).

The applications of d-SPE include clinical [281,282] and environmental applications [283,284]. One of the clinical applications include the work of M.A. Farajzadeh [281] who developed a d-SPE of atorvastatin, iosartan, and valsartan from human plasma followed by analysis by LC-UV.

The advantages of d-SPE are simplicity, longer time of contact, larger surface area and lower cost compared to conventional SPE [285]. Disadvantages are longer extraction procedure with the need of centrifugation or filtration step.

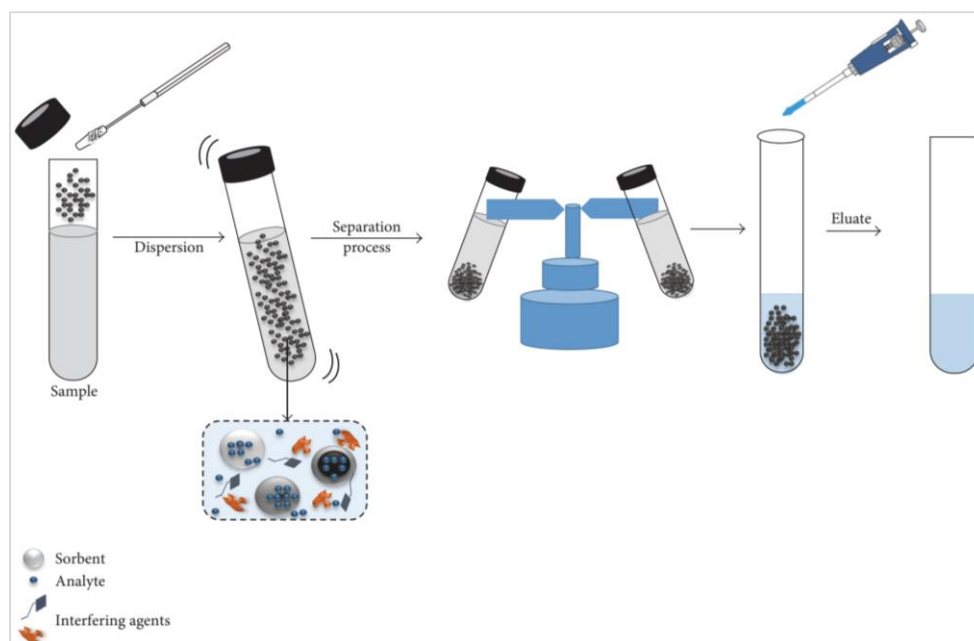


Figure 13: Schema of dispersion methodology by dispersive solid phase extraction.

5.5. QuEChERS

QuEChERS, another recent technique of extraction, introduced first by M. Anastassiades in 2003 [286] for the determination of pesticides. The acronym QuEChERS stands for quick, easy, cheap, effective, rugged and safe. This technique involves microscale extraction using ACN and dispersive solid-phase extraction (d-SPE) by using a salt. The idea is based on the dispersion of salts to extract, clean-up and isolate analytes of interest from very complex matrices. This effective and easy preparation approach involves two steps: 1/ an extraction step based on partitioning via salting-out extraction where an equilibrium between an aqueous and an organic layer (ACN or methanol) is promoted, 2/ a d-SPE step that involves further clean-up using several combinations of porous sorbents and salts to remove matrix interfering substances. This latter step requires a smaller amount of extract and sorbent, and permits to avoid additional centrifugation, filtration and/or precipitation. QuEChERS were used in many fields including environmental, food and clinical analysis. Some of the commercially available kits of QuEChERS are shown in Fig. 14.



Figure 14: Commercially available Quechers kits

In clinical analysis, J.L. Westland [287] used QuEChERS for the extraction of benzodiazepines in human urine. S. Mizuno [288] developed a determination method of valproate in human samples by QuEChERS extraction salt (400 mg of MgSO_4 and 100 mg of sodium acetate) then, adding 1.0 ml of ACN. The mixture was vigorously mixed then, centrifuged at 2000 g for 10 min. The supernatant was treated with d-SPE kit (containing 150 mg of magnesium sulfate (MgSO_4) and 50 mg of octadecylsilyl silica gel, C18) for sample cleanup followed by GC-MS/MS analysis. QuEChERS were also used for the extraction of lipids from plasma and urine for LC-MS analysis [289].

5.6. Microextraction techniques

In recent years, microextraction techniques were developed to address the need for a reduction in the use of organic solvents (environmentally friendly procedures), and sample. These techniques are also developed to explore and to facilitate sample preparation in a rapid and a convenient way inside the laboratory or for on-site applications [290]. They were used in many applications in different fields including environmental, pharmaceutical, clinical and forensic analysis.

Microextraction techniques are classified into liquid phase microextraction (LPME) and solid phase microextraction (SPME) [291]. The extraction phase should always represent the same proportion of analyte from a sample, taking into account that the sample volume in micro extraction is not limited [290].

LPME method is a sample pretreatment technique that uses small volumes of organic solvents to extract a wide variety of analytes from different matrices. The development of these techniques focuses on

providing simple, inexpensive, and environmentally friendly extraction procedures for sample preparation or pretreatment [292].

On the other hand, SPME is based on the sorption of analytes directly from the aqueous or gaseous samples, or in headspace vials by a thin film of an extracting phase immobilized over the surface of a sorbent-coated silica fiber. It combines sampling, analyte isolation, and enrichment into one single step. The extracts can be then thermally desorbed by inserting into a GC system, or using small amounts of organic solvents for injection into a LC-MS. The biggest advantage of SPME is the reduction of time and solvent, and the combination of the whole extraction process in one step [293].

Nowadays, there are several microextraction techniques formats available as shown in Fig. 15. At the left, LPME is classified into single-drop and membrane-assisted microextractions variants. On the right, SPME can be classified according to the diffusion process into diffusion by stirring and diffusion by flow through. In the next lines, some examples of SPME and LPME will be discussed.

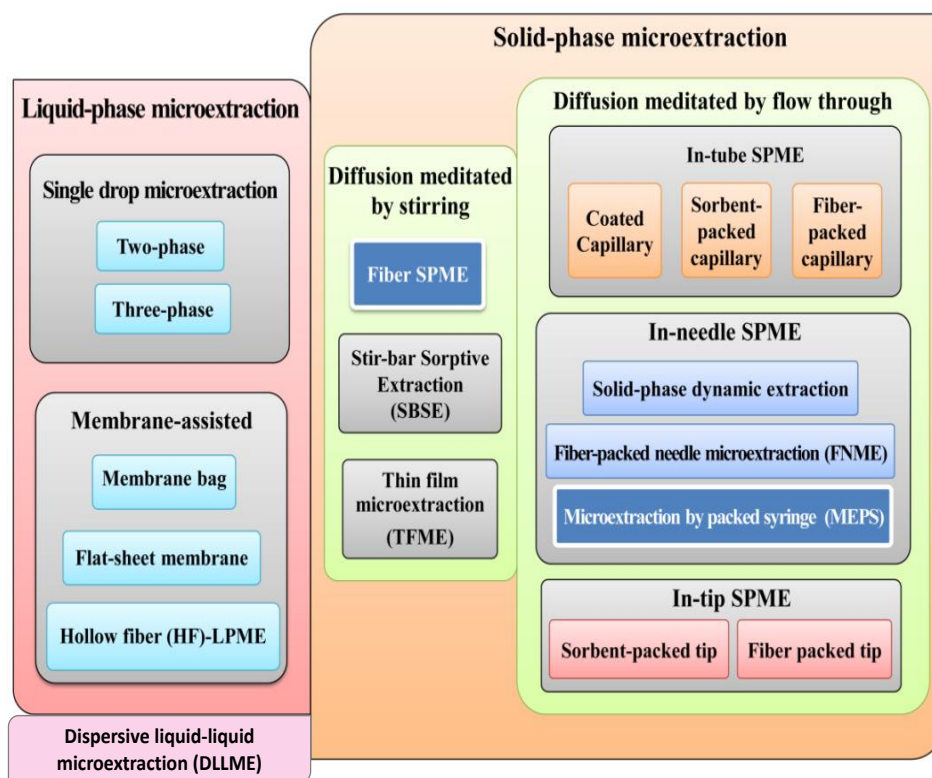


Figure 15: Classification of different microextraction techniques [291]. LPME: liquid phase microextraction, SPME: solid phase microextraction, SDME: single drop microextraction, FNME: fiber-packed needle microextraction, MEPS: microextraction by packed syringe, HF-LPME: hollow fiber liquid phase microextraction, DLLME: dispersive liquid-liquid microextraction.

5.4.1 Single drop microextraction (SDME)

Single drop microextraction (SDME) which is a type of LPME, where a drop of extracting solvent is suspended into the sample (or in the headspace above the sample) from the tip of a rod (often made of polytetrafluoroethylene, (PTFE)) or a syringe needle. Extraction from the sample occurs under equilibrium [294,295] into two phases (drop phase and sample phase) or three phases (drop phase, sample phase and organic phase) [296] (Fig. 16). Extraction occurs by flowing of the sample to the solvent drop. L. Dong [297] developed GC-MS method for the determination of Z-ligustilide in plasma following headspace SDME. The same author also developed a GC-MS following headspace SDME and simultaneous derivatization for fast determination of the diabetes biomarker, acetone in human blood samples [298]. Some drawbacks are also encountered such as impermanence of the drop generated and lack of sensitivity and precision [299].

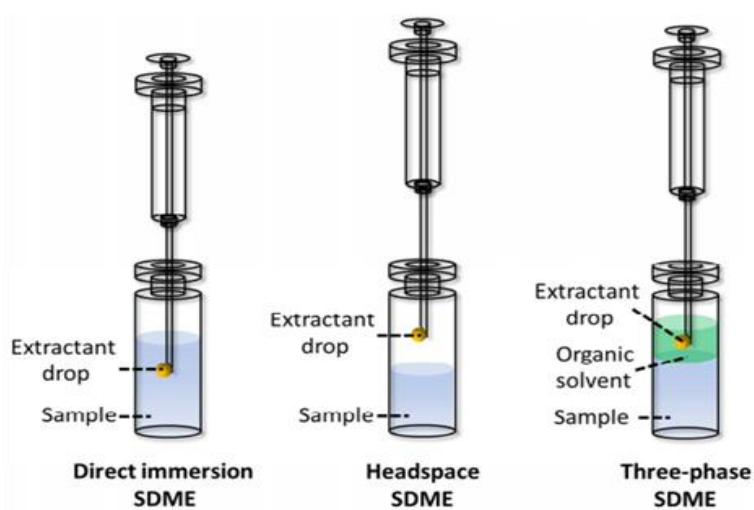


Figure 16: Various modes of SDME including direct immersion SDME, headspace SDME and three-phase SDME [296].

5.4.2 Membrane assisted extraction

Membrane assisted extraction is when the sample and extracting solvent are separated by a porous membrane. The membrane is typically hydrophobic polymeric materials that come in the form of a flat membrane (Fig. 17.A) [300] or are filled with extracting solvent and are typically assembled using a hollow fiber (Fig. 17.B) [301]. These extractions can be either static (without using a stirrer) or dynamic (by using a stirrer). The target analyte is isolated from the aqueous solution and dispersed into the organic solvent impregnated in the wall pores supported liquid membrane (SLM) in the hollow fiber. Subsequently, the

analyte is then transferred into the organic solvent (acceptor phase). M. Hadjmohammadi [302] developed a hollow fiber LPME of warfarin from human plasma followed by analysis LC-UV. Also, some drawbacks are encountered such as long extraction time needed besides the possibility of the fiber pores to get blocked.

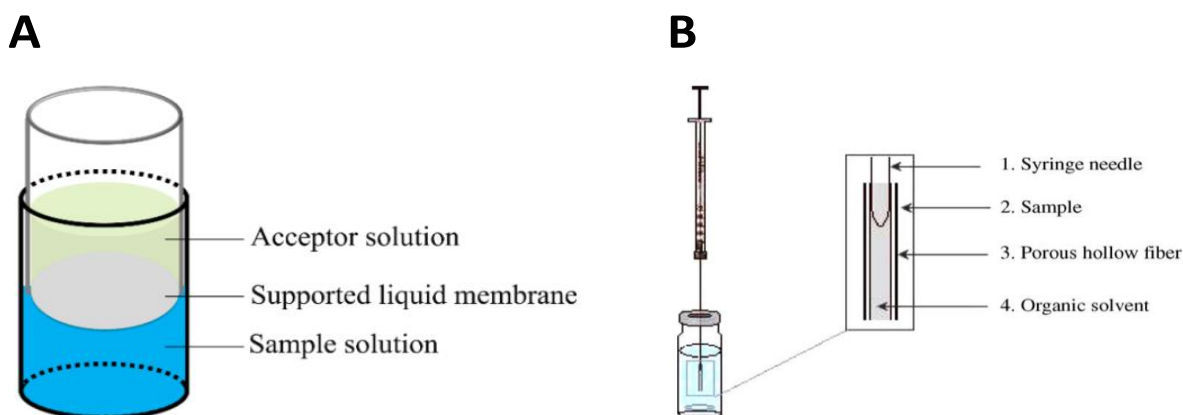


Figure 17: (A) Schematic representation of flat membrane-based liquid-phase microextraction [300]. (B) Schematic representation of HF-LPME system [301].

5.4.3 Dispersive liquid-liquid microextraction (DLLME)

Another type of LPME is dispersive liquid-liquid microextraction (DLLME) where the extraction of analytes takes place by dispersion of the extracting solvent in water containing analytes. Dispersion is achieved by using a second dispersing solvent. The extraction process involves two steps: 1/ the mixture of extracting and dispersing solvents is rapidly injected to a water sample. A dispersion is formed which facilitates fast extraction of analytes from the water sample. 2/ the dispersion is removed by centrifugation and the extracting solvent containing analytes is taken for analysis with a microsyringe (Fig. 18) [303]. Several requirements are needed to achieve DLLME [303]. The dispersing solvent has to be fully soluble with the water phase such as ACN. The extracting solvent must have the potential for extracting analytes with sufficient solubility in the dispersing solvent. In addition, its solubility in water has to be very low. Moreover, the density of the extracting solvent has to have a significant difference from the density of water to enable phase separation. DLLME has been successfully applied to the extraction and concentration of a wide variety of organic compounds [304] and metal ions [305], mainly from water samples. Also, X. Shen [306] used DLLME for the preconcentration of eight parabens in real samples (plasma and urine) followed by their determination using LC-UV. Although the cheapness, rapidity and high recovery obtained when using DLLME, disadvantages were also encountered. These disadvantages

include the need to use three solvent, step of centrifugation and limited solvent choices that can fulfill the requirements of DLLME.

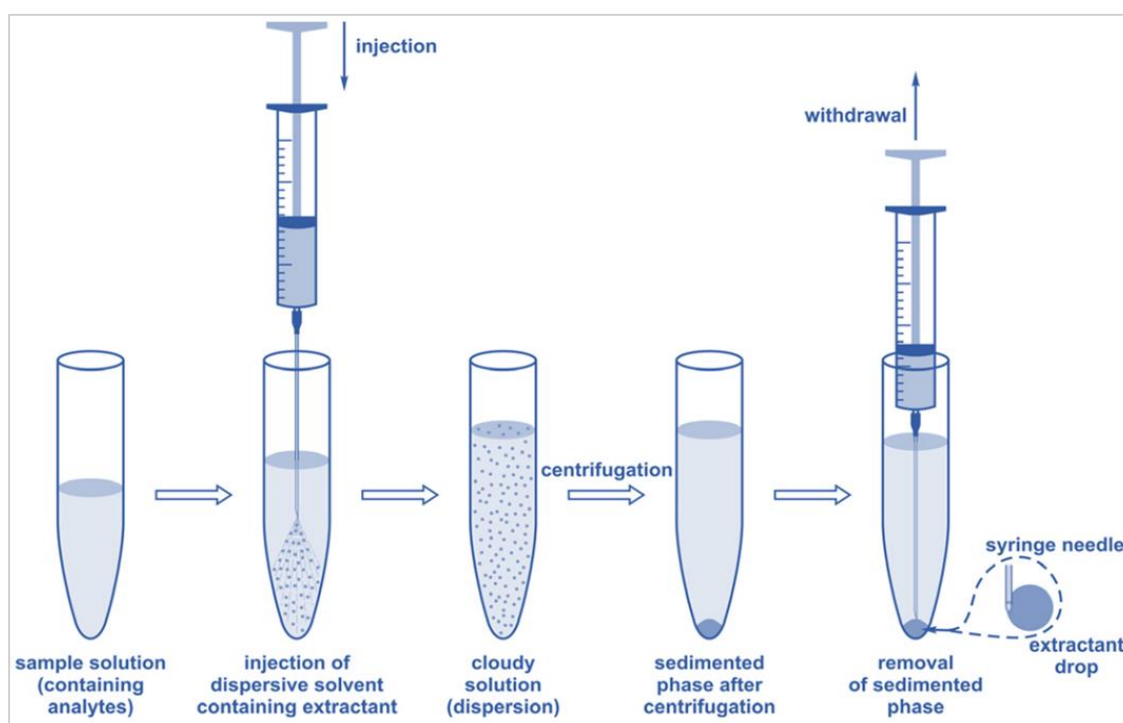


Figure 18: The DLLME procedure [303]

5.4.4 Microextraction by packed sorbent (MEPS)

MEPS is a major upgrade of SPE to a more efficient and sophisticated format. It was developed by Abdel-Rehim et al. in 2004 [307]. In MEPS, sample extraction, concentration and cleanup are performed in a single device composed of a syringe and MEPS sorbent. The sample is drawn through the syringe, the analytes are retained onto the solid phase and eluted in successive steps, allowing the purification or speciation of samples as shown in Fig. 19.

Some clinical applications of MEPS were done. R. Wietecha-Posłuszny [308] developed a MEPS for the isolation of psychotropic drugs from human serum followed by LC-UV analysis. MEPS was also successfully applied for the analysis of drugs such as antidepressants from human serum [308], immunosuppressives in whole blood [309] and cardiac drugs in human urine [310]. Also, it was used in environmental analysis for the determination of pesticides in sugarcane juice [311] and of organophosphorous pesticides from aquatic samples [312]. The advantages of MEPS are the durability of the packed sorbent which can be used more than 100 times, even when using plasma or urine sample. Besides, the reduction of the solvent

used and sample volume needed, as well as reduction in the waste production. The reduction of sample volume needed, will be beneficial in reducing the chance of infection when dealing with biological samples [291]. Nevertheless several optimization steps are needed to achieve extraction efficiency besides, the limited number of sorbents available [291].

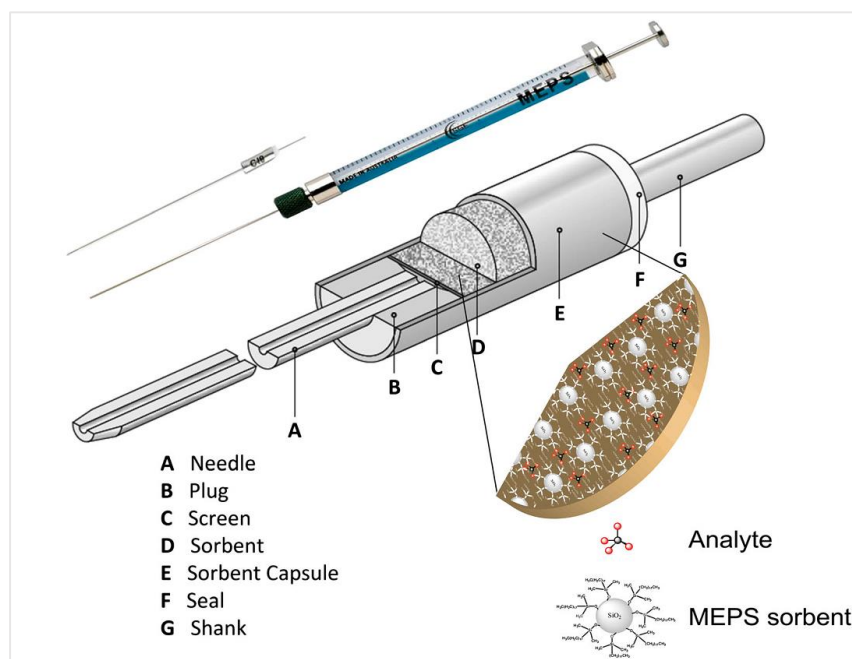


Figure 19: Schematic overview of the micro-extraction by packed sorbent (MEPS) syringe [307]

5.4.5 Stir bar sorptive extraction (SBSE)

SBSE is considered as another type of SPME based on a similar principal. It was introduced in 1999 as a solventless sample preparation method for the extraction and enrichment of organic compounds from aqueous matrices [313]. It is based on sorptive extraction where the targeted analytes are extracted into a polymer coating on a magnetic stirring rod. The partitioning coefficient of the analytes between the polymer coating and the sample matrix control the extraction and also, it is controlled by the phase ratio between the polymer coating and the sample volume [313].

Stir bars made of quartz coated with the sorbent polydimethylsiloxane (PDMS) (Fig. 20) [314] was used for the analysis of volatile and semivolatile micropollutants from aqueous samples [315]. Compared to SPME, the SBSE has more coated polymer (>50 times) with higher extraction efficiency. SBSE was applied in bioanalysis for the extraction of drugs such as central nervous system drugs [316] and antidepressants [317]. Also it was used in environmental applications including the analysis of off-flavor compounds in

water samples [318] and the determination of polybrominated diphenyl ethers in environmental matrices [319]. Some limitations are mentioned in reviews concerning SBSE. Samples with high organic matter or suspended solid components such as environmental samples, biological fluids or foods, are very difficult to extract with SBSE. Adsorption of the analytes onto the organic matter surface competes with the stir bar in the sorption [320]. Also, contamination of the sample by new pollution during the time between purification and reuse of the stirrer was also encountered [321].

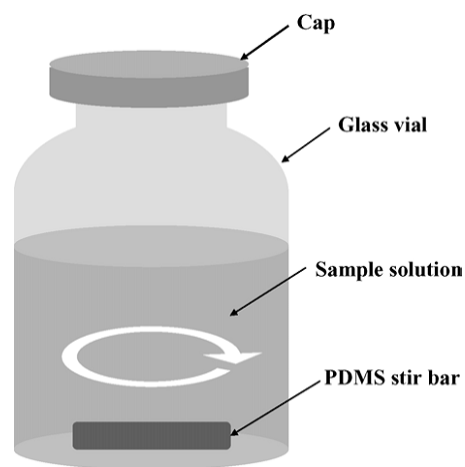


Figure 20: Schematic of SBSE [314]

5.4.6 Conclusion of sample pretreatment part:

Sample preparation is crucial in analytical chemistry. It is often labor intensive and time consuming. Biological sample pretreatment is an important part of biopharmaceutical analysis and the most troublesome aspect in the entire analytical process. There is no extraction method better than the other. The choice of suitable extraction method is based on the expected goals of the whole process including the extraction efficiency, the used analytical methodology, the nature and the property of the matrix.

In the context of our project, PP and SALLE methods were thought to be the most suitable for our project due to simplicity, cost effective and easy to apply procedures. The fact that TKIs are strongly bound to biological proteins has confined our choice since both methods use organic solvent (usually ACN).

In the next point, we will expose some principle of Capillary Electrophoresis technique that was at the heart of our developments. Applications of CE for Therapeutic Drug Monitoring are also discussed.

6. Capillary electrophoresis (CE)

6.1. Introduction to CE

CE is the combination of the powerful separation mechanisms of electrophoresis with the instrumentation and concepts of chromatography. As a separation technique, electrophoresis was first performed using a moving boundary method by Tiselius in 1937 [322]. He used a U-shaped tube filled with a buffer solution that contain the sample to be separated, with no defined boundary between the sample and the buffer solutions. This required a significant amount of sample and, more importantly, allowed complete isolation of only part of the fastest and slowest migrating components. The desire to perform electrophoresis using a defined sample zone in order to isolate individual component zones led to the concept of zone electrophoresis. He found that sample components migrated in a direction and at a rate determined by their charge and mobility. Followed to this work, in 1967, Stellan Hjertén [323], rotated millimeter capillaries along their longitudinal axis to minimize the effects of thermal diffusion and convection caused by electrical current. Later on, J.W. Jorgenson and K.D. Lukacs [324] advanced the technique by using 75 μm internal diameter (id) fused silica capillaries. They also described different parameters affecting separation quality and the potential of CE as an analytical technique. Since then, numerous reviews, books and scientific papers were published describing theory of CE and its applications in different fields. In the following lines, we will present some principle of CE technique especially concerning capillary zone electrophoresis (CZE) that was the core of our project.

6.2. CZE theory

6.2.1. Electrophoresis

As mentioned above, CZE analysis in a silica capillary is done under the application of an electrical field [325]. The velocity of an ion can then be given by equation (I.1):

$$\mathbf{v} = \mu_{\text{ep}}\mathbf{E} \quad (\text{I.1})$$

where \mathbf{v} is the ion velocity, μ_{ep} is electrophoretic mobility of ion and \mathbf{E} is the applied electric field.

The electrophoretic mobility (μ_{ep}) is a specific characteristic of the ion under given experimental conditions. The μ_{ep} of an analyte depends directly on its size and charge. In addition, the electrophoretic mobility is dependent on analysis conditions such as the pH, the ionic strength (I), composition and viscosity of the separating electrolyte. According to the above equation (I.2):

$$\mu_{\text{ep}} = \mathbf{v}/\mathbf{E} = q/6\pi\eta r \quad (\text{I.2})$$

where q is the net charge of the analyte, r is Stoke's radius and η is the buffer viscosity.

6.2.2. Electro-osmotic flow

The second fundamental factor that affects the migration of compounds is the electro-osmotic flow (EOF) [326] especially in CZE mode. This phenomenon comes from the bulk movement of the electrolyte solution through the capillary as a consequence to the surface charge on the inner capillary wall. At pH levels greater than 2.5, the silanol groups (SiOH) ionize to form anionic form (SiO⁻) according to their pKa (3-4) as shown in Fig. 21. The negative surface charges of silanol group are balanced by cations attracted from the buffer solution and built up near the surface. This forms what is called a double layer creating a potential difference very close to the wall called zeta-potential (ζ). When the voltage is applied, the cations forming the diffuse bilayer are attracted towards the cathode. Because these cations are solvated, their movement drags the bulk solution in the capillary towards the cathode forming EOF. The magnitude of EOF is expressed by electro-osmotic mobility (μ_{eo}) which is defined by the following equation (I.3):

$$\mu_{eo} = \mathbf{u}_{eo}/E = \varepsilon \zeta / 6\pi\eta \quad (I.3)$$

where ε is the dielectric constant of the buffer solution and ζ is the zeta potential.

The zeta potential is determined by the surface charge on the capillary wall. Since this charge is strongly pH dependent, the magnitude of the EOF varies with pH. At high pH, the silanol groups are deprotonated so, the EOF is higher than that at low pH.

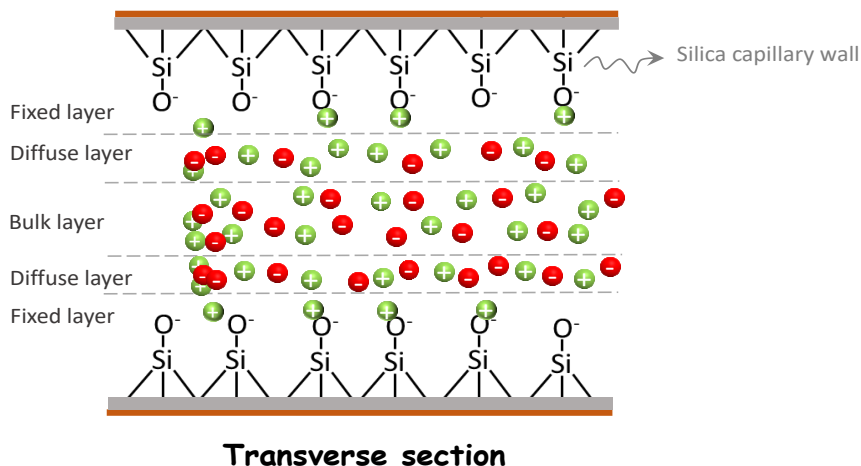


Figure 21: Schema showing electro-osmotic mobility, electrophoretic mobility and apparent mobility of cations, anions and neutral substances.

The apparent mobility μ_{app} of an ion corresponds to the algebraic sum of its electrophoretic mobility (μ_{ep}) and μ_{eo} [327]. This apparent mobility depends on the nature of the analyte (anion, cation or neutral) as shown in Fig. 22.

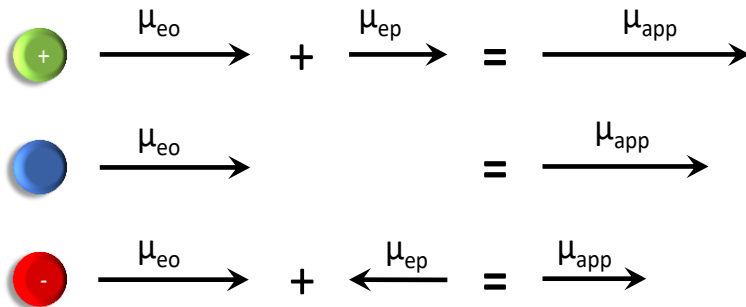


Figure 22: Schema showing electro-osmotic mobility, electrophoretic mobility and apparent mobility of cations, anions and neutral substances.

6.2.3. Factors affecting the mobility values

In the presence of EOF [328], the effective mobility (μ_{ep}), can be extracted from μ_{app} by independently measuring the EOF using a neutral marker that moves at a velocity equal to the EOF. Examples of neutral markers include dimethylsulphoxide (DMSO) and acetone. On the other hand, ζ is greatly affected by the ionic strength (I) of the separating buffer. As the I increased, the double layer is compressed and both ζ and EOF are reduced.

When the injection of the sample is done at the anodic side, the EOF is from anode to cathode. Cations will move at the same direction with the EOF so, they will move faster than neutral species and anions. Neutral compounds will be carried with EOF at the same velocity. If the μ_{ep} of anions is smaller than the EOF, they will move towards the cathode. The size of charged species will also play predominant role i.e. smaller cations move faster than larger cations while, larger anions moves faster towards the cathode than smaller anions (as shown in Fig. 23).

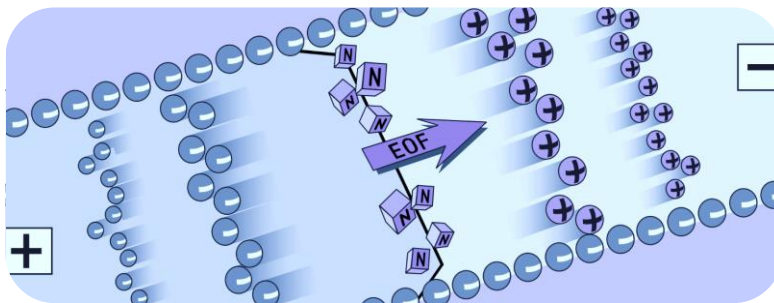


Figure 23: Differential solute migration superimposed on electro-osmotic flow in capillary zone electrophoresis [328]

6.3. Analytical parameters and CE instrumentation

6.3.1. Mobility and migration time

The time required for an ion to migrate to the point of detection is called the migration time (t). The migration time can be used to calculate the apparent solute mobility by the following equation (I.4):

$$\mu_{\text{app}} = l/tE = IL/Vt \quad (\text{I.4})$$

where V is the applied voltage, l is the effective capillary length (until the detector) and L is the total capillary length. Note that, the effective length of a capillary is length from the point of injection to the point of detection.

Generally, the CE system (Fig. 24.A) consists of vials containing both sample/electrolyte solutions, a silica capillary, two electrodes connected to a high voltage power supply and an optical detector. The power supply is used to supply up to 30 kV, which generates current levels between 200 to 300 μA . The capillary is covered outside by a polyimide coat to give rigidity to the capillary (Fig. 24.B). The capillary is filled with an appropriate buffer called back ground electrolyte (BGE) loaded from vials containing BGE. The introduction of the sample is done either hydrodynamic or electrokinetic injection.

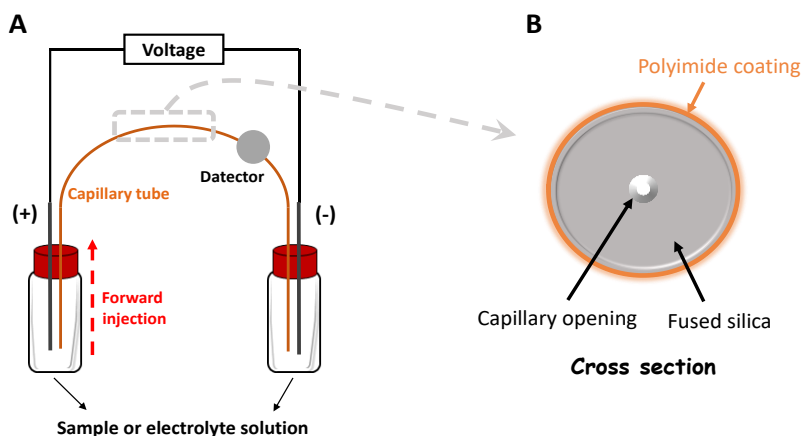


Figure 24: (A) Schematic diagram of the basic instrumentation for CE. The sample and the electrolyte solution are switched when making injections. (B) Cross section of a capillary column for capillary electrophoresis.

6.3.2. Factors affecting the separation

Separation in electrophoresis is based on differences in analyte mobility and efficiency. The difference necessary to resolve two zones is dependent on the length of the zones. Zone length is strongly dependent on dispersive processes [328].

On the other hand, the heat generated by the passage of electrical current is called joule heating which limits the benefit of increasing the electrical field [329]. Joule heating causes a temperature rise and temperature gradients in the BGE affecting the molecular diffusion, EOF and electrophoretic flow [330]. This effect is independent on capillary dimensions and efficient temperature control. The narrow-bore silica capillaries help to reduce joule heating.

In the next lines, modes of injection in CE will be discussed.

6.4. Hydrodynamic injection

Hydrodynamic sample injection is the most widely used method. It can be accomplished by application of pressure at the injection end of the capillary, vacuum at the exit end of the capillary, or by siphoning action or (hydrostatic injection) obtained by elevating the injection reservoir relative to the exit reservoir (Fig 25.A, B and C).

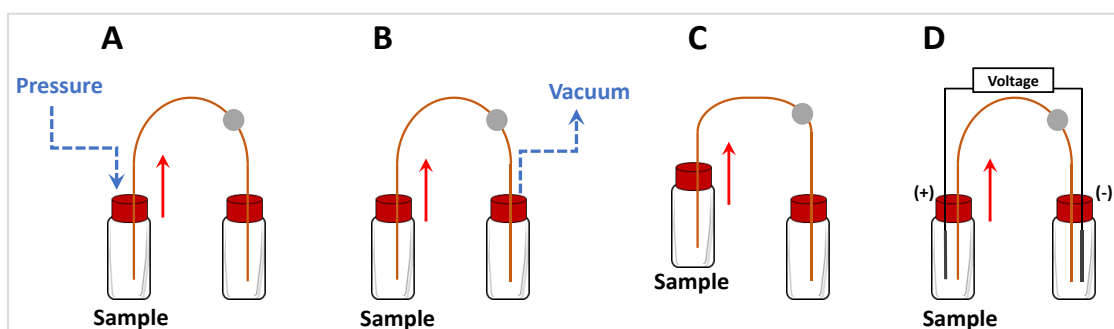


Figure 25: Methods of sample injection. (A), (B) and (C) represent hydrodynamic injection while, (D) represent electrokinetic injection. (A) hydrodynamic injection by applying pressure at the inlet. (B) hydrodynamic injection by vacuum at the outlet. (C) hydrodynamic injection by elevating the injection reservoir relative to the exit reservoir. (D) electrokinetic injection.

With hydrodynamic injection, the volume of sample loaded will be a function of the capillary dimensions, the viscosity of the buffer in the capillary, the applied pressure, and the time. This volume can be calculated by using the Hagen-Poiseuille equation (I.5):

$$\text{Volume loaded} = (\Delta P i d^4 \pi t) / 128 \eta L \quad (I.5)$$

where ΔP is the pressure difference across the capillary, $i d$ is the capillary internal diameter, t is the time of injection, η is the buffer viscosity and L is the total capillary length.

From an instrumental point of view, the reproducibility of the injection sample volume can be between 1 to 2 % RSD. Precise temperature control ($\pm 0.1^\circ\text{C}$) of the capillary is necessary to maintain constant injection volume. As with migration time, viscosity of BGE in the capillary and thus the injected quantity

varies with temperature. The sample viscosity does not significantly affect injection volume since the sample plug is only a very small volume relative to the total volume in the capillary. The later fact is true except an on-line concentration technique (e.g. stacking) was used, allowing to inject larger sample volume.

Sample injection by siphoning effect could be avoided by decreasing as much as possible the duration of the injection. Besides, the liquid levels of the sample and BGE in the CE vials should be at the same level. Siphoning effect can cause poor peak area reproducibility and even overloading of the sample. It has also been found that simply placing the capillary in a sample reservoir will cause an injection due to capillary action. This phenomenon has been called a zero-injection effect. While often insignificant, with concentrated samples, the injected amount can be quantifiable and should be considered during quantitative analysis [331].

6.5. Electrokinetic injection

Electrokinetic, or electromigration, injection is performed by replacing the injection-end reservoir with the sample vial and applying the voltage (Fig. 25.D). The driving force here is the electrical field produced by the injection voltage applied to the electrode immersed in the sample solution [332]. Usually a field strength up to 3 to 5 times lower than that used for separation is applied. Analyte enters the capillary by two forces. The first one concerns analytes migration according to their charges while, the second force is related to the pumping action of the EOF. The quantity loaded by electrokinetic injection is dependent on the electrophoretic mobility of analytes. Electrokinetic injection is discriminative. Ions of high mobility are introduced into the capillary at higher rate than ions of low mobility. The quantity injected, Q (g or moles), can be calculated according to equation (I.6):

$$Q = ((\mu_{ep} - \mu_{eo})V\pi^2rCt)/L \quad (I.6)$$

Where μ_{ep} is the electrophoretic mobility of the analyte, μ_{eo} is the EOF mobility, V is the applied voltage, r is the capillary radius, C is the analyte concentration, t is the time of injection and L is the capillary total length. So, sample loading is dependent on the EOF, sample concentration, and sample mobility. Due to these phenomena electrokinetic injection is generally not as reproducible as its hydrodynamic injection [332].

The sample volume should be optimized to avoid reduction in efficiency and resolution. It is often recommended to use sample volumes that are less than 1 to 2 % of the total capillary volume to avoid sample zone dispersion.

6.6. Capillary zone electrophoresis (CZE) and other modes

Among different modes of CE, the most widely used mode is CZE due to its simplicity, easy to apply and its diverse high expediency for many practical applications [333]. Separation in CZE is based on differences in the electrophoretic mobilities of analytes in discrete zones and at different velocities, which, in turn, depend on the charge-to-size ratios. Many applications of CZE are encountered in environmental analysis [334–336], food analysis [337,338], forensic analysis [339,340], bioanalysis [341,342] and pharmaceutical analysis [343,344].

On the other hand, micellar electrokinetic chromatography (MEKC) is another mode of CE achieved by adding micelles to the BGE. Neutral compounds could be separated by this mode [345]. Analytes distribute themselves between the hydrophobic interior of the micelle at the critical micelle concentration (CMC) and hydrophilic buffer solution [346]. Sodium dodecyl sulfate (SDS) is the most commonly used surfactant in MEKC applications. The electrophoretic mobility of SDS (anionic surfactant) cause the surfactant and micelles to slowly migrate in a counter direction to the stronger EOF. Many applications of MEKC are encountered in environmental analysis [347,348], food analysis [349] and bioanalysis [350].

Capillary gel electrophoresis (CGE) [351] is very similar to CZE. The main difference is that in CGE the column is packed with a gel, which affects the mobility of the analytes. Accordingly, the size of analyte molecules is the additional factor contributing in separation besides, electrophoretic separation.

Another mode of CE is capillary isoelectric focusing (CIEF) [352]. CIEF is based on isoelectric point (pI) values. Carrier ampholytes are used to form a pH gradient within the capillary, and the ampholyte molecules (e.g proteins) are separated (focused) through the carrier ampholyte medium until they become uncharged at their pI values. Many applications of CIEF are encountered in proteomics [353,354].

Capillary electrochromatography (CEC), another technique of CE based on the analytes' stationary–mobile phase interactions. However, in the case of charged compounds, the different electrophoretic mobilities have to be considered. The process takes place in a capillary column, containing a selected stationary phase, where the mobile phase is delivered by an EOF controlled by the application of a relatively high electric field [355,356]. Also, many applications of CIEF are encountered in proteomics [357] and enantioseparation of pharmaceuticals [358]

All the above mentioned modes are summarized in [Table 6](#). CZE is the best choice for routine analysis due to its simplicity and easy to apply (as mentioned earlier) compared to other CE modes.

Table 6: Summary of the CE modes and their applications

CE mode	Mechanism of separation	Type of molecules separated	Ref
CZE	Based on the mobility of analytes inside the capillary when applying an electric field which based to charge-to-size ratio of the analytes.	Charged molecules	[333,359]
MEKC	Based on the partition of the analyte between hydrophobic interior part of the micelles at the CMC and the aqueous phase in the BGE.	Neutral molecules and could be applied also for charged molecules	[345]
CGE	Based on the size of analyte and its electrophoretic mobility.	Macromolecules such as proteins and DNA (biopolymers)	[351,360]
CIEF	Based on the isoelectric point of analytes reaches in a carrier ampholyte.	Amphoteric molecules	[352]
CEC	Based on analytes' stationary–mobile phase interactions and electrophoretic mobilities of analytes.	Charged molecules	[355]

6.7. Detection in CE

Detection in CE is a significant challenge as a result of the small dimensions of the capillary and nanoliter volumes of the sample. Concentrated analyte solutions or pre-concentration methods are often necessary to ameliorate the sensitivity of CE analysis. A number of detection methods have been used in CE and are similar to those used in LC. Mostly, all detectors used in LC, can also be used in CE. Most of CE detection modes, either destructive (*e.g.* mass spectrometry) or non-destructive (*e.g.* optical), positioned on column, end-column or post-column, so far have been adapted from HPLC, of which the most commonly employed will be described. Among the most common detection techniques are UV-Vis, laser induced fluorescence [361], electrochemical [362] and refractive index [363]. Other detection technique such as mass spectrometry can be hyphenated to CE [364]. For on-line (on-capillary) detection, a detector window is made manually by burning off a portion of the separation capillary which render this part optically transparent.

6.7.1. UV-Vis detection

UV-Visible detection is by-far the most common and the most widely used detection method primarily due to its nearly universal detection nature [328] besides, its availability in most laboratories. Part of the

high efficiency observed in CE is due to on-line capillary detection. Commercial CE instruments usually contain UV-Vis detector. The design of the detector window is critical and the optical path length is equal to the capillary diameter, which limits the sensitivity. The bubble cell [365], the Z-shape cell [366], and similar flow cells (Fig. 26) have been developed to increase the optical path length, but peak broadening may occur and the cells are not often employed. Another strategy dealt with on-line sample pre-concentration by what is called stacking phenomena. This phenomena is based on the manipulation of the mobility of both analytes and BGE [367] (will be discussed in details later). [368].

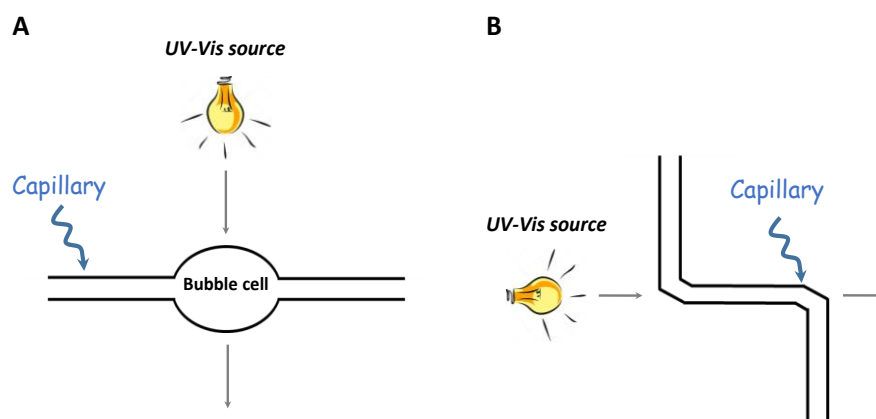


Figure 26: Techniques for increasing the path length of the capillary. (A) Bubble cell and (B) Z-shape cell

6.7.2. Fluorescence detection

Fluorescence detection is the most sensitive on-line detection technique coupled to CE, especially when laser induced fluorescence (LIF) is used as the excitation source [361]. A small portion of the capillary's polyimide coating is removed (burned off) and the laser beam is focused on the inner walls of the capillary tubing. Emission is measured at an angle of 90° to the laser taking into consideration that the BGE have low emission compared to analytes especially if they are naturally fluorescent. Because the laser provides an intense source of radiation that can be focused to a narrow spot, detection limits are as low as 10^{-16} M [369]. Disadvantages concerning the use of LIF, are the highly expensive laser price and the fact that few analytes are naturally fluorescent. The latter drawback could be solved by derivatization to make the analytes fluorescent.

6.7.3. Contactless conductivity detection (CCD)

The use of contactless conductivity detection (CCD) has great advantages in CE analysis [370]. CCD was first introduced by Gas et al. in 1980 [371]. CCD is a non-selective detection method convenient for all charged ions and when coupled to CE, its response is proportional to the difference in the mobility of the

analyte and the co-ion of the BGE. The basic arrangement of an axial CCD, which was first introduced independently by J.A. Fracassi Da Silva [370,372] in 1998, and is still widely used nowadays [373–376].

6.7.4. *Mass (MS) detection*

During the past few years CE-MS has undergone significant development in both instrumentation and application. Several ionization methods have been used for CE-MS including electrospray ionization [377,378] or pneumatically assisted electrospray ionization [379], and continuous-flow fast atom bombardment [380]. But, although the high sensitivity achieved when using CE-MS, several limitations are considered including the high cost, non-availability and the need for a specific sample pretreatment protocol before analysis. These drawbacks make it difficult to use CE-MS for routine analysis.

6.8. Stacking phenomenon in CE

As mentioned above, sensitivity of CE is limited by the dimensions of the capillary and the short path length of the detector window. Techniques that involve different extraction mechanisms, such as LLE and SPE could be used to solve the sensitivity problem of CE. These techniques are used to clean-up the extract from interfering compounds and to concentrate the target analyte. In addition, the limit of detection (LOD) is proportional to the amount of sample injected. Increasing the sample volume injected could ameliorate the LOD. However, injecting large sample volumes under non-optimized conditions could lead to peak broadening, as other electrophoretic parameters, such as buffer conductivities, pH, I , the magnitude and direction of the EOF play an important role also.

To resolve this problem, several methods based on the optimization of different electrophoretic conditions, can on-line concentrate the sample by what is called stacking [381]. Many stacking techniques will be discussed in the next paragraphs.

6.8.1. *Field amplified sample stacking (FASS)*

FASS is the simplest technique of sample stacking. The sample is solubilized in a low conductivity matrix (i.e. organic solvent). The BGE is usually aqueous with high conductivity. When applying the electrical field, ions will migrate faster in the low conductivity region (high field strength) while slowing down when reaching the high conductivity BGE (lower field strength). Therefore, the sample ions will stack at the boundary between the two regions, into a narrow zone increasing the sensitivity. Fig. 27 shows the mechanism of FASS. Applications of FASS include drug analysis [382–384], evaluation of the DNA methylation [385] and chiral separation [386].



Figure 27: The mechanism of FASS

6.8.2. Field amplified sample injection (FASI)

In FASI, also reported in some publication as field enhance sample injection (FESI), the sample is introduced by electrokinetic injection [387]. Applications of FASI include analysis of peptides [388], phenolic compounds [389] and plant extract (alkaloids) [390].

6.8.3. Large volume sample stacking (LVSS)

LVSS can be performed by using a similar buffer system as for FASS. The sample is dissolved either in a low conductivity buffer or water and injected to 1/2 or 1/3 of the capillary. The polarity is inverted making the EOF towards the inlet. The EOF directs the sample out of the capillary (cationic species) while, the anionic species are stacked at the interface (boundary) between the BGE and sample zone as shown in Fig. 28. After the current reaches 95-99% of its' original value, the polarity is then switched to normal. Anionic species are then separated normally based on their size and charge. Applications of this technique include the analysis of food colorants [391], bacteria [392], metallothioneins analysis in eel liver [393], analysis of rutin, hyperoside, and chlorogenic acid in Flos Farfarae [394] and analysis of many drugs [395–397].

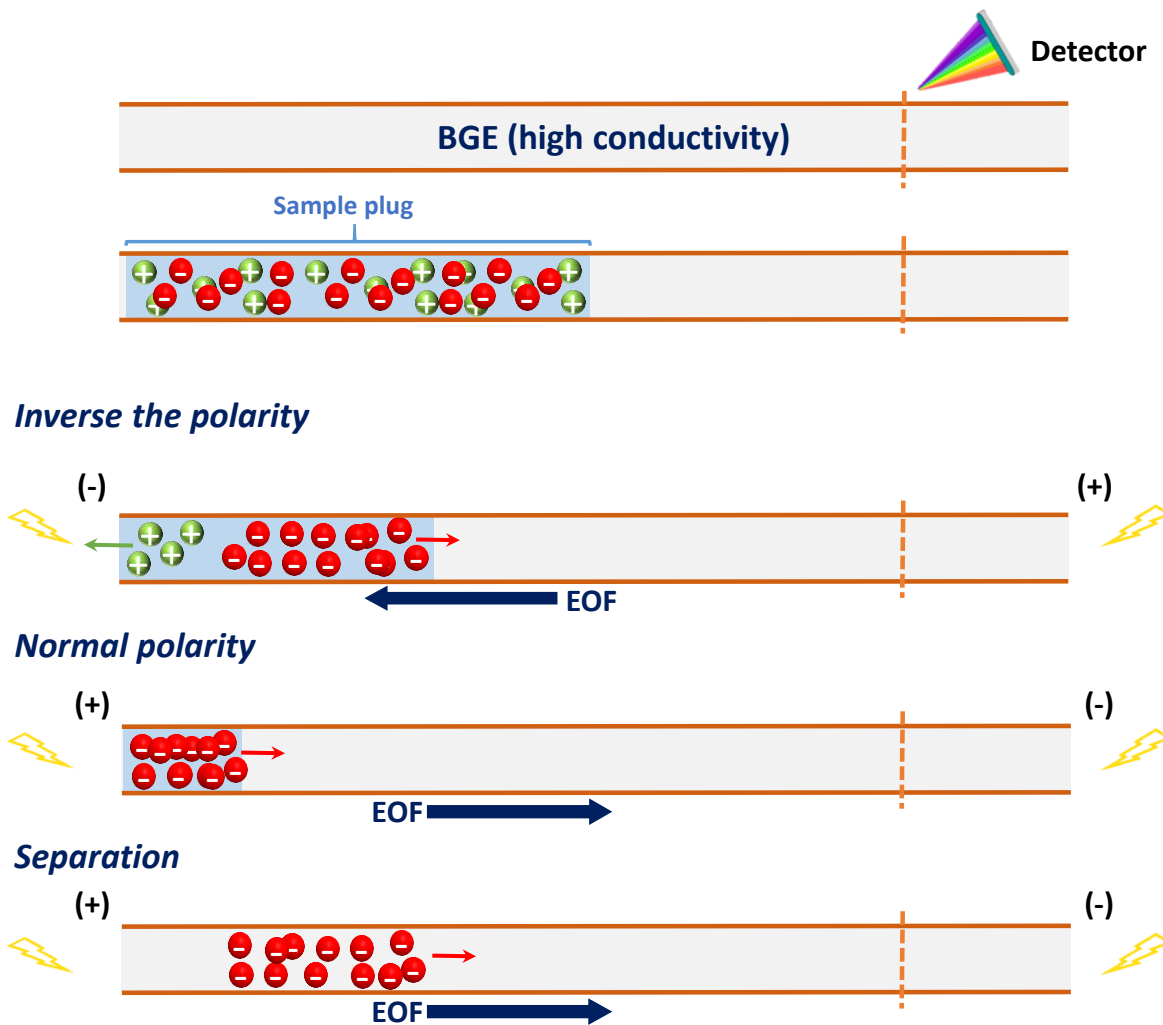


Figure 28: The mechanism of LVSS

6.8.4. Sweeping

Sweeping is another type of stacking which can be used for charged or neutral species. The sample concentration effect relies on how the pseudo stationary phase (PS) enters the sample solution zone (non-micelle buffer) and sweeps the analytes [395,398]. The BGE contains surfactants (such as, anionic micelles) to form a micelle buffer. The samples are prepared in a non-micelle buffer. The pH of these solutions is low (weak EOF). A negative polarity is applied and the separation begins. The cations move toward the inlet (cathode), anions move in the reverse direction (anode) (Fig. 29). As a result, anionic micelles enter the capillary and sweep the analytes followed by separation by MEKC mode. Some applications of this method include analysis of proguanil [399], analysis of morphine and its metabolites [400] and the separation of lysergic acid diethylamide [401].

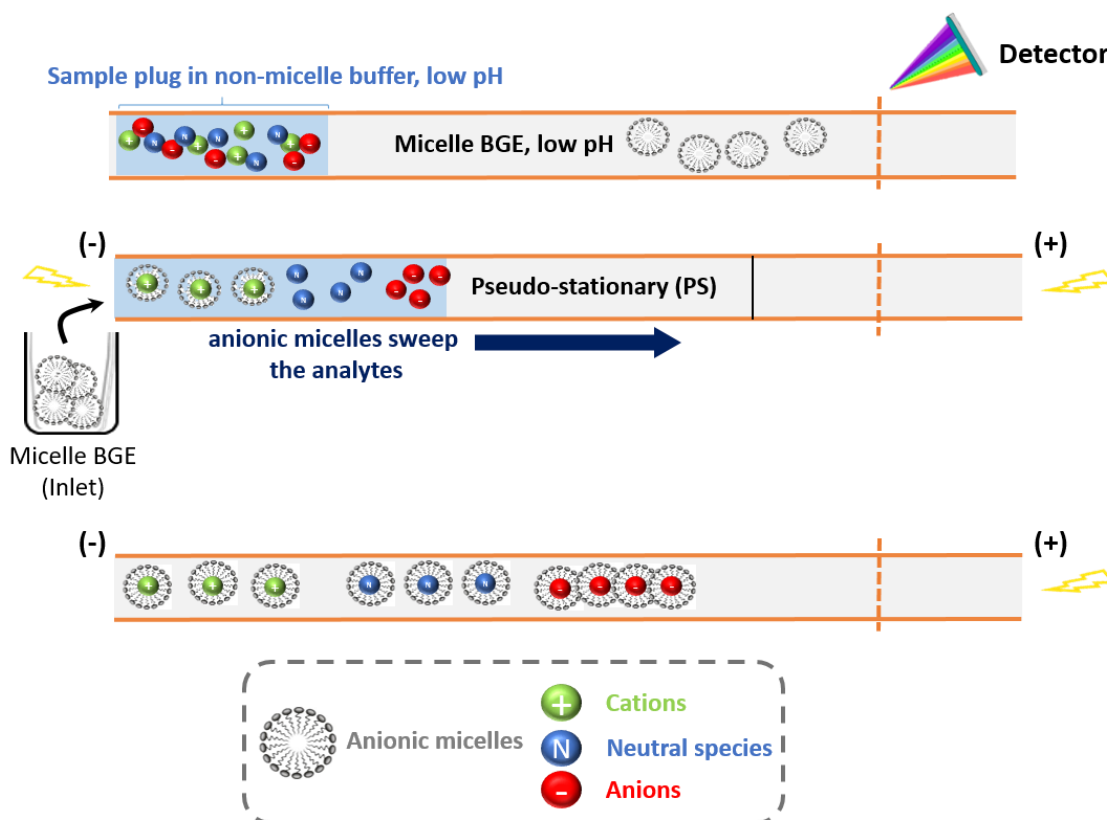


Figure 29: Mechanism of sweeping

6.8.5. pH mediated stacking

Most of the above on-line methods require the sample to be dissolved in a low conductivity matrix to have a stacking phenomenon. But, this is not always suitable especially in case of biological samples (such as urine or plasma) which contain salts increasing I of the sample which leads to diffusion of the sample ions instead of stacking [402]. pH mediated stacking method could be used to overcome such behavior. Fig. 30 shows how pH mediated stacking is happening. At first, the sample is prepared in a high I medium and is electrokinetically injected into the capillary. Then, a plug of strong acid is electrophoretically injected and a positive separation voltage is applied. The strong acid titrates the sample solution to create a highly resistance neutral zone. A higher electrical field will develop, and the ions will migrate faster. Therefore, the analytes are stacked at the boundary between the titrated zone and the BGE. Some applications of this method include the analysis of coumarin metabolites in microsomal incubations [403] and pre-concentration of anions in physiological samples [404].

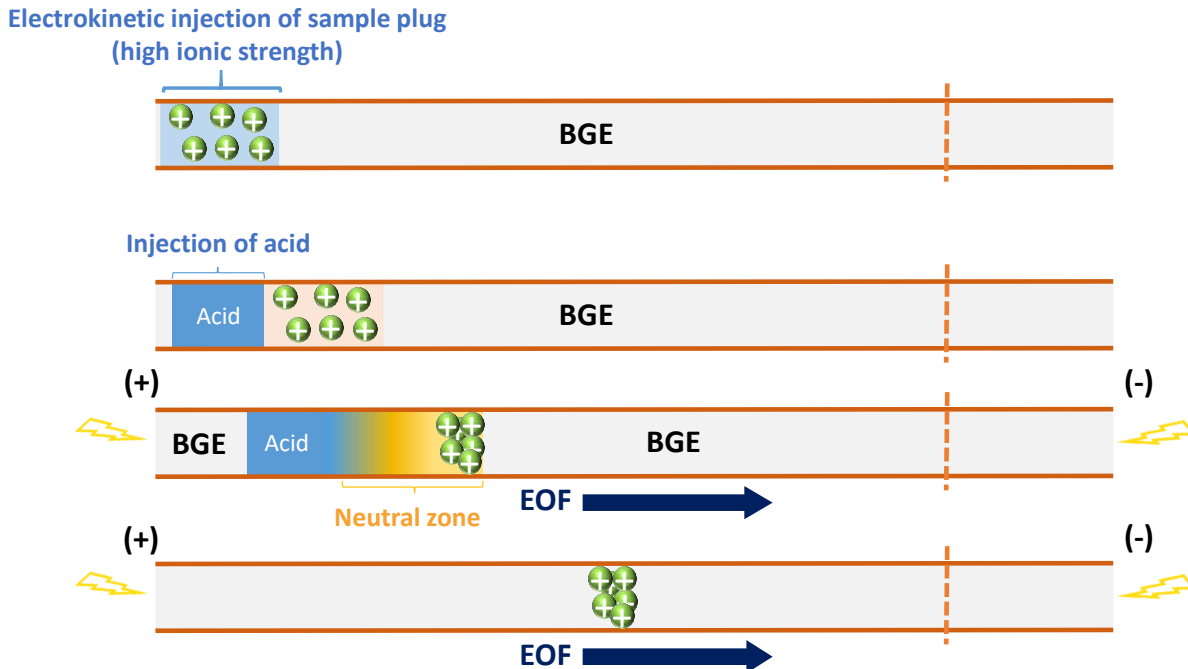


Figure 30: Mechanism of pH mediated stacking

6.8.6. Isotachopheresis (ITP)

In this mode, sample is introduced between a leading electrolyte and a terminating electrolyte solution. The μ_{ep} of the leading electrolyte (LE) is higher than the analytes while the terminating electrolyte (TE) has lower μ_{ep} than the analytes. When the electrical field is applied, the analytes are compacted (sandwiched) between the LE and TE. In ITP, the concentrations of the analyte ions are regulated by the concentration of the leading ion (as shown in Fig. 31). Thus, the concentration of the leading ion is adjusted to be relatively high (mM) to obtain high concentration efficiency. The limitation of conventional ITP that it has limited separation capacity because of analyte zone could overlap at final.

- Transient isotachopheresis (t-ITP)

This mode is also sometimes called pseudo-isotachopheresis as analytes are first separated by ITP then, the sample bands are separated by CZE according to their size and charge. Some applications of ITP include the analysis of hippurate in serum [405], determination of chloride, nitrate, sulfate, nitrite, fluoride, and phosphate [406], analysis of serotonin inhibitor [407] and the analysis also of proteins [408].

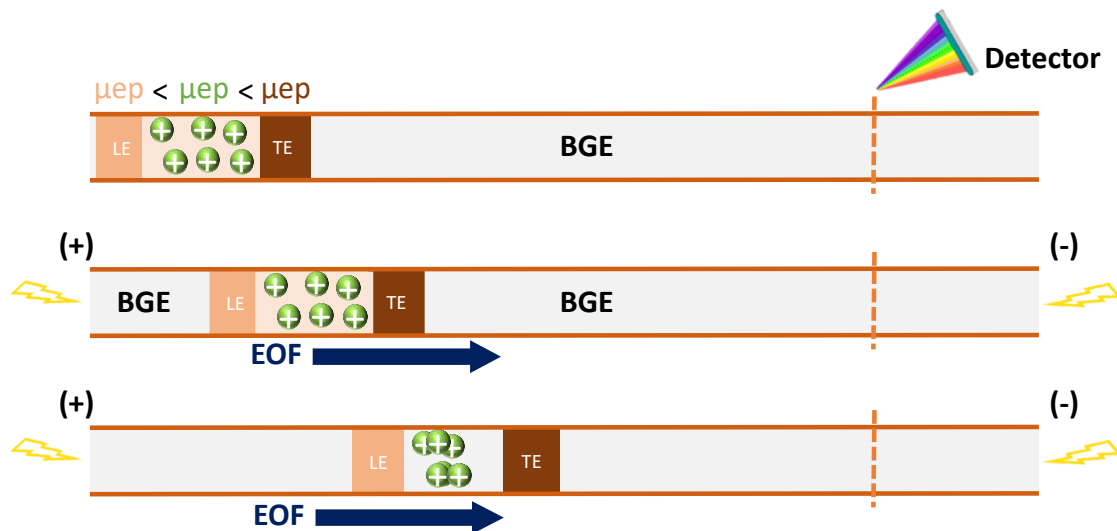


Figure 31: Mechanism of ITP

6.8.7. Analyte focusing by micelle collapse (AFMC)

AFMC can be considered as a type of MEKC except the fact that micelles are used to focus the analyte at the beginning of separation and then collapses to release the analytes in between the sample and BGE. [409]. Sample is prepared in a matrix that contains the micelles and an electrolyte anion of high mobility, while the BGE has lower conductivity solution compared to the sample (see Fig. 32). To ensure the collapse of the micelles, the concentration of surfactant micelle in the sample must be kept low and slightly above the critical micelle concentration and the conductivity must be adjusted to a minimum to ensure effective collapsing of the micelles. Neutral AFMC [410] was used for on-line pre-concentration of alkaloids. Many factors affecting neutral AFMC were published by Quirino J [411] specifying sample injection length, conductivity ratio, surfactant micelle concentration and different electrolyte salt added into the sample in order to have the maximum sensitivity of analysis. Eight cationic drugs, five neutral steroids, three quaternary ammonium and three neutral organophosphate pesticides were successfully analyzed by AFMC in a work published by Kukusamude C [412].

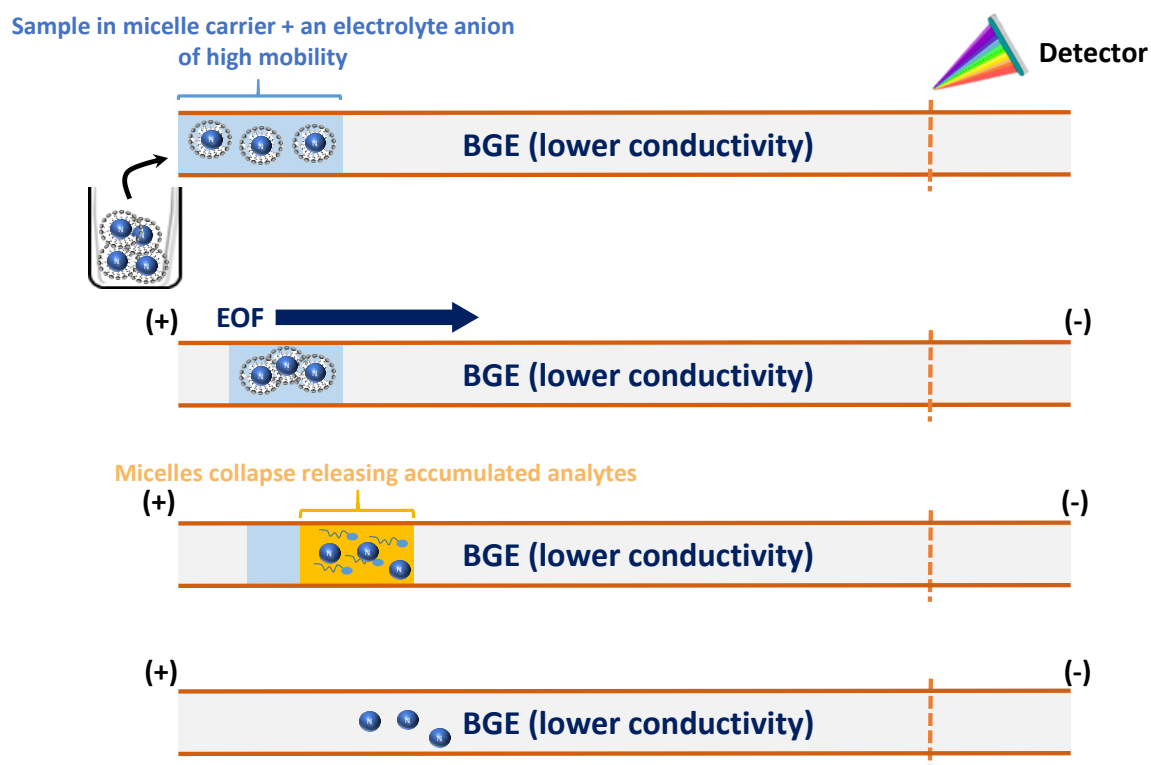


Figure 32: Mechanism of AFMC

6.9. TDM and CE

As mentioned before, TDM is used for adjusting the patient drug dose to achieve optimum clinical response. The analytical method developed for TDM objective of drugs has to be cost effective, easy to operate, sensitive and precise. Most of the analytical methods developed for the quantification of drugs in biological fluids (e.g. plasma, urine ...) is based on LC coupled to MS (as explained before). Although it offers high sensitivity and high specificity compared to other analytical methods [413], it suffers from 1/high operating cost, 2/ highly expensive instrument and 3/non-availability in all institutions.

Recently, CE has shown to offer several advantages for TDM. CE is not popular yet as LC in routine analysis but, the operating cost is much lower than that of LC. In contrast, CE suffers from high sensitivity to matrix effects especially when dealing with biological matrices such as human plasma. Plasma samples contain high concentration of proteins and salts. Biological proteins tend to adhere to the capillary wall due to interactions between negatively charged silanol groups and positively charged moieties of the protein molecules like arginine and lysine residues. This causes a decrease in the EOF resulting in peak broadening and loss of efficiency and reproducibility. Salts on the other hand, cause the peak height of analytes to diminish and sample zone to spread inside the capillary causing distortion and broadening of analytes peaks [402]. These negative effects become significant when the sample volume injected is greatly

increased. Another limitation concerning the use of CE is the poor detection related to the small dimension of the capillary and nanoliter volumes of the sample. Peak areas of analytes obtained by CE usually have lower signal-to-noise ratios than those of LC. So, there is always a need to increase the sensitivity and reproducibility when using CE technique either by off-line or on-line methods.

The off-line methods are based on using different sample preparation techniques prior to CE analysis. PP, LLE, SPE and microextraction techniques are well established and accounted for the vast majority of sample preparation steps used in the current CE assays. [Table 7](#) represents the applications of CE in the field of TDM of drugs. In this table, several validated CE-based TDM assays have been described including those for various antiepileptics, antibiotics, antimycotics, analgesics and beta blockers to name but a few [414–416]. 88% of the CE methods used were based on CZE mode. This was attributed as previously mentioned to the simplicity of CZE and its easy to apply procedure. Only 11% were based on MEKC mode.

49% of the extraction methods mentioned in [table 7](#) are based on PP using ACN which was performed in many works due to its effectiveness and simplicity to precipitate proteins from the sample [376,416–420]. In addition, the supernatant could be injected directly to CE without further treatment. The fact that the supernatant is an ACN rich solution could be advantageous to apply ACN stacking [421]. The latter is used for samples with high concentrations of salts and/or proteins such as in the case of plasma. However, different electrophoretic conditions such as pH, type and *I* of BGE have to be optimized in order to obtain maximum benefits [422]. These factors affect greatly the plate number, resolution and migration time of analytes. Also, PP by other solvents are mentioned such as methanol [423] or acetone [424] or methanol/ACN [425] or more recently ACN/dithiothreitol [426]. But, they are less common than PP by ACN. Other case involved the use of two sample pretreatment techniques (PP and DLLME) to enhance sensitivity or to give cleaner extract [427]. SPE [414,428,429] and LLE [430–433] are also used prior to CE analysis. Most of the sample pretreatment methods dealt with evaporation of the organic layer obtained after LLE or extract obtained after PP and reconstitution in water or in the BGE to ameliorate the sensitivity. [Table 7](#) lists many of the drugs analyzed mainly by CZE and to lesser extent with MEKC. The majority of these reports have been validated for their linearity, detection limits, accuracy and precision.

Table 7: Application of CE in bioanalysis

CE mode	Sample	Matrix	Sample pretreatment	Comments	Year	Ref(s)
CZE	Cytosine- β -D-arabinoside	Plasma	SPE by C18 cartridge	ACN elution then, evaporation and reconstitution in water	1991	[414]
MEKC	<i>Antiepileptic drugs</i> - Ethosuccimide - phenytoin - primidone - phenobarbital - carbamazepine - valproic acid	Plasma	LLE by ethylacetate	The organic layer was evaporated and reconstituted in 5% methanol in water	1992	[430]
MEKC	Theophylline	Plasma	LLE by ethylacetate	The organic layer was evaporated and reconstituted in water	1992	[431]
CZE	Cefixime and its metabolites	Urine	-----	Direct determination of urine samples	1992	[415]
MEKC	Theophylline	Plasma	PP by ACN	The supernatant was directly injected into the capillary	1993	[416]
CZE	Fosfomycin	Serum	PP by methanol	The supernatant was evaporated and reconstituted in water	1993	[423]
CZE	7-hydroxycoumarin	Serum and urine	LLE by diethylether	The upper layer was evaporated to dryness and reconstituted in phosphate buffer	1995	[432]
CZE	<i>Hypoglycemic drugs</i> - glipizide - glyburide - chlorpropamide - acetohexamide - tolbutamide	Urine	SPE	On-line SPE extraction by C18 tips	1995	[428]

	- tolazamide					
CZE	Iohexol	Plasma and urine	PP by ACN	Direct injection of the supernatant	1996	[417]
CZE	Ibuprofen	Serum	PP by ACN	Direct injection of the supernatant	1996	[418]
CZE	lamotrigine	Serum	PP by ACN	Direct injection of the supernatant	1996	[434]
CZE	procainamide and N-acetyl procainamide	Urine	-----	Direct injection of urine samples at pH 7.7 to avoid matrix effect	1997	[435]
CZE	Acetaminophen and salicylic acid	Plasma	-----	A stable and reproducible separation could only be achieved using a 1:1 mixture of acetonitrile and SDS-buffer as rinsing reagent	1997	[436]
CZE	Tamoxifen and metabolites	Serum	LLE by 98:2 hexane-isoamyl alcohol	1:1 methanol-acetonitrile containing 10mM ammonium acetate and 1% acetic acid	1997	[433]
CZE	Taurine	Plasma	PP by ACN	Derivatisation with flouriscamine	2000	[419]
CZE	b-blocker atenolol	Plasma	SPE	After SPE, the extract was evaporated and reconstituted in water	2001	[437]
CZE	clopidogrel carboxylic acid	Plasma and urine	SPE	Organic extract evaporated and reconstituted in methanol and BGE	2010	[429]

CZE	Valine, isoleucine, and leucine	Plasma	PP by ACN	Injection of the supernatant to CE-C ⁴ D	2015	[376]
CZE	Carvedilol	Plasma	PP by acetone followed by DLLME	Evaporation of the extract followed by reconstitution in ACN/water, FASI was used to improve sensitivity	2015	[427]
CZE	Piperacillin, tazobactam and cefepime	Plasma	PP by methanol and ACN	-----	2015	[425]
CZE and HPLC	Thiocarbonyldiimidazole	Plasma	PP by ACN	pH mediated stacking was used to increase the sensitivity	2015	[420]
CZE	<i>Antiarrhythmic drugs</i> - Metoprolol - Propranolol hydrochloride - Sotalol hydrochloride - diltiazem - verapamil	Plasma	DLLME	FASS used to increase sensitivity	2015	[438]
CZE	Tamoxifen	Plasma	LLE with (95:5, v/v) ethyl acetate:2 propanol	Evaporation and reconstitution in methanol then, injection to CE-C ⁴ D	2015	[439]
CZE	Dexrazoxane	Plasma	PP by acetone	Evaporation and reconstitution in water then, injection to CE-MS	2016	[424]
CZE	Ceftazidime	Plasma	PP by ACN	-----	2016	[440]
CZE	Tamoxifen	Plasma	LLE by ethylacetate	FASI used to increase sensitivity	2016	[441]

CZE	Capecitabine	Plasma	HF-SPME	FASI used to increase sensitivity	2016	[442]
CZE	Glutamic acid	Plasma	PP by ACN and dithiothreitol	-----	2017	[426]

General conclusion of the chapter

This chapter gives a state-of-art on the importance of TKIs in targeted cancer therapy and the significance to measure their concentration by TDM. This chapter also gives an overview about the importance of CE in bioanalysis as an alternative technique to LC. CE has shown to offer several advantages for TDM including lower operational cost and high separation ability. With stacking methods, CE has enough sensitivity for the analysis of many of the drugs in biological matrices such as plasma. There is always a need for further sensitivity and to give a great attention to sample pretreatment technique specially when dealing with plasma samples.

The objective of this work is to develop an analytical method using CE that can be used for the TDM of TKIs. Developing a new technique for sample pretreatment of TKIs from patients' plasma is an objective but, also to adapt this technique to be coupled to CE coupled to a UV detection is another objective. The whole methodology should be fast, consumes less organic solvents, cheaper to apply and easy to automate compared to other traditional extraction techniques.

References

- [1] Definition of cancer - NCI Dictionary of Cancer Terms - National Cancer Institute, (n.d.). <https://www.cancer.gov/publications/dictionaries/cancer-terms/def/cancer> (accessed September 16, 2019).
- [2] R. Lakhtakia, A Brief History of Breast Cancer: Part I: Surgical domination reinvented., Sultan Qaboos Univ. Med. J. 14 (2014) e166-9.
- [3] What is cancer? | Cancer Research UK, (n.d.). <https://www.cancerresearchuk.org/about-cancer/what-is-cancer> (accessed September 16, 2019).
- [4] A. Jemal, R. Siegel, E. Ward, Y. Hao, J. Xu, T. Murray, M.J. Thun, Cancer statistics, 2008, CA Cancer J. Clin. 58 (2008) 71–96.
- [5] State of Health in the EU FranceCountry Health Profile 2017, (n.d.). <https://doi.org/10.1787/888933593532>.
- [6] A. -J Tuyns, J. Esteve, L. Raymond, F. Berrino, E. Benhamou, F. Blanchet, P. Boffetta, P. Crosignani, A. Del Moral, W. Lehmann, F. Merletti, G. Pequignot, E. Rreou, H. Sancho-Garnier, B. Terracini, A. Zubiri, L. Zubiri, Cancer of the larynx/hypopharynx, tobacco and alcohol: larc international case-control study in Turin and Varese (Italy), Zaragoza and Navarra (Spain), Geneva (Switzerland) and Calvados (France), Int. J. Cancer. 41 (1988) 483–491.
- [7] J.A. Knight, J. Fan, K.E. Malone, E.M. John, C.F. Lynch, R. Langballe, L. Bernstein, R.E. Shore, J.D. Brooks, A.S. Reiner, M. Woods, X. Liang, J.L. Bernstein, Alcohol consumption and cigarette smoking in combination: A predictor of contralateral breast cancer risk in the WECARE study, Int. J. Cancer. 141 (2017) 916–924.
- [8] How cancer rates have exploded in France in the last 30 years - The Local, (n.d.). <https://www.thelocal.fr/20190702/how-cancer-numbers-have-exploded-in-france-in-the-last-30-years> (accessed September 16, 2019).
- [9] D. Hanahan, R.A. Weinberg, The hallmarks of cancer., Cell. 100 (2000) 57–70.
- [10] D. Hanahan, R.A. Weinberg, Hallmarks of cancer: the next generation., Cell. 144 (2011) 646–74.
- [11] J.H. Walsh, W.E. Karnes, F. Cuttitta, A. Walker, Autocrine growth factors and solid tumor malignancy., West. J. Med. 155 (1991) 152–63.

- [12] N. Cheng, A. Chytil, Y. Shyr, A. Joly, H.L. Moses, Transforming Growth Factor- Signaling-Deficient Fibroblasts Enhance Hepatocyte Growth Factor Signaling in Mammary Carcinoma Cells to Promote Scattering and Invasion, *Mol. Cancer Res.* 6 (2008) 1521–1533.
- [13] N.A. Bhowmick, E.G. Neilson, H.L. Moses, Stromal fibroblasts in cancer initiation and progression., *Nature.* 432 (2004) 332–7.
- [14] R.E. Reiter, Z. Gu, T. Watabe, G. Thomas, K. Szigeti, E. Davis, M. Wahl, S. Nisitani, J. Yamashiro, M.M. Le Beau, M. Loda, O.N. Witte, Prostate stem cell antigen: a cell surface marker overexpressed in prostate cancer., *Proc. Natl. Acad. Sci. U. S. A.* 95 (1998) 1735–40.
- [15] B. Ozanne, C.S. Richards, F. Hendler, D. Burns, B. Gusterson, Over-expression of the EGF receptor is a hallmark of squamous cell carcinomas, *J. Pathol.* 149 (1986) 9–14.
- [16] M.A. Davies, Y. Samuels, Analysis of the genome to personalize therapy for melanoma, *Oncogene.* 29 (2010) 5545–5555.
- [17] B.H. Jiang, L.Z. Liu, Chapter 2 PI3K/PTEN Signaling in Angiogenesis and Tumorigenesis, in: *Adv. Cancer Res.*, 2009: pp. 19–65.
- [18] T.L. Yuan, L.C. Cantley, PI3K pathway alterations in cancer: Variations on a theme, *Oncogene.* 27 (2008) 5497–5510.
- [19] N. Bardeesy, N.E. Sharpless, RAS unplugged: Negative feedback and oncogene-induced senescence, *Cancer Cell.* 10 (2006) 451–453.
- [20] K.E. O'Reilly, F. Rojo, Q.B. She, D. Solit, G.B. Mills, D. Smith, H. Lane, F. Hofmann, D.J. Hicklin, D.L. Ludwig, J. Baselga, N. Rosen, mTOR inhibition induces upstream receptor tyrosine kinase signaling and activates Akt, *Cancer Res.* 66 (2006) 1500–1508.
- [21] S. Sudarsanam, D.E. Johnson, Functional consequences of mTOR inhibition., *Curr. Opin. Drug Discov. Devel.* 13 (2010) 31–40.
- [22] S. Lee, C.A. Schmitt, The dynamic nature of senescence in cancer, *Nat. Cell Biol.* 21 (2019) 94–101.
- [23] B.E. Engel, W.D. Cress, P.G. Santiago-Cardona, The retinoblastoma protein: A master tumor suppressor acts as a link between cell cycle and cell adhesion, *Cell Health Cytoskelet.* 7 (2014) 1–10.

- [24] B.J. Aubrey, A. Strasser, G.L. Kelly, Tumor-suppressor functions of the TP53 pathway, *Cold Spring Harb. Perspect. Med.* 6 (2016) 1–16.
- [25] T. Hamzehloie, M. Mojarrad, M. Hasanzadeh-Nazarabadi, S. Shekouhi, The role of tumor protein 53 mutations in common human cancers and targeting the murine double minute 2-P53 interaction for cancer therapy, *Iran. J. Med. Sci.* 37 (2012) 3–8.
- [26] H. Ikushima, K. Miyazono, TGF β 2 signalling: A complex web in cancer progression, *Nat. Rev. Cancer.* 10 (2010) 415–424.
- [27] J. Massagué, TGF β in Cancer, *Cell.* 134 (2008) 215–230.
- [28] B. Bierie, H.L. Moses, Tumour microenvironment - TGF β : The molecular Jekyll and Hyde of cancer, *Nat. Rev. Cancer.* 6 (2006) 506–520.
- [29] J. Xu, S. Lamouille, R. Derynck, TGF- β -induced epithelial to mesenchymal transition, *Cell Res.* 19 (2009) 156–172.
- [30] J.M. Adams, S. Cory, The Bcl-2 apoptotic switch in cancer development and therapy, *Oncogene.* 26 (2007) 1324–1337.
- [31] S.W. Lowe, E. Cepero, G. Evan, Intrinsic tumour suppression, *Nature.* 432 (2004) 307–315.
- [32] M.R. Junttila, G.I. Evan, P53 a Jack of all trades but master of none, *Nat. Rev. Cancer.* 9 (2009) 821–829.
- [33] R. O’Connor, C. Fennelly, D. Krause, Regulation of survival signals from the insulin-like growth factor-I receptor, *Biochem. Soc. Trans.* 28 (2015) 47–51.
- [34] B. Levine, G. Kroemer, Autophagy in the Pathogenesis of Disease, *Cell.* 132 (2008) 27–42.
- [35] E. Hiyama, K. Hiyama, Telomere and telomerase in stem cells, *Br. J. Cancer.* 96 (2007) 1020–1024.
- [36] N.W. Kim, M.A. Piatyszek, K.R. Prowse, C.B. Harley, M.D. West, P.L.C. Ho, G.M. Coviello, W.E. Wright, S.L. Weinrich, J.W. Shay, Specific association of human telomerase activity with immortal cells and cancer, *Science* (80-.). 266 (1994) 2011–2015.
- [37] J.W. Shay, W.N. Keith, Targeting telomerase for cancer therapeutics, *Br. J. Cancer.* 98 (2008) 677–683.

- [38] D. Hanahan, J. Folkman, Patterns and emerging mechanisms of the angiogenic switch during tumorigenesis, *Cell*. 86 (1996) 353–364.
- [39] N. Ferrara, Vascular Endothelial Growth Factor, *Brenner's Encycl. Genet. Second Ed.* 29 (2013) 274–276.
- [40] V. Baeriswyl, G. Christofori, The angiogenic switch in carcinogenesis, *Semin. Cancer Biol.* 19 (2009) 329–337.
- [41] T.T. Onder, P.B. Gupta, S.A. Mani, J. Yang, E.S. Lander, R.A. Weinberg, Loss of E-cadherin promotes metastasis via multiple downstream transcriptional pathways, *Cancer Res.* 68 (2008) 3645–3654.
- [42] I.J. Fidler, The pathogenesis of cancer metastasis: the “seed and soil” hypothesis revisited., *Nat. Rev. Cancer.* 3 (2003) 453–8.
- [43] B.-Z. Qian, J.W. Pollard, Macrophage diversity enhances tumor progression and metastasis., *Cell.* 141 (2010) 39–51.
- [44] R.A. Gatenby, R.J. Gillies, Why do cancers have high aerobic glycolysis?, *Nat. Rev. Cancer.* 4 (2004) 891–899.
- [45] R.J. DeBerardinis, J.J. Lum, G. Hatzivassiliou, C.B. Thompson, The Biology of Cancer: Metabolic Reprogramming Fuels Cell Growth and Proliferation, *Cell Metab.* 7 (2008) 11–20.
- [46] R.G. Jones, C.B. Thompson, Tumor suppressors and cell metabolism: A recipe for cancer growth, *Genes Dev.* 23 (2009) 537–548.
- [47] M. Jang, S.S. Kim, J. Lee, Cancer cell metabolism: Implications for therapeutic targets, *Exp. Mol. Med.* 45 (2013) 1–8.
- [48] C. V Dang, G.L. Semenza, Oncogenic alterations of metabolism, *Trends Biochem. Sci.* 24 (1999) 68–72.
- [49] B. Muz, P. de la Puente, F. Azab, A.K. Azab, The role of hypoxia in cancer progression, angiogenesis, metastasis, and resistance to therapy, *Hypoxia.* 3 (2015) 83.
- [50] B. Lakshmi Narendra, K. Eshvendar Reddy, S. Shantikumar, S. Ramakrishna, Immune system: A double-edged sword in cancer, *Inflamm. Res.* 62 (2013) 823–834.

- [51] S.-R. Woo, L. Corrales, T.F. Gajewski, Innate Immune Recognition of Cancer, *Annu. Rev. Immunol.* 33 (2015) 445–474.
- [52] R.J. Binder, Functions of Heat Shock Proteins in Pathways of the Innate and Adaptive Immune System, *J. Immunol.* 193 (2014) 5765–5771.
- [53] P.C. Rodríguez, A.H. Zea, A.C. Ochoa, Mechanisms of tumor evasion from the immune response., *Cancer Chemother. Biol. Response Modif.* 21 (2003) 351–64.
- [54] M.W.L. Teng, J.B. Swann, C.M. Koebel, R.D. Schreiber, M.J. Smyth, Immune-mediated dormancy: an equilibrium with cancer, *J. Leukoc. Biol.* 84 (2008) 988–993.
- [55] C. Ferrone, G. Dranoff, Dual roles for immunity in gastrointestinal cancers, *J. Clin. Oncol.* 28 (2010) 4045–4051.
- [56] M. Esteller, Cancer epigenomics: DNA methylomes and histone-modification maps, *Nat. Rev. Genet.* 8 (2007) 286–298.
- [57] S. Negrini, V.G. Gorgoulis, T.D. Halazonetis, Genomic instability an evolving hallmark of cancer, *Nat. Rev. Mol. Cell Biol.* 11 (2010) 220–228.
- [58] H.F. Dvorak, Tumors: Wounds that do not heal-redux, *Cancer Immunol. Res.* 3 (2015) 1–11.
- [59] D.S. Foster, R.E. Jones, R.C. Ransom, M.T. Longaker, J.A. Norton, The evolving relationship of wound healing and tumor stroma, *JCI Insight.* 3 (2018). <https://doi.org/10.1172/jci.insight.99911>.
- [60] D.G. DeNardo, P. Andreu, L.M. Coussens, Interactions between lymphocytes and myeloid cells regulate pro-versus anti-tumor immunity, *Cancer Metastasis Rev.* 29 (2010) 309–316.
- [61] S.I. Grivennikov, F.R. Greten, M. Karin, Immunity, Inflammation, and Cancer, *Cell.* 140 (2010) 883–899.
- [62] J. Lokich, A. Bothe, N. Fine, J. Perri, The delivery of cancer chemotherapy by constant venous infusion ambulatory management of venous access and portable pump, *Cancer.* 50 (1982) 2731–2735.
- [63] S. Tohme, R.L. Simmons, A. Tsung, Surgery for cancer: A trigger for metastases, *Cancer Res.* 77 (2017) 1548–1552.
- [64] R. Baskar, K.A. Lee, R. Yeo, K.W. Yeoh, Cancer and radiation therapy: Current advances and future

- directions, *Int. J. Med. Sci.* 9 (2012) 193–199.
- [65] D.S. Shewach, R.D. Kuchta, Introduction to cancer chemotherapeutics, *Chem. Rev.* 109 (2009) 2859–2861.
- [66] R.K. Singh, S. Kumar, D.N. Prasad, T.R. Bhardwaj, Therapeutic journey of nitrogen mustard as alkylating anticancer agents: Historic to future perspectives, *Eur. J. Med. Chem.* 151 (2018) 401–433.
- [67] Y. Chen, Y. Jia, W. Song, L. Zhang, Therapeutic Potential of Nitrogen Mustard Based Hybrid Molecules, *Front. Pharmacol.* 9 (2018) 1449–1453.
- [68] E. Scholar, Antimetabolites, *XPharm Compr. Pharmacol. Ref.* (2007) 1–4.
- [69] M. Ivancich, Z. Schrank, L. Wojdyla, B. Leviskas, A. Kuckovic, A. Sanjali, N. Puri, Treating Cancer by Targeting Telomeres and Telomerase, *Antioxidants.* 6 (2017) 15.
- [70] R.S.Y. Wong, Role of Nonsteroidal Anti-Inflammatory Drugs (NSAIDs) in Cancer Prevention and Cancer Promotion, *Adv. Pharmacol. Sci.* 2019 (2019) 1–10.
- [71] Z. Zhang, F. Chen, L. Shang, Advances in antitumor effects of NSAIDs, *Cancer Manag. Res.* 10 (2018) 4631–4640.
- [72] D. Li, P. Wang, Y. Yu, B. Huang, X. Zhang, C. Xu, X. Zhao, Z. Yin, Z. He, M. Jin, C. Liu, Tumor-preventing activity of aspirin in multiple cancers based on bioinformatic analyses, *PeerJ.* 6 (2018) 1–15.
- [73] H. Zhang, J. Chen, Current status and future directions of cancer immunotherapy., *J. Cancer.* 9 (2018) 1773–1781.
- [74] M.K. Callahan, J.D. Wolchok, J.P. Allison, AntiCTLA-4 antibody therapy: Immune monitoring during clinical development of a novel immunotherapy, *Semin. Oncol.* 37 (2010) 473–484.
- [75] T. Chodon, R.C. Koya, K. Odunsi, Active Immunotherapy of Cancer, *Immunol. Invest.* 44 (2015) 817–836.
- [76] G. Manning, D.B. Whyte, R. Martinez, T. Hunter, S. Sudarsanam, The protein kinase complement of the human genome, *Science* (80-.). 298 (2002) 1912–1934.
- [77] M.A. Lemmon, J. Schlessinger, Cell signaling by receptor tyrosine kinases., *Cell.* 141 (2010) 1117–

1134.

- [78] A. Ullrich, J. Schlessinger, Signal transduction by receptors with tyrosine kinase activity, *Cell*. 61 (1990) 203–212.
- [79] C.W. Ward, M.C. Lawrence, V.A. Streltsov, T.E. Adams, N.M. McKern, The insulin and EGF receptor structures: new insights into ligand-induced receptor activation, *Trends Biochem. Sci.* 32 (2007) 129–137.
- [80] E. Gocek, A.N. Moulas, G.P. Studzinski, Non-receptor protein tyrosine kinases signaling pathways in normal and cancer cells, *Crit. Rev. Clin. Lab. Sci.* 51 (2014) 125–137.
- [81] C.C. Uphoff, S. Habig, S. Fombonne, Y. Matsuo, H.G. Drexler, ABL-BCR expression in BCR-ABL-positive human leukemia cell lines, *Leuk. Res.* 23 (1999) 1055–1060.
- [82] R.P. Million, J. Aster, D. Gary Gilliland, R.A. Van Etten, The Tel-Abl (ETV6-Abl) tyrosine kinase, product of complex (9;12) translocations in human leukemia, induces distinct myeloproliferative disease in mice, *Blood*. 99 (2002) 4568–4577.
- [83] C.N. Prabhakar, Epidermal growth factor receptor in non-small cell lung cancer., *Transl. Lung Cancer Res.* 4 (2015) 110–118.
- [84] J. Carlsson, K. Wester, M. De La Torre, P.U. Malmström, T. Gårdmark, EGFR-expression in primary urinary bladder cancer and corresponding metastases and the relation to HER2-expression. on the possibility to target these receptors with radionuclides, *Radiol. Oncol.* 49 (2015) 50–58.
- [85] H. Masuda, D. Zhang, C. Bartholomeusz, H. Doihara, G.N. Hortobagyi, N.T. Ueno, Role of epidermal growth factor receptor in breast cancer, *Breast Cancer Res. Treat.* 136 (2012) 331–345.
- [86] T. Sasaki, K. Hiroki, Y. Yamashita, The Role of Epidermal Growth Factor Receptor in Cancer Metastasis and Microenvironment, *Biomed Res. Int.* 2013 (2013) 1–8.
- [87] I. Carvalho, F. Milanezi, A. Martins, R.M. Reis, F. Schmitt, Overexpression of platelet-derived growth factor receptor α in breast cancer is associated with tumour progression, *Breast Cancer Res.* 7 (2005) 788–795.
- [88] I. Nazarenko, S.M. Hede, X. He, A. Hedrén, J. Thompson, M.S. Lindström, M. Nistér, PDGF and PDGF receptors in glioma, *Ups. J. Med. Sci.* 117 (2012) 99–112.

- [89] S.M. Farabaugh, D.N. Boone, A. V Lee, Role of IGF1R in breast cancer subtypes, stemness, and lineage differentiation, *Front. Endocrinol. (Lausanne)*. 6 (2015) 1–12.
- [90] R. Shi, H.J. Berkel, H. Yu, Insulin-like growth factor-I and prostate cancer: A meta-analysis, *Br. J. Cancer*. 85 (2001) 991–996.
- [91] A. Arora, E.M. Scholar, Role of tyrosine kinase inhibitors in cancer therapy., *J. Pharmacol. Exp. Ther.* 315 (2005) 971–9.
- [92] N. Iqbal, N. Iqbal, Imatinib: A Breakthrough of Targeted Therapy in Cancer, *Chemother. Res. Pract.* 2014 (2014) 1–9.
- [93] J.C. Van Der Mijn, H.J. Broxterman, J.C. Knol, S.R. Piersma, R.R. De Haas, H. Dekker, T. V. Pham, V.W. Van Beusechem, B. Halmos, J.W. Mier, C.R. Jiménez, H.M.W. Verheul, Sunitinib activates Axl signaling in renal cell cancer, *Int. J. Cancer*. 138 (2016) 3002–3010.
- [94] Q. Jiao, L. Bi, Y. Ren, S. Song, Q. Wang, Y. shan Wang, Advances in studies of tyrosine kinase inhibitors and their acquired resistance, *Mol. Cancer*. 17 (2018) 1–12.
- [95] W. Jurczak, M. Długosz-Danecka, M. Wang, Acalabrutinib for adults with mantle cell lymphoma, *Expert Rev. Clin. Pharmacol.* 12 (2019) 179–187.
- [96] E.D. Deeks, G.M. Keating, Afatinib in advanced NSCLC: a profile of its use, *Drugs Ther. Perspect.* 34 (2018) 89–98.
- [97] T. Vavalà, S. Novello, Alectinib in the treatment of ALK-positive non-small cell lung cancer: an update on its properties, efficacy, safety and place in therapy., *Ther. Adv. Med. Oncol.* 10 (2018) 1–12.
- [98] R.J. Motzer, K. Penkov, J. Haanen, B. Rini, L. Albiges, M.T. Campbell, B. Venugopal, C. Kollmannsberger, S. Negrier, M. Uemura, J.L. Lee, A. Vasiliev, W.H. Miller, H. Gurney, M. Schmidinger, J. Larkin, M.B. Atkins, J. Bedke, B. Alekseev, J. Wang, M. Mariani, P.B. Robbins, A. Chudnovsky, C. Fowst, S. Hariharan, B. Huang, A. di Pietro, T.K. Choueiri, Avelumab plus Axitinib versus Sunitinib for Advanced Renal-Cell Carcinoma, *N. Engl. J. Med.* 380 (2019) 1103–1115.
- [99] Z.T. Al-Salama, L.J. Scott, Baricitinib: A Review in Rheumatoid Arthritis, *Drugs*. 78 (2018) 761–772.
- [100] S. Isfort, T.H. Brümmendorf, Bosutinib in chronic myeloid leukemia: patient selection and perspectives, *J. Blood Med.* Volume 9 (2018) 43–50.

- [101] R. Ali, J. Arshad, S. Palacio, R. Mudad, Brigatinib for ALK-positive metastatic non-small-cell lung cancer: Design, development and place in therapy, *Drug Des. Devel. Ther.* 13 (2019) 569–580.
- [102] R. Elisei, M.J. Schlumberger, S.P. Müller, P. Schöffski, M.S. Brose, M.H. Shah, L. Licitra, B. Jarzab, V. Medvedev, M.C. Kreissl, B. Niederle, E.E.W. Cohen, L.J. Wirth, H. Ali, C. Hessel, Y. Yaron, D. Ball, B. Nelkin, S.I. Sherman, Cabozantinib in progressive medullary thyroid cancer, *J. Clin. Oncol.* 31 (2013) 3639–3646.
- [103] Z. Zhu, Y. Chai, Crizotinib resistance overcome by ceritinib in an ALK-positive non-small cell lung cancer patient with brain metastases, *Med. (United States)*. 96 (2017) 1–3.
- [104] J.J. Lin, A.T. Shaw, Recent Advances in Targeting ROS1 in Lung Cancer, *J. Thorac. Oncol.* 12 (2017) 1611–1625.
- [105] A. Passaro, F. de Marinis, Dacomitinib in EGFR-positive non-small cell lung cancer: an attractive but broken option, *Transl. Lung Cancer Res.* 7 (2018) 100–102.
- [106] D. Keskin, S. Sadri, A.E. Eskazan, Dasatinib for the treatment of chronic myeloid leukemia: Patient selection and special considerations, *Drug Des. Devel. Ther.* 10 (2016) 3355–3361.
- [107] J.P. Wang, C.Y. Wu, Y.C. Yeh, Y.M. Shyr, Y.Y. Wu, C.Y. Kuo, Y.P. Hung, M.H. Chen, W.P. Lee, J.C. Luo, Y. Chao, C.P. Li, Erlotinib is effective in pancreatic cancer with epidermal growth factor receptor mutations: A randomized, open-label, prospective trial, *Oncotarget.* 6 (2015) 18162–18173.
- [108] Y. Wang, C. Zhou, G. Schmid Bindert, Erlotinib in the treatment of advanced non-small cell lung cancer: An update for clinicians, *Ther. Adv. Med. Oncol.* 4 (2012) 19–29.
- [109] M.E. Royce, D. Osman, Everolimus in the treatment of metastatic breast cancer, *Breast Cancer Basic Clin. Res.* 9 (2015) 73–79.
- [110] J.C. Yao, M.H. Shah, T. Ito, C.L. Bohas, E.M. Wolin, E. Van Cutsem, T.J. Hobday, T. Okusaka, J. Capdevila, E.G.E. de Vries, P. Tomassetti, M.E. Pavel, S. Hoosen, T. Haas, J. Lincy, D. Lebwohl, K. Öberg, Everolimus for Advanced Pancreatic Neuroendocrine Tumors, *N. Engl. J. Med.* 364 (2011) 514–523.
- [111] S. Buti, A. Leonetti, A. Dallatomasina, M. Bersanelli, Everolimus in the management of metastatic renal cell carcinoma: an evidence-based review of its place in therapy, *Core Evid.* 11 (2016) 23–

- 36.
- [112] D.N. Franz, K. Agricola, M. Mays, C. Tudor, M.M. Care, K. Holland-Bouley, N. Berkowitz, S. Miao, S. Peyrard, D.A. Krueger, Everolimus for subependymal giant cell astrocytoma: 5-year final analysis, *Ann. Neurol.* 78 (2015) 929–938.
- [113] N.T. Connell, N. Berliner, Fostamatinib for the treatment of chronic immune thrombocytopenia, *Blood.* 133 (2019) 2027–2030.
- [114] E.H. Sim, I.A. Yang, R. Wood-Baker, R. V Bowman, K.M. Fong, Gefitinib for advanced non-small cell lung cancer, 2018.
- [115] A.E. Perl, J.K. Altman, J. Cortes, C. Smith, M. Litzow, M.R. Baer, D. Claxton, H.P. Erba, S. Gill, S. Goldberg, J.G. Jurcic, R.A. Larson, C. Liu, E. Ritchie, G. Schiller, A.I. Spira, S.A. Strickland, R. Tibes, C. Ustun, E.S. Wang, R. Stuart, C. Röllig, A. Neubauer, G. Martinelli, E. Bahceci, M. Levis, Selective inhibition of FLT3 by gilteritinib in relapsed or refractory acute myeloid leukaemia: a multicentre, first-in-human, open-label, phase 1–2 study, *Lancet Oncol.* 18 (2017) 1061–1075.
- [116] L.K. Shea, F.M. Mikhail, A. Forero-Torres, R.S. Davis, Concomitant imatinib and ibrutinib in a patient with chronic myelogenous leukemia and chronic lymphocytic leukemia, *Clin. Case Reports.* 5 (2017) 899–901.
- [117] D.M. Stephens, S.E. Spurgeon, Ibrutinib in mantle cell lymphoma patients: Glass half full? Evidence and opinion, *Ther. Adv. Hematol.* 6 (2015) 242–252.
- [118] C. Owen, N.L. Berinstein, A. Christofides, L.H. Sehn, Review of Bruton tyrosine kinase inhibitors for the treatment of relapsed or refractory mantle cell lymphoma, *Curr. Oncol.* 26 (2019) 233–240.
- [119] T. Liu-Dumlao, H. Kantarjian, D.A. Thomas, S. O’Brien, F. Ravandi, Philadelphia-positive acute lymphoblastic leukemia: Current treatment options, *Curr. Oncol. Rep.* 14 (2012) 387–394.
- [120] S. V Labropoulos, E.D. Razis, Imatinib in the treatment of dermatofibrosarcoma protuberans, *Biol. Targets Ther.* 1 (2007) 347–353.
- [121] G. Helbig, Imatinib for the treatment of hypereosinophilic syndromes, *Expert Rev. Clin. Immunol.* 14 (2018) 163–170.
- [122] L.F. Lopes, C.E. Bacchi, Imatinib treatment for gastrointestinal stromal tumour (GIST), *J. Cell. Mol.*

- Med. 14 (2010) 42–50.
- [123] J. Cortes, F. Giles, S. O'Brien, D. Thomas, M. Albitar, M.B. Rios, M. Talpaz, G. Garcia-Manero, S. Faderl, L. Letvak, A. Salvado, H. Kantarjian, Results of imatinib mesylate therapy in patients with refractory or recurrent acute myeloid leukemia, high-risk myelodysplastic syndrome, and myeloproliferative disorders, *Cancer*. 97 (2003) 2760–2766.
- [124] Z.Q. Xu, Y. Zhang, N. Li, P.J. Liu, L. Gao, X. Gao, X.J. Tie, Efficacy and safety of lapatinib and trastuzumab for HER2-positive breast cancer: A systematic review and meta-analysis of randomised controlled trials, *BMJ Open*. 7 (2017) 1–9.
- [125] B. Ricciuti, C. Genova, L. Crinò, M. Libra, G.C. Leonardi, Antitumor activity of larotrectinib in tumors harboring NTRK gene fusions: a short review on the current evidence, *Onco. Targets. Ther.* Volume 12 (2019) 3171–3179.
- [126] U. J. Patel, PharmD, MPH, M. May, PharmD, BCOP, Lenvatinib in the Treatment of Differentiated Thyroid Cancer and Advanced Renal Cell Carcinoma, *J. Adv. Pract. Oncol.* 8 (2017) 757–764.
- [127] B.J. Solomon, B. Besse, T.M. Bauer, E. Felip, R.A. Soo, D.R. Camidge, R. Chiari, A. Bearz, C.-C. Lin, S.M. Gadgeel, G.J. Riely, E.H. Tan, T. Seto, L.P. James, J.S. Clancy, A. Abbattista, J.-F. Martini, J. Chen, G. Peltz, H. Thurm, S.-H. Ignatius Ou, A.T. Shaw, Lorlatinib in patients with ALK-positive non-small-cell lung cancer: results from a global phase 2 study., *Lancet. Oncol.* 19 (2018) 1654–1667.
- [128] M. Levis, Midostaurin approved for FLT3-mutated AML, *Blood*. 129 (2017) 3403–3406.
- [129] D.J. DeAngelo, T.I. George, A. Linder, C. Langford, C. Perkins, J. Ma, P. Westervelt, J.D. Merker, C. Berube, S. Coutre, M. Liedtke, B. Medeiros, D. Sternberg, C. Dutreix, P.A. Ruffie, C. Corless, T.J. Graubert, J. Gotlib, Efficacy and safety of midostaurin in patients with advanced systemic mastocytosis: 10-year median follow-up of a phase II trial, *Leukemia*. 32 (2018) 470–478.
- [130] K.L. Blackwell, K. Zaman, S. Qin, K.H.R. Tkaczuk, M. Campone, D. Hunt, R. Bryce, L.J. Goldstein, 202 Study Group, Neratinib in Combination With Trastuzumab for the Treatment of Patients With Advanced HER2-positive Breast Cancer: A Phase I/II Study, *Clin. Breast Cancer*. 19 (2019) 97–104.
- [131] H. Kantarjian, F. Giles, L. Wunderle, K. Bhalla, S. O'Brien, B. Wassmann, C. Tanaka, P. Manley, P. Rae, W. Mietlowski, K. Bochinski, A. Hochhaus, J.D. Griffin, D. Hoelzer, M. Albitar, M. Dugan, J.

- Cortes, L. Alland, O.G. Ottmann, Nilotinib in Imatinib-Resistant CML and Philadelphia Chromosome-Positive ALL, *N. Engl. J. Med.* 354 (2006) 2542–2551.
- [132] E. Bendstrup, W. Wuyts, T. Alfaro, N. Chaudhuri, R. Cornelissen, M. Kreuter, K. Melgaard Nielsen, A.M.B. Münster, M. Myllärniemi, C. Ravaglia, T. Vanuytsel, M. Wijsenbeek, Nintedanib in idiopathic pulmonary fibrosis: Practical management recommendations for potential adverse events, *Respiration.* 97 (2019) 173–184.
- [133] T. Jiang, C. Su, S. Ren, F. Cappuzzo, G. Rocco, J.D. Palmer, N. van Zandwijk, F. Blackhall, X. Le, N.A. Pennell, C. Zhou, A consensus on the role of osimertinib in non-small cell lung cancer from the AME Lung Cancer Collaborative Group, *J. Thorac. Dis.* 10 (2018) 3909–3921.
- [134] D. Cella, J.L. Beaumont, Pazopanib in the treatment of advanced renal cell carcinoma, *Ther. Adv. Urol.* 8 (2016) 61–69.
- [135] E.D. Deeks, Pazopanib: In Advanced soft tissue sarcoma, *Drugs.* 72 (2012) 2129–2140.
- [136] J.E. Cortes, D.W. Kim, J. Pinilla-Ibarz, P.D. le Coutre, R. Paquette, C. Chuah, F.E. Nicolini, J.F. Apperley, H.J. Khoury, M. Talpaz, D.J. DeAngelo, E. Abruzzese, D. Rea, M. Baccarani, M.C. Müller, C. Gambacorti-Passerini, S. Lustgarten, V.M. Rivera, F.G. Haluska, F. Guilhot, M.W. Deininger, A. Hochhaus, T.P. Hughes, N.P. Shah, H.M. Kantarjian, Ponatinib efficacy and safety in Philadelphia chromosome-positive leukemia: final 5-year results of the phase 2 PACE trial, *Blood.* 132 (2018) 393–404.
- [137] A. Sartore-Bianchi, A. Zeppellini, A. Amatu, R. Ricotta, K. Bencardino, S. Siena, Regorafenib in metastatic colorectal cancer, *Expert Rev. Anticancer Ther.* 14 (2014) 255–265.
- [138] H.M. Kvasnicka, J. Thiele, C.E. Bueso-Ramos, W. Sun, J. Cortes, H.M. Kantarjian, S. Verstovsek, Long-term effects of ruxolitinib versus best available therapy on bone marrow fibrosis in patients with myelofibrosis, *J. Hematol. Oncol.* 11 (2018) 1–10.
- [139] M. Griesshammer, G. Saydam, F. Palandri, G. Benevolo, M. Egyed, J. Callum, T. Devos, S. Sivgin, P. Guglielmelli, C. Bensasson, M. Khan, J.P. Ronco, F. Passamonti, Ruxolitinib for the treatment of inadequately controlled polycythemia vera without splenomegaly: 80-week follow-up from the RESPONSE-2 trial, *Ann. Hematol.* 97 (2018) 1591–1600.
- [140] G.M. Keating, A. Santoro, Sorafenib: A review of its use in advanced hepatocellular carcinoma,

- Drugs. 69 (2009) 223–240.
- [141] C. Guevremont, C. Jeldres, P.I. Karakiewicz, F.I. Mija, Sorafenib in the Management of Metastatic Renal Cell Carcinoma, *Curr. Oncol.* 16 (2009) 27–32.
- [142] D.L.S. Danilovic, G. Castro, F.S.R. Roitberg, F.A.B. Vanderlei, F.A. Bonani, R.M.C. Freitas, G.B. Coura-Filho, R.Y. Camargo, M.A. Kulcsar, S. Marui, A.O. Hoff, Potential role of sorafenib as neoadjuvant therapy in unresectable papillary thyroid cancer, *Arch. Endocrinol. Metab.* 62 (2018) 370–375.
- [143] A.S. Abdelhameed, M.W. Attwa, N.S. Al-Shaklia, A.A. Kadi, A highly sensitive LC-MS/MS method to determine novel Bruton’s tyrosine kinase inhibitor spebrutinib: Application to metabolic stability evaluation, *R. Soc. Open Sci.* 6 (2019) 1–10.
- [144] N. Mulet-Margalef, X. Garcia-Del-Muro, Sunitinib in the treatment of gastrointestinal stromal tumor: Patient selection and perspectives, *Onco. Targets. Ther.* 9 (2016) 7573–7582.
- [145] S. Faivre, P. Niccoli, D. Castellano, J.W. Valle, P. Hammel, J.L. Raoul, A. Vinik, E. Van Cutsem, Y.J. Bang, S.H. Lee, I. Borbath, C. Lombard-Bohas, P. Metrakos, D. Smith, J.S. Chen, P. Ruzsniwski, J.F. Seitz, S. Patyna, D.R. Lu, K.J. Ishak, E. Raymond, Sunitinib in pancreatic neuroendocrine tumors: Updated progression-free survival and final overall survival from a phase III randomized study, *Ann. Oncol.* 28 (2017) 339–343.
- [146] B.I. Rini, T.E. Hutson, R.A. Figlin, M.J. Lechuga, O. Valota, L. Serfass, B. Rosbrook, R.J. Motzer, Sunitinib in Patients With Metastatic Renal Cell Carcinoma: Clinical Outcome According to International Metastatic Renal Cell Carcinoma Database Consortium Risk Group, *Clin. Genitourin. Cancer.* 16 (2018) 298–304.
- [147] Z.T. Al-Salama, L.J. Scott, Baricitinib: A Review in Rheumatoid Arthritis, *Drugs.* 78 (2018) 761–772.
- [148] S.A. Wells, B.G. Robinson, R.F. Gagel, H. Dralle, J.A. Fagin, M. Santoro, E. Baudin, R. Elisei, B. Jarzab, J.R. Vasselli, J. Read, P. Langmuir, A.J. Ryan, M.J. Schlumberger, Vandetanib in patients with locally advanced or metastatic medullary thyroid cancer: A randomized, double-blind phase III trial, *J. Clin. Oncol.* 30 (2012) 134–141.
- [149] H.J. Klümper, C.F. Samer, R.H.J. Mathijssen, J.H.M. Schellens, H. Gurney, Moving towards dose individualization of tyrosine kinase inhibitors, *Cancer Treat. Rev.* 37 (2011) 251–260.

- [150] B. Gao, S. Yeap, A. Clements, B. Balakrishnar, M. Wong, H. Gurney, Evidence for therapeutic drug monitoring of targeted anticancer therapies, *J. Clin. Oncol.* 30 (2012) 4017–4025.
- [151] H. Glavinas, P. Krajcsi, J. Cserepes, B. Sarkadi, The role of ABC transporters in drug resistance, metabolism and toxicity., *Curr. Drug Deliv.* 1 (2004) 27–42.
- [152] S. Marchetti, N.A. de Vries, T. Buckle, M.J. Bolijn, M.A.J. van Eijndhoven, J.H. Beijnen, R. Mazzanti, O. van Tellingen, J.H.M. Schellens, Effect of the ATP-binding cassette drug transporters ABCB1, ABCG2, and ABCC2 on erlotinib hydrochloride (Tarceva) disposition in in vitro and in vivo pharmacokinetic studies employing *Bcrp1*^{-/-}/*Mdr1a/1b*^{-/-} (triple-knockout) and wild-type mice, *Mol. Cancer Ther.* 7 (2008) 2280–2287.
- [153] J.S. Lagas, R.A.B. van Waterschoot, R.W. Sparidans, E. Wagenaar, J.H. Beijnen, A.H. Schinkel, Breast Cancer Resistance Protein and P-glycoprotein Limit Sorafenib Brain Accumulation, *Mol. Cancer Ther.* 9 (2010) 319–326.
- [154] T. Mizuno, M. Fukudo, T. Fukuda, T. Terada, M. Dong, T. Kamba, T. Yamasaki, O. Ogawa, T. Katsura, K.I. Inui, A.A. Vinks, K. Matsubara, The Effect of ABCG2 genotype on the population pharmacokinetics of sunitinib in patients with renal cell carcinoma, *Ther. Drug Monit.* 36 (2014) 310–316.
- [155] J. Li, M. Zhao, P. He, M. Hidalgo, S.D. Baker, Differential metabolism of gefitinib and erlotinib by human cytochrome P450 enzymes, *Clin. Cancer Res.* 13 (2007) 3731–3737.
- [156] F. Thomas, P. Rochaix, M. White-Koning, I. Hennebelle, J. Sarini, A. Benlyazid, L. Malard, J.L. Lefebvre, E. Chatelut, J.P. Delord, Population pharmacokinetics of erlotinib and its pharmacokinetic/pharmacodynamic relationships in head and neck squamous cell carcinoma, *Eur. J. Cancer.* 45 (2009) 2316–2323.
- [157] T. Mizuno, T. Terada, T. Kamba, M. Fukudo, T. Katsura, E. Nakamura, O. Ogawa, K. Inui, ABCG2 421C>A polymorphism and high exposure of sunitinib in a patient with renal cell carcinoma, *Ann. Oncol.* 21 (2010) 1382–1383.
- [158] Z.P. Jiang, X.L. Zhao, N. Takahashi, S. Angelini, B. Dubashi, L. Sun, P. Xu, Trough concentration and ABCG2 polymorphism are better to predict imatinib response in chronic myeloid leukemia: A meta-analysis, *Pharmacogenomics.* 18 (2017) 35–56.

- [159] T. Mizuno, M. Fukudo, T. Terada, T. Kamba, E. Nakamura, O. Ogawa, K.-I. Inui, T. Katsura, Impact of Genetic Variation in Breast Cancer Resistance Protein (BCRP/ABCG2) on Sunitinib Pharmacokinetics, *Drug Metab. Pharmacokinet.* 27 (2012) 631–639.
- [160] H.R. Kim, H.S. Park, W.S. Kwon, J.H. Lee, Y. Tanigawara, S.M. Lim, H.S. Kim, S.J. Shin, J.B. Ahn, S.Y. Rha, Pharmacogenetic determinants associated with sunitinib-induced toxicity and ethnic difference in Korean metastatic renal cell carcinoma patients, *Cancer Chemother. Pharmacol.* 72 (2013) 825–835.
- [161] K.M. Giacomini, P. V Balimane, S.K. Cho, M. Eadon, T. Edeki, K.M. Hillgren, S.M. Huang, Y. Sugiyama, D. Weitz, Y. Wen, C.Q. Xia, S.W. Yee, H. Zimdahl, M. Niemi, International transporter consortium commentary on clinically important transporter polymorphisms, *Clin. Pharmacol. Ther.* 94 (2013) 23–26.
- [162] K. Furukawa, J. Ishida, M. Inagaki, K. Takabe, S. Ishikawa, M. Sakai, H. Ichimura, K. Kamiyama, T. Kaburagi, K. Hayashihara, K. Kishi, M. Saito, H. Satoh, A population-based study of gefitinib in patients with postoperative recurrent non-small cell lung cancer, *Exp. Ther. Med.* 3 (2012) 53–59.
- [163] J.R. Hecht, Y.J. Bang, S.K. Qin, H.C. Chung, J.M. Xu, J.O. Park, K. Jeziorski, Y. Shparyk, P.M. Hoff, A. Sobrero, P. Salman, J. Li, S.A. Protsenko, Z.A. Wainberg, M. Buyse, K. Afenjar, V. Houè, A. Garcia, T. Kaneko, Y. Huang, S. Khan-Wasti, S. Santillana, M.F. Press, D. Slamon, Lapatinib in combination with capecitabine plus oxaliplatin in human epidermal growth factor receptor 2-positive advanced or metastatic gastric, esophageal, or gastroesophageal adenocarcinoma: TRIO-013/LOGiC - A randomized phase III trial, *J. Clin. Oncol.* 34 (2016) 443–451.
- [164] T. Yoshino, Y. Komatsu, Y. Yamada, K. Yamazaki, A. Tsuji, T. Ura, A. Grothey, E. Van Cutsem, A. Wagner, F. Cihon, Y. Hamada, A. Ohtsu, Randomized phase III trial of regorafenib in metastatic colorectal cancer: Analysis of the CORRECT Japanese and non-Japanese subpopulations, *Invest. New Drugs.* 33 (2015) 740–750.
- [165] J.R. Johnson, M. Cohen, R. Sridhara, Y.F. Chen, G.M. Williams, J. Duan, J. Gobburu, B. Booth, K. Benson, J. Leighton, L.S. Hsieh, N. Chidambaram, P. Zimmerman, R. Pazdur, Approval summary for erlotinib for treatment of patients with locally advanced or metastatic non-small cell lung cancer after failure of at least one prior chemotherapy regimen, *Clin. Cancer Res.* 11 (2005) 6414–6421.

- [166] P. Di Gion, F. Kanefendt, A. Lindauer, M. Scheffler, O. Doroshenko, U. Fuhr, J. Wolf, U. Jaehde, Clinical pharmacokinetics of tyrosine kinase inhibitors: Focus on pyrimidines, pyridines and pyrroles, *Clin. Pharmacokinet.* 50 (2011) 551–603.
- [167] R.W.F. van Leeuwen, F.G.A. Jansman, N.G. Hunfeld, R. Peric, A.K.L. Reyners, A.L.T. Imholz, J.R.B.J. Brouwers, J.G. Aerts, T. van Gelder, R.H.J. Mathijssen, Tyrosine Kinase Inhibitors and Proton Pump Inhibitors: An Evaluation of Treatment Options, *Clin. Pharmacokinet.* 56 (2017) 683–688.
- [168] K.S. Thomas, A. Billingsley, N. Amarshi, B.A. Nair, Elevated international normalized ratio associated with concomitant warfarin and erlotinib, *Am. J. Heal. Pharm.* 67 (2010) 1426–1429.
- [169] A.E.C.A.B. Willemsen, F.J.E. Lubberman, J. Tol, W.R. Gerritsen, C.M.L. Van Herpen, N.P. Van Erp, Effect of food and acid-reducing agents on the absorption of oral targeted therapies in solid tumors, *Drug Discov. Today.* 21 (2016) 962–976.
- [170] R.C. Kane, A.T. Farrell, H. Saber, S. Tang, G. Williams, J.M. Jee, C. Liang, B. Booth, N. Chidambaram, D. Morse, R. Sridhara, P. Garvey, R. Justice, R. Pazdur, Sorafenib for the treatment of advanced renal cell carcinoma, *Clin. Cancer Res.* 12 (2006) 7271–7278.
- [171] M. Hamilton, J.L. Wolf, J. Rusk, S.E. Beard, G.M. Clark, K. Witt, P.J. Cagnoni, Effects of smoking on the pharmacokinetics of erlotinib, *Clin. Cancer Res.* 12 (2006) 2166–2171.
- [172] D. Marin, A. Bazeos, F.X. Mahon, L. Eliasson, D. Milojkovic, M. Bua, J.F. Apperley, R. Szydlo, R. Desai, K. Kozlowski, C. Paliompeis, V. Latham, L. Foroni, M. Molimard, A. Reid, K. Rezvani, H. De Lavallade, C. Guallar, J. Goldman, J.S. Khorashad, Adherence is the critical factor for achieving molecular responses in patients with chronic myeloid leukemia who achieve complete cytogenetic responses on imatinib, *J. Clin. Oncol.* 28 (2010) 2381–2388.
- [173] D.M. Geynisman, K.E. Wickersham, Adherence to targeted oral anticancer medications., *Discov. Med.* 15 (2013) 231–41.
- [174] L. Timmers, C.C. Boons, D. Mangnus, J.E. Moes, E.L. Swart, E. Boven, E.F. Smit, J.G. Hugtenburg, The use of erlotinib in daily practice: A study on adherence and patients' experiences, *BMC Cancer.* 11 (2011) 284.
- [175] T.H. Booij, H. Bange, W.N. Leonhard, K. Yan, M. Fokkelman, S.J. Kunnen, J.G. Dauwerse, Y. Qin, B. van de Water, G.J.P. van Westen, D.J.M. Peters, L.S. Price, High-Throughput Phenotypic Screening

- of Kinase Inhibitors to Identify Drug Targets for Polycystic Kidney Disease, *SLAS Discov.* 22 (2017) 974–984.
- [176] D. Bertholee, J.G. Maring, A.B.P. van Kuilenburg, Genotypes Affecting the Pharmacokinetics of Anticancer Drugs, *Clin. Pharmacokinet.* 56 (2017) 317–337.
- [177] D. Sabanathan, A. Zhang, P. Fox, S. Coulter, V. Gebiski, B. Balakrishnar, M. Chan, C. Liddle, H. Gurney, Dose individualization of sunitinib in metastatic renal cell cancer: toxicity-adjusted dose or therapeutic drug monitoring, *Cancer Chemother. Pharmacol.* 80 (2017) 385–393.
- [178] B.A. Wolf, Overview of therapeutic drug monitoring and biotechnologic drugs, *Ther. Drug Monit.* 18 (1996) 402–404.
- [179] E. Spina, C. Hiemke, J. De Leon, Assessing drug-drug interactions through therapeutic drug monitoring when administering oral second-generation antipsychotics, *Expert Opin. Drug Metab. Toxicol.* 12 (2016) 407–422.
- [180] M. Boffito, E. Acosta, D. Burger, C. V Fletcher, C. Flexner, R. Garaffo, G. Gatti, M. Kurowski, C.F. Perno, G. Peytavin, M. Regazzi, D. Back, Therapeutic drug monitoring and drug-drug interactions involving antiretroviral drugs, *Antivir. Ther.* 10 (2005) 469–477.
- [181] A.S. Gross, Best practice in therapeutic drug monitoring, *Br. J. Clin. Pharmacol.* 46 (1998) 95–99.
- [182] H.L. McLeod, Therapeutic drug monitoring opportunities in cancer therapy, *Pharmacol. Ther.* 74 (1997) 39–54.
- [183] M.E. De Jonge, A.D.R. Huitema, J.H.M. Schellens, S. Rodenhuis, J.H. Beijnen, Individualised cancer chemotherapy: Strategies and performance of prospective studies on therapeutic drug monitoring with dose adaptation: A review, *Clin. Pharmacokinet.* 44 (2005) 147–173.
- [184] H.R. Ashbee, R.A. Barnes, E.M. Johnson, M.D. Richardson, R. Gorton, W.W. Hope, Therapeutic drug monitoring (TDM) of antifungal agents: Guidelines from the british society for medical mycology, *J. Antimicrob. Chemother.* 69 (2014) 1162–1176.
- [185] T. Terada, S. Noda, K.I. Inui, Management of dose variability and side effects for individualized cancer pharmacotherapy with tyrosine kinase inhibitors, *Pharmacol. Ther.* 152 (2015) 125–134.
- [186] J. Rodríguez, G. Castañeda, L. Muñoz, J.C. Villa, Quantitation of sunitinib, an oral multitarget tyrosine kinase inhibitor, and its metabolite in urine samples by nonaqueous capillary

- electrophoresis time of flight mass spectrometry, *Electrophoresis*. 36 (2015) 1580–1587.
- [187] T. Velpandian, R. Mathur, N.K. Agarwal, B. Arora, L. Kumar, S.K. Gupta, Development and validation of a simple liquid chromatographic method with ultraviolet detection for the determination of imatinib in biological samples, *J. Chromatogr. B Anal. Technol. Biomed. Life Sci.* 804 (2004) 431–434.
- [188] R.L. Oostendorp, J.H. Beijnen, J.H.M. Schellens, O. van Tellingen, Determination of imatinib mesylate and its main metabolite (CGP74588) in human plasma and murine specimens by ion-pairing reversed-phase high-performance liquid chromatography, *Biomed. Chromatogr.* 21 (2007) 747–754.
- [189] A. Davies, A.K. Hayes, K. Knight, S.J. Watmough, M. Pirmohamed, R.E. Clark, Simultaneous determination of nilotinib, imatinib and its main metabolite (CGP-74588) in human plasma by ultra-violet high performance liquid chromatography, *Leuk. Res.* 34 (2010) 702–707.
- [190] E. Pirro, S. De Francia, F. De Martino, C. Fava, S. Ulisciani, G.R. Cambrin, S. Racca, G. Saglio, F. Di Carlo, A new HPLC-UV validated method for therapeutic drug monitoring of tyrosine kinase inhibitors in leukemic patients, *J. Chromatogr. Sci.* 49 (2011) 753–757.
- [191] A.A. Golabchifar, M.R. Rouini, B. Shafaghi, S. Rezaee, A. Foroumadi, M.R. Khoshayand, Optimization of the simultaneous determination of imatinib and its major metabolite, CGP74588, in human plasma by a rapid HPLC method using D-optimal experimental design, *Talanta*. 85 (2011) 2320–2329.
- [192] M. Miura, N. Takahashi, K.I. Sawada, Quantitative determination of imatinib in human plasma with high-performance liquid chromatography and ultraviolet detection, *J. Chromatogr. Sci.* 49 (2011) 412–415.
- [193] L. Faivre, C. Gomo, O. Mir, F. Taieb, A. Schoemann-Thomas, S. Ropert, M. Vidal, D. Dusser, A. Dauphin, F. Goldwasser, B. Blanchet, A simple HPLC-UV method for the simultaneous quantification of gefitinib and erlotinib in human plasma, *J. Chromatogr. B Anal. Technol. Biomed. Life Sci.* 879 (2011) 2345–2350.
- [194] Y. Zheng, A. Thomas-Schoemann, L. Sakji, P. Boudou-Rouquette, N. Dupin, L. Mortier, M. Vidal, F. Goldwasser, B. Blanchet, An HPLC-UV method for the simultaneous quantification of vemurafenib and erlotinib in plasma from cancer patients, *J. Chromatogr. B Anal. Technol.*

- Biomed. Life Sci. 928 (2013) 93–37.
- [195] B. Blanchet, B. Billefont, J. Cramard, A.S. Benichou, S. Chhun, L. Harcouet, S. Ropert, A. Dauphin, F. Goldwasser, M. Tod, Validation of an HPLC-UV method for sorafenib determination in human plasma and application to cancer patients in routine clinical practice, *J. Pharm. Biomed. Anal.* 49 (2009) 1109–1114.
- [196] M. Dziadosz, R. Lessig, H. Bartels, HPLC-DAD protein kinase inhibitor analysis in human serum, *J. Chromatogr. B Anal. Technol. Biomed. Life Sci.* 893 (2012) 77–81.
- [197] V. Escudero-Ortiz, J.J. Pérez-Ruixo, B. Valenzuela, Development and Validation of a High-Performance Liquid Chromatography Ultraviolet Method for Lapatinib Quantification in Human Plasma, *Ther. Drug Monit.* 35 (2013) 796–802.
- [198] V. Escudero-Ortiz, J.J. Pérez-Ruixo, B. Valenzuela, Development and validation of an HPLC-UV method for pazopanib quantification in human plasma and application to patients with cancer in routine clinical practice, *Ther. Drug Monit.* 37 (2015) 172–179.
- [199] M. Ohgami, M. Homma, Y. Suzuki, K. Naito, M. Yamada, S. Mitsuhashi, F. Fujisawa, H. Kojima, T. Kaburagi, K. Uchiumi, Y. Yamada, H. Bando, H. Hara, K. Takei, A simple high-performance liquid chromatography for determining lapatinib and erlotinib in human plasma, *Ther. Drug Monit.* 38 (2016) 657–662.
- [200] B. Blanchet, C. Saboureau, A.S. Benichou, B. Billefont, F. Taieb, S. Ropert, A. Dauphin, F. Goldwasser, M. Tod, Development and validation of an HPLC-UV-visible method for sunitinib quantification in human plasma, *Clin. Chim. Acta.* 404 (2009) 134–139.
- [201] M.C. Etienne-Grimaldi, N. Renée, H. Izzedine, G. Milano, A routine feasible HPLC analysis for the anti-angiogenic tyrosine kinase inhibitor, sunitinib, and its main metabolite, SU12662, in plasma, *J. Chromatogr. B Anal. Technol. Biomed. Life Sci.* 877 (2009) 3757–3761.
- [202] B. Pang, Y. Zhu, L. Lu, F. Gu, H. Chen, The Applications and Features of Liquid Chromatography-Mass Spectrometry in the Analysis of Traditional Chinese Medicine, *Evidence-Based Complement. Altern. Med.* 2016 (2016) 1–7.
- [203] R. Bakhtiar, J. Lohne, L. Ramos, L. Khemani, M. Hayes, F. Tse, High-throughput quantification of the anti-leukemia drug STI571 (Gleevec™) and its main metabolite (CGP 74588) in human plasma

- using liquid chromatography-tandem mass spectrometry, *J. Chromatogr. B Anal. Technol. Biomed. Life Sci.* 768 (2002) 325–340.
- [204] R.A. Parise, R.K. Ramanathan, M.J. Hayes, M.J. Egorin, Liquid chromatographic-mass spectrometric assay for quantitation of imatinib and its main metabolite (CGP 74588) in plasma, *J. Chromatogr. B Anal. Technol. Biomed. Life Sci.* 791 (2003) 39–44.
- [205] G. Guetens, G. De Boeck, M. Highley, H. Dumez, A.T. Van Oosterom, E.A. De Bruijn, Quantification of the anticancer agent STI-571 in erythrocytes and plasma by measurement of sediment technology and liquid chromatography-tandem mass spectrometry, *J. Chromatogr. A.* 1020 (2003) 27–34.
- [206] L. Couchman, M. Birch, R. Ireland, A. Corrigan, S. Wickramasinghe, D. Josephs, J. Spicer, R.J. Flanagan, An automated method for the measurement of a range of tyrosine kinase inhibitors in human plasma or serum using turbulent flow liquid chromatography–tandem mass spectrometry, *Anal. Bioanal. Chem.* 403 (2012) 1685–1695.
- [207] N.A.G. Lankheet, M.J.X. Hillebrand, H. Rosing, J.H.M. Schellens, J.H. Beijnen, A.D.R. Huitema, Method development and validation for the quantification of dasatinib, erlotinib, gefitinib, imatinib, lapatinib, nilotinib, sorafenib and sunitinib in human plasma by liquid chromatography coupled with tandem mass spectrometry, *Biomed. Chromatogr.* 27 (2013) 466–476.
- [208] A. Chahbouni, J.C.G. Den Burger, R.M. Vos, A. Sinjewel, A.J. Wilhelm, Simultaneous quantification of erlotinib, gefitinib, and imatinib in human plasma by liquid chromatography tandem mass spectrometry, *Ther. Drug Monit.* 31 (2009) 683–687.
- [209] S. Bouchet, E. Chauzit, D. Ducint, N. Castaing, M. Canal-Raffin, N. Moore, K. Titier, M. Molimard, Simultaneous determination of nine tyrosine kinase inhibitors by 96-well solid-phase extraction and ultra performance LC/MS-MS, *Clin. Chim. Acta.* 412 (2011) 1060–1067.
- [210] N.P. Van Erp, D. de Wit, H.J. Guchelaar, H. Gelderblom, T.J. Hesting, J. den Hartigh, A validated assay for the simultaneous quantification of six tyrosine kinase inhibitors and two active metabolites in human serum using liquid chromatography coupled with tandem mass spectrometry, *J. Chromatogr. B Anal. Technol. Biomed. Life Sci.* 937 (2013) 33–43.
- [211] A. Haouala, B. Zanolari, B. Rochat, M. Montemurro, K. Zaman, M.A. Duchosal, H.B. Ris, S. Leyvraz, N. Widmer, L.A. Decosterd, Therapeutic Drug Monitoring of the new targeted anticancer agents

- imatinib, nilotinib, dasatinib, sunitinib, sorafenib and lapatinib by LC tandem mass spectrometry, *J. Chromatogr. B.* 877 (2009) 1982–1996.
- [212] E. Kralj, J. Trontelj, T. Pajič, A. Kristl, Simultaneous measurement of imatinib, nilotinib and dasatinib in dried blood spot by ultra high performance liquid chromatography tandem mass spectrometry, *J. Chromatogr. B Anal. Technol. Biomed. Life Sci.* 903 (2012) 150–156.
- [213] A.R. Masters, C.J. Sweeney, D.R. Jones, The quantification of erlotinib (OSI-774) and OSI-420 in human plasma by liquid chromatography-tandem mass spectrometry, *J. Chromatogr. B Anal. Technol. Biomed. Life Sci.* 848 (2007) 379–383.
- [214] L. Li, M. Zhao, F. Navid, K. Pratz, B.D. Smith, M.A. Rudek, S.D. Baker, Quantitation of sorafenib and its active metabolite sorafenib N-oxide in human plasma by liquid chromatography-tandem mass spectrometry, *J. Chromatogr. B.* 878 (2010) 3033–3038.
- [215] M. Allard, N. Khoudour, B. Rousseau, C. Joly, C. Costentin, B. Blanchet, C. Tournigand, A. Hulin, Simultaneous analysis of regorafenib and sorafenib and three of their metabolites in human plasma using LC-MS/MS, *J. Pharm. Biomed. Anal.* 142 (2017) 42–48.
- [216] M. Zhao, M.A. Rudek, P. He, F.T. Hafner, M. Radtke, J.J. Wright, B.D. Smith, W.A. Messersmith, M. Hidalgo, S.D. Baker, A rapid and sensitive method for determination of sorafenib in human plasma using a liquid chromatography/tandem mass spectrometry assay, *J. Chromatogr. B Anal. Technol. Biomed. Life Sci.* 846 (2007) 1–7.
- [217] F. Bai, B.B. Freeman, C.H. Fraga, M. Fouladi, C.F. Stewart, Determination of lapatinib (GW572016) in human plasma by liquid chromatography electrospray tandem mass spectrometry (LC-ESI-MS/MS), *J. Chromatogr. B Anal. Technol. Biomed. Life Sci.* 831 (2006) 169–175.
- [218] J. Musijowski, M. Filist, P.J. Rudzki, Sensitive single quadrupole LC/MS method for determination of lapatinib in human plasma, *Acta Pol. Pharm. - Drug Res.* 71 (2014) 1029–1036.
- [219] S. Roche, G. McMahon, M. Clynes, R. O'Connor, Development of a high-performance liquid chromatographic-mass spectrometric method for the determination of cellular levels of the tyrosine kinase inhibitors lapatinib and dasatinib, *J. Chromatogr. B Anal. Technol. Biomed. Life Sci.* 877 (2009) 3982–3990.
- [220] C. Pressiat, H.H. Huynh, A. Plé, H. Sauvageon, I. Madelaine, C. Chougnnet, C. Le Maignan, S.

- Mourah, L. Goldwirt, Development and validation of a simultaneous quantification method of ruxolitinib, vismodegib, olaparib, and pazopanib in human plasma using liquid chromatography coupled with tandem mass spectrometry, *Ther. Drug Monit.* 40 (2018) 337–343.
- [221] M. Birch, P.E. Morgan, S. Handley, A. Ho, R. Ireland, R.J. Flanagan, Simple methodology for the therapeutic drug monitoring of the tyrosine kinase inhibitors dasatinib and imatinib, *Biomed. Chromatogr.* 27 (2013) 335–342.
- [222] A. D’Avolio, M. Simiele, S. De Francia, A. Ariaudo, L. Baietto, J. Cusato, C. Fava, G. Saglio, F. Di Carlo, G. Di Perri, HPLC-MS method for the simultaneous quantification of the antileukemia drugs imatinib, dasatinib and nilotinib in human peripheral blood mononuclear cell (PBMC), *J. Pharm. Biomed. Anal.* 59 (2012) 109–116.
- [223] R.A. Parise, M.J. Egorin, S.M. Christner, D.D. Shah, W. Zhou, J.H. Beumer, A high-performance liquid chromatography-mass spectrometry assay for quantitation of the tyrosine kinase inhibitor nilotinib in human plasma and serum, *J. Chromatogr. B Anal. Technol. Biomed. Life Sci.* 877 (2009) 1894–1900.
- [224] A.S. Abdelhameed, M.W. Attwa, A.A. Kadi, An LC–MS/MS method for rapid and sensitive high-throughput simultaneous determination of various protein kinase inhibitors in human plasma, *Biomed. Chromatogr.* 31 (2017) e3793.
- [225] C. Merienne, M. Rousset, D. Ducint, N. Castaing, K. Titier, M. Molimard, S. Bouchet, High throughput routine determination of 17 tyrosine kinase inhibitors by LC–MS/MS, *J. Pharm. Biomed. Anal.* 150 (2018) 112–120.
- [226] M. Herbrink, N. de Vries, H. Rosing, A.D.R. Huitema, B. Nuijen, J.H.M. Schellens, J.H. Beijnen, Quantification of 11 Therapeutic Kinase Inhibitors in Human Plasma for Therapeutic Drug Monitoring Using Liquid Chromatography Coupled With Tandem Mass Spectrometry., *Ther. Drug Monit.* 38 (2016) 649–656.
- [227] M. van Dyk, J.O. Miners, G. Kichenadasse, R.A. McKinnon, A. Rowland, A novel approach for the simultaneous quantification of 18 small molecule kinase inhibitors in human plasma: A platform for optimised KI dosing, *J. Chromatogr. B Anal. Technol. Biomed. Life Sci.* 1033 (2016) 17–26.
- [228] S.J.K.A. Ubhayasekera, W. Aluthgedara, B. Ek, J. Bergquist, Simultaneous quantification of imatinib and CGP74588 in human plasma by liquid chromatography-time of flight mass

- spectrometry (LC-TOF-MS), *Anal. Methods*. 8 (2016) 3046–3054.
- [229] S.M. Amer, A.A. Kadi, H.W. Darwish, M.W. Attwa, Liquid chromatography tandem mass spectrometry method for the quantification of vandetanib in human plasma and rat liver microsomes matrices: Metabolic stability investigation, *Chem. Cent. J.* 11 (2017) 1–8.
- [230] A. Svedberg, H. Gréen, A. Vikström, J. Lundeberg, S. Vikingsson, A validated liquid chromatography tandem mass spectrometry method for quantification of erlotinib, OSI-420 and didesmethyl erlotinib and semi-quantification of erlotinib metabolites in human plasma, *J. Pharm. Biomed. Anal.* 107 (2015) 186–195.
- [231] C.L. Braal, G.D.M. Veerman, R. Peric, J.G.J.V. Aerts, R.H.J. Mathijssen, S.L.W. Koolen, P. de Bruijn, Quantification of the tyrosine kinase inhibitor erlotinib in human scalp hair by liquid chromatography-tandem mass spectrometry: pitfalls for clinical application, *J. Pharm. Biomed. Anal.* 172 (2019) 175–182.
- [232] M. V. Chatziathanasiadou, E.K. Stylos, E. Giannopoulou, M.H. Spyridaki, E. Briasoulis, H.P. Kalofonos, T. Crook, N. Syed, G.B. Sivolapenko, A.G. Tzakos, Development of a validated LC-MS/MS method for the in vitro and in vivo quantitation of sunitinib in glioblastoma cells and cancer patients, *J. Pharm. Biomed. Anal.* 164 (2019) 690–697.
- [233] R.B. Verheijen, B. Thijssen, H. Rosing, J.H.M. Schellens, L. Nan, N. Venekamp, J.H. Beijnen, N. Steeghs, A.D.R. Huitema, Fast and Straightforward Method for the Quantification of Pazopanib in Human Plasma Using LC-MS/MS, *Ther. Drug Monit.* 40 (2018) 230–236.
- [234] E. Cardoso, T. Mercier, A.D. Wagner, K. Homicsko, O. Michielin, K. Ellefsen-Lavoie, L. Cagnon, M. Diezi, T. Buclin, N. Widmer, C. Csajka, L. Decosterd, Quantification of the next-generation oral anti-tumor drugs dabrafenib, trametinib, vemurafenib, cobimetinib, pazopanib, regorafenib and two metabolites in human plasma by liquid chromatography-tandem mass spectrometry, *J. Chromatogr. B Anal. Technol. Biomed. Life Sci.* 1083 (2018) 124–136.
- [235] T. Kawaguchi, A. Hamada, C. Hirayama, R. Nakashima, T. Nambu, Y. Yamakawa, H. Watanabe, K. Horikawa, H. Mitsuya, H. Saito, Relationship between an effective dose of imatinib, body surface area, and trough drug levels in patients with chronic myeloid leukemia, *Int. J. Hematol.* 89 (2009) 642–648.
- [236] Y. Yin, J. Xiang, S. Tang, J. Chen, Q. Yu, B. Zhang, A lower dosage of imatinib in patients with

- gastrointestinal stromal tumors with toxicity of the treatment, *Medicine (Baltimore)*. 95 (2016) 1–5.
- [237] T.I. Mughal, A. Schrieber, Principal long-term adverse effects of imatinib in patients with chronic myeloid leukemia in chronic phase, *Biol. Targets Ther.* 4 (2010) 315–323.
- [238] B. Peng, M. Hayes, D. Resta, A. Racine-Poon, B.J. Druker, M. Talpaz, C.L. Sawyers, M. Rosamilia, J. Ford, P. Lloyd, R. Capdeville, Pharmacokinetics and pharmacodynamics of imatinib in a phase I trial with chronic myeloid leukemia patients, *J. Clin. Oncol.* 22 (2004) 935–942.
- [239] V.M. Rezende, A.J. Rivellis, M.M. Gomes, F.A. Dörr, M.M.Y. Novaes, L. Nardinelli, A.L. de L. Costa, D. de A.F. Chamone, I. Bendit, Determination of serum levels of imatinib mesylate in patients with chronic myeloid leukemia: Validation and application of a new analytical method to monitor treatment compliance, *Rev. Bras. Hematol. Hemoter.* 35 (2013) 103–108.
- [240] Y. Liu, Y. Zhang, G. Feng, Q. Niu, S. Xu, Y. Yan, S. Li, M. Jing, Comparison of effectiveness and adverse effects of gefitinib, erlotinib and icotinib among patients with non-small cell lung cancer: A network meta-analysis, *Exp. Ther. Med.* 14 (2017) 4017–4032.
- [241] N.A.G. Lankheet, L.M. Knapen, J.H.M. Schellens, J.H. Beijnen, N. Steeghs, A.D.R. Huitema, Plasma concentrations of tyrosine kinase inhibitors imatinib, erlotinib, and sunitinib in routine clinical outpatient cancer care, *Ther. Drug Monit.* 36 (2014) 326–334.
- [242] N.A.G. Lankheet, E.E. Schaake, H. Rosing, J.A. Burgers, J.H.M. Schellens, J.H. Beijnen, A.D.R. Huitema, Quantitative determination of erlotinib and O-desmethyl erlotinib in human EDTA plasma and lung tumor tissue, *Bioanalysis.* 4 (2012) 2563–2577.
- [243] M. Steffens, T. Paul, V. Hichert, C. Scholl, D. Von Mallek, C. Stelzer, F. Sörgel, B. Reiser, C. Schumann, S. Rüdiger, S. Boeck, V. Heinemann, V. Kächele, T. Seufferlein, J. Stingl, Dosing to rash? - The role of erlotinib metabolic ratio from patient serum in the search of predictive biomarkers for EGFR inhibitor-mediated skin rash, *Eur. J. Cancer.* 55 (2016) 131–139.
- [244] W. De Hsiao, C.Y. Peng, P.H. Chuang, H.C. Lai, K.S. Cheng, J.W. Chou, Y.Y. Chen, C.J. Yu, C.L. Feng, W.P. Su, S.H. Chen, J.T. Kao, Evaluation of dose-efficacy of sorafenib and effect of transarterial chemoembolization in hepatocellular carcinoma patients: A retrospective study, *BMC Gastroenterol.* 16 (2016) 1–9.

- [245] Y. Li, Z.H. Gao, X.J. Qu, The adverse effects of sorafenib in patients with advanced cancers, *Basic Clin. Pharmacol. Toxicol.* 116 (2015) 216–221.
- [246] N.P. van Erp, H. Gelderblom, H.J. Guchelaar, Clinical pharmacokinetics of tyrosine kinase inhibitors, *Cancer Treat. Rev.* 35 (2009) 692–706.
- [247] F.L. Opdam, H.-J. Guchelaar, J.H. Beijnen, J.H.M. Schellens, Lapatinib for Advanced or Metastatic Breast Cancer, *Oncologist.* 17 (2012) 536–542.
- [248] B. Thiessen, C. Stewart, M. Tsao, S. Kamel-Reid, P. Schaiquevich, W. Mason, J. Easaw, K. Belanger, P. Forsyth, L. McIntosh, E. Eisenhauer, A phase I/II trial of GW572016 (lapatinib) in recurrent glioblastoma multiforme: Clinical outcomes, pharmacokinetics and molecular correlation, *Cancer Chemother. Pharmacol.* 65 (2010) 353–361.
- [249] D. Chatsipiroios, Safety profile and clinical recommendations for the use of lapatinib, *Breast Care.* 5 (2010) 16–21.
- [250] K.D. Hardy, M.D. Wahlin, I. Papageorgiou, J.D. Unadkat, A.E. Rettie, S.D. Nelson, Studies on the role of metabolic activation in tyrosine kinase inhibitor-dependent hepatotoxicity: Induction of CYP3A4 enhances the cytotoxicity of lapatinib in HepaRG cells, *Drug Metab. Dispos.* 42 (2014) 162–171.
- [251] P. Mlejnek, P. Dolezel, E. Faber, P. Kosztyu, Interactions of N-desmethyl imatinib, an active metabolite of imatinib, with P-glycoprotein in human leukemia cells, *Ann. Hematol.* 90 (2011) 837–842.
- [252] J. Ling, K.A. Johnson, Z. Miao, A. Rakhit, M.P. Pantze, M. Hamilton, B.L. Lum, C. Prakash, Metabolism and excretion of erlotinib, a small molecule inhibitor of epidermal growth factor receptor tyrosine kinase, in healthy male volunteers, *Drug Metab. Dispos.* 34 (2006) 420–426.
- [253] D.T. Rossi, K.G. Miller, Sample preparation methods for the analysis of pharmaceutical materials, *Sep. Sci. Technol.* 5 (2004) 165–201.
- [254] N.Y. Ashri, M. Abdel-Rehim, Sample treatment based on extraction techniques in biological matrices, *Bioanalysis.* 3 (2011) 2003–2018.
- [255] C. Polson, P. Sarkar, B. Incledon, V. Raguvaran, R. Grant, Optimization of protein precipitation based upon effectiveness of protein removal and ionization effect in liquid chromatography-

- tandem mass spectrometry., *J. Chromatogr. B. Analyt. Technol. Biomed. Life Sci.* 785 (2003) 263–75.
- [256] D.A. Wells, *Bioanalytical applications: solid-phase extraction*, in: *Encycl. Sep. Sci.*, Academic Press, 2000: pp. 2142–2146.
- [257] O. Kretz, H.M. Weiss, M.M. Schumacher, G. Gross, *In vitro* blood distribution and plasma protein binding of the tyrosine kinase inhibitor imatinib and its active metabolite, CGP74588, in rat, mouse, dog, monkey, healthy humans and patients with acute lymphatic leukaemia, *Br. J. Clin. Pharmacol.* 58 (2004) 212–216.
- [258] S.R. Christiansen, A. Broniscer, J.C. Panetta, C.F. Stewart, Pharmacokinetics of erlotinib for the treatment of high-grade glioma in a pediatric patient with cystic fibrosis: Case report and review of the literature, *Pharmacotherapy.* 29 (2009) 858–866.
- [259] M.C. Villarroel, K.W. Pratz, L. Xu, J.J. Wright, B.D. Smith, M.A. Rudek, Plasma protein binding of sorafenib, a multi kinase inhibitor: *In vitro* and in cancer patients, *Invest. New Drugs.* 30 (2012) 2096–2102.
- [260] A. Haouala, B. Zanolari, B. Rochat, M. Montemurro, K. Zaman, M.A. Duchosal, H.B. Ris, S. Leyvraz, N. Widmer, L.A. Decosterd, Therapeutic Drug Monitoring of the new targeted anticancer agents imatinib, nilotinib, dasatinib, sunitinib, sorafenib and lapatinib by LC tandem mass spectrometry, *J. Chromatogr. B Anal. Technol. Biomed. Life Sci.* 877 (2009) 1982–1996.
- [261] Z. Berk, *Food Process Engineering and Technology: Second Edition*, 2013.
- [262] S. Pedersen-Bjergaard, K.E. Rasmussen, T. Grønhaug Halvorsen, Liquid-liquid extraction procedures for sample enrichment in capillary zone electrophoresis, *J. Chromatogr. A.* 902 (2000) 91–105.
- [263] D. Remane, M.R. Meyer, F.T. Peters, D.K. Wissenbach, H.H. Maurer, Fast and simple procedure for liquid-liquid extraction of 136 analytes from different drug classes for development of a liquid chromatographic-tandem mass spectrometric quantification method in human blood plasma, *Anal. Bioanal. Chem.* 397 (2010) 2303–2314.
- [264] C.S. Højskov, L. Heickendorff, H.J. Møller, High-throughput liquid-liquid extraction and LCMSMS assay for determination of circulating 25(OH) vitamin D3 and D2 in the routine clinical laboratory,

- Clin. Chim. Acta. 411 (2010) 114–116.
- [265] G. Ling, J. Sun, J. Tang, X. Xu, Y. Sun, Z. He, Liquid chromatography-electrospray ionization mass spectrometric method for determination of gliclazide in human plasma, *Anal. Lett.* 39 (2006) 1381–1391.
- [266] C. Kratzsch, O. Tenberken, F.T. Peters, A.A. Weber, T. Kraemer, H.H. Maurer, Screening, library-assisted identification and validated quantification of 23 benzodiazepines, flumazenil, zaleplone, zolpidem and zopiclone in plasma by liquid chromatography/mass spectrometry with atmospheric pressure chemical ionization, *J. Mass Spectrom.* 39 (2004) 856–872.
- [267] O. Quintela, A. Cruz, A. De Castro, M. Concheiro, M. López-Rivadulla, Liquid chromatography-electrospray ionisation mass spectrometry for the determination of nine selected benzodiazepines in human plasma and oral fluid, *J. Chromatogr. B Anal. Technol. Biomed. Life Sci.* 825 (2005) 63–71.
- [268] S. Paterson, R. Cordero, S. Burlinson, Screening and semi-quantitative analysis of post mortem blood for basic drugs using gas chromatography/ion trap mass spectrometry, *J. Chromatogr. B Anal. Technol. Biomed. Life Sci.* 813 (2004) 323–330.
- [269] D. Liu, X. Han, X. Liu, M. Cheng, M. He, G. Rainer, H. Gao, X. Zhang, Measurement of ultra-trace level of intact oxytocin in plasma using SALLE combined with nano-LC–MS, *J. Pharm. Biomed. Anal.* 173 (2019) 62–67.
- [270] A. Gure, F.J. Lara, D. Moreno-González, N. Megersa, M. Del Olmo-Iruela, A.M. García-Campaña, Salting-out assisted liquid-liquid extraction combined with capillary HPLC for the determination of sulfonylurea herbicides in environmental water and banana juice samples, *Talanta.* 127 (2014) 51–58.
- [271] M.C. Hennion, Solid-phase extraction: Method development, sorbents, and coupling with liquid chromatography, *J. Chromatogr. A.* 856 (1999) 3–54.
- [272] C.F. Poole, New trends in solid-phase extraction, *TrAC - Trends Anal. Chem.* 22 (2003) 362–373.
- [273] W. Naidong, W.Z. Shou, T. Addison, S. Maleki, X. Jiang, Liquid chromatography/tandem mass spectrometric bioanalysis using normal-phase columns with aqueous/organic mobile phases - A novel approach of eliminating evaporation and reconstitution steps in 96-well SPE, *Rapid*

- Commun. Mass Spectrom. 16 (2002) 1965–1975.
- [274] M.J.M. Wells, J.L. Michael, M.J.M. Wells, Reversed-Phase Solid-Phase Extraction for Aqueous Environmental Sample Preparation in Herbicide Residue Analysis, *J. Chromatogr. Sci.* 25 (1987) 345–350.
- [275] P.D. Majors, J.S. McLean, J.C.M. Scholten, NMR bioreactor development for live in-situ microbial functional analysis, *J. Magn. Reson.* 192 (2008) 159–166.
- [276] U.J. Nilsson, E.J.L. Fournier, O. Hindsgaul, Solid-phase extraction on C18 silica as a purification strategy in the solution synthesis of a 1-Thio- β -D-galactopyranoside library, *Bioorganic Med. Chem.* 6 (1998) 1563–1575.
- [277] H. Bagheri, A. Mohammadi, A. Salemi, On-line trace enrichment of phenolic compounds from water using a pyrrole-based polymer as the solid-phase extraction sorbent coupled with high-performance liquid chromatography, *Anal. Chim. Acta.* 513 (2004) 445–449.
- [278] M. Gilar, A. Belenky, B.H. Wang, High-throughput biopolymer desalting by solid-phase extraction prior to mass spectrometric analysis, *J. Chromatogr. A.* 921 (2001) 3–13.
- [279] L. Han, Y. Sapozhnikova, S.J. Lehotay, Streamlined sample cleanup using combined dispersive solid-phase extraction and in-vial filtration for analysis of pesticides and environmental pollutants in shrimp, *Anal. Chim. Acta.* 827 (2014) 40–46.
- [280] G. Islas, I.S. Ibarra, P. Hernandez, J.M. Miranda, A. Cepeda, Dispersive Solid Phase Extraction for the Analysis of Veterinary Drugs Applied to Food Samples: A Review, *Int. J. Anal. Chem.* 2017 (2017) 1–16.
- [281] M.A. Farajzadeh, A. Yadeghari, M. Abbaspour, Dispersive solid phase extraction using magnetic nanoparticles performed in a narrow-bored tube for extraction of atorvastatin, losartan, and valsartan in plasma, *Adv. Pharm. Bull.* 9 (2019) 138–146.
- [282] V. Ferrone, M. Carlucci, V. Ettorre, R. Cotellesse, P. Palumbo, A. Fontana, G. Siani, G. Carlucci, Dispersive magnetic solid phase extraction exploiting magnetic graphene nanocomposite coupled with UHPLC-PDA for simultaneous determination of NSAIDs in human plasma and urine, *J. Pharm. Biomed. Anal.* 161 (2018) 280–288.
- [283] M. Salimi, M. Behbahani, H.R. Sobhi, M. Ghambarian, A. Esrafil, Dispersive solid-phase extraction

- of selected nitrophenols from environmental water samples using a zirconium-based amino-tagged metal–organic framework nanosorbent, *J. Sep. Sci.* 41 (2018) 4159–4166.
- [284] M.A. Farajzadeh, A. Mohebbi, Development of magnetic dispersive solid phase extraction using toner powder as an efficient and economic sorbent in combination with dispersive liquid–liquid microextraction for extraction of some widely used pesticides in fruit juices, *J. Chromatogr. A.* 1532 (2018) 10–19.
- [285] G. Islas, I.S. Ibarra, P. Hernandez, J.M. Miranda, A. Cepeda, Dispersive Solid Phase Extraction for the Analysis of Veterinary Drugs Applied to Food Samples: A Review, *Int. J. Anal. Chem.* 2017 (2017) 1–16.
- [286] M. Anastassiades, S.J. Lehotay, D. Stajnbaher, F.J. Schenck, Fast and easy multiresidue method employing acetonitrile extraction/partitioning and “dispersive solid-phase extraction” for the determination of pesticide residues in produce., *J. AOAC Int.* 86 (2003) 412–31.
- [287] J.L. Westland, F.L. Dorman, QuEChERS extraction of benzodiazepines in biological matrices, *J. Pharm. Anal.* 3 (2013) 509–517.
- [288] S. Mizuno, X.P. Lee, M. Fujishiro, T. Matsuyama, M. Yamada, Y. Sakamoto, M. Kusano, K. Zaitso, C. Hasegawa, I. Hasegawa, T. Kumazawa, A. Ishii, K. Sato, High-throughput determination of valproate in human samples by modified QuEChERS extraction and GC-MS/MS, *Leg. Med.* 31 (2018) 66–73.
- [289] D.Y. Bang, S.K. Byeon, M.H. Moon, Rapid and simple extraction of lipids from blood plasma and urine for liquid chromatography-tandem mass spectrometry, *J. Chromatogr. A.* 1331 (2014) 19–26.
- [290] J. Pawliszyn, Solid-Phase Microextraction in Perspective, in: *Handb. Solid Phase Microextraction*, Elsevier, 2012: pp. 1–12.
- [291] C. Silva, C. Cavaco, R. Perestrelo, J. Pereira, J.S. Câmara, Microextraction by packed Sorbent (MEPS) and solid-phase microextraction (SPME) as sample preparation procedures for the metabolomic profiling of urine, *Metabolites.* 4 (2014) 71–97.
- [292] J. Moreda-Piñeiro, A. Moreda-Piñeiro, Recent Advances in the Combination of Assisted Extraction

- Techniques, *Compr. Anal. Chem.* 76 (2017) 519–573.
- [293] J.M. Kokosa, Selecting an Appropriate Solvent Microextraction Mode for a Green Analytical Method, *Compr. Anal. Chem.* 76 (2017) 403–425.
- [294] S.K. Kailasa, H.F. Wu, Single-drop microextraction for bioanalysis: present and future., *Bioanalysis.* 5 (2013) 2593–2596.
- [295] S.E. Ebeler, Gas Chromatographic Analysis of Wines, in: *Gas Chromatogr.*, Elsevier, 2012: pp. 689–710.
- [296] S. Tang, T. Qi, P.D. Ansah, J.C. Nalouzebi Fouemina, W. Shen, C. Basheer, H.K. Lee, Single-drop microextraction, *TrAC - Trends Anal. Chem.* 108 (2018) 306–313.
- [297] L. Dong, C. Deng, B. Wang, X. Shen, Fast determination of Z-ligustilide in plasma by gas chromatography/mass spectrometry following headspace single-drop microextraction, *J. Sep. Sci.* 30 (2007) 1318–1325.
- [298] L. Dong, X. Shen, C. Deng, Development of gas chromatography-mass spectrometry following headspace single-drop microextraction and simultaneous derivatization for fast determination of the diabetes biomarker, acetone in human blood samples, *Anal. Chim. Acta.* 569 (2006) 91–96.
- [299] M. Rutkowska, K. Dubalska, P. Konieczka, J. Namieśnik, Microextraction techniques used in the procedures for determining organomercury and organotin compounds in environmental samples, *Molecules.* 19 (2014) 7581–7609.
- [300] R. Zhu, Y. Dong, X. Cai, C. Huang, Determination of barbiturates in biological specimens by flat membrane-based liquid-phase microextraction and liquid chromatography-mass spectrometry, *Molecules.* 24 (2019) 1494–1506.
- [301] D.A. Lambropoulou, T.A. Albanis, Application of hollow fiber liquid phase microextraction for the determination of insecticides in water, *J. Chromatogr. A.* 1072 (2005) 55–61.
- [302] M. Hadjmohammadi, H. Ghambari, Three-phase hollow fiber liquid phase microextraction of warfarin from human plasma and its determination by high-performance liquid chromatography, *J. Pharm. Biomed. Anal.* 61 (2012) 44–49.
- [303] Y. Assadi, M.A. Farajzadeh, A. Bidari, Dispersive liquid-liquid microextraction, *Compr. Sampl. Sample Prep.* 2 (2012) 181–212.

- [304] M. Rezaee, Y. Assadi, M.-R. Milani Hosseini, E. Aghaee, F. Ahmadi, S. Berijani, Determination of organic compounds in water using dispersive liquid–liquid microextraction, *J. Chromatogr. A.* 1116 (2006) 1–9.
- [305] G. Peng, Y. Lu, Q. He, D. Mmereki, G. Zhou, J. Chen, X. Tang, Dispersive Liquid–Liquid Microextraction Using Low-Toxic Solvent for the Determination of Heavy Metals in Water Samples by Inductively Coupled Plasma–Mass Spectrometry, *J. AOAC Int.* 99 (2016) 260–266.
- [306] X. Shen, J. Liang, L. Zheng, Q. Lv, H. Wang, Application of dispersive liquid–liquid microextraction for the preconcentration of eight parabens in real samples and their determination by high-performance liquid chromatography, *J. Sep. Sci.* 40 (2017) 4385–4393.
- [307] J. Pereira, J.S. Câmara, A. Colmsjö, M. Abdel-Rehim, Microextraction by packed sorbent: An emerging, selective and high-throughput extraction technique in bioanalysis, *Biomed. Chromatogr.* 28 (2014) 839–847.
- [308] R. Wietecha-Posłuszny, A. Garbacik, M. Woźniakiewicz, A. Moos, M. Wieczorek, P. Kościelniak, Application of microextraction by packed sorbent to isolation of psychotropic drugs from human serum, *Anal. Bioanal. Chem.* 402 (2012) 2249–2257.
- [309] R. Said, A. Pohanka, M. Abdel-Rehim, O. Beck, Determination of four immunosuppressive drugs in whole blood using MEPS and LC-MS/MS allowing automated sample work-up and analysis, *J. Chromatogr. B Anal. Technol. Biomed. Life Sci.* 897 (2012) 42–49.
- [310] S. Magiera, Fast, simultaneous quantification of three novel cardiac drugs in human urine by MEPS-UHPLC-MS/MS for therapeutic drug monitoring, *J. Chromatogr. B Anal. Technol. Biomed. Life Sci.* 938 (2013) 86–95.
- [311] B.H. Fumes, F.N. Andrade, Á.J. dos S. Neto, F.M. Lanças, Determination of pesticides in sugarcane juice employing microextraction by packed sorbent followed by gas chromatography and mass spectrometry, *J. Sep. Sci.* 39 (2016) 2823–2830.
- [312] H. Bagheri, Z. Ayazi, A. Aghakhani, N. Alipour, Polypyrrole/polyamide electrospun-based sorbent for microextraction in packed syringe of organophosphorous pesticides from aquatic samples, *J. Sep. Sci.* 35 (2012) 114–120.
- [313] F. David, P. Sandra, Stir bar sorptive extraction for trace analysis, *J. Chromatogr. A.* 1152 (2007)

54–69.

- [314] M. Kawaguchi, R. Ito, K. Saito, H. Nakazawa, Novel stir bar sorptive extraction methods for environmental and biomedical analysis, *J. Pharm. Biomed. Anal.* 40 (2006) 500–508.
- [315] E. Baltussen, P. Sandra, F. David, C. Cramers, Stir bar sorptive extraction (SBSE), a novel extraction technique for aqueous samples: Theory and principles, *J. Microcolumn Sep.* 11 (1999) 737–747.
- [316] M.G. Kassem, Stir bar sorptive extraction for central nervous system drugs from biological fluids, *Arab. J. Chem.* 4 (2011) 25–35.
- [317] A.R. Chaves, S.M. Silva, R.H.C. Queiroz, F.M. Lanças, M.E.C. Queiroz, Stir bar sorptive extraction and liquid chromatography with UV detection for determination of antidepressants in plasma samples, *J. Chromatogr. B Anal. Technol. Biomed. Life Sci.* 850 (2007) 295–302.
- [318] D. Benanou, F. Acobas, M.R. Deroubin, F. David, P. Sandra, Analysis of off-flavors in the aquatic environment by stir bar sorptive extraction-thermal desorption-capillary GC/MS/olfactometry, *Anal. Bioanal. Chem.* 376 (2003) 69–77.
- [319] P. Serôdio, M.S. Cabral, J.M.F. Nogueira, Use of experimental design in the optimization of stir bar sorptive extraction for the determination of polybrominated diphenyl ethers in environmental matrices, *J. Chromatogr. A.* 1141 (2007) 259–270.
- [320] F.J. Camino-Sánchez, R. Rodríguez-Gómez, A. Zafra-Gómez, A. Santos-Fandila, J.L. Vílchez, Stir bar sorptive extraction: Recent applications, limitations and future trends, *Talanta.* 130 (2014) 388–399.
- [321] P. Popp, C. Bauer, L. Wennrich, Application of stir bar sorptive extraction in combination with column liquid chromatography for the determination of polycyclic aromatic hydrocarbons in water samples, *Anal. Chim. Acta.* 436 (2001) 1–9.
- [322] M.A. Jenkins, Serum and urine electrophoresis for detection and identification of monoclonal proteins., *Clin. Biochem. Rev.* 30 (2009) 119–11922.
- [323] S. Hjertén, Free zone electrophoresis, *Chromatogr. Rev.* 9 (1967) 122–143.
- [324] J.W. Jorgenson, K.D. Lukacs, Free-zone electrophoresis in glass capillaries., *Clin. Chem.* 27 (1981) 1551–1553.

- [325] J.P. Landers, Handbook of capillary and microchip electrophoresis and associated microtechniques, CRC Press, 2007.
- [326] M.G. Khaledi, High-performance capillary electrophoresis : theory, techniques, and applications, Wiley, 1998.
- [327] J. Frenz, High performance capillary electrophoresis, Trends Biotechnol. 9 (2003) 243–250.
- [328] J.P. Landers, High performance capillary electrophoresis of biomolecules, Hewlett-Packard GmbH, 1991.
- [329] X. Xuan, D. Li, Analytical study of Joule heating effects on electrokinetic transportation in capillary electrophoresis, J. Chromatogr. A. 1064 (2005) 227–237.
- [330] X. Xuan, D. Li, Joule heating effects on peak broadening in capillary zone electrophoresis, J. Micromechanics Microengineering. 14 (2004) 1171–1180.
- [331] B.X. Mayer, How to increase precision in capillary electrophoresis, J. Chromatogr. A. 907 (2001) 21–37.
- [332] Z. Krivácsy, A. Gelencsér, J. Hlavay, G. Kiss, Z. Sárvári, Electrokinetic injection in capillary electrophoresis and its application to the analysis of inorganic compounds, J. Chromatogr. A. 834 (1999) 21–44.
- [333] H.J. Issaq, Capillary zone electrophoresis Electrophoresis Library, J. Chromatogr. A. 675 (2002) 286–287.
- [334] M.I. Turnes Carou, P. López Mahía, S. Muniategui Lorenzo, E. Fernández Fernández, D. Prada Rodríguez, Capillary zone electrophoresis for the determination of light-absorbing anions in environmental samples, J. Chromatogr. A. 918 (2001) 411–421.
- [335] D.T.R. Stewart, M.D. Celiz, G. Vicente, L.A. Colón, D.S. Aga, Potential use of capillary zone electrophoresis in size characterization of quantum dots for environmental studies, TrAC - Trends Anal. Chem. 30 (2011) 113–122.
- [336] M.M. Barbooti, Environmental applications of spectrochemical analysis, in: Environ. Appl. Instrum. Chem. Anal., Apple Academic Press, 2015: pp. 365–398.
- [337] E. Bermudo, O. Núñez, L. Puignou, M.T. Galceran, Analysis of acrylamide in food products by in-

- line preconcentration capillary zone electrophoresis, *J. Chromatogr. A.* 1129 (2006) 129–134.
- [338] T. Dai, J. Duan, X. Li, X. Xu, H. Shi, W. Kang, Determination of sulfonamide residues in food by capillary zone electrophoresis with on-line chemiluminescence detection based on an Ag(III) complex, *Int. J. Mol. Sci.* 18 (2017) 1–11.
- [339] R. Gottardo, I. Mikšík, Z. Aturki, D. Sorio, C. Seri, S. Fanali, F. Tagliaro, Analysis of drugs of forensic interest with capillary zone electrophoresis/time-of-flight mass spectrometry based on the use of non-volatile buffers, *Electrophoresis.* 33 (2012) 599–606.
- [340] F. Tagliaro, F.P. Smith, S. Turrina, V. Equisetto, M. Marigo, Complementary use of capillary zone electrophoresis and micellar electrokinetic capillary chromatography for mutual confirmation of results in forensic drug analysis, *J. Chromatogr. A.* 735 (1996) 227–235.
- [341] H. Yao, J. Vandebossche, C.E. Sanger-van de Griend, Y. Janssens, C.S. Fernandez, X. Xu, E. Wynendaele, G.W. Somsen, R. Haselberg, B. De Spiegeleer, Development of a capillary zone electrophoresis method to quantify *E. coli* L-asparaginase and its acidic variants, *Talanta.* 182 (2018) 83–91.
- [342] R. Wojcik, G. Zhu, Z. Zhang, X. Yan, Y. Zhao, L. Sun, M.M. Champion, N.J. Dovichi, Capillary zone electrophoresis as a tool for bottom-up protein analysis, *Bioanalysis.* 8 (2016) 89–92.
- [343] S. Fanali, M. Cristalli, A. Nardi, L. Ossicini, S.K. Shukla, Capillary zone electrophoresis in pharmaceutical analysis., *Farmaco.* 45 (1990) 693–702.
- [344] J.P. Mufusama, L. Hoellein, D. Feineis, U. Holzgrabe, G. Bringmann, Capillary zone electrophoresis for the determination of amodiaquine and three of its synthetic impurities in pharmaceutical formulations, *Electrophoresis.* 39 (2018) 2530–2539.
- [345] G. Hancu, B. Simon, A. Rusu, E. Mircea, . Gyeresi, Principles of micellar electrokinetic capillary chromatography applied in pharmaceutical analysis, *Adv. Pharm. Bull.* 3 (2013) 1–8.
- [346] S. Terabe, K. Otsuka, K. Ichikawa, A. Tsuchiya, T. Ando, Electrokinetic Separations with Micellar Solutions and Open-Tubular Capillaries, *Anal. Chem.* 56 (1984) 111–113.
- [347] C. Copper, K. Brensinger, C. Rollman, A. Clark, M. Perez, A. Genzman, J. Rine, M. Moini, MEKC-UV as an effective tool for the separation and identification of explosives, high explosives, and their degradation products in environmental samples, *Electrophoresis.* 37 (2016) 2554–2557.

- [348] G. Vasas, D. Szydłowska, A. Gáspár, M. Welker, M. Trojanowicz, G. Borbély, Determination of microcystins in environmental samples using capillary electrophoresis, *J. Biochem. Biophys. Methods.* 66 (2006) 87–97.
- [349] A. Cifuentes, B. Bartolomé, C. Gómez-Cordovés, Fast determination of procyanidins and other phenolic compounds in food samples by micellar electrokinetic chromatography using acidic buffers, *Electrophoresis.* 22 (2001) 1561–1567.
- [350] M. Katayama, Y. Matsuda, T. Sasaki, K.I. Shimokawa, S. Kaneko, T. Iwamoto, Determination of bisphenol A and 10 alkylphenols in serum using SDS micelle capillary electrophoresis with γ -cyclodextrin, *Biomed. Chromatogr.* 15 (2001) 437–442.
- [351] K. Nagy, K. Vékey, Separation methods, in: *Med. Appl. Mass Spectrom.*, Elsevier, 2008: pp. 61–92.
- [352] D. Otter, PROTEIN | Determination and Characterization, in: *Encycl. Food Sci. Nutr.*, Academic Press, 2003: pp. 4824–4830.
- [353] D. Suba, Z. Urbányi, A. Salgó, Capillary isoelectric focusing method development and validation for investigation of recombinant therapeutic monoclonal antibody, *J. Pharm. Biomed. Anal.* 114 (2015) 53–61.
- [354] M.G. Johlfs, P. Gorjala, Y. Urasaki, T.T. Le, R.R. Fiscus, Capillary isoelectric focusing immunoassay for fat cell differentiation proteomics, *PLoS One.* 10 (2015) 1–11.
- [355] F. Svec, CEC: Selected developments that caught my eye since the year 2000, *Electrophoresis.* 30 (2009) 68–82.
- [356] A. Rocco, G. D’Orazio, Z. Aturki, S. Fanali, Capillary Electrochromatography: A Look at Its Features and Potential in Separation Science, in: *Liq. Chromatogr. Fundam. Instrum.*, Elsevier, 2013: pp. 469–492.
- [357] R. Wu, H. Zou, M. Ye, Z. Lei, J. Ni, Capillary electrochromatography for separation of peptides driven with electrophoretic mobility on monolithic column, *Anal. Chem.* 73 (2001) 4918–4923.
- [358] S. Declerck, Y. Vander Heyden, D. Mangelings, Enantioseparations of pharmaceuticals with capillary electrochromatography: A review, *J. Pharm. Biomed. Anal.* 130 (2016) 81–99.
- [359] N. Guichard, M. Ogereau, L. Falaschi, S. Rudaz, J. Schappler, P. Bonnabry, S. Fleury-Souverain, Determination of 16 antineoplastic drugs by capillary electrophoresis with UV detection:

- Applications in quality control, *Electrophoresis*. 39 (2018) 2512–2520.
- [360] A.S. Cohen, D.L. Smisek, P. Keohavong, Capillary gel electrophoresis of biopolymers, *Trends Anal. Chem.* 12 (1993) 195–202.
- [361] J. Bergquist, M.J. Vona, C.O. Stiller, W.T. O'Connor, T. Falkenberg, R. Ekman, Capillary electrophoresis with laser-induced fluorescence detection: A sensitive method for monitoring extracellular concentrations of amino acids in the periaqueductal grey matter, *J. Neurosci. Methods*. 65 (1996) 33–42.
- [362] R.P. Baldwin, Recent advances in electrochemical detection in capillary electrophoresis, *Electrophoresis*. 21 (2000) 4017–4028.
- [363] B. Krattiger, A.E. Bruno, H.M. Widmer, M. Geiser, R. Dändliker, Laser-based refractive-index detection for capillary electrophoresis: ray-tracing interference theory, *Appl. Opt.* 32 (1993) 956–956.
- [364] K. Swinney, D.J. Bornhop, Detection in capillary electrophoresis, in: *Electrophoresis, 2000*: pp. 1239–1250.
- [365] A. Rodat, P. Gavard, F. Couderc, Improving detection in capillary electrophoresis with laser induced fluorescence via a bubble cell capillary and laser power adjustment, *Biomed. Chromatogr.* 23 (2009) 42–47.
- [366] J.P. Chervet, R.E.J. Van Soest, M. Ursem, Z-shaped flow cell for UV detection in capillary electrophoresis, *J. Chromatogr. A*. 543 (1991) 439–449.
- [367] D.M. Osbourn, D.J. Weiss, C.E. Lunte, On-line preconcentration methods for capillary electrophoresis, *Electrophoresis*. 21 (2000) 2768–2779.
- [368] J.P. Quirino, S. Terabe, Approaching a Million-Fold Sensitivity Increase in Capillary Electrophoresis with Direct Ultraviolet Detection: Cation-Selective Exhaustive Injection and Sweeping, *Anal. Chem.* 72 (2000) 1023–30.
- [369] L.N. Amankwa, M. Albin, W.G. Kuhr, Fluorescence detection in capillary electrophoresis, *TrAC Trends Anal. Chem.* 11 (1992) 114–120.
- [370] J.A. Fracassi Da Silva, N. Guzman, C.L. Do Lago, Contactless conductivity detection for capillary electrophoresis: Hardware improvements and optimization of the input-signal amplitude and

- frequency, *J. Chromatogr. A.* 942 (2002) 249–258.
- [371] B. Gaš, M. Demjanenko, J. Vacík, High-frequency contactless conductivity detection in isotachopheresis, *J. Chromatogr. A.* 192 (1980) 253–257.
- [372] J.A. Fracassi Da Silva, C.L. Do Lago, An Oscillometric Detector for Capillary Electrophoresis, *Anal. Chem.* 70 (1998) 4339–4343.
- [373] F.S. Felix, M.S.M. Quintino, A.Z. Carvalho, L.H.G. Coelho, C.L. Do Lago, L. Angnes, Determination of salbutamol in syrups by capillary electrophoresis with contactless conductivity detection (CE-C4D), *J. Pharm. Biomed. Anal.* 40 (2006) 1288–1292.
- [374] W.S. Law, P. Kubáň, J.H. Zhao, S.F.Y. Li, P.C. Hauser, Determination of vitamin C and preservatives in beverages by conventional capillary electrophoresis and microchip electrophoresis with capacitively coupled contactless conductivity detection, *Electrophoresis.* 26 (2005) 4648–4655.
- [375] S. Nussbaumer, S. Fleury-Souverain, S. Rudaz, P. Bonnabry, J.L. Veuthey, Determination of suxamethonium in a pharmaceutical formulation by capillary electrophoresis with contactless conductivity detection (CE-C4D), *J. Pharm. Biomed. Anal.* 49 (2009) 333–337.
- [376] P. Tůma, J. Gojda, Rapid determination of branched chain amino acids in human blood plasma by pressure-assisted capillary electrophoresis with contactless conductivity detection, *Electrophoresis.* 36 (2015) 1969–1975.
- [377] R.D. Smith, C.J. Barinaga, H.R. Udseth, Improved Electrospray Ionization Interface for Capillary Zone Electrophoresis-Mass Spectrometry, *Anal. Chem.* 60 (1988) 1948–1952.
- [378] E.D. Lee, W. Mück, J.D. Henion, T.R. Covey, Liquid junction coupling for capillary zone electrophoresis/ion spray mass spectrometry, *Biomed. Environ. Mass Spectrom.* 18 (1989) 844–850.
- [379] Y. Tanaka, K. Otsuka, S. Terabe, Evaluation of an atmospheric pressure chemical ionization interface for capillary electrophoresis-mass spectrometry, *J. Pharm. Biomed. Anal.* 30 (2003) 1889–1895.
- [380] N.J. Reinhoud, W.M.A. Niessen, U.R. Tjaden, L.G. Gramberg, E.R. Verheij, J. van der Greef, Performance of a liquid-junction interface for capillary electrophoresis mass spectrometry using continuous-flow fast-atom bombardment, *Rapid Commun. Mass Spectrom.* 3 (1989) 348–351.

- [381] Z.K. Shihabi, Stacking in capillary zone electrophoresis, *J. Chromatogr. A.* 902 (2000) 107–117.
- [382] F. Tagliaro, G. Manetto, F. Crivellente, D. Scarcella, M. Marigo, Hair analysis for abused drugs by capillary zone electrophoresis with field-amplified sample stacking., *Forensic Sci. Int.* 92 (1998) 201–11.
- [383] C.C. Chen, S.M. Wu, Y.H. Huang, W.K. Ko, H.S. Kou, H.L. Wu, On-line field-amplified sample stacking in capillary electrophoresis for analysis of amitriptyline and its metabolite nortriptyline in plasma, *Anal. Chim. Acta.* 517 (2004) 103–110.
- [384] Y. Shi, Y. Huang, J. Duan, H. Chen, G. Chen, Field-amplified on-line sample stacking for separation and determination of cimaterol, clenbuterol and salbutamol using capillary electrophoresis, *J. Chromatogr. A.* 1125 (2006) 124–128.
- [385] A. Zinellu, S. Sotgia, V. De Murtas, P. Cossu-Rocca, M.R. De Miglio, M.R. Muroni, A. Mura, M.G. Uras, M. Contini, L. Deiana, C. Carru, Evaluation of methylation degree from formalin-fixed paraffin-embedded DNA extract by field-amplified sample injection capillary electrophoresis with UV detection, *Anal. Bioanal. Chem.* 399 (2011) 1181–1186.
- [386] Z. Wang, H. Guo, M. Chen, G. Zhang, R. Chang, A. Chen, Separation and determination of corynoxine and corynoxine B using chiral ionic liquid and hydroxypropyl- β -cyclodextrin as additives by field-amplified sample stacking in capillary electrophoresis, *Electrophoresis.* 39 (2018) 2195–2201.
- [387] M.C. Breadmore, R.M. Tubaon, A.I. Shallan, S.C. Phung, A.S.A. Keyon, D. Gstoettenmayr, P. Prapatpong, A.A. Alhusban, L. Ranjbar, H. Heng See, M. Dawod, J.P. Quirino, Recent advances in enhancing the sensitivity of electrophoresis and electrochromatography in capillaries and microchips (2012-2014), *Electrophoresis.* 36 (2015) 36–61.
- [388] Y. Yang, R.I. Boysen, M.T.W. Hearn, Optimization of field-amplified sample injection for analysis of peptides by capillary electrophoresis-mass spectrometry, *Anal. Chem.* 78 (2006) 4752–4758.
- [389] D. Martínez, F. Borrull, M. Calull, Sample stacking using field-amplified sample injection in capillary zone electrophoresis in the analysis of phenolic compounds, *J. Chromatogr. A.* 788 (1997) 185–193.
- [390] X. Chen, Y. Tang, S. Wang, Y. Song, F. Tang, X. Wu, Field-amplified sample injection in capillary

- electrophoresis with amperometric detection for the ultratrace analysis of diastereomeric ephedrine alkaloids, *Electrophoresis*. 36 (2015) 1953–1961.
- [391] H.Y. Huang, C.W. Chiu, S.L. Sue, C.F. Cheng, Analysis of food colorants by capillary electrophoresis with large-volume sample stacking, *J. Chromatogr. A*. 995 (2003) 29–36.
- [392] L. Yu, S.F.Y. Li, Large-volume sample stacking with polarity switching for the analysis of bacteria by capillary electrophoresis with laser-induced fluorescence detection, *J. Chromatogr. A*. 1161 (2007) 308–313.
- [393] G. Álvarez-Llamas, A. Rodríguez-Cea, M.R. Fernández De La Campa, A. Sanz-Medel, Large volume sample stacking capillary electrophoresis for metallothioneins analysis in eel liver, *Anal. Chim. Acta*. 486 (2003) 183–190.
- [394] H. Yu, Z.-Y. Hao, L. Li, Y. Huang, H.-F. Zhang, A. Chen, Analysis of Three Compounds in Flos Farfarae by Capillary Electrophoresis with Large-Volume Sample Stacking, *Int. J. Anal. Chem.* 2017 (2017) 1–6.
- [395] C. Cruces-Blanco, A.M. García-Campaña, Capillary electrophoresis for the analysis of drugs of abuse in biological specimens of forensic interest, *TrAC - Trends Anal. Chem.* 31 (2012) 85–95.
- [396] G. McGrath, W.F. Smyth, Large-volume sample stacking of selected drugs of forensic significance by capillary electrophoresis, *J. Chromatogr. B Biomed. Sci. Appl.* 681 (1996) 125–131.
- [397] N.L. Deñola, N.S. Quiming, Y. Saito, K. Jinno, Simultaneous enantioseparation and sensitivity enhancement of basic drugs using large-volume sample stacking, *Electrophoresis*. 28 (2007) 3542–3552.
- [398] J.P. Quirino, J.B. Kim, S. Terabe, Sweeping: Concentration mechanism and applications to high-sensitivity analysis in capillary electrophoresis, *J. Chromatogr. A*. 965 (2002) 357–373.
- [399] R.B. Taylor, R.G. Reid, A.S. Low, Analysis of proguanil and its metabolites by application of the sweeping technique in micellar electrokinetic chromatography, *J. Chromatogr. A*. 916 (2001) 201–206.
- [400] Y.H. Lin, J.F. Chiang, M.R. Lee, R.J. Lee, W.K. Ko, S.M. Wu, Cation-selective exhaustive injection and sweeping micellar electrokinetic chromatography for analysis of morphine and its four metabolites in human urine, *Electrophoresis*. 29 (2008) 2340–2347.

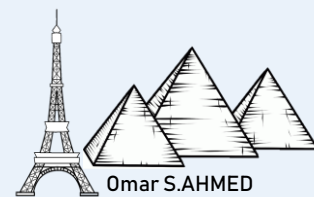
- [401] C. Fang, J.T. Liu, C.H. Lin, Optimization of the separation of lysergic acid diethylamide in urine by a sweeping technique using micellar electrokinetic chromatography, *J. Chromatogr. B Anal. Technol. Biomed. Life Sci.* 775 (2002) 37–47.
- [402] Z.K. Shihabi, Field amplified injection in the presence of salts for capillary electrophoresis, *J. Chromatogr. A.* 853 (1999) 3–9.
- [403] E.M. Ward, M.R. Smyth, R. O’Kennedy, C.E. Lunte, Application of capillary electrophoresis with pH-mediated sample stacking to analysis of coumarin metabolites in microsomal incubations, *J. Pharm. Biomed. Anal.* 32 (2003) 813–822.
- [404] Y. Zhao, C.E. Lunte, pH-mediated field amplification on-column preconcentration of anions in physiological samples for capillary electrophoresis, *Anal. Chem.* 71 (1999) 3985–3991.
- [405] L. Křivánková, A. Vraná, P. Gebauer, P. Boček, On-line isotachopheresis-capillary zone electrophoresis versus sample self stacking capillary zone electrophoresis. Analysis of hippurate in serum, *J. Chromatogr. A.* 772 (1997) 283–295.
- [406] D. Kaniansky, I. Zelenský, A. Hybenová, F.I. Onuska, Determination of Chloride, Nitrate, Sulfate, Nitrite, Fluoride, and Phosphate by On-Line Coupled Capillary Isotachopheresis-Capillary Zone Electrophoresis with Conductivity Detection, *Anal. Chem.* 66 (1994) 4258–4264.
- [407] T. Buzinkaiová, J. Polonský, Determination of four selective serotonin reuptake inhibitors by capillary isotachopheresis, *Electrophoresis.* 21 (2000) 2839–2841.
- [408] F. Acevedo, Isotachopheresis of proteins, *J. Chromatogr. A.* 470 (1989) 407–414.
- [409] S. Jeong, F. Shakerian, D.S. Chung, Analyte focusing by micelle collapse for liquid extraction surface analysis coupled with capillary electrophoresis of neutral analytes on a solid surface, *Electrophoresis.* (2019). <https://doi.org/10.1002/elps.201900113>.
- [410] X. Hou, X. Zhang, Y. Lu, The application of capillary electrophoretic on-line preconcentration in alkaloid analysis, *Anal. Methods.* 9 (2017) 10–17.
- [411] J.P. Quirino, Neutral analyte focusing by micelle collapse in micellar electrokinetic chromatography, *J. Chromatogr. A.* 1214 (2008) 171–177.
- [412] C. Kukulamude, S. Srijaranai, J.P. Quirino, Stacking and separation of neutral and cationic analytes in interface-free two-dimensional heart-cutting capillary electrophoresis, *Anal. Chem.* 86

- (2014) 3159–3166.
- [413] J.E. Adaway, B.G. Keevil, Therapeutic drug monitoring and LC-MS/MS, *J. Chromatogr. B Anal. Technol. Biomed. Life Sci.* 883 (2012) 33–49.
- [414] D.K. Lloyd, A.M. Cypess, I.W. Wainer, Determination of cytosine- β -d-arabinoside in plasma using capillary electrophoresis, *J. Chromatogr. B Biomed. Sci. Appl.* 568 (1991) 117–124.
- [415] S. Honda, A. Taga, K. Kakehi, S. Koda, Y. Okamoto, Determination of cefixime and its metabolites by high-performance capillary electrophoresis, *J. Chromatogr. A.* 590 (1992) 364–368.
- [416] I.M. Johansson, M.B. Grön-Rydberg, B. Schmekel, Determination of theophylline in plasma using different capillary electrophoretic systems, *J. Chromatogr. A.* 652 (1993) 487–493.
- [417] M. V Rocco, V.M. Buckalew, L.C. Moore, Z.K. Shihabi, Capillary Electrophoresis for the Determination of Glomerular, *Am. J. Kidney Dis.* 28 (1996) 173–177.
- [418] Z.K. Shihabi, M.E. Hinsdale, Analysis of ibuprofen in serum by capillary electrophoresis, *J. Chromatogr. B Biomed. Appl.* 683 (1996) 115–118.
- [419] M.T. Kelly, H. Fabre, D. Perrett, Determination of taurine in plasma by capillary zone electrophoresis following derivatisation with fluorescamine, *Electrophoresis.* 21 (2000) 699–705.
- [420] A.V. Ivanov, E.D. Virus, B.P. Luzyanin, A.A. Kubatiev, Capillary electrophoresis coupled with 1,1'-thiocarbonyldiimidazole derivatization for the rapid detection of total homocysteine and cysteine in human plasma, *J. Chromatogr. B.* 1004 (2015) 30–36.
- [421] Z.K. Shihabi, Peptide stacking by acetonitrile-salt mixtures for capillary zone electrophoresis, *J. Chromatogr. A.* 744 (1996) 231–240.
- [422] M.A. Friedberg, M. Hinsdale, Z.K. Shihabi, Effect of pH and ions in the sample on stacking in capillary electrophoresis, *J. Chromatogr. A.* 781 (1997) 35–42.
- [423] A. Baillet, G.A. Pianetti, M. Taverna, G. Mahuzier, D. Baylocq-Ferrier, Fosfomycin determination in serum by capillary zone electrophoresis with indirect ultraviolet detection, *J. Chromatogr. B Biomed. Sci. Appl.* 616 (1993) 311–316.
- [424] A. Tycova, M. Vido, P. Kovarikova, F. Foret, Interface-free capillary electrophoresis-mass spectrometry system with nanospray ionization—Analysis of dexrazoxane in blood plasma, *J.*

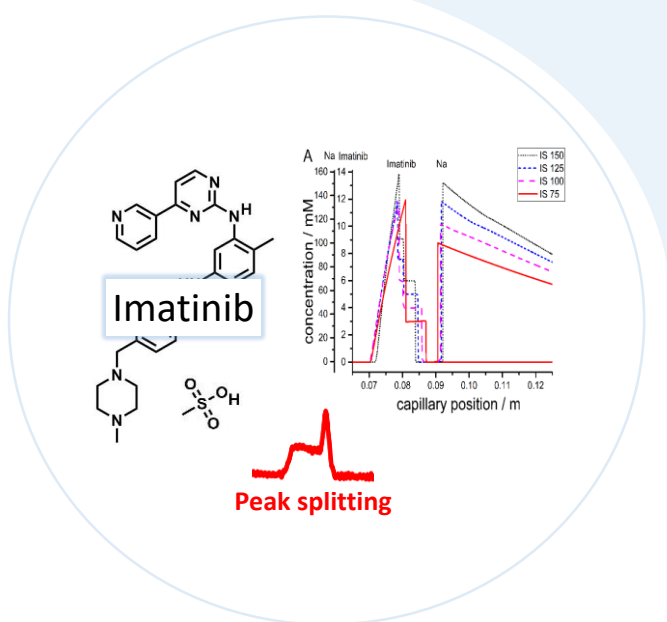
- Chromatogr. A. 1466 (2016) 173–179.
- [425] A. Al-Attas, J.J. Nasr, N. El-Enany, F. Belal, A green capillary zone electrophoresis method for the simultaneous determination of piperacillin, tazobactam and cefepime in pharmaceutical formulations and human plasma, *Biomed. Chromatogr.* 29 (2015) 1811–1818.
- [426] Z. Cieslarova, F.S. Lopes, C.L. do Lago, M.C. França, A.V. Colnaghi Simionato, Capillary electrophoresis tandem mass spectrometry determination of glutamic acid and homocysteine's metabolites: Potential biomarkers of amyotrophic lateral sclerosis, *Talanta*. 170 (2017) 63–68.
- [427] S. Hamidi, S. Soltani, A. Jouyban, A dispersive liquid-liquid microextraction and chiral separation of carvedilol in human plasma using capillary electrophoresis, *Bioanalysis*. 7 (2015) 1107–1117.
- [428] M.A. Strausbauch, S.J. Xu, J.E. Ferguson, M.E. Nunez, D. Machacek, G.M. Lawson, P.J. Wettstein, J.P. Landers, Concentration and separation of hypoglycemic drugs using solid-phase extraction-capillary electrophoresis, *J. Chromatogr. A*. 717 (1995) 279–291.
- [429] M. Karażniewicz-Łada, F. Główska, G. Oszkinis, Capillary Zone Electrophoresis method for determination of (+)-S clopidogrel carboxylic acid metabolite in human plasma and urine designed for biopharmaceutical studies, *J. Chromatogr. B*. 878 (2010) 1013–1018.
<https://doi.org/10.1016/J.JCHROMB.2010.02.033>.
- [430] K.J. Lee, G.S. Heo, N.J. Kim, D.C. Moon, Analysis of antiepileptic drugs in human plasma using micellar electrokinetic capillary chromatography, *J. Chromatogr. A*. 608 (1992) 243–250.
- [431] K.J. Lee, G.S. Heo, N.J. Kim, D.C. Moon, Separation of theophylline and its analogues by micellar electrokinetic chromatography: application to the determination of theophylline in human plasma, *J. Chromatogr. B Biomed. Sci. Appl.* 577 (1992) 135–141.
- [432] D.P. Bogan, B. Deasy, R. O'Kennedy, M.R. Smyth, U. Fuhr, Determination of free and total 7-hydroxycoumarin in urine and serum by capillary electrophoresis, *J. Chromatogr. B Biomed. Sci. Appl.* 663 (1995) 371–378.
- [433] J.M. Sanders, L.T. Burka, M.D. Shelby, R.R. Newbold, M.L. Cunningham, Determination of tamoxifen and metabolites in serum by capillary electrophoresis using a nonaqueous buffer system, *J. Chromatogr. B Biomed. Appl.* 695 (1997) 181–185.
- [434] Z.K. Shihabi, K.S. Oles, Serum lamotrigine analysis by capillary electrophoresis, *J. Chromatogr. B*

- Biomed. Appl. 683 (1996) 119–123.
- [435] G. Vargas, J. Havel, E. Hadašová, Direct determination of procainamide and N-acetylprocainamide by capillary zone electrophoresis in pharmaceutical formulations and urine, *J. Chromatogr. A.* 772 (1997) 271–276.
- [436] A. Kunkel, S. Günter, H. Wätzig, Quantitation of acetaminophen and salicylic acid in plasma using capillary electrophoresis without sample pretreatment Improvement of precision, *J. Chromatogr. A.* 768 (1997) 125–133.
- [437] R. Arias, R.M. Jiménez, R.M. Alonso, M. Téllez, I. Arrieta, P. Flores, E. Ortiz-Lastra, Determination of the β -blocker atenolol in plasma by capillary zone electrophoresis, *J. Chromatogr. A.* 916 (2001) 297–304.
- [438] R. Fazeli-Bakhtiyari, M.H. Sorouraddin, M.A. Farajzadeh, A. Jouyban, Detection limit enhancement of antiarrhythmic drugs in human plasma using capillary electrophoresis with dispersive liquid-liquid microextraction and field-amplified sample stacking method, *Bioanalysis.* 7 (2015) 21–37.
- [439] L.Y. Thang, S. Shahir, H.H. See, Determination of tamoxifen and its metabolites in human plasma by nonaqueous capillary electrophoresis with contactless conductivity detection, *Electrophoresis.* 36 (2015) 2713–2719.
- [440] P. Tůma, M. Jaček, V. Fejfarová, J. Polák, Electrophoretic stacking for sensitive determination of antibiotic ceftazidime in human blood and microdialysates from diabetic foot, *Anal. Chim. Acta.* 942 (2016) 139–145.
- [441] L.Y. Thang, M.C. Breadmore, H.H. See, Electrokinetic supercharging in nonaqueous capillary electrophoresis for online preconcentration and determination of tamoxifen and its metabolites in human plasma, *J. Chromatogr. A.* 1461 (2016) 185–191.
- [442] M. Forough, K. Farhadi, R. Molaei, H. Khalili, R. Shakeri, A. Zamani, A.A. Matin, Capillary electrophoresis with online stacking in combination with AgNPs@MCM-41 reinforced hollow fiber solid-liquid phase microextraction for quantitative analysis of Capecitabine and its main metabolite 5-Fluorouracil in plasma samples isolated from can, *J. Chromatogr. B.* 1040 (2017) 22–37.

Chapter II



Influence of salt and acetonitrile in the sample on CE analysis of TKIs



This chapter is the subject of:

- 📄 **A scientific paper:** *Influence of salt and acetonitrile on the capillary zone electrophoresis analysis of imatinib in plasma samples.* Accepted in *Electrophoresis*. 40 (2019), 2810–2819.
- 📄 **A poster:** *Electrophoretic analysis of high salt content samples. Application to imatinib mesylate for possible therapeutic drug monitoring.* 13eme congrès francophone sur les sciences séparatives et les couplages de l'AFSEP-April 2019, Paris, France.



Preface

In this chapter, the effect of salt present in the sample on the analysis of TKIs by CE was studied. Salt which is normally found in biological samples, is considered as an important factor affecting analysis by CE. As mentioned in chapter I, plasma is the main matrix for the TDM of TKIs and it contains salt at a concentration of about 1.0% (m/v). In this context, the effect of salt on the analysis of TKIs was our first concern. Imatinib mesylate was first chosen to monitor its analytical behavior by CE at different concentrations of salt, including 1.0% (m/v) in regards of salt concentration in plasma. Also, we have studied how the judicious choice of the pH and the I of the BGE can counterbalance the negative effects due to the presence of salt in the sample. A second concern is the presence of high % of biological proteins in plasma that could interfere with the analysis and the strong conjugation between TKIs and proteins. PP by adding ACN solvent to the sample is the most common technique used to eliminate biological proteins. Therefore, another part in our study dealt with the effect of adding of ACN on the analysis of imatinib in the presence of salt in the sample matrix.

In section I, preliminary results are demonstrated on the effect of the presence of salt in the samples of imatinib mesylate when analyzed by CZE. In section II, a simple, sensitive, fast and cost-effective analytical methodology was developed for the analysis of imatinib in human plasma by CZE in the presence of salt in the sample matrix (the subject of an accepted scientific paper). Several analytical conditions including I , pH of the BGE and % of ACN used were studied. Moreover, a collaboration was achieved between our group and the electrophoretic and chromatographic separation methods (ECHMET) group in Charles university in Prague, Czech Republic for one week training on Simul program financed by Balard doctoral school of chemistry under the supervision of Dr. Pavel Dubský with his PhD student Michael Malý. This collaboration was initiated to understand the electrophoretic behavior of imatinib in the presence of salt in the matrix. ECHMET group developed Simul program, a CZE simulator which displays the dynamics of separation process inside the capillary based on encoded mathematical model. Thanks to this collaboration, we succeeded to understand the behavior of imatinib mesylate in high saline aqueous matrix. Simulations and interpretations are given in details in this chapter and were used to optimize analytical conditions for the analysis of imatinib in human plasma. In section III, supplementary results concerning all the simulations by Simul program are given in details. In section IV, the method developed for the analysis of imatinib, was also applied for the analysis of the three other TKIs namely lapatinib ditosylate, erlotinib hydrochloride and sorafenib.

Section I

As mentioned in chapter I, human plasma contains high concentration of proteins and salts. Proteins can bind to the silica capillary walls affecting greatly the reproducibility and the quality of results obtained [1]. Salts, on the other hand, cause sample band spreading and consequently reduced peak efficiency of analytes obtained [2]. These deleterious effects become more significant when the sample injected volume is greatly increased. Our strategy at first was to study the effect of salt naturally present in human plasma on the electrophoretic behavior of TKIs and based on the results obtained, to determine optimal electrophoretic analysis conditions. Imatinib mesylate was chosen to start the trials with it. In addition, propranolol hydrochloride was used as another model compound, belonging to another therapeutic class but, with common physico-chemical features such as solubility and pKa, to compare its electrophoretic behavior with the behavior of imatinib.

I.1 Materials and methods of sections II and IV

I.1.1 Materials

All reagents were of analytical grade and used as received without further purification. Acetonitrile (ACN, purity $\geq 99.9\%$) was from Honeywell Riedel de Haen (Seelze, Germany). ϵ -amino caproic acid (purity $\geq 99\%$) was from Acros organics (Geel, Belgium). Sodium chloride (NaCl, purity $\geq 99.5\%$), sodium hydroxide (purity $\geq 99\%$), citric acid (purity $\geq 99\%$), imatinib mesylate (purity ≥ 98), Sorafenib (purity $\geq 99\%$), erlotinib hydrochloride (purity $\geq 99\%$) and lapatinib ditosylate (purity $\geq 99\%$) were purchased from Molekula (Munich, Germany). Human plasma for reconstitution were purchased from Sigma Aldrich (Saint-Quentin-Fallavie, France).

I.1.2 Apparatus and software

All CE separations were carried out using a Beckman P/ACE MDQ instrument (Fullerton, USA) equipped with a UV detection system. Data were acquired by 32 Karat software (Version 8.0, Beckman Coulter). Uncoated fused-silica capillaries (50 μ m ID) were obtained from Polymicro Technologies (Phoenix, USA). The capillary length was chosen to be 50 cm with effective length of 40 cm.

I.1.3 CE method

New capillaries were pre-conditioned with 1.0 M NaOH for 3.0 min under 20 psi followed by distilled water for 3.0 min under 20 psi. Then, the capillary was flushed with the BGE for 5.0 min under 20 psi. Hydrodynamic injections of the samples were varied between 0.4 to 0.5 psi and injection times were

varied between 20 to 94 seconds (s) to obtain injection volumes comprised between 20–118 nl. All separations were carried out with an applied voltage of 15 kV. The capillary was thermostated at 25 °C. UV detection was performed at 254 nm. Corrected areas were calculated by dividing each TKIs area by its corresponding migration time.

1.1.4 Preparation of the BGE and stock sample solutions

The background electrolytes were mixtures of citric acid and ϵ -amino caproic acid at different pH and I , based on a previous study of our group. BGE composition with the desired I and pH was calculated using the software “Peakmaster” 5.3 [3]: 1/ pH 2.0 and I 150 mM: citric acid (1800 mM) and ϵ -amino caproic acid (137 mM), 2/ pH 2.0 and I 50 mM: citric acid (700 mM) and ϵ -amino caproic acid (37 mM), 3/ pH 4.0 and I 50 mM: citric acid (37 mM) and ϵ -amino caproic acid (55 mM), 4/ pH 4.0 and I 100 mM: citric acid (67 mM) and ϵ -amino caproic acid (109 mM), 5/ pH 4.0 and I 150 mM: citric acid (100 mM) and ϵ -amino caproic acid (163 mM), 6/ pH 4.0 and I 200 mM: citric acid (120 mM) and ϵ -amino caproic acid (230 mM).

Aqueous stock solutions of imatinib mesylate and propranolol hydrochloride were prepared at a concentration of 100 mg/L in pure distilled water. Stock solutions of erlotinib hydrochloride, sorafenib and lapatinib ditosylate were prepared at a concentration of 1.0 g/L in dimethyl sulfoxide (DMSO) solvent. Stock solution of NaCl was prepared at a concentration of 10% (w/v) in pure distilled water. All stock samples were stored frozen at -20 °C.

1.1.5 Preparation of standard solutions

- Standard mixed solution of imatinib mesylate and propranolol hydrochloride in 100% water: relevant volumes (depending on desired concentration) of distilled water and stock solutions of both imatinib mesylate and propranolol hydrochloride were vortexed in an eppendorf centrifuge tube.

- Solution to study the effect of salt (section I): standard mixed solutions of imatinib mesylate and propranolol hydrochloride in water containing specific % of NaCl (m/v) ranging from 1.0 to 2.0% (m/v) were prepared. Relevant volumes (depending on desired concentration) of distilled water, imatinib mesylate, propranolol hydrochloride and NaCl stock solutions were vortexed in an eppendorf centrifuge tube to obtain a final concentration of NaCl ranging from 1.0 to 2.0% (m/v).

- Solution to study the effect of ACN and of salt (section IV): standard mixed solution of the four TKIs in the presence of 1.0% of NaCl (m/v) was prepared. Relevant volumes of imatinib, erlotinib hydrochloride, lapatinib ditosylate, sorafenib, NaCl stock solutions and ACN were vortexed in an eppendorf centrifuge

tube to have a ratio of 50/50 ACN/standard solution (v/v) with 1.0 % of NaCl (m/v) with the four TKIs at a concentration of 5 µg/mL each. After vortexing for 1 minute, the solution was left to stand for 3.0 min. All solutions were stored in refrigerator at 4 °C.

1.1.6 Preparation of plasma sample spiked with the four TKIs

Briefly, human plasma was placed in an eppendorf centrifuge tube and spiked with appropriate volumes of imatinib, erlotinib hydrochloride, lapatinib ditosylte and sorafenib stock solutions to obtain final concentration of 5 µg/mL for each TKIs. Then, the spiked plasma was mixed during 1 hour at room temperature. 400 µl of ACN was added to have a ratio of 50/50 ACN/plasma (v/v) with the four TKIs at a concentration of 5 µg/mL each. The addition of ACN induced PP. The supernatant was vortexed for 1 minute and centrifuged for 5 minutes (11000 rpm, 4°C).

1.2 Preliminary results

Standard mixed solutions of imatinib mesylate and propranolol hydrochloride were prepared with different concentrations of salt ranging from 0 to 2.0%, m/v (see part 1.1.5). The BGE was a mixture of citric acid and ε-amino caproic acid at pH 4.0. The I of the BGE was varied between 50 to 200 mM in order to study the effect of increasing the I of BGE on the electrophoretic analysis of imatinib with/without salt in the sample matrix.

1.2.1 Study of the effect of salt and I of the BGE on the analysis of imatinib mesylate by CE

Fig. 1 shows the analysis of imatinib and propranolol at different I of the BGE and different concentration of salt ranging from 0 to 2.0% (m/v) at pH 4.0. Both analytes are basic having one positive charge at pH 4.0 according to their pKa. Accordingly, propranolol was detected first followed by imatinib. This is due to the lower molecular weight of propranolol hydrochloride (259.34 g/mol) compared to imatinib mesylate (493.6 g/mol). As the concentration of salt (i.e NaCl) in the sample increases, a dramatic decrease in the peak heights of both analytes was observed for all the I of the BGE. Moreover, the efficiency and form of peak were also greatly affected by the presence of high concentration of salt starting from 1.0% (m/v). This electrophoretic behavior was related at first to the high I of the sample compared to BGE. In the case of a sample with 1.0 % NaCl (m/v) (as in plasma), the ionic strength of the sample was about 850 mM compared to 50 mM of BGE. This caused the sample band to disperse inside the capillary. Also, the analysis time increases by a factor of 1.5 when the I of the BGE increased. The reason behind this observation is that the mobility of analytes decreases when the I of the BGE increases. The tested TKIs molecules are basic in nature (cations), there μ_{app} will be the sum between EOF and electrophoretic mobility μ_{ep} . The

increase in the I of BGE will cause the decrease in the double bilayer thickness of the silanol group on the capillary wall which will cause a decrease in zeta potential and a decrease in EOF (as mentioned in chapter I) [4]. In addition, according to Henry equation (II.7) describing the relation between zeta potential and electrophoretic velocity,

$$v = \varepsilon\zeta/\eta \quad (\text{II.7})$$

where v is the electrophoretic velocity, ε is the dielectric constant of the buffer solution, ζ is the zeta potential and η is the BGE viscosity [5]. So, μ_{ep} will be calculated according to equation (II.8):

$$\mu_{ep} = \varepsilon\zeta/\eta E \quad (\text{II.8})$$

where E is the applied electric field. So, increasing the I of the BGE will decrease ζ which will lead to a decrease in the μ_{ep} of analytes and an increase in their migration time. So, their apparent mobility will be decreased.

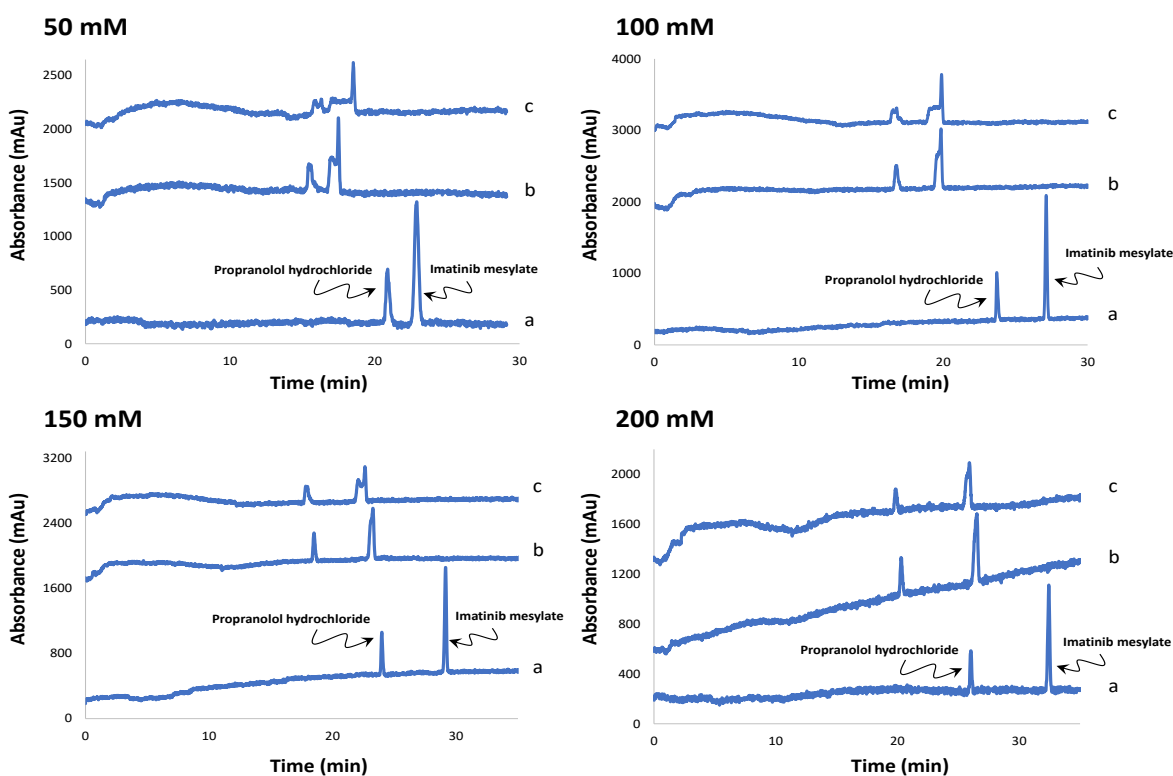


Figure 1: Analysis of imatinib mesylate and propranolol hydrochloride at the concentration of 5 and 20 $\mu\text{g}/\text{mL}$ respectively at different I of the BGE 50, 100, 150 and 200 mM. Both compounds were prepared in (a) 100 % water (b) 1.0% NaCl (m/v) in water and (c) 2.0% NaCl (m/v) in water. Analysis conditions: silica capillary 50 μm i.d., total length 50 cm, effective length 40 cm. BGE: citric acid – ε -aminocaproic acid at pH 4.0. Temperature: 25°C. Separation voltage: 15 kV. Sample injection volume: 120 nL (corresponding to 15% of the capillary volume till the detector window). Detection: 254 nm.

A splitting of imatinib peak was also observed with two maxima at high concentration of salt. The smaller maxima is the first to be detected followed by the second larger maxima. The distance between two maxima (plateau) decreased with increasing I of the BGE from 50 to 200 mM by a factor of 0.6 (as shown in Fig. 2). The height of imatinib peak increased by a factor of 1.43 when the I of BGE increased from 50 to 100 mM. In contrast, the height of imatinib peak decreased by a factor of 1.67 for I of BGE > 100 mM. On the other hand, the width of peak baseline decreased by a factor 1.67 when the I increased from 50 to 200 mM. So, it is better to work at high I of the BGE.

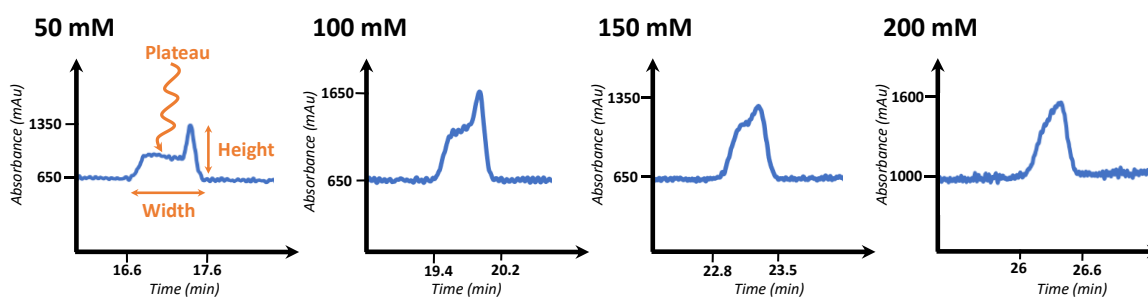


Figure 2: Effect of increasing I of the BGE on the form of peak of imatinib in the presence of 1.0% salt (m/v).

In section II, several analytical conditions such as I and pH of the BGE were studied to better understand the behavior of imatinib in the presence of salt. Also, an overview about simulations achieved by Simul program to explain why imatinib peak was splitted in the presence of salt were discussed. Thanks to this works realized in collaboration with ECHMET group, an optimized CZE analytical methodology was proposed for the analysis of imatinib mesylate in human plasma. This work was the subject of an accepted paper in Electrophoresis journal (doi:10.1002/elps.201900188).

References of section I

- [1] Z.K. Shihabi, Therapeutic drug monitoring by capillary electrophoresis, *J. Chromatogr. A.* 807 (1998) 27–36.
- [2] Z.K. Shihabi, Field amplified injection in the presence of salts for capillary electrophoresis, *J. Chromatogr. A.* 853 (1999) 3–9.
- [3] M. Jaroš, V. Hruška, M. Štědrý, I. Zusková, B. Gaš, Eigenmobilities in background electrolytes for capillary zone electrophoresis: IV. Computer program PeakMaster, *Electrophoresis.* 25 (2004) 3080–3085.
- [4] J.C. Reijenga, T.P.E.M. Verheggen, J.H.P.A. Martens, F.M. Everaerts, Buffer capacity, ionic strength

and heat dissipation in capillary electrophoresis, *J. Chromatogr. A.* 744 (1996) 147–153.

- [5] P. Fonte, F. Andrade, F. Araújo, C. Andrade, J. das Neves, B. Sarmiento, Chitosan-coated solid lipid nanoparticles for insulin delivery, *Methods Enzymol.* 508 (2012) 295–314.

Section II

Influence of salt and acetonitrile on the capillary electrophoresis analysis of imatinib in plasma samples

Omar S. Ahmed^{1,4}, Michal Malý², Yoann Ladner¹, Laurent Philibert³, Pavel Dubský², Catherine Perrin¹

¹Institut des Biomolécules Max Mousseron (IBMM), UMR 5247-CNRS-UM-ENSCM, Montpellier, France

²Department of Physical and Macromolecular Chemistry, Faculty of Science, Charles University, Prague, Albertov 6, Prague 2, Czech Republic

³Institut régional du Cancer de Montpellier (ICM), Département de Pharmacie et Pharmacologie, Montpellier, France

⁴Department of Analytical Chemistry, Faculty of Pharmacy, Misr University of Science and Technology (MUST). Al-Motamayez District, 6th of October City, P.O.Box: 77, Egypt.

Research article accepted in

Electrophoresis, Wiley

Electrophoresis. 40 (2019), 2810–2819.

Keywords:

Acetonitrile, peak splitting, salt, simul software, tyrosine Kinase Inhibitor.

Highlights:

1. Investigation about imatinib mesylate peak splitting in high saline matrix using Simul program.
2. Direct analysis of imatinib mesylate by capillary electrophoresis (CE) technique.
3. On-line concentration by acetonitrile stacking at high sample volume injected.

List of abbreviation:

- Ionic strength (I)
- Acetonitrile (ACN)
- Sodium chloride (NaCl)
- Therapeutic Drug Monitoring (TDM)
- Tyrosine kinase inhibitor (TKI)

Abstract

A simple, sensitive, specific and cost-effective analytical methodology was developed for the analysis of human plasma samples spiked with imatinib by capillary zone electrophoresis (CZE) with on-line UV detection in the context of Therapeutic Drug Monitoring (TDM). Several analytical conditions such as the ionic strength (I) and the pH of the background electrolyte (BGE) composed of citric acid and ϵ -amino caproic acid were studied in regards of the presence of sodium chloride (NaCl) in plasma samples (1.0% (m/v)). Computer simulations (Simul software) were used to confirm the experimental results and to understand imatinib electrophoretic behavior in the presence of NaCl. Furthermore, the advantages of adding acetonitrile (ACN) to the sample containing NaCl to combine efficient protein precipitation and on-line CZE stacking of imatinib was demonstrated. LOD and LOQ values of 48 and 191 ng/ml were obtained from plasma sample supernatant after protein precipitation with ACN, which is much lower than mean imatinib plasma level observed for patients treated by imatinib mesylate (about 1000 ng/ml). Good linearity was obtained in the concentration range 191–5000 ng/ml ($r^2 > 0.997$). Relative standard deviations (RSD) of less than 1.68% and 2.60% ($n=6$) for migration times and corrected peak areas, respectively, were observed at the LOQ.

1. Introduction

In the last decades, capillary electrophoresis (CE) has been demonstrated to offer promising, effective, fast and economic approaches for the separation and quantification of a large variety of therapeutic substances in biological samples [1]. Nevertheless, the analysis of plasma samples by CE can be difficult to realize due to the high concentration of interfering compounds (i.e. proteins, salts at about 1.0% (w/v)) that affect the analysis. The presence of salts in the sample may lead to peak broadening and baseline distortion limiting the amount of sample which can be loaded inside the capillary [2–5]. Therefore, the first (most applied) approach is to use sample preparation techniques (desalting, extraction) prior to CE to reduce interferences, to concentrate the analytes of interest and to obtain efficient electrophoretic peaks [6,7]. However, these methods are based on the use of complex, long and expensive sample preparation protocols, which is not advantageous for routine analysis. The second approach is based on the judicious choice of CE conditions, such as ionic strength (I), pH, type of buffer and addition of organic solvent to the sample to allow the direct CE analysis of samples containing salts/proteins without the need to apply sophisticated desalting and extraction steps [8,9].

The present study fits in with this latter approach and has the objective to propose a simple, sensitive, specific and cost-effective analytical methodology for the analysis of imatinib mesylate in human plasma by CZE. Imatinib mesylate is an orally administered tyrosine kinase inhibitors (TKIs) which is considered as the gold standard for the treatment of chronic myeloid leukemia and gastrointestinal stromal tumor [10]. However, due to its narrow therapeutic range and high inter-individual variability [11,12], therapeutic drug monitoring (TDM) of imatinib is compulsory to adapt the dose to each individual patient, to understand the absence/decrease of response to the treatment (therapeutic failure) and to manage drug interactions. Survey of the literature shows that liquid chromatography (LC) coupled to UV [13,14] or mass (MS) [15–18] detection is the main analytical technique used for the analysis of imatinib in plasma. Few studies report the use of CE methods including direct CZE [19–21], non-aqueous capillary electrophoresis (NACE) [22] and CE coupled to mass spectrometry [23]. Nevertheless, sample pretreatment techniques such as liquid-liquid extraction (LLE) [19], solid-phase extraction (SPE) [22], LLE/SPE combination [23] or electromembrane extraction [21] were used prior to the CE analysis of imatinib. Therefore, simpler analytical methodologies that do not require complex desalting and extraction protocol are needed for the routine analysis of imatinib in plasma samples such as for TDM.

Our strategy was based on keeping the salt naturally present in the plasma sample and adding acetonitrile (ACN) as a deproteinization agent. At first, specific attention was paid to the influence of salt, i.e., sodium

chloride (NaCl), on the analysis of imatinib. Several electrophoretic conditions including I and pH of the BGE were tested, optimized and compared to the simulations obtained by Simul program (<https://echmet.natur.cuni.cz/software/download>) [24]. Simulations provided detailed information on the lifetime of the moving imatinib/sodium boundaries as a function of the BGE pH and I , sample pH and injection length. Furthermore, the advantages of adding acetonitrile (ACN) to the sample containing NaCl to combine efficient protein precipitation and on-line CZE stacking of imatinib was demonstrated. From the results obtained, a CZE-UV methodology based on the direct analysis of the plasma sample supernatant was proposed and the performances of the method was evaluated in terms of recovery, specificity, repeatability, LOD, LOQ and linearity.

2. Experimental

2.1. Chemicals and reagents

All reagents were of analytical grade and used as received without further purification. Acetonitrile (ACN, purity $\geq 99.9\%$) was from Honeywell Riedel de Haen (Seelze, Germany). ϵ -amino caproic acid ($C_6H_{13}NO_2$, MW 131.17, $pK_{a1} = 4.42$, $pK_{a2} = 10.75$, purity $\geq 99\%$) was from Acros organics (Geel, Belgium). Sodium chloride (NaCl, purity $\geq 99.5\%$), sodium hydroxide pellets (purity $\geq 99\%$), citric acid ($C_6H_8O_7$, MW 192.12, $pK_{a1} = 3.13$, $pK_{a2} = 4.76$, $pK_{a3} = 6.4$, purity $\geq 99\%$), imatinib mesylate (purity $\geq 98\%$). Human plasma for reconstitution were purchased from Sigma Aldrich (Saint-Quentin-Fallavie, France).

2.2. CE apparatus and software

All CZE separations were carried out using a Beckman P/ACE-MDQ instrument (Fullerton, USA) equipped with a UV filter detection system. Data were acquired by 32 Karat software (Version 8.0, Beckman Coulter). Uncoated fused-silica capillaries (50 μm ID) were obtained from Polymicro Technologies (Phoenix, USA). Two lengths of capillary were used for the experiments, 50 and 30 cm (40 and 20 cm effective lengths to the detector respectively).

CE expert software (Beckman, USA) was used for injection volumes calculation.

2.3. CZE methods

New capillaries were pre-conditioned with 1.0 M NaOH for 3.0 min under 20 psi followed by distilled water for 3.0 min under 20 psi. Then, the capillary was flushed with the background electrolyte (BGE) for 5.0 min under 20 psi. For 50 cm capillaries, sample injection volumes comprised between 57 to 295 nl, representing 7.5 to 40% of the capillary effective length, were used. To achieve this, hydrodynamic injections of the samples were performed by varying the injection pressures between 0.4 and 1.4 psi and the injection times between 60 and 89 seconds (s). For 30 cm capillaries, sample injection volumes

comprised between 30 to 156 nl, representing 7.5 to 40% of the capillary effective length, were used. To achieve this, hydrodynamic injections of the samples were performed by varying the injection pressures between 0.4 and 0.6 psi and the injection times between 19 and 66 s. All separations were carried out with an applied voltage of 15 kV. The capillary was thermostated at 25°C. UV detection was performed at 254 nm. Corrected areas were calculated by dividing each peak area by its corresponding migration time.

2.4. Preparation of background electrolyte and stock sample solutions

Imatinib being a basic compound, it was analyzed under acidic conditions to have sufficient electrophoretic mobility. The background electrolytes were mixtures of citric acid and ϵ -amino caproic acid at different pH and I , as a previous study of our group [25] has shown that it was appropriate for the analysis of tyrosine kinase inhibitors with high efficiency and selectivity. BGEs composition with desired I and pH was calculated using the software "Peakmaster" 5.3 (section 2.7): 1/ pH 2.0 and I 150 mM: citric acid (1800 mM) and ϵ -amino caproic acid (137 mM), 2/ pH 2.0 and I 50 mM: citric acid (700 mM) and ϵ -amino caproic acid (37 mM), 3/ pH 4.0 and I 50 mM: citric acid (37 mM) and ϵ -amino caproic acid (55 mM), 4/ pH 4.0 and I 100 mM: citric acid (67 mM) and ϵ -amino caproic acid (109 mM), 5/ pH 4.0 and I 150 mM: citric acid (100 mM) and ϵ -amino caproic acid (163 mM), 6/ pH 4.0 and I 200 mM: citric acid (120 mM) and ϵ -amino caproic acid (230 mM). I was limited to 150 mM to avoid excessive Joule heating.

Aqueous stock solutions of imatinib were prepared at a concentration of 100 mg/L. Stock solution of NaCl was prepared at a concentration of 10% (w/v) in pure distilled water. All Stock sample solutions were stored at -20°C. All other solutions were stored in refrigerator at 4°C.

2.5. Imatinib standard solutions

- *Imatinib standard solutions in 100% water* were prepared at 5.0 mg/l with relevant volumes of distilled water and imatinib stock solution.

- *Imatinib aqueous standard solutions containing 1.0% (w/v) of NaCl* were prepared at 5.0 mg/L with relevant volumes of distilled water, imatinib stock solution and NaCl stock solution.

- *Imatinib standard solutions containing NaCl and ACN* were prepared at 5.0 mg/L with relevant volumes of imatinib stock solution, NaCl stock solution and ACN; and mixed in an eppendorf centrifuge tube to have a ratio of 50/50 ACN/standard solution (v/v) with a final concentration of 0.5% NaCl (w/v). After vortexing for 1 minute, the solution was left to stand for 3.0 min. Then, a specific volume of the standard sample solution (corresponding to a specific percentage of the capillary length till detector window) was injected and analyzed by CZE with on-line UV detection.

2.6. Preparation of human plasma sample spiked with imatinib

Briefly, human plasma was placed in an eppendorf centrifuge tube and spiked with appropriate volumes of imatinib stock solution to obtain final imatinib concentrations between 191 and 5000 ng/ml. Then, the spiked plasma was mixed during 1 hour at room temperature ($25 \pm 3^\circ\text{C}$) with an oscillating mixer at 300 rpm. 400 μl of ACN was added to have a ratio of 50/50 ACN/plasma (v/v). The addition of ACN induced protein precipitation. The supernatant was vortexed for 1 minute and centrifuged for 5 minutes (11000 rpm, 4°C). Then, a specific volume of the supernatant (corresponding to a specific percentage of the capillary length till detector window) was injected and analyzed by CZE with on-line UV detection.

2.7. Peakmaster and Simul 5 softwares

PeakMaster (<https://echmet.natur.cuni.cz/software/download>) is a capillary zone electrophoresis simulator for personal computers intended to aid with common analytical laboratory tasks [26]. PeakMaster has proven to be a valuable tool for CE buffer design because it features a powerful engine capable of calculating equilibrium composition of arbitrarily complex chemical solution and the corresponding parameters such as pH, buffer capacity and effective mobilities of all contained compounds.

Simul 5 implements numerical solver of the electromigration continuity equations, enabling it to solve any kind of one-dimensional capillary electrophoresis problem. Unlike PeakMaster, Simul 5 is an advanced tool for in-depth studies of electromigration processes [24].

Simulations of imatinib in various buffers were performed in a 12.5 cm long space divided into 60000 grid points using a developer version of Simul 5 (faster parallel algorithm in the computational core that can handle high grid densities, not yet released for public use). Driving voltage was 3750 V (field strength 300 v/cm). Length of sample zone was 5 cm. Capillary diameter was set to 50 μm . This setup is a good approximation of the actual experimental conditions. Length of the simulated capillary was reduced by a factor of 4 to save computation time. System with BGE ionic strength of 75 mM and pH 4.0 exhibited severe oscillations during the phase of chloride and sodium zones separation. In order to obtain useful results for this system, grid resolution had to be increased to 160000 points.

Exact sample and BGE compositions can be found in supporting information. Simulations were performed in the two buffers, pH 2.0 and pH 4.0, at I values of 75, 100, 125 and 150 mM. I correction (to limiting mobilities and pKa values) was not applied during the simulations. We use I value solely as an indicator of the actual buffer concentration in this context.

3. Results and discussion

Simple, specific and fast are the main criteria required for the development of analytical methods dedicated to routine analysis such as TDM. Sample preparation steps applied prior the analysis of drugs in plasma samples can induce a lack of robustness and an increase in the cost of the method due to the use of sophisticated desalting and extraction procedures. Therefore, an electrophoretic analytical methodology requiring no desalting of the samples and using ACN as deproteinization agent was developed. ACN was added to the sample, and the supernatant was directly analyzed by CZE with on-line UV detection.

3.1. Effect of sample salts on the electrophoretic analysis of imatinib: experimental

Imatinib mesylate is a basic molecule having 4 pKa(s) ($pK_{a1} = 1.52$, $pK_{a2} = 2.56$, $pK_{a3} = 3.73$ and $pK_{a4} = 8.07$) (structure shown in Fig. 1A).

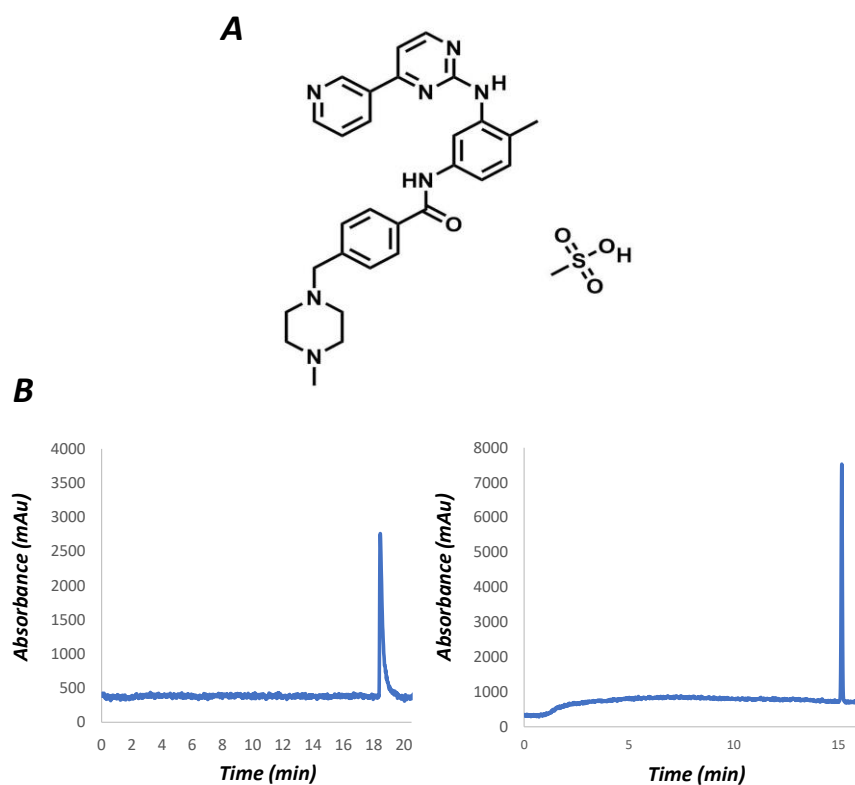


Figure 1: (A) Molecular structure of imatinib mesylate. (B) analysis of imatinib mesylate in 100% water at two different pH of the BGE. Analysis conditions: silica capillary: 50 μ m i.d., total length: 50 cm. BGE: citric acid – ϵ -aminocaproic acid buffer / 50 at pH 4.0 and at pH 2.0. Temperature: 25°C. Separation voltage: 15 kV. Sample injection volume: 60 nl (corresponding to 7.5% of the capillary length till the detector window). Detection: 254 nm.

Preliminary trials showed that the CZE analysis of imatinib diluted in 100% water to 5 mg/L (see section 2.5) gave an efficient imatinib peak at pH 2.0 and 4.0, I 50 mM (Fig. 1B). The electrophoretic mobilities μ_{ep} of imatinib at pH 2.0 and pH 4.0 were determined as being equal to 2.02×10^{-2} and 9.95×10^{-3} cm²/V/s, respectively. Then, imatinib electrophoretic behavior in the presence of salt was studied. Aqueous solution of imatinib at 5 mg/L containing 1.0% w/v of salt (see section 2.5) was first analyzed with a BGE pH 4.0 and I 50 mM. CZE analyses were done with a sample injected volume equal to 7.5% of the capillary length till detector window to obtain a good sensitivity of the method (see section 2.3).

A splitting of imatinib peak (Fig. 2A) was observed. This result showed that the presence of salt induced peak splitting by comparing imatinib peak form in the presence (Fig. 2A) and the absence (Fig. 2B) of salt. Increasing the I of the BGE to 150 mM allowed to ameliorate the peak form (no peak splitting due to stacking effect [2]) (Fig. 2B).

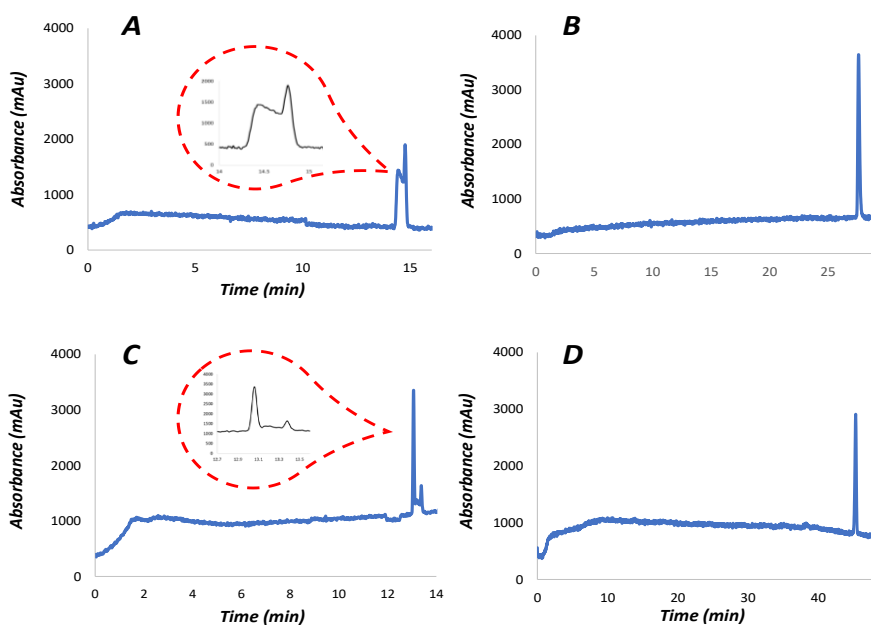


Figure 2: Analysis of imatinib mesylate at two different I and pH of the BGE. Analysis conditions: silica capillary: 50 μ m i.d., total length: 50 cm. BGE: citric acid – ϵ -aminocaproic acid buffer (A) / 50 mM pH 4.0, (B) / 150 mM pH 4, (C) / 50 mM pH 2.0 (D) / 150 mM pH 2.0. Temperature: 25°C. Separation voltage: 15 kV. Sample injection volume: 60 nl (corresponding to 7.5% of the capillary length till the detector window). Detection: 254 nm.

When analyses were performed at pH 2.0 (increasing the electrophoretic mobility of imatinib and decreasing the electroosmotic mobility) and at I 50 mM, peak splitting was also observed but with a different pattern from that obtained at pH 4. Two sharp zones were observed at the beginning and at the end of the sample zone connected with a plateau in between (Fig. 2C). Similarly, to pH 4.0, peak splitting disappeared with increasing I of BGE to 150 mM (Fig. 2D). Similar observations were obtained with

aqueous solution of imatinib at 5 mg/L containing 0.5% w/v of salt confirming the effect of salt on peak splitting (results not shown). Similar observations were obtained with small sample injected volume (1.0% of the capillary volume till detector window) and lower injected concentration of imatinib (191-5000 ng/mL) confirming the dependency of peak splitting on the I of the BGE.

3.1. Effect of sample salts on the analysis of imatinib: computer simulation

A computer simulation using Simul 5 software was performed (see section 2.7) in order to visualize how the peak splitting patterns at pH 4.0 (Fig. 2A) and pH 2.0 (Fig. 2C), and vanishing of peak splitting at high I vs. low I buffers, occurred. Simulation were performed with a shorter capillary compared to experimental trials to spare computational time. Therefore, the simulation was stopped before the peak reaches the experimental position of the detector. Simulation with an I of 50 mM could not be completed due to the development of too sharp boundaries and regions of too low ionic concentrations that could not be handled by Simul 5. Nevertheless, the results clearly demonstrate peak splitting dynamics in the two buffers and its dependency on I . Detailed description of the simulation results for the four corner-cases of pH 4.0/ I 150 mM, pH 4.0/ I 75 mM, pH 2.0/ I 150 mM, and pH 2.0/ I 75 mM can be found in supplementary information. Herein, we showed the final results and inspected their I dependency.

Apart from some studies reporting peak splitting due to complexation reactions between the analyte and the BGE [27], peak splitting is to be attributed to the formation of various boundaries and thus different electrophoretic properties zones that develop in long injection plugs (large sample volume injected). These phenomena are specifically observed under mismatch conditions between the sample zone and BGE. This may result, e.g., in trapping of a portion of weak electrolyte analyte in a zone of low/high pH values [28], or development of rather complicated transient states (transient pH junctions, transient ITP, mixed boundaries) reported specifically in high-saline samples as in the present study [29,30]. Development of such boundaries can be predicted or anticipated by means of the so-called velocity diagrams [31,32]. This approach is useful in understanding the peak splitting mechanism, yet the theory cannot be generalized into simple rules that would allow for a genuine explanation of differences in peak splitting dynamics in particular BGEs. Computer simulation thus remains the easiest way to verify the experimental results against the theory of electrophoresis.

In the present study, the key transition state that the system passes through is splitting of injected sodium zone into two (interconnected) parts (cf. Supporting information, Fig. S1D). This effect was described and elucidated in the frame of the velocity diagrams by Malá at al. [30] (with the difference that an anionic system with a weak acidic analyte was studied under the presence of highly concentrated salt in the

sample, so that chloride ions took the role of sodium ions). The two sodium zone parts exhibit sharp boundaries at their backs, which cause accumulation of imatinib analyte on them. Thus, two zones of stacked imatinib arise in the system: one (herein referred to as primary stacked zone) following the very end of the sodium zone (primary sodium boundary) as it passes through the injection region, and the second (secondary stacked zone) at the secondary sodium boundary that develops roughly in the middle of the injection zone. The simulations reveal that it is the behavior of that secondary boundary that is responsible for various peak splitting patterns of imatinib observed under different pH and I conditions.

Figure 3.A demonstrates that the peak splitting pattern as observed in Figure 2A, indeed, develops in the system with a BGE of pH 4. Notice that the simulation results are depicted in the x domain (inside the capillary) so that the peak becomes mirrored in the time domain, being recorded from right to left. In these conditions (pH 4), the secondary sodium boundary develops close to the primary one. The primary boundary has passed through almost half of the injection plug before the secondary boundary starts to develop and the secondary boundary moves slowly so that the primary and secondary boundaries (and thus the stacked zones of imatinib) merge together before they can leave the injection zone. From then on, separation of the stacked zone of imatinib from sodium back begins. Still a portion of imatinib stays trapped in the sodium zone, which exhibits as the “chair-like” splitting pattern observed in the electropherograms.

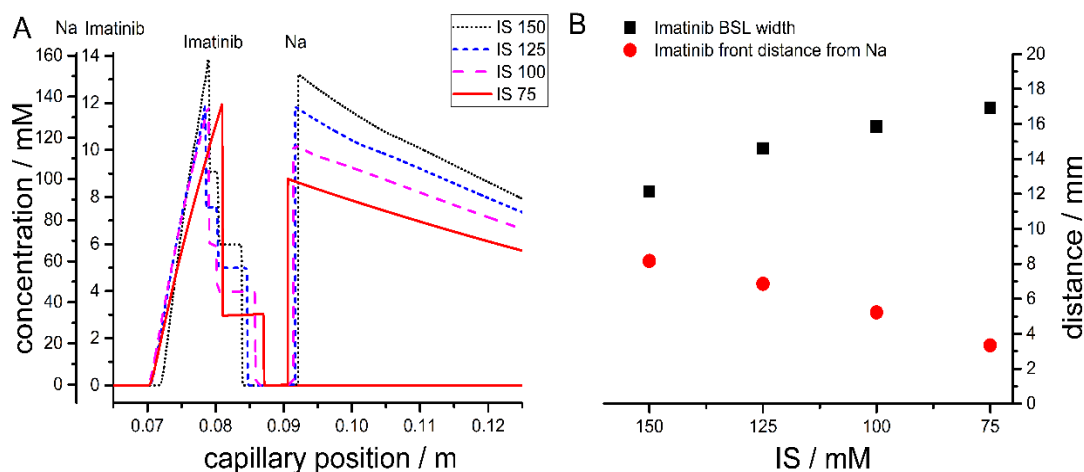


Figure 3: Simulation results of imatinib peak development in buffers of pH 4 and various I values (in mM). See Experimental for simulation conditions. Time-frames at 2 min (120 s); the time is relevant to simulation conditions and do not correspond to experimental time. A) concentration profiles, Na and imatinib have separate y axes. B) trends of two measures, imatinib peak baseline (BSL) width and its separation from Na rear boundary, with IS. x-axis goes from higher IS values to lower IS values.

The same peak pattern is observed for every I at pH 4.0, albeit its life-time decreases with increasing I . As the I of the BGE increases, the primary and secondary boundaries get closer to each other (no secondary boundary effectively develops at I 150 mM) and the peak of imatinib gets separated from Na zone sooner. The difference in heights between the peak top and the plateau decreases, and the peak baseline width shortens (cf. Fig. 3B, x axis goes from higher to lower I values). Thus, the peak splitting pattern is likely smeared out by electromigration dispersion before it can reach the detector in high I buffers, pH 4.

Figure 4.A shows peak patterns observed in BGEs at pH 2.0 under various I conditions. The dynamics of imatinib peak development is more complicated in these systems. The secondary boundary develops relatively far away from the primary boundary and moves to the cathode fast, so it is not so easily caught up by the primary boundary. This keeps the two stacked zones of imatinib separated from each other.

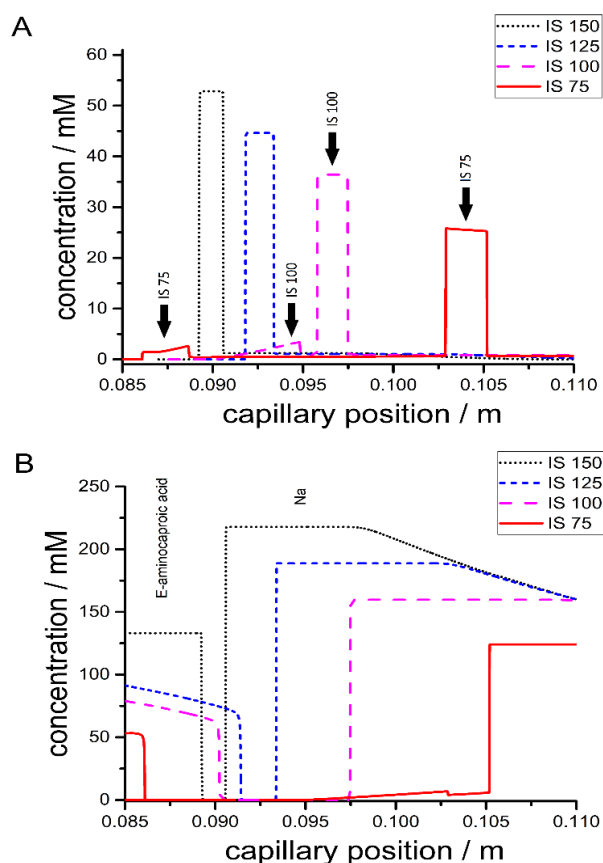


Figure 4: Simulation results of imatinib peak development in buffers of pH 2 and various I values (in mM). See Experimental for simulation conditions. Time-frames at 2 min (120 s); the time is relevant to simulation conditions and do not correspond to experimental time. A) profiles of imatinib. Arrows indicate stacked zones of imatinib that belongs to the same IS profile. B) profiles of the BGE co-ion, ϵ -aminocaproic acid (more to the left), and the sample co-ion, Na (more to the right).

Nevertheless, at higher I values, the secondary boundary vanishes when it reaches another (stationary) boundary that stays at the end of the injection zone. Thus, the secondary stacked zone of imatinib gets stuck at this position until it merges with the primary zone, and the two continue migration as a single stacked zone following the rear of the sodium peak. Additionally, imatinib has higher effective mobility than its BGE co-ion, ϵ -aminocaproic acid, at pH 2.0. Thus transient-ITP (t-ITP) establishes and the imatinib plug is confined between sodium boundary at its front and ϵ -aminocaproic acid boundary at its rear as shown in [Figure 4.B](#). At low I values, the secondary boundary becomes able to pass through the stationary boundary at the end of the injection zone and drags the secondary stacked zone of imatinib down the capillary. The two stacked zones of imatinib thus remain separated for a long time resulting in the “higher peak – plateau – lower peak” splitting pattern recorded by the detector. This provides a computational support for the experimental observations obtained at different I /pH of the BGE.

3.1. Effect of adding ACN to the samples

The addition of ACN volumes representing 50 to 70% (v/v) of the initial sample volume causes the precipitation of 88 to 92.1% of plasma proteins according to the work of Polson [32]. For ACN volumes of less than 50% (v), the protein precipitation decreases to less than 5%. Preliminary trials were realized by varying the percentage of ACN in the sample from 40 to 70 % (v/v) (results not shown). The amount of salt in the initial sample was maintained constant at 1.0% (w/v) as in the section 3.1 to evaluate only the effect of ACN on imatinib electrophoretic behavior. The first results showed that the addition of ACN volumes representing more than 50% of the initial sample volume caused instability of the electrical current even with low injected sample volumes. Therefore, a ratio of 50/50 ACN/1.0% NaCl (m/v) water (v/v) was selected for the experiments to ensure both an efficient precipitation of proteins and a stable electrical current (see section 2.5). While no splitting of imatinib peak was observed using BGE at pH 4.0 and I 150 mM with aqueous sample (as discussed before in part 3.1), the addition of ACN to the sample lead to a splitting of imatinib peak under the same analysis conditions ([Fig. 5A](#)). The peak splitting pattern observed is somewhat “inversed chair like pattern” compared to that obtained at the same pH (i.e. 4.0) but at lower I , i.e. 50 mM without ACN in the sample matrix (see [Fig. 2A](#)). Unfortunately, there is no theoretical model that can describe in details this kind of behavior of molecules inside the capillary when organic solvent is present in the sample matrix. So, our hypothesis is that imatinib stacked zone was not completely separated from sodium back and still a part of imatinib stayed trapped in the sodium zone (as discussed before in section 3.2). Changing the pH from 4.0 to 2.0 keeping the same I of BGE, imatinib peak efficiency improved with the disappearance of splitting ([Fig. 5B](#)). This also could be due to the fact that

imatinib gets a higher ionization state at pH 2.0 allowing imatinib stacked zone to be completely separated from sodium back. So, an ϵ -amino caproic – citric acid separation buffer (BGE) at pH 2.0 and / 150 mM had to be used to obtain an efficient peak of imatinib when dissolved in 50/50 ACN/1.0% NaCl (m/v) water (v/v).

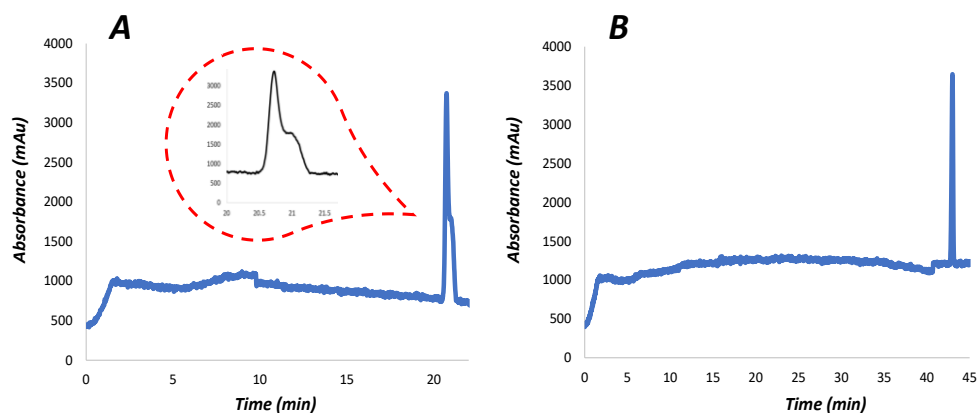


Figure 5: Electropherograms of imatinib mesylate obtained after adding ACN solvent with a total capillary length of 50 cm. Analysis conditions: BGE: citric acid – ϵ -aminocaproic acid buffer / 150 mM (A) pH 4.0 and (B) pH 2.0. Temperature: 25°C. Separation voltage: 15 kV. Sample injection volume corresponding to 7.5 % of the capillary length till the detector window. Detection: 254 nm.

It is well known that the addition of a high proportion of organic solvent, i.e., ACN in the sample can improve the sensitivity of CE analysis due to the existence of stacking phenomena [33]. So, in order to evaluate the performance of the on-line stacking at pH 2.0 and / 150 mM, the injected volume of imatinib dissolved in 50/50 ACN/1.0% NaCl (m/v) water (v/v) was varied from 57 to 295 nl (corresponding to 7.5 to 40% of the capillary volume till the detector window) by varying hydrodynamic injection pressure and injection time (see part 2.3). As the injected sample volume increased, symmetric and efficient peaks of imatinib were obtained (Fig. 6A) improving the sensitivity of the method due to on-line acetonitrile stacking. Fig. 6B shows the effect of the injected sample volume on imatinib peak height in several solubilizing media. Imatinib dissolved in 50/50 ACN/1.0% NaCl (m/v) water (v/v) allowed to inject up to 40% of the capillary effective length without instability of the electrical current as often observed with high volume injected. In comparison, only 20 and 10% of the capillary effective length could be injected for imatinib samples dissolved in 100% water or in water containing 1.0% NaCl (m/v). Moreover, good linearity between peak height and injected volume was obtained for imatinib in 50/50 ACN/1.0% NaCl (m/v) water (v/v) with r^2 of 0.995. In case of imatinib dissolved in 100% water or in water containing 1.0% NaCl (m/v), the linear increase in peak height stopped at 10 and 15% sample injected volume, respectively. In addition, sensitivity enhancement factors of 5.5 and 3.6 were obtained for imatinib in 50/50 ACN/1.0%

NaCl (m/v) water (v/v) with 40% volume injected compared to the maximum injected volumes of imatinib in water with 1.0% salt and in 100% water, respectively. So, the addition of 50% (v/v) of ACN in the sample containing 1.0% (v/w) of salt allowed to inject a large amount of sample without peak broadening and was defined as the best optimal sample preparation condition for the CZE analysis of imatinib.

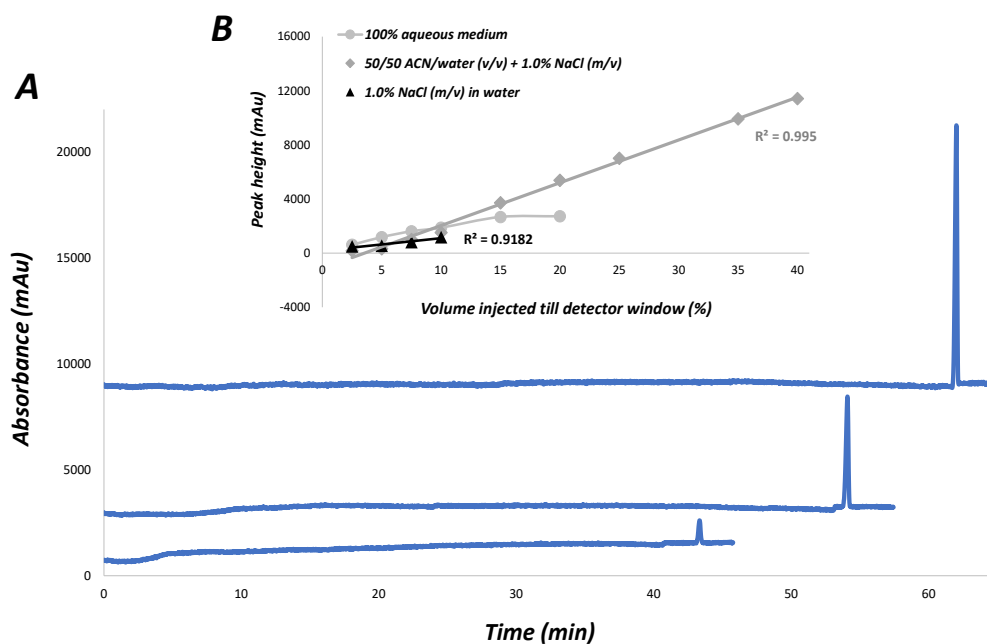


Figure 6: Analysis of imatinib samples in 50/50 ACN/1.0% NaCl m/v water v/v. (A) Effect of sample injected volumes (57, 148, 295 nL corresponding to 7.5, 20 and 40% of the capillary length till the detector window) on the analysis of imatinib mesylate. Analysis conditions: silica capillary 50 μm i.d., total length: 50 cm. BGE: citric acid – ϵ -aminocaproic acid buffer / 150 mM pH 2.0. Temperature: 25°C. Separation voltage: 15 kV. Sample injection volumes are expressed in percentage corresponding to the capillary length filled with the sample till the detector window. Detection: 254 nm. (B) Effect of injected sample volume (57 to 295 nL corresponding to 2.5 to 40% of the capillary length till the detector window) on imatinib peak height in different solubilizing medium (100% water, 1.0% NaCl m/v in water and 50/50 ACN/1.0% NaCl m/v water v/v).

3.1. Application to plasma samples

The performance of the proposed methodology was evaluated for the analysis of imatinib in plasma sample (see part 2.6). Due the dilution of plasma sample in acetonitrile (50/50 ACN/plasma (v/v)), the amount of salt in the sample analyzed by CZE is about 0.5% (w/v). The BGE was at pH 2.0 and I 150 mM. The capillary length was decreased from 50 to 30 cm (effective length 20 cm) while the separation voltage was kept at 15 kV in order to reduce the analysis time. Fig. 7A and 7B show the electropherograms obtained for blank (no imatinib) plasma and plasma spiked with imatinib. No interfering peaks of endogenous proteins were observed at the migration time of imatinib demonstrating the specificity of the proposed methodology. Moreover, the migration time of imatinib was decreased from 65 to 18

minutes compared to prior experiments due to the use of shorter capillary (30 cm capillary length). The maximum injected sample volume without peak broadening was of 156 nL (corresponding to 40% of the capillary volume till the detector window) and was similar to that obtained with a standard imatinib sample solution (see part 3.3). This result indicated that on-line stacking performances were similar for both injected solutions (standard and plasma solution) and confirmed the robustness of the proposed methodology for the analysis of imatinib in plasma samples.

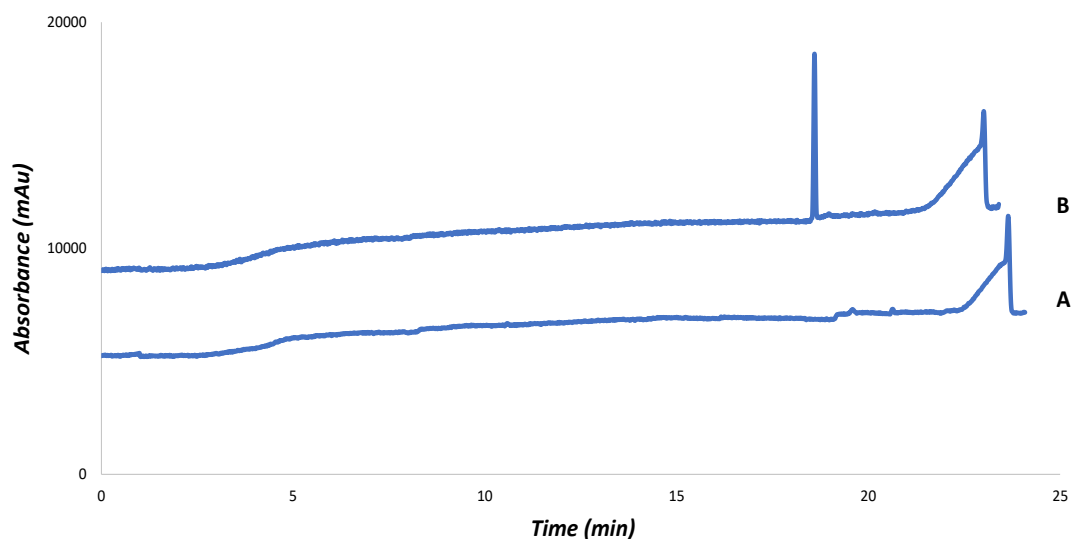


Figure 7: Electropherograms of the imatinib mesylate obtained from (A) blank sample (no imatinib) and (B) human plasma sample. Analysis conditions: silica capillary 50 μm i.d., total length: 30 cm. BGE: citric acid – ϵ -aminocaproic acid buffer / 150 mM pH 2.0. Temperature: 25°C. Separation voltage: 15 kV. Sample injection volume: 156 nL (corresponding to 40% of the capillary length till the detector window). Detection: 254 nm.

Then, the analytical performances of the methodology were evaluated and were resumed in [table 1](#). LOD and LOQ values of 48 and 191 ng/ml were obtained, respectively, which are values much lower than mean imatinib plasma level observed for patients treated by imatinib mesylate, which is estimated at 1000 ng/ml [34]. Good repeatability was obtained at LOQ level ($n = 6$) on the migration time (RSD: 1.68%) and corrected peak areas (RSD: 2.60%). Good linearity of calibration curve from 191 to 5000 ng/ml were obtained with correlation coefficient (r^2) of 0.997. So, the proposed methodology based on a simple, fast and cost-effective sample preparation protocol is well suited for the routine analysis of imatinib in plasma sample such as TDM.

Table 1: Summary of the quantitative results achieved on plasma samples with injected sample volume equal to 40% of the capillary volume till detector window.

Performance parameters	Values
Recovery (%)	90.3
Linearity (ng/ml)	191-5000
Correlation coefficient (r^2)	0.997

LOD (ng/ml)	48
LOQ (ng/ml)	191
% RSD ^a (corrected peak area)	2.60
% RSD ^a (migration time)	1.68
Total analysis time (min)	26

4. Conclusion

Studies were done to understand the electrophoretic behavior of imatinib in samples containing salt (NaCl) under various analytical conditions. Different peak splitting patterns of imatinib at different pH (2 and 4) and I (from 50 to 150 mM) of BGE were experimentally observed and were consistent with computer simulation performed with Simul software. These simulations proved that imatinib peak splitting is a consequence of the presence of salt (sodium ion) in the sample with the formation of imatinib/sodium boundaries that develop to different extends and propagate with various velocities within the sample zone depending on pH and I of BGE. ACN solvent was added to the sample to eliminate plasma protein and to allow on-line stacking of imatinib increasing the sensitivity of the method. At the same time, the addition of ACN eliminated the peak splitting at pH 2, allowing for the analysis of imatinib in plasma samples with simplicity, low cost, easy operational procedure and low consumption of organic solvent compared to other traditional sample preparation procedures (LLE, SPE). Further studies will be realized on clinical human samples to show the applicability of the proposed methodology for the possible TDM of TKI in patients' plasma.

Acknowledgments:

The authors appreciate the efforts of the Ecole Doctorale Chimie Balard (University of Montpellier, France) for the grant, giving the opportunity to Omar S. AHMED to realize a scientific exchange with the ECHMET group in Prague. Development of the new version of Simul is supported by "Czech Science Foundation, grant No. 18-11776S". The authors would like to thank Prof. Joseph Joachim and Prof. Emmanuel Cornillot the coordinators of the collaboration between MUST university and the university of Montpellier. The authors would like also to thank Mr Khaled El-toukhy chancellor, chairman of trustees in MUST university, Pr Mohamed Mostafa (vice president of MUST university) and Dr Yasmin El kashef, the responsible of foreign affairs in MUST university for their support.

References

- [1] Von Heeren, F., Thormann, W., *Electrophoresis* 1997, 18, 2415–2426.
- [2] Shihabi, Z.K., *J. Chromatogr. A.* 1993, 652, 471–475.
- [3] Øtergaard, J., Heegaard, N.H.H., *Electrophoresis* 2003, 24, 2903–2913.
- [4] Leone, A.M., Francis, P.L., Rhodes, P., Moncada, S., *Biochem. Biophys. Res. Commun.* 1994, 200, 951–957.
- [5] Ashri, N.Y., Abdel-Rehim, M., *Bioanalysis* 2011, 3, 2003–2018.
- [6] Lloyd, D.K., *J. Chromatogr. A.* 1996, 735, 29–42.
- [7] Clarke, N.J., Tomlinson, A.J., Schomburg, G., Naylor, S., *Anal. Chem.* 1997, 69, 2786–2792.
- [8] Friedberg, M.A., Hinsdale, M., Shihabi, Z.K., *J. Chromatogr. A.* 1997, 781, 35–42.
- [9] Carou, M.I.T., Mahía, P.L., Lorenzo, S.M., Fernández, E.F., Rodríguez, D.P., *J. Chromatogr. Sci.* 2001, 39, 397–401.
- [10] Peng, B., Lloyd, P., Schran, H., *Clin. Pharmacokinet.* 2005, 44, 879–894.
- [11] Petain, A., Kattygnarath, D., Azard, J., Chatelut, E., Delbaldo, C., Geoerger, B., Barrois, M., Seronie-Vivien, S., LeCesne, A., Vassal, G., *Clin. Cancer Res.* 2008, 14, 7102–7109.
- [12] Herviou, P., Thivat, E., Richard, D., Roche, L., Dohou, J., Pouget, M., Eschalier, A., Durando, X., Authier, N., *Oncol. Lett.* 2016, 12, 1223–1232.
- [13] Medenica, M., Jancic, B., Ivanovic, D., Malenovic, A., *J. Chromatogr. A.* 2004, 1031, 243–248.
- [14] Roth, O., Spreux-Varoquaux, O., Bouchet, S., Rousselot, P., Castaigne, S., Rigaudeau, S., Ragueneau, V., Therond, P., Devillier, P., Molimard, M., Maneglier, B., *Clin. Chim. Acta.* 2010, 411, 140–146.
- [15] D’Avolio, A., Simiele, M., De Francia, S., Ariaudo, A., Baietto, L., Cusato, J., Fava, C., Saglio, G., Di Carlo, F., Di Perri, G., *J. Pharm. Biomed. Anal.* 2012, 59, 109–116.
- [16] De Francia, S., D’Avolio, A., De Martino, F., Pirro, E., Baietto, L., Siccardi, M., Simiele, M., Racca, S., Saglio, G., Di Carlo, F., Di Perri, G., *J. Chromatogr. B Anal. Technol. Biomed. Life Sci.* 2009, 877, 1721–1726.
- [17] Bakhtiar, R., Lohne, J., Ramos, L., Khemani, L., Hayes, M., Tse, F., *J. Chromatogr. B Anal. Technol. Biomed. Life Sci.* 2002, 768, 325–340.
- [18] Xu, Z., Zhang, Y., Yang, L., Qiang, S., Zhang, W., Yu, Z., Hang, T., Wen, A., *J. Chromatogr. Sci.* 2013, 52, 344–350.
- [19] Ajimura, T.O., Borges, K.B., Ferreira, A.F., de Castro, F.A., de Gaitani, C.M., *Electrophoresis* 2011, 32, 1885–1892.

- [20] Rodríguez Flores, J., Berzas, J.J., Castañeda, G., Rodríguez, N., J. Chromatogr. B Anal. Technol. Biomed. Life Sci. 2003, 794, 381–388.
- [21] Forough, M., Farhadi, K., Eyshi, A., Molaei, R., Khalili, H., Javan Kouzegaran, V., Matin, A.A., J. Chromatogr. A. 2017, 1516, 21–34.
- [22] Rodríguez, J., Castañeda, G., Muñoz, L., López, S., Anal. Methods. 2014, 6, 3842–3848.
- [23] Elhamili, A., Bergquist, J., Electrophoresis 2011, 32, 1778–1785.
- [24] Hruška, V., Jaroš, M., Gaš, B., Electrophoresis 2006, 27, 984–991.
- [25] Ahmed, O.S., Ladner, Y., Montels, J., Philibert, L., Perrin, C., J. Chromatogr. A. 2018, 1579, 121–128.
- [26] Malý, M., Dvohunová, M., Dvořák, M., Gerlero, G.S., Kler, P.A., Hruška, V., Dubský, P., Electrophoresis 2019 elps.201800400. doi:10.1002/elps.201800400.
- [27] Revilla, A.L., Havel, J., Jandik, P., J. Chromatogr. A. 1996, 745, 225–232.
- [28] Ermakov, S.V., Zhukov, M.Y., Capelli, L., Righetti, P.G., Anal. Chem. 1994, 66, 4034–4042.
- [29] Malá, Z., Gebauer, P., Electrophoresis 2006, 27, 4601–4609.
- [30] Malá, Z., Gebauer, P., Boček, P., Electrophoresis 2009, 30, 866–874.
- [31] Gebauer, P., Boček, P., Electrophoresis 2005, 26, 453–462.
- [32] Polson, C., Sarkar, P., Incledon, B., Raguvaran, V., Grant, R., J. Chromatogr. B. 2003, 785, 263–275.
- [33] Tůma, P., Bursová, M., Sommerová, B., Horsley, R., Čabala, R., Hložek, T., J. Pharm. Biomed. Anal. 2018, 160, 368–373.
- [34] Lankheet, N.A.G., Knapen, L.M., Schellens, J.H.M., Beijnen, J.H., Steeghs, N., Huitema, A.D.R., Ther. Drug Monit. 2014, 36, 326–334.

Section III (Supplementary results)

In this section, the detailed transition states and mixed boundaries that the sample of imatinib in high saline matrix (explained in section II) pass through at different I and pH of the BGE are explained in details by simulations obtained by Simul program.

1 Simulations of development of imatinib peak splitting

1.1 Chemical composition

- *Sample*

Constituent	Concentration / mM
Imatinib	1.7
Methanesulfonic acid	1.7
Na	171
Cl	171

- *BGE pH 4.0:*

Constituent	Concentration / mM			
	I 150 mM	I 125 mM	I 100 mM	I 75 mM
E-aminocaproic acid	163	136.25	109	81.75
Citric acid	100	83.75	67	50.25

- *BGE pH 2.0:*

Constituent	Concentration / mM			
	I 150 mM	I 125 mM	I 100 mM	I 75 mM
E-aminocaproic acid	137	114	91.2	63.84
Citric acid	1800	1500	1200	840

1.2 Legend

Below are figures illustrating simulations of development of sample zone in various BGEs. In order to get more space in the figures and to improve their readability, we do not provide legends and x and y axis units in every figure. Instead, we provide a legend common to all figures here:

x axis All figures have x axis in meters.

y axis All figures have several y axes. Every axis belongs to one or more profiles and has units that correspond to that profile(s)

Profiles All figures share the same color-coding for different profiles and their assignment to a y axis as follows

Profile	color	axis	axis units
Imatinib	Red	left red	mM
Sodium	Brown	left black	mM
Chloride	Green	left black	mM
E-aminocaproic acid	Blue	left black	mM
pH	Pink	right pink	pH units
Conductivity	Silver	right silver	10^{-2} S/m

1.3 Simulation of imatinib peak development at pH 4.0 and I 75 mM

Figure S 1: Simulation time-frames at pH 4.0, I 75 mM. Legend and units provided in section 1.1. Description of panels follows in the text. Horizontal dashed lines signify individual boundaries. Arrows (flags) points to the direction of boundary movement. Scales of x and y axes may differ for different panels.

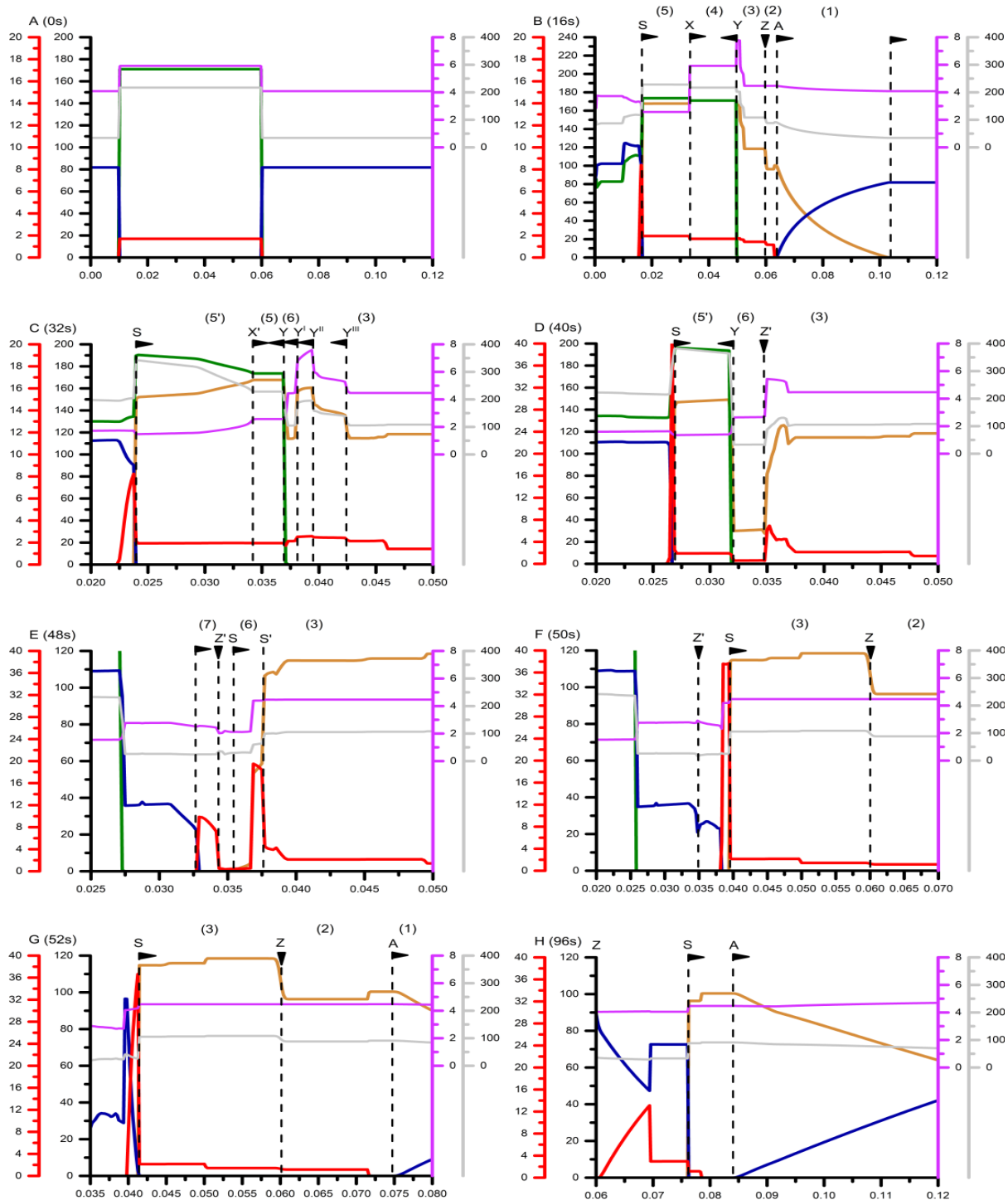


Figure S 1A, 0s:

At the beginning, 50 mm long zone of 1.7 mM imatinib mesylate with 1% (171 mM) NaCl is introduced into homogeneous BGE. Conductivity in the sample zone is approximately 6 times higher than conductivity in BGE and pH of the sample is almost 6.0, pH of BGE is 4.0.

Figure S 1B, 16s:

Upon the voltage application, several boundaries and transition zones form with a relatively long lifetime due to the large width of the injection zone. A typical electromigration dispersion (EMD) boundary is seen at the front of Na profile as the fast strong-electrolyte ion penetrates into BGE with a slower co-ion (1). This region is followed by a transient zone (2) between the beginning of the EMD boundary (A) and the end of the original sample zone (Z), where the concentration of Na is regulated by BGE to a value of approx. 95 mM. Next is a transition region (zone 3) that forms as Cl ions penetrates through the original sample zone (Y). The original sample zone is still preserved in zone (4). Another sharp boundary (X) moves through the sample region that bounds zone (5) where a disproportion between Cl and Na ions exists making the zone acidic. Finally, a sharp moving boundary (S) is formed at the rear of the sample plug as a counterpart [1] to the diffusive boundary, zone 1.

Boundary (S) moves faster than imatinib analyte so that it penetrates through imatinib zone leaving a portion of imatinib behind. That portion of imatinib, however, experiences much higher electric field (BGE with lower conductivity), which speeds up the analyte until it hits the boundary (S) again. This causes an accumulation (field-amplified sample stacking) of imatinib at the rare boundary of Na. Simultaneously, the decrease in pH in zone (5) speeds up imatinib as well. Nevertheless, the pH effect can apparently not overweight the effect of the huge disproportion in the electric fields inside and outside NaCl plug. The front of imatinib zone is determined by point (A). The concentration profile of imatinib between points (S), (A) is approximately flat, and spreads forward only very slowly compared to the speed of boundary (S). Imatinib plug thus shortens as the peak accumulated at the rear of the plug is chasing imatinib plug front.

Noticeable is also boundary (Y) right after which pH attains a value as high as almost 8.0, which makes imatinib molecules virtually immobilized. Nevertheless, imatinib does not accumulate at this boundary as the boundary itself is moving to the anode, i.e., gradually penetrating through the imatinib plug.

Figure S 1C, 32s:

Should the peak profile depicted in Figure 2A (main article) result, the peak of imatinib accumulated at boundary (S) must not reach the front of imatinib zone (A) before imatinib gets completely separated from Na peak and reaches the detector. The simulation reveals, however, that the situation is more difficult since the system undergoes one more important transition. First, zone (4) of the original sample composition disappears as boundaries (X) and (Y) reach each other. At this point, a wave (the front of which is depicted with boundary (X')) of even more disproportional concentrations of Na and Cl ions develops at boundary (S) and spreads into region (5) forming a new composition of region (5'). This leads to a decrease in pH, which is however related to a huge increase in conductivity in this sub-region, leading to further profound accumulation of imatinib at boundary (S). Simultaneously, a dip in Na profile starts to develop (zone 6) along with several anodic boundaries (Y^I - Y^{III}) that altogether form a zone of an elevated pH value (zone 7).

Figure S 1D, 40s:

The amount of imatinib accumulating at boundary (S) is reaching a value comparable to that of the BGE and NaCl constituents, so that it allows for a formation of a transient-ITP with the BGE-co-ion (E-aminocaproic acid) as a terminating ion, imatinib the middle-ion, and Na the leading ion. This would not be possible if the disproportion of Na and Cl ions had not caused the decrease in pH down to a value of 2.0 in this region, which gives to imatinib higher effective mobility than that of E-aminocaproic acid (while the opposite applies at the actual pH of BGE).

In the meantime, zone (5') evolved completely into the composition with the high disproportion in Na and Cl ion concentrations. After that point, a stationary boundary (Z') arises at the position of approx. 35mm that now bounds region (6). As the process continues, boundary (Z') somewhat absorbs anodic boundaries Y^I - Y^{III} (panel C), gradually shortening region (7). Boundary (Y) moves out of the stationary boundary (Z') and the dip in Na concentration in region (6) grows into a deep depression in Na profile so that Na distribution itself becomes split into two parts (regions (5') and (3)).

Simultaneously, another portion of imatinib starts to accumulate at the secondary Na boundary (Z'). Interestingly, the accumulation of imatinib takes place ahead of that boundary (i.e. inside Na zone). Formation of stacked zone of an analyte either behind or ahead of a transient pH boundary (depending on the analyte's pKa value) was reported in a theoretical study by Thormann [2], albeit without any further explanation. It should be rather attributed to a complicated, not completely understandable process of

formation of boundary (Z'). Anyway, two accumulation zones of imatinib now exist in the system, ahead the newly formed boundary (Z') and behind the rear boundary (S).

Figure S 1E, 48s

Boundaries (S) and (Y) have reached each other, region (5') disappeared and Na and Cl zones became completely separated. This is associated with an abrupt decrease in conductivity that Na boundary (S) experiences ahead of it. Consequently, the boundary literally sneaks out of its position bounded to the transient-ITP formed between the stacked portion of imatinib and Na (panel D), and turns into a Na tail (S, panel E) that detaches from the imatinib stacked plug. That portion of imatinib still continues its ITP-pattern migration (followed by the slower BGE co-ion), yet the leading Na ion is not present. The detachment of Na plug from the front of the stacked portion of imatinib causes another drop in pH in front of the imatinib-stacked zone. At the low pH value, imatinib molecules have higher effective mobility than in the stacked zone. Thus, it is likely hydroxonium ions or even the imatinib itself that constitutes leading ions for the transient-ITP of the stacked portion of imatinib from now on.

As boundary (Y^{III}) continues its anodic movement to the stationary boundary (Z'), the region of elevated pH (7.0) shrinks until it completely disappears. At that point, a new cathodic boundary (S') separates from the stationary boundary (Z'). Boundary (S') penetrates through the portion of imatinib accumulated in zone (7) (panel D).

Figure S 1F, 50s:

Na tail (S, panel E) reaches the cathodic boundary (S', panel E), and the two merge into a single boundary (S), which will finally become the rear of Na peak that is evolving in the separation system from the injection zone. Boundary (S) continues its penetration into imatinib zone as the two sample components (Na and imatinib) separates from each other, followed by the portion of imatinib accumulated in zone (7, panel D). Simultaneously, the transient-ITP imatinib zone moves ahead, still in a region of pH 2.0, until the two accumulated zones of imatinib merge into a single zone as well. This zone will become the actual imatinib peak registered by the detector as seen in Figure 2A (main article).

Figure S 1G, 52s:

The pH value in Na peak and in the newly established zone of imatinib and E-aminocaproic acid behind Na peak reaches its expected value in BGE, i.e., the value of 4.0. This slows down imatinib molecules and gives them an effective mobility lower than that of E-aminocaproic acid. Thus, E-aminocaproic acid

penetrates into imatinib zone (up to boundary (S)), the transient-ITP process vanishes, and an EMD-dispersed peak of imatinib is formed as expected in the given BGE.

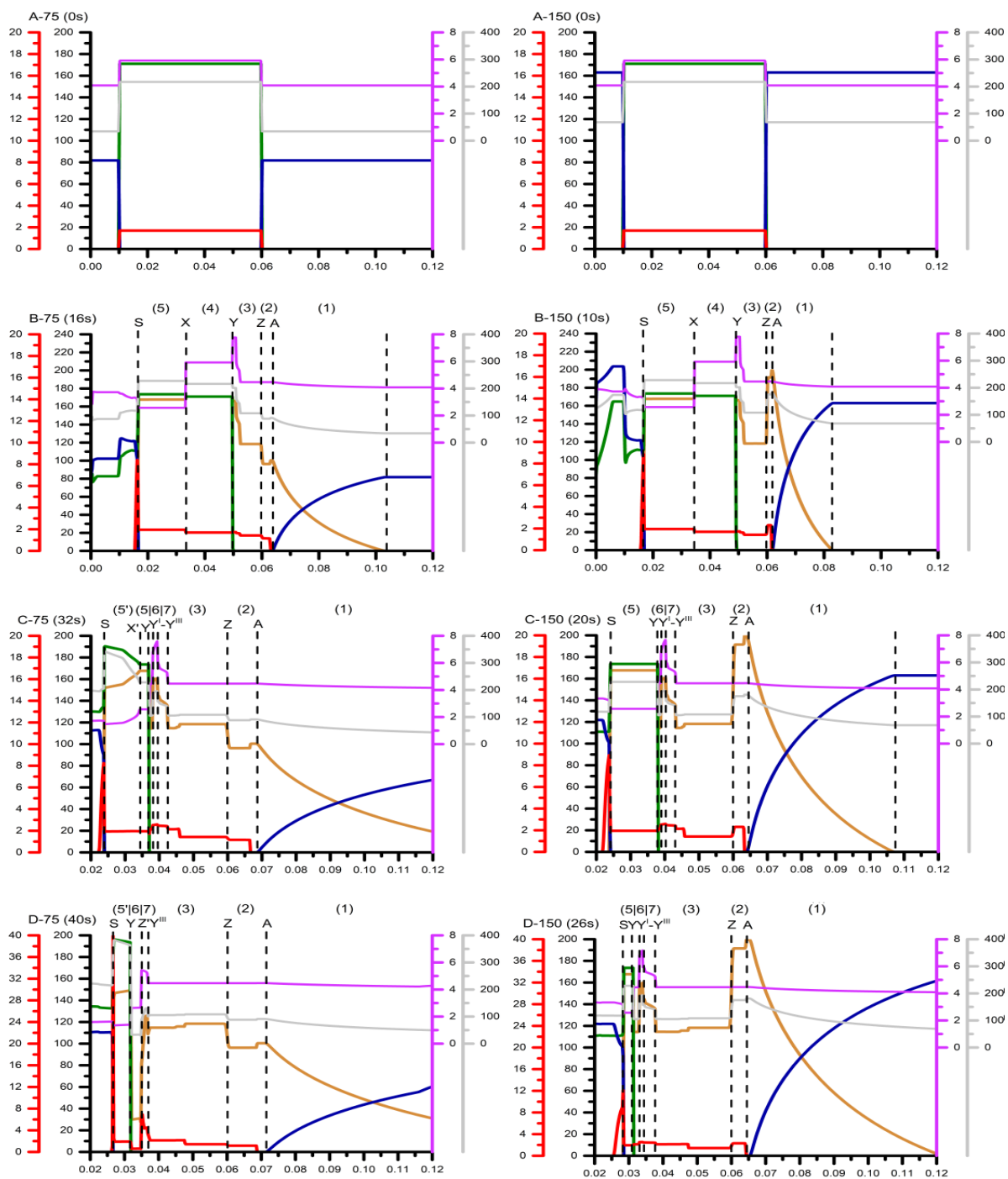
Nevertheless, the peak still has not escaped the original sample zone (Z) and a portion of imatinib has propagated into region (2), which itself widened with a slow movement of point (A). This portion of imatinib plug will become the step registered by the detector as seen in Figure 2A (main article).

Figure S 1H, 96s:

Na boundary (S) now moves with so high velocity relative to imatinib at pH 4.0 that although a field-amplified sample stacking of imatinib could continue at this boundary, the accumulated zone of imatinib is unable to catch up with the boundary and the close-to-the-original amount of imatinib leaves the Na peak. This concentration profile pattern of imatinib is further stabilized by the fact that the analyte develops into an EMD-tailing peak with sharp front. Thus, the pattern survives for a certain period of time even after imatinib has become completely separated from Na peak (Figure 3, main article).

1.4 Comparison between I 75 mM and I 150 mM at pH 4.0

Figure S 2 (two pages): Comparison between I 75 mM (left) and I 150 mM (right) at pH 4.0. Legend and units provided in section 1.1. Description of panels follows in the text. Horizontal dashed lines signify individual boundaries. Scales of x and y axes may differ for different panels but are kept the same for each pair of left and right panels. Time frames for I 75 mM are the same as in Figure S 1.



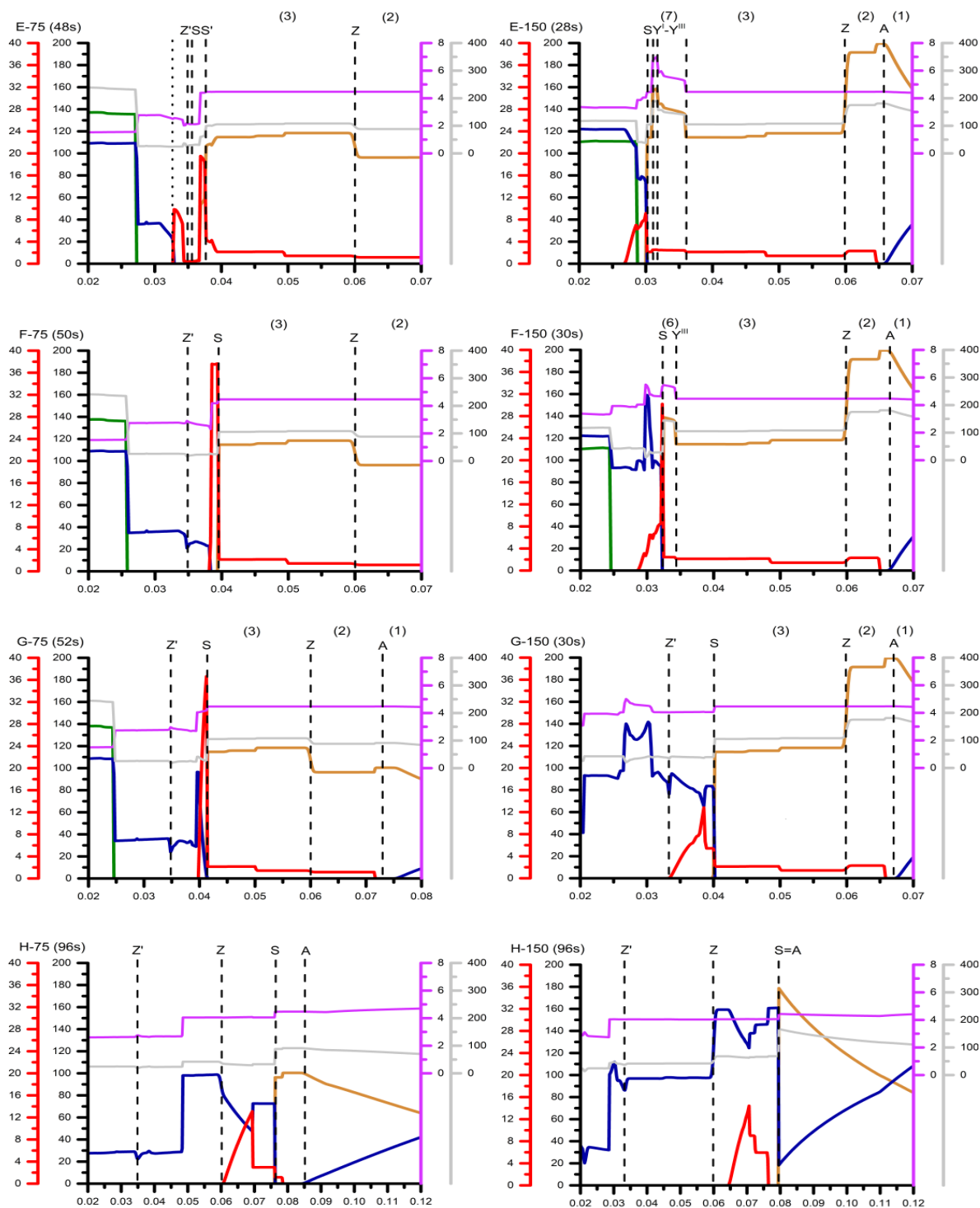


Figure S 2 compares the aforementioned processes at two BGEs of 75 mM and 150 mM. I correction was not applied in simulations. The difference in I reflects the difference in ionic concentrations in the two

BGEs and thus in their conductivities. We will refer to the two BGEs of I 75 mM and I 150 mM as to BGE4@75 and BGE4@150, respectively.

Figure S 2A:

Initial states differ only in conductivity values in the two BGEs. Conductivities in sample zones are the same since the same sample composition is introduced into both systems. Nevertheless, the electric field in the low-conductivity-BGE system (BGE4@75) and the high-conductivity-BGE system (BGE4@150) must be distributed in such a way that a higher electric field is found in the low-conductivity (high-resistance) regions, while the overall integral of the electric field remains the same since the same voltage is applied across the same capillary length in both cases.

These results in a slightly lower initial electric field in the BGE region accompanied by a significantly higher initial electric field in the sample plug region in BGE4@150 compared to those of BGE4@75. For example, let us consider a 50 mm long sample plug injected into the two systems in a 250 mm long capillary. Then, $E_{\text{BGE150-BGE}}$ would be 96% of the value of $E_{\text{BGE75-BGE}}$, while $E_{\text{BGE150-SAMPLE}}$ be 2-times the value of $E_{\text{BGE75-SAMPLE}}$; where $E_{\text{BGE}\{150/75\}\text{-[BGE/SAMPLE]}}$ stands for electric field [in BGE (outside the sample plug)] / [in sample plug] in system {BGE4@150} / {BGE4@75}, respectively, at the beginning of the separation process.

Figure S 2B:

As a consequence of electric field distribution, the front of Na peak (zone 1) and point (A) propagate slower in BGE4@150 than in BGE4@75. Similarly, boundaries (S, X, Y) that develop inside the sample plug propagate much faster. Notice nearly the same positions of these boundaries in panels (B-75) and (B-150), although 16 s vs. 10 s of the process has elapsed in the former (B-75) vs. the later (B-150) case. Consequently, the life-time of all the transient states shortens in the high-conductivity BGE4@150.

Development of all profiles are nearly identical in both systems at the beginning (though with different overall speeds) except for the concentration level of Na in region (2), which establishes at significantly higher value in BGE4@150 than in BGE4@75, as expected.

Figure S 2C:

The simulation reveals first, yet minor, difference in the dynamics of development of the two systems. The secondary wave (X') and the related region (5') do not develop in BGE4@150. Instead, region (5) remains stable even after boundary (X) hits boundary (Y) and disappears. Otherwise, the systems behave very similarly up to this point.

Figure S 2D:

This panel shows the time-frames of the two systems right before Na and Cl get separated, i.e., boundaries (S) and (Y) are about to reach each other and region (5) to disappear. This happens after 40 s and only 26 s of voltage application in BGE4@75 and BGE4@150, respectively (the times are related to applied voltage and capillary length in simulation and are not absolute times as expected in an experiment).

The simulation reveals that the stationary boundary (Z') has not (yet, cf. panel G) developed in BGE4@150, and thus boundaries Y^I-Y^{III} continue their anodic movement until they actually vanish as they meet boundary (S), which is approaching from the anodic site. Therefore, the secondary concentration zone of imatinib adjacent to boundary (Z') (region 7, BGE4@75) does not rise in BGE4@150. Similarly, the large concentration dip in Na profile (6) does not develop either. This is an important difference observed between the two systems, albeit it is difficult to explain by any simple (elementary) rules of electrophoresis.

Figure S 2E:

While the transient-ITP is established in BGE4@75, it never happens in BGE4@150. Instead, the front of E-aminocaproic acid co-ion profile keeps up with Na boundary (S) in BGE4@150 for the entire process. This may be attributed to the stationary boundary (Z') along with the Na concentration dip in region (6) not to be present in BGE4@150 and/or to the fact that imatinib is not so profoundly concentrated at boundary (S) in that BGE. The less profound preconcentration of imatinib in BGE4@150 is caused by a higher pH value (and thus lower effective mobility of imatinib) that is seen in the zone of E aminocaproic acid right preceding boundary (S). This, in turn, is likely contributed by the higher buffering capacity of the highly concentrated BGE.

Figure S 2F:

As the two stacked zones of imatinib merge in BGE4@75, imatinib concentration distributions become again similar in both BGEs. Yet, imatinib is less stacked at Na boundary (S) in BGE4@150, where field-amplified sample stacking takes place rather than transient ITP observed in BGE4@75.

Figure S 2G:

Panel G shows time frames in BGE4@75 and BGE4@150 when Na boundary (S) reached a position of 40 mm in both systems. It takes 52 s and approx. half that time in BGE4@75 and BGE4@150, respectively. Furthermore, the "peak" (accumulated zone) of imatinib has already started separating from Na peak boundary (S) in BGE4@150, while the preconcentration process still continues in BGE4@75. The "peak"

of imatinib is also lower and wider, while the imatinib step (ahead of the “peak”) is higher in BGE4@150 compared to BGE4@75. Finally, the forehead of imatinib profile has penetrated deeper along the capillary in BGE4@75 than in BGE4@150, making imatinib plug shorter in BGE4@150. This all contributes to a longer life-time of the peak splitting pattern in BGE4@75 compared to BGE4@150.

Figure S 2H:

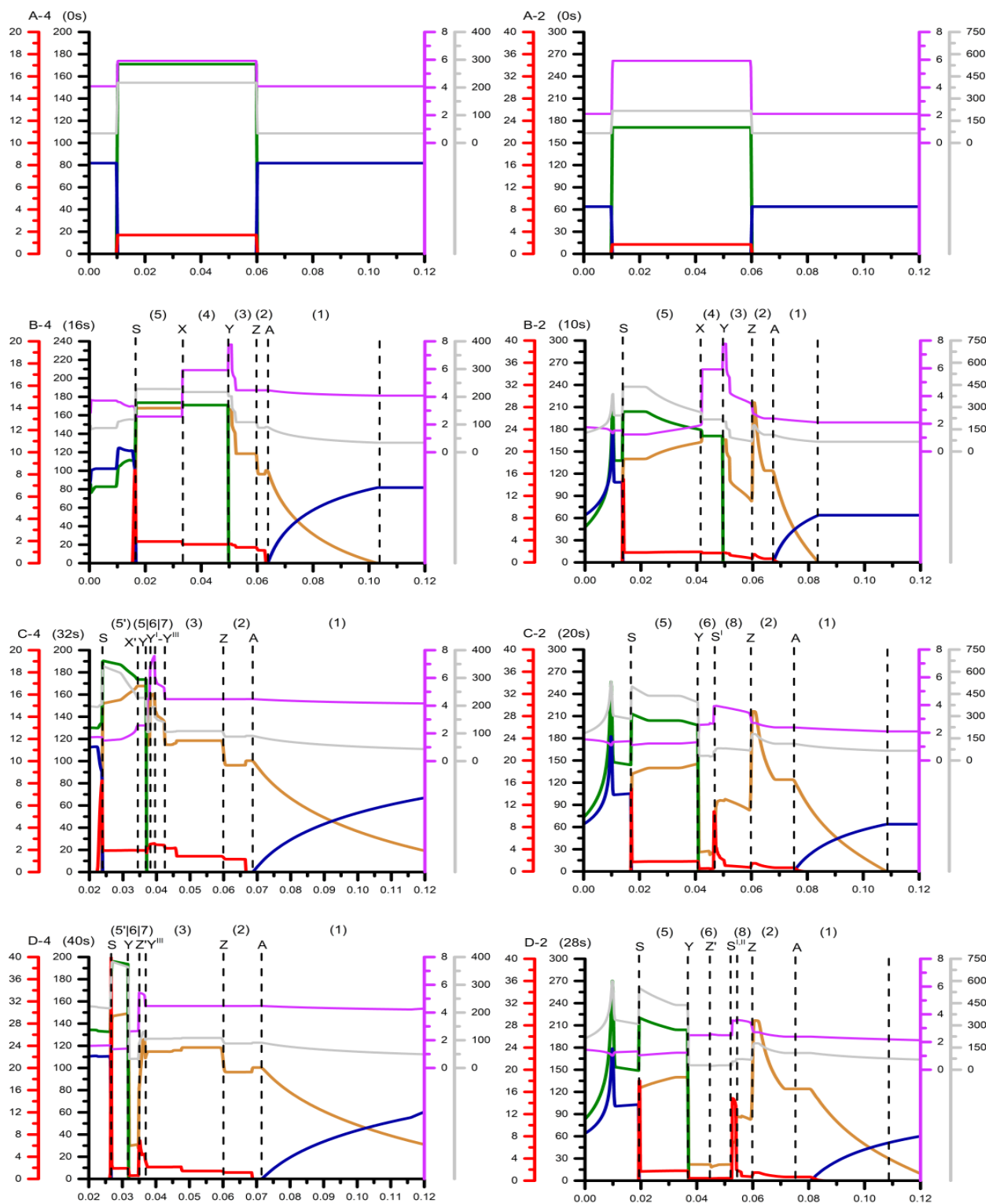
Final frames show the separation process after 96 s. Both “peaks” of imatinib are approximately of the same size, nevertheless the difference between the peak top and the plateau region is significantly higher in BGE4@75. In that BGE, and in contrast to BGE4@150, Na peak has still not fully developed and imatinib has not yet been separated from Na boundary (S).

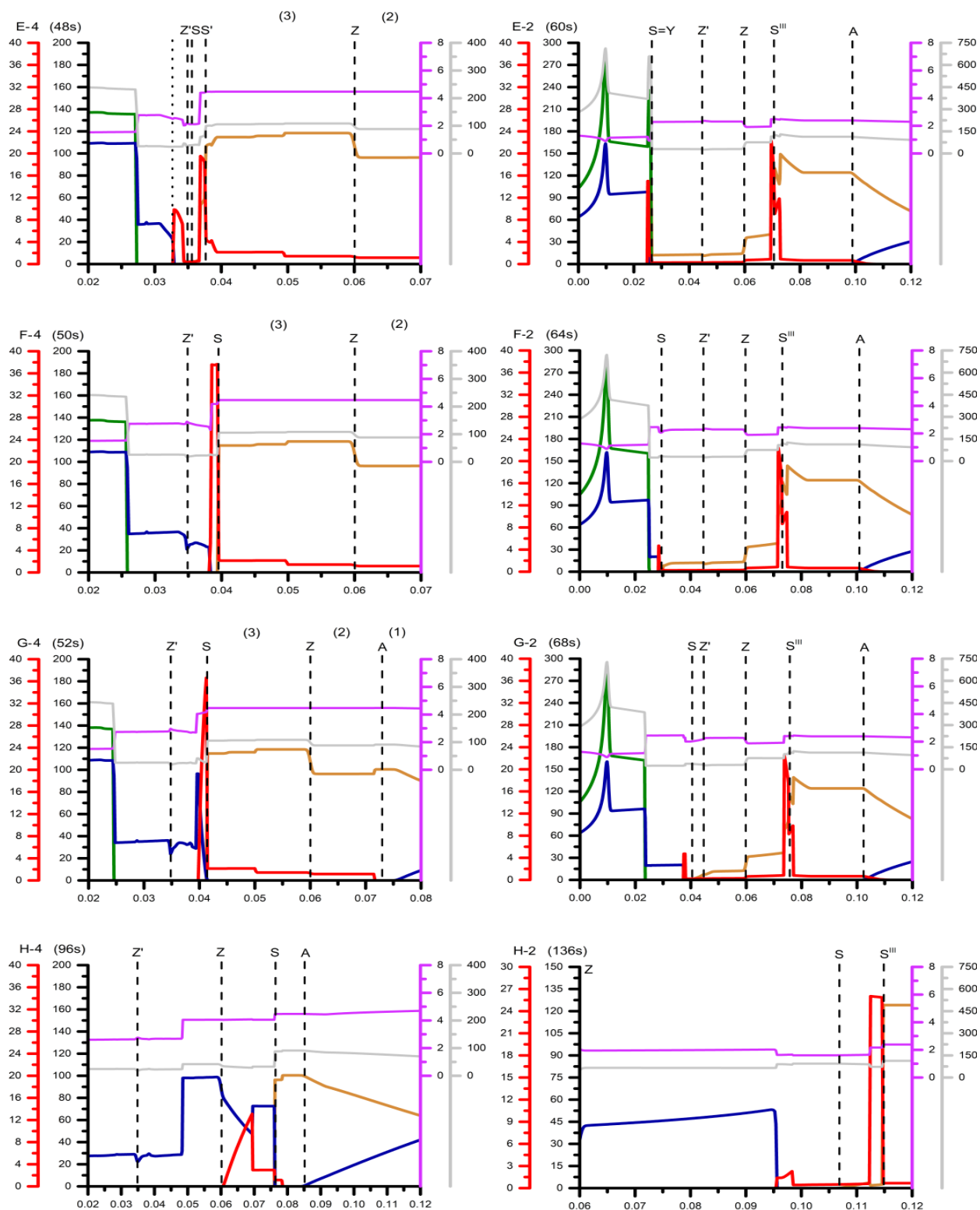
Consequently, the initial peak splitting pattern of imatinib is smeared out to the expected triangular peak distribution before it can reach the detector at high-conductivity (i.e. high I) BGEs. The simulation was performed in a shorter capillary than in experiment for performance reasons. Thus, the survival of the peaks till the actual position of the detector was not studied. Additionally, simulation in BGE of the experimental value of I 50 mM could not be performed within a reasonable time, since too sharp boundaries and regions of almost zero conductivity (cf. e.g. zone (6) in Figure S 1D) developed to an extent that could not be supported by Simul.

The trend of prolongation of the peak splitting pattern with decreasing I (conductivity) of BGE was nevertheless confirmed (Figure 3B, main article) and it can be anticipated that lowering I down to 50 mM would easily lead to the peak splitting observable in the detector.

1.5 Comparison between pH 4.0 and pH 2.0 at I 75 mM

Figure S 3 (two pages): Comparison between pH 4.0 (left) and pH 2.0 (right) at I 75 mM. Legend and units provided in section 1.1. Description of panels follows in the text. Horizontal dashed lines signify individual boundaries. Scales of x and y axes may differ for every panel as well as within every pair of left and right panels. Time-frames for I 75 mM are the same as in **Figure S 1**.





Next simulations were performed in BGE of pH 2.0. Here we compare the results between systems comprising of BGEs of pH 4.0 and pH 2.0, both at I 75 mM (BGE4@75 and BGE2@75, respectively).

Figure S 3A:

Initial conditions differ only in pH (and thus concentrations of constituents) of the two BGEs.

Figure S 3B:

Zone (5), boundary (X), in BGE2@75 develops in a way similar to that as zone (5'), boundary (X'), develops in the later stage (panel C-4) in BGE4@75. Closer look at panels (B-2) and (C-4) reveals that BGE composition right preceding boundary S is similar in both cases (B-2 and C-2), which makes similar development of zone (5) in BGE2@75 and zone (5') in BGE4@75 expectable. However, the system needs to go through one extra transition step (panel B-4) in BGE4@75.

Another difference is seen in zone (3) where no plateau in Na concentration profile exists in BGE2@75 as it does in BGE4@75. Finally, lower pH gives imatinib higher effective mobility so that it penetrates deeper into Na front in BGE2@75.

Figure S 3C-D:

The most important difference between the two systems is observed as boundaries (Y^I - Y^{III}) along with region (6) starts being developed. In BGE4@75 (panel C-4), these boundaries have anionic mobilities and follow Cl boundary (Y) until the stationary boundary (Z' panel D-4) emerges that later absorbs them. From then on, depletion of Na ions takes place in zone (6) and the Na zone becomes split in itself. Simultaneously, the secondary stacked zone of imatinib raises at boundary Z' in zone (7).

In contrast to BGE4@75, the newly developed boundary (in place of boundaries (Y^I - Y^{III})) has cationic mobility and is thus denoted as (S') in BGE2@75. This causes an immediate accumulation of the secondary stacked zone of imatinib on this boundary and imatinib is further stacked as boundary (S') penetrates through the imatinib plug. Additionally, Na concentration depletion is more profound and region (6) widened as the two boundaries (Y) and (S') move in opposite directions in BGE2@75. Finally, boundary (S') moves with considerably higher velocity than boundary (S), which pulls the two stacked zones of imatinib (rare zone stacked at boundary (S) and second zone developed on boundary (S')) apart.

These two paragraphs reveal the difference in the dynamics of the imatinib peak development in BGEs of pH 4.0 and pH 2.0, that are most likely responsible for the different peak splitting patterns observed in these two BGEs at 175 mM (Figure 2, main article). Nevertheless, as stated earlier, these effects are easily observable by means of the computer simulation, yet not so easily transferable into a logic of any elementary rules of electrophoresis.

Besides, a few additional minor observations can be made in BGE2@75, as is the zone of an elevated pH (region 8) as a counterpart to region (7) in BGE4@75 and the development of temporal boundaries such as S^{II} (panel D-2) as a counterpart to boundaries Y^{II} - Y^{III} in BGE4@75.

Figure S 3E-G:

These panels demonstrate how the two systems develop after the depletion zone (6), i.e., sodium peak splitting emerged. In BGE4@75, region (6) is relatively narrow and the rear stacked zone of imatinib plug (S) soon catches up with the secondary stacked zone of imatinib (S') going through the transient-ITP phase. Similar process takes place in BGE2@75. Nevertheless, the two “peaks” (accumulated zones) of imatinib has got far away from each other due to the cathodic character of the boundaries (S^I - S^{III}) (the boundaries have consecutively arisen in the system – not demonstrated – so that we finally refer to boundary S^{III} in place of boundary S^I) before they really start approaching each other. For example, at the time point when Na separates from Cl (i.e., boundaries (S) and (Y) cross over each other), boundary (S') along with the accumulated portion of imatinib on it has already escaped the separation zone (panel E-2).

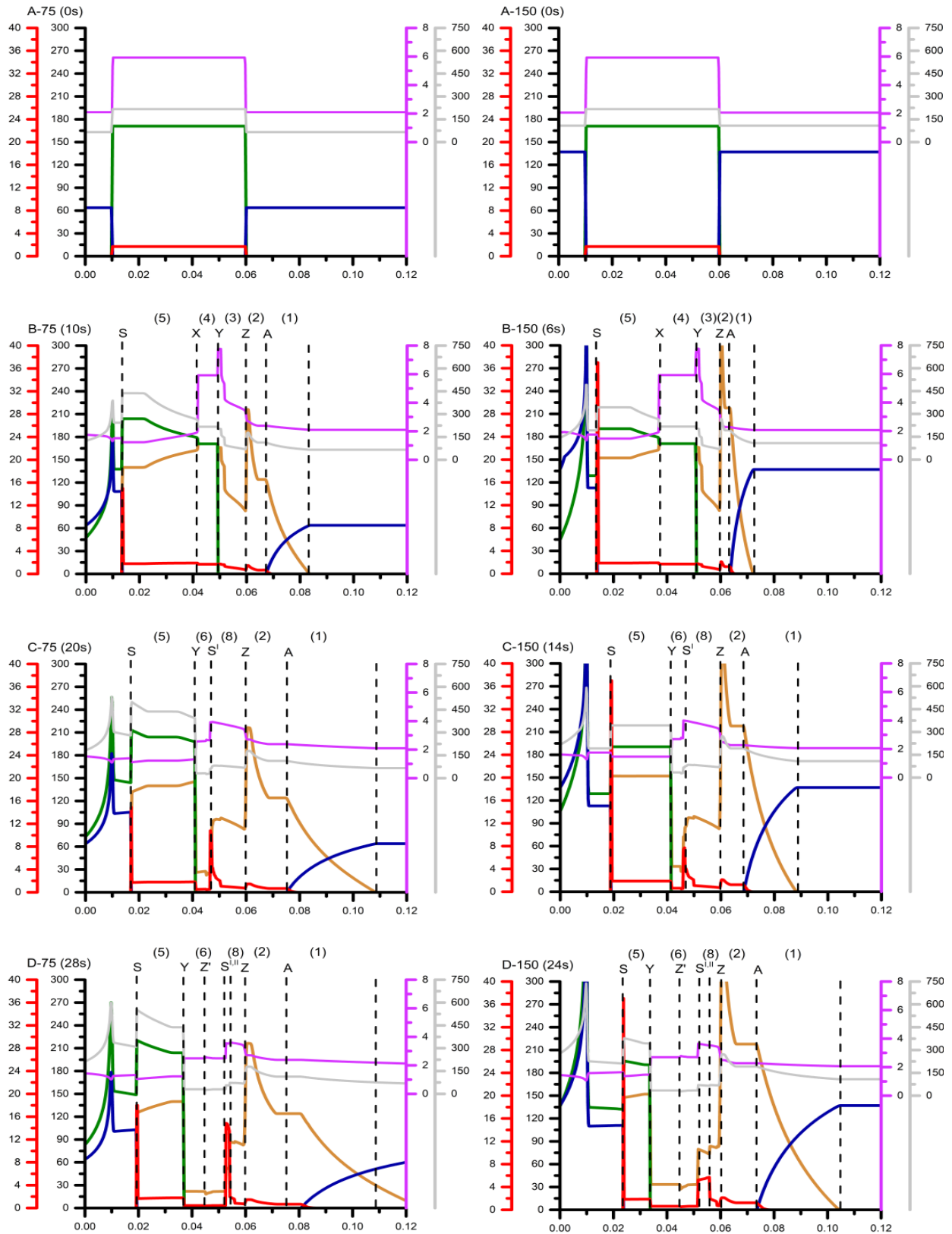
Not earlier than that, boundary (S) speeds up and starts chasing the head of the sodium peak that split from its rear earlier (Figure S 3C). Still, the rear portion of stacked imatinib is slower than that boundary continuing its movement in the transient-ITP mode (followed by E-aminocaproic acid).

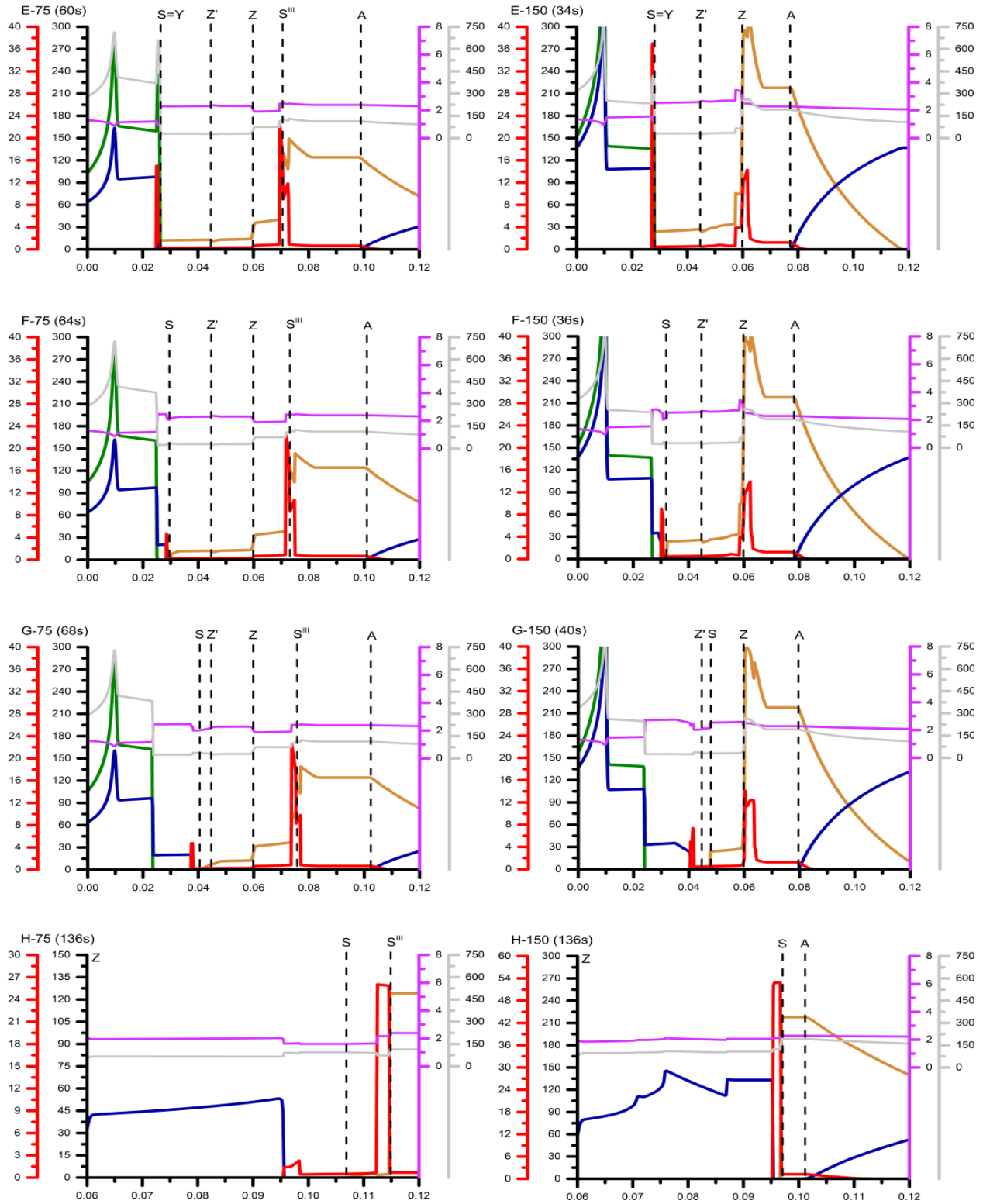
Figure S 3H:

Consequently, the two-stacked zone of imatinib has not merged after 136 s of the separation process in BGE2@75, while they already form a single stacked zone in BGE4@75 in 50 s. This demonstrate itself as “two peaks connected with a plateau” splitting pattern in the BGE of pH 2, and as “chair-like” splitting pattern in the other BGE of pH 4.0.

1.6 Comparison between I 75 mM and I 150 mM at pH 2.0

Figure S 4 (two pages): Comparison between I 75mM (left) and I 150 mM (right) at pH 4.0. Legend and units provided in section 1.1. Description of panels follows in the text. Horizontal dashed lines signify individual boundaries. Scales of x and y axes are the same throughout the entire figure (except for x-axis, panel H). Time-frames for I 75 mM are the same as in **Figure S 3**.





The last simulation demonstrates the difference between low and high I (concentrations) BGEs of pH 2.0. Two main factors that affect final imatinib peak shape in these two BGEs, i.e., peak splitting recorded in BGE2@75 and not recorded in BGE2@150, are revealed.

Figure S 4A-D:

The systems behave similarly till Na and Cl do not get separated. Nevertheless, the BGE2@150 system develops faster/slower inside/outside the injection zone due to the different electric field distributions as discussed earlier (chapter 1.4 Comparison between I 75 mM and I 150 mM at pH 4.0, Figure S 2A).

Figure S 4E:

Thus, it takes 60 s to the BGE2@75 system to reach the point of separation of Na and Cl sample components ($S=Y$), while the same point is reached already in approx. half that time in BGE2@150.

Figure S 4D-G:

More importantly, though, the two systems differ in how boundary (S^{III}) interacts with the stationary boundary (Z). In both cases (BGE2@75 and BGE2@150), the temporary cathodic boundaries S^{II} - S^{III} develop at which the secondary stacked zone of imatinib accumulates. Nevertheless, boundary (S^{III}) can overtake the stationary boundary of the injection zone (Z) pushing this secondary stacked zone of imatinib further down the capillary. To the contrary, the boundary (S^{III}) is absorbed by the stationary boundary (Z) in BGE2@150 leaving the secondary stacked zone of imatinib was stuck there until the rear Na boundary (S) reaches it. (The second stationary boundary (Z') also develops in pH 2 albeit it does not play any particular role here.)

Figure S 4H:

After that point, the two hitherto separated stacked zone of imatinib merge in BGE2@150, and Na leaves the injection zone as a single peak followed by the stacked zone of imatinib (while a portion of imatinib is still escaping from Na peak). Since imatinib has higher effective mobility than the E-aminocaproic acid co-ion at pH 2.0, the three components, E-aminocaproic acid|stacked imatinib|Na, form a transient-ITP track in the BGE2@150. Thus, the point of a complete separation of imatinib from Na rear was not achieved in these simulations.

References of supplementary results

- [1] Dvořák, M., Dubský, P., Dohunová, M., Gaš, B., *Electrophoresis*, 2019, 40, 668-682
- [2] Breadmore, M.C., Mosher, R.A., Thormann, W., *Anal. Chem.* 2006, 78, 538-546.

Section IV

IV.1 Application of the developed CE-UV methodology (section II) to human plasma spiked with the four TKIs

The method developed for the analysis of imatinib mesylate (section II), was applied for the analysis of the three other TKIs namely lapatinib ditosylate, erlotinib hydrochloride and sorafenib. Fig. 1 shows electropherograms obtained for the analysis of standard solution and plasma spiked both with the four TKIs (5.0 mg/l each).

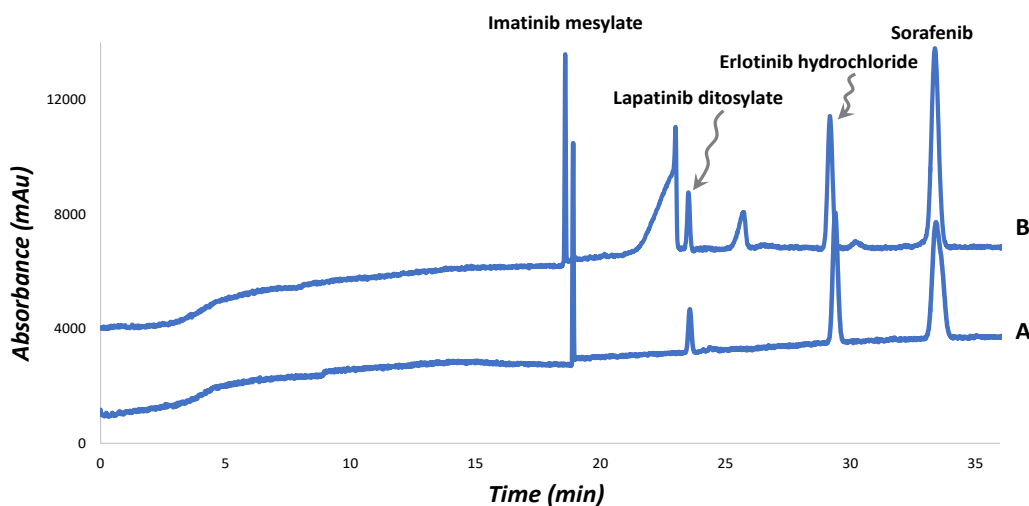


Figure 1: Electropherogram of 4 TKIs obtained from (A) standard and (B) human plasma samples. Analysis conditions: silica capillary 50 μm i.d., total length 30 cm, effective length 20 cm. BGE: citric acid – 6-aminocaproic acid buffer / 150 mM pH 2.0. Temperature: 25 $^{\circ}\text{C}$. Separation voltage: 15 kV. Sample injection volume: 156 nl (corresponding to 40% of the capillary volume till the detector window). Detection: 254 nm.

In comparison, a standard sample solution containing the four TKIs was analyzed following the same analytical procedure as for human plasma. Similar electrophoretic profiles in terms of migration times and resolutions of peaks were obtained for the four TKIs. Imatinib is the first to be detected in CZE as it has three positive charges (pKa 8.07, 3.73, 2.56 and 1.52) and lowest molecular weight (493.6 g/mol). Although, lapatinib has the largest molecular weight (925.5 g/mol), it was detected second as it is completely charged according to its pKa 7.2. Erlotinib was partially positively charged (pKa of 2.66) and it was detected third as it has lower molecular weight (393.4 g/mol) compared to sorafenib (464.8 g/mol) which was detected at last (pKa of 5.18). Every TKIs was also verified by injecting standard solution of every TKIs and compare the obtained electropherogram with the plasma solution. These results also showed that the peak heights of lapatinib ditosylate and sorafenib obtained from plasma were larger than

those obtained from standard sample. Maybe it is related to the difference in composition of the supernatant obtained from standard and plasma solution in term of salt, water and ACN which could lead to peak broadening (as described in section I and II). Another remark in the electropherogram of plasma, is the large peak detected just before lapatinib peak which may be related to plasma protein. The specificity was verified by injecting blank samples prepared by the same method mentioned in point (I.1.6) but without TKIs. No interfering peaks were detected at the time of migration of the four TKIs (result not shown). On the other hand, peak areas of both compounds were the same confirming that the recovery is the same between standard and plasma samples. The measured LOQ of imatinib was 191 ng/mL. LOQ of lapatinib ditosylate, erlotinib hydrochloride and sorafenib were estimated at 2400, 625 and 441 ng/mL respectively for an injected volume equal to 40% of the capillary volume till the detector window. These LOQ values arrive to plasma levels observed for patients treated by imatinib, erlotinib and sorafenib which are 1000, 1200 and 1440 ng/mL respectively [1,2]. In contrast, the estimated LOQ value of lapatinib doesn't arrive to its trough plasma level which is 1740 ng/mL [3]. So, in the next chapter, another strategy will be tested in order to improve the analytical performance, extract and analyze the four TKIs by CE.

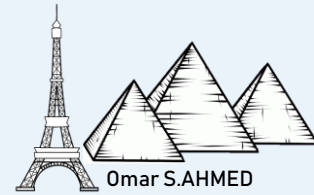
References of section IV

- [1] N.A.G. Lankheet, L.M. Knapen, J.H.M. Schellens, J.H. Beijnen, N. Steeghs, A.D.R. Huitema, Plasma concentrations of tyrosine kinase inhibitors imatinib, erlotinib, and sunitinib in routine clinical outpatient cancer care, *Ther. Drug Monit.* 36 (2014) 326–334
- [2] H. Akaza, T. Tsukamoto, M. Murai, K. Nakajima, S. Naito, Phase II study to investigate the efficacy, safety, and pharmacokinetics of sorafenib in Japanese patients with advanced renal cell carcinoma, *Jpn. J. Clin. Oncol.* 37 (2007) 755–762.
- [3] B. Thiessen, C. Stewart, M. Tsao, S. Kamel-Reid, P. Schaiquevich, W. Mason, J. Easaw, K. Belanger, P. Forsyth, L. McIntosh, E. Eisenhauer, A phase I/II trial of GW572016 (lapatinib) in recurrent glioblastoma multiforme: Clinical outcomes, pharmacokinetics and molecular correlation, *Cancer Chemother. Pharmacol.* 65 (2010) 353–361.

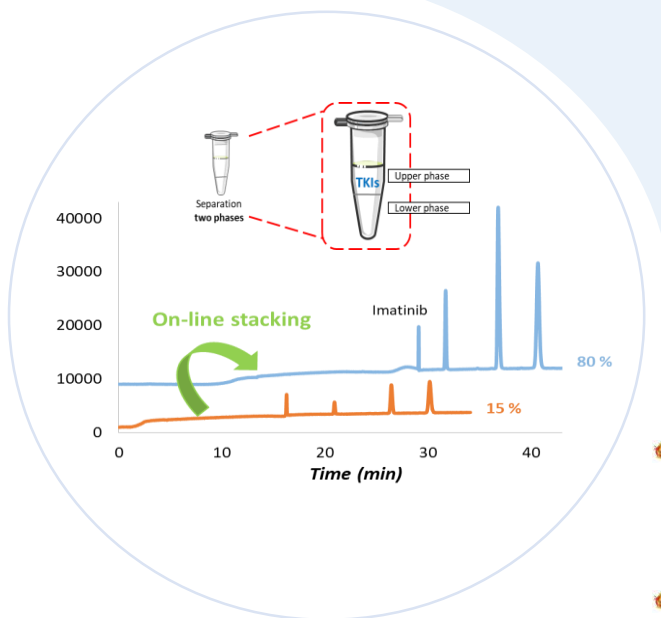
General conclusion of the chapter

Several factors related to biological matrix (e.g. salts and proteins) have a direct effect on the analytical performance of analysis of TKIs by CE. In this chapter, the analysis of imatinib mesylate in high-salty matrix by CZE was studied. According to the results obtained, increasing the presence of salt at high concentration affect negatively the form of peak of analytes. Experimentally observed peak splitting of imatinib analyte in the presence of salt and its dependency on pH and I of the BGE was confirmed by means of computer simulation (Simul program). Peak splitting can be suppressed by increasing I of BGE if caused by the presence of salt in highly-saline samples. Based on these facts, optimal analytical conditions were proposed for the analysis of imatinib mesylate by CZE in human plasma. ACN solvent was added to the sample having the advantage to eliminate simultaneously proteins and to ameliorate the sensitivity of analysis. The supernatant (containing mostly ACN) could be injected up to 40 % of the capillary volume till the detector window due to the existence of on-line stacking phenomenon inside the capillary. This approach was successfully applied to human plasma spiked with at first only imatinib mesylate. The developed methodology offers a number of features including easy operational procedure, low consumption of organic solvent, environmental benignity and applicability to high salinity matrix. This confirms the significance of the proposed methodology for the TDM of imatinib in human plasma. Moreover, the same methodology was applied for the three other TKIs. Although the efficient forms of peaks obtained, the performance of the method in terms of LOQ and resolution of peaks especially in case of lapatinib was not sufficient. Another strategy to extract and to concentrate the four TKIs will be discussed in details in the next chapter.

Chapter III



Salting-out assisted liquid-liquid extraction (SALLE) as an extraction technique: Application to the CZE analysis of TKIs



This chapter is the subject of:

- **An oral presentation:** *salting-out assisted liquid-liquid extraction with in-line stacking in capillary zone electrophoresis for the determination of tyrosine kinase inhibitors in human plasma.* ISC 2018, Cannes-Mandelieu, France.
- **A scientific paper:** *Coupling of salting-out assisted liquid-liquid extraction with on-line stacking for the analysis of tyrosine kinase inhibitors in human plasma by capillary zone electrophoresis.* J. Chromatogr. A. 1579 (2018) 121–128.
- **A poster:** *Apport de l'électrophorèse capillaire pour le Suivi Thérapeutique Personnalisé (STP) de patients traités par Chimiothérapie : Application aux Inhibiteurs de Tyrosine Kinase (ITK).* 12^{ème} congrès francophone sur les sciences séparatives et les couplages de l'AFSEP-Avril 2017, Paris, France.



Preface

As mentioned in chapter II, the presence of salt in human plasma sample has a significant effect on the CZE analysis of TKIs. The addition of ACN to the sample as a protein precipitant besides, optimizing the electrophoretic conditions such as I and pH of the BGE, could ameliorate the CE analysis performance. As shown in section IV of the chapter II, the developed analytical methodology was used for the analysis of imatinib mesylate in human plasma. This method also gave acceptable LOQ in case of erlotinib and sorafenib. But, lack of sensitivity was observed in case of lapatinib ditosylate. In addition, a large peak of protein was detected just before lapatinib peak, affecting both resolution and quantification.

From these results, we could conclude that the plasma matrix adversely affected the analytical performance in terms of sensitivity and thus there was a need to reduce or to eliminate this effect by optimizing extraction steps. A salting-out assisted liquid-liquid extraction (SALLE) was developed for the extraction of TKIs from human plasma. The SALLE technique was successfully coupled to CE-UV for the analysis of the four selected TKIs.

This chapter is divided into four sections, the first one provides a state-of-art about salting-out phenomena, SALLE technique and its application in different fields. In addition, the preliminary results obtained to optimize SALLE technique was also discussed. In section II, the optimization of SALLE-CE-UV methodology for the quantification of the four selected TKIs in human plasma was discussed. This work was the subject of a published paper in the journal of chromatography A. In section III, a comparison between performances of the method developed in chapter II and the SALLE-CE-UV methodology for the quantification of four TKIs in human plasma was done. From the results obtained in sections II, an optimization of the analytical conditions for imatinib has been proved to be necessary. Therefore, optimization of the pH used for the analysis of imatinib mesylate by CZE at high sample volume injected was discussed in section IV.

Section I

I.1 Salting-out effect & SALLE

Salting-out effect also known as salt-induced precipitation or salt fractionation is a phenomenon that occurs when the salt concentration in an aqueous solution is very high. The solubility of miscible organic solvents in water in the presence of high concentration of salt is decreased which leads to separation into two phases (upper organic and lower aqueous phases) [1]. Moreover, if molecules are partially water-soluble organic compounds (soluble in both water and organic mediums), there will then be a remarkable decrease of compound solubility in water, causing the compounds to either precipitate as solids, or increase the partition into the other more favorable organic phase [2]. If proteins are present in the sample, then the salting-out effect will cause their PP due to the presence of organic solvent (e.g. ACN). The mechanism behind this phenomena was accounted to many theories but, the exact mechanism is still unclear [3–5]. Two theories have been proposed to explain salting-out phenomena. The first one supposes the decrease in the mutual solubility of the solvents. It assumes that molecules, not necessarily ionic in nature, are preferentially solvated by one of the solvents, making this solvent unavailable for dissolving the second [6]. The second theory concerning only ionic compounds, assumes that the more polar of the two solvents (e.g. water) preferentially surrounds the salt because of electrostatic attraction, leading to non-ideal behavior and positive deviation from the Raoult's law [7]. Thus, the vapor pressure above the aqueous phase is increased and the tendency of the second solvent to separate from the first solvent (e.g. aqueous phase) is increased (its solubility in the first solvent is decreased) [7].

As mentioned in chapter I, SALLE is defined as a homogeneous LLE method in which the addition of salts into a sample solution composed of a miscible mixture of water and an organic solvent (such as ACN or acetone) induces a two phases separation (organic phase from bulk aqueous phase) [2]. SALLE particularly uses the salting-out phase separation phenomenon (as previously mentioned) to extract organic compounds from various aqueous samples by water-miscible organic solvents [8]. SALLE combines PP (achieved by using an organic solvent), extraction of targeted analytes by partitioning into the organic solvent and contribution to a cleaner extract with better recovery compared to other classical sample pretreatment techniques [9,10]. Since the solvent used in SALLE is totally water miscible, and the analytes of interest are fully dissolved in the water–solvent mixture before salting-out, no lengthy and vigorous mechanical mixing is needed to promote extraction recovery [11]. For decades, numerous researches used SALLE with different salting-out agents and water-miscible organic solvents, frequently ACN. Applications of SALLE included the extraction of metal chelates [12,13], volatile organic solutes [14] and a

wide range of hydrophilic and hydrophobic organic compounds [14,15] into the organic phase prior to analysis. SALLE can be coupled with many analytical techniques including atomic absorption [12], absorption spectrometry [16], GC [14,17–19], CE [20,21] and LC [10,13,15,22–28] as shown in Fig 1.

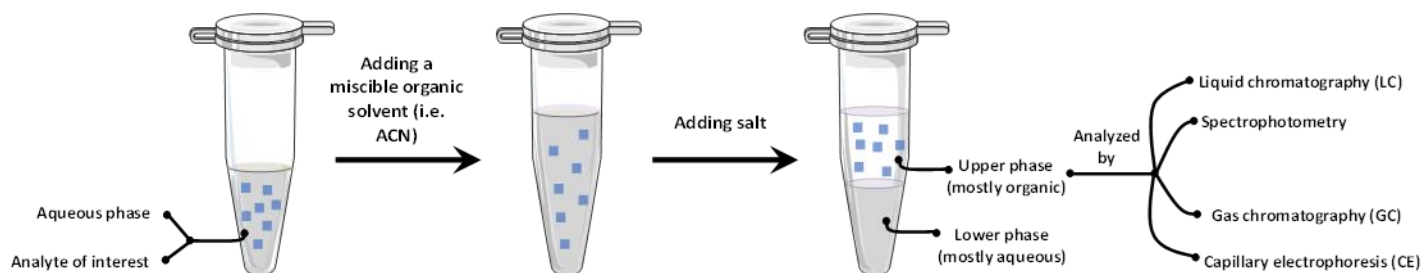


Figure 1: Concept of SALLE

Applications of SALLE were involved into many fields including clinical (will be discussed part I.2), environmental and food analysis applications (as mentioned in table 1). The diverse applications of SALLE in different fields show the advantage of SALLE as an extraction technique compared to other traditional extraction techniques such as LLE, PP and SPE.

Table 1: Most recent applications of SALLE in different fields

Analytical method	Analyte	Organic solvent	Salt	Medium	Ref
LC-MS	Tetracycline	ACN	Ammonium sulfate	Enfant food (meat, vegetables and milk)	[29]
LC-UV	Thiaclopred	ACN	Sodium chloride and sodium sulfate	Fruit and vegetables	[30]
UV/visible	Phenol and chlorophenol	ACN	Sodium chloride	water samples	[31]
LC-MS	Amphetamines	ACN	Ammonium sulfate	Meconium specimens (first stool of newborn)	[32]
UV/visible	Cysteine	ACN	Sodium sulfate	Food	[33]
LC-UV	Paraquat	ACN	Sodium chloride	Environmental and food samples	[34]

LC-UV	Flavanoids	Ethanol	Ammonium sulfate	Seeds of <i>Cuscuta chinensis</i> Lam	[35]
LC-FL	Benzimidazole	Methanol	Ammonium sulfate	Farm fish samples	[36]
LC-UV	17- β -Estradiol	ACN	NaCl	Water samples	[37]
GC-MS	Topiramate	Toluene	NaCl	Water samples	[38]
LC-DAD	Ciprofloxacin residues	ACN	Magnesium sulphate	Water samples	[39]
LC-MS/MS	5-nitroimidazoles	ACN	Magnesium sulphate	Fish roe samples	[40]

1.2 Clinical and bioanalytical applications of SALLE

Many and many clinical and bioanalytical applications are accounted for the use of SALLE as an extraction technique of various targeted analytes and biological matrices. The high salt concentration with the organic solvent in a SALLE can all effectively precipitate biological proteins prior to phase separation [9]. Most of salts, matrix components and particle residues are retained in the lower aqueous phase during phase separation giving cleaner extract in the upper organic phase in simple and fast ways. So, SALLE combines PP with LLE in a simple way giving the capability to extract many compounds from biological matrices that are difficult to be extracted by classical LLE and SPE [8,9,41–43]. This difficulty is attributed to the low recoveries of analytes, multistep time-consuming protocols used, etc. SALLE also consumes less solvent and need mostly no tedious evaporation or reconstitution steps as previously discussed for classical LLE in chapter I. In addition, SALLE need no steps of sample loading, sorbent conditioning, washing and elution which are needed for SPE. Therefore, such sample preparation method can be integrated into the overall bioanalytical process with optimal extraction efficiency, and be streamlined with different analytical techniques [44]. By the same theory of SALLE, sugaring-out assisted liquid-liquid extraction (SULLE) was achieved with high concentrations of sugars such as saccharides [45] for the extraction of many compounds [46,47]. Compared with SALLE, SULLE shows advantages of rapid phase separation and a friendlier environment to biomolecules [48], less erosion to the analytical apparatus. But, due to the fact that biological samples such as plasma naturally contain salt (about 1.0% m/v), the implementation of SALLE is easier.

Table 2 shows most of the researches published on SALLE technique and its application in clinical and bioanalytical fields. Many of these works were published for a number of water-miscible organics solvents such as methanol, ethyl acetate, isopropanol and ACN. 81% of these works were based on using ACN solvent due to its efficient deproteinization property, to numerate a few [10,22,23]. Also, different salts and different salt concentrations have also been established for the extraction from biological matrices. The type and amount of salt are based on different factors such as type detection technique used and extraction efficiency [49]. Mass-spectrometry-friendly salts such as potassium carbonate, ammonium carbonate, magnesium sulphate and ammonium acetate are used as salting-out agents when MS detection is used. Other salts such as NaCl, potassium carbonate, potassium chloride and potassium sulphate were used when UV detection is employed as shown in table 2.

Table 2: Clinical and bioanalytical applications of SALLE

Analytical method	Analyte	Organic solvent	Salt	Matrix	Ref
GC-MS	Phenobarbital, pentobarbital	Isopropanol	Potassium carbonate	Plasma	[17]
GC-MS	Secobarbital, Pentobarbital Phenobarbital, Diazepam, Caffeine, Diphenyl hydantoin Meperidine, Morphine, Antipyrine, Glutethimide	Ethyl acetate	Ammonium carbonate	Urine, plasma and breast milk	[18]
GC-UV	Amitriptyline, Amphetamine Caffeine, Chlordiazepoxide Chlorpromazine, Diazepam Methamphetamine Methaqualone, Morphine Propoxyphene, Quinine	Ether-ethanol	Potassium carbonate	Urine	[50]
LC-UV	Cyclophosphamide	ACN	Potassium carbonate	Plasma	[10]
LC-UV	Cadralazine	ACN	Potassium carbonate	Plasma	[22]

LC-UV	Diltiazem	ACN	Ammonium sulphate	Plasma	[23]
LC-UV	Cyclosporin-A	ACN	Ammonium sulphate	Plasma	[24]
LC-UV	Lamotrigine	ACN	Sodium carbonate	Plasma	[25]
LC-UV	Valproic acid	ACN	NaCl	Plasma	[26]
LC-UV	Efavirenz	ACN	Potassium chloride	Plasma	[51]
LC-MS/MS	Lopinavir and ritonavir	ACN	Magnesium sulphate	Plasma	[8]
LC-MS/MS	Abbott investigational new drug ABT-869	ACN	Ammonium acetate	Plasma	[41]
LC-MS/MS	Abbott investigational new drug compound A	ACN	Ammonium acetate	Plasma	[42]
LC-MS/MS	Simvastatin, simvastatin acid	ACN	Ammonium formate	Plasma	[43]
LC-MS/MS	Lopinavir and ritonavir	ACN	Zinc sulphate	Plasma	[9]
LC-MS/MS	Lopinavir and ritonavir	ACN	Ammonium acetate	Plasma	[52]
LC-MS/MS	Synthetic cannabinoid metabolites	ACN	Ammonium acetate	Urine	[53]
LC-MS	Entecavir	ACN	Magnesium acetate	Plasma	[54]
CE-UV	Warfarin	ACN	NaCl	Urine	[55]
CE-UV	Hydrophobic porphyrins	ACN	NaCl	Urine	[21]
HILIC-UV	β -blockers	ACN	Ammonium sulphate	Urine	[56]

LC-UV	Temozolomide	Ethyl acetate, dichloromethane, ACN and methanol	NaCl and potassium sulphate	Plasma	[57]
-------	--------------	---	-----------------------------------	--------	------

The first use of SALLE to extract drug and metabolites from biological fluids (e.g. plasma or urine) can be traced back to the 1970s [17,18,50]. Such an extraction approach was further explored in the 1980s and 2000s [10,23–26,51]. All of the above SALLE applications involved the use of solid salt to avoid dilution of the sample and to achieve a two phases separation. In 2008, Zhang et al. [8] accounted the first real high-throughput SALLE procedure coupled to LC–MS/ MS analysis by using an automated liquid handler and 96-well plate. A potential concern of the SALLE method coupled to LC–MS analysis is that a portion of the salt added at high concentration might be extracted in the upper mostly organic phase (not 100% organic, will be discussed in point I.3). In Zhangs’ work, magnesium sulphate, a mass friendly salt, was used as the salting-out agent for the LC–MS/MS analysis of many drugs in biofluids [41–43]. Also, zinc sulphate was used as the salting-out agent. Sometimes, ACN and zinc sulphate are used together as a double PP to get cleaner upper phase extract after SALLE [9,58]. Different salting-out agents such as magnesium sulfate [8], ammonium acetate [52] and also a sugaring out agent such as glucose [47] were compared and validated for the extraction and the analysis of lopinavir and ritonavir. Wang et al. developed a CE method coupled to a salting-out extraction with ACN stacking and the use of dimethyl-beta-cyclodextrin as the chiral selector for the sensitive and enantioselective separation of warfarin enantiomers in urine samples [55]. Based on his work, ACN upper rich phase will offer improved sensitivity compared to conventional CE analysis leading to higher enrichment factor (> 1000x) compared to conventional CE method. Another work [21] reported the effect of pH on extraction efficiency after SALLE of various porphyrins from urine. He concluded that by controlling the pH of SALLE extraction, a number of hydrophobic porphyrins could be extracted efficiently into a smaller volume of ACN phase to achieve high enrichment factor. Another work dealt with a developed SALLE-HPLC method for estimation of temozolomide in plasma [57]. The author showed that upon the utilization of two salts (NaCl and potassium sulphate) for the extraction of temozolomide, the extraction efficiency (%) was further improved (87.75%) and was twice of conventional LLE (46.23%).

More recently, S. Magiera [56] used SALLE coupled to hydrophilic interaction liquid chromatography (HILIC) for the determination of selected β -blockers and their metabolites in human urine. In HILIC, the

elution strength of the solvents is opposite to the reversed-phase and, typically, a polar stationary phase such as bare silica or its polar derivatives is used. ACN has weaker elution strength than water on the HILIC, and gradient elution on HILIC starts with a high organic content mobile phase. For this reason, HILIC provides an attractive retention for many polar analytes, and the typical supernatant from PP and extract from reversed-phase SPE such as ACN and methanol can be injected directly without going through the tedious solvent evaporation and reconstitution steps. This advantage could be used to inject the upper ACN phase directly to HILIC [2,56].

SALLE has been already coupled to CE technique. Examples are given in the publication in section II. As mentioned in chapter II, ACN is a highly efficient protein precipitant besides, the fact that the extracted solution is mainly composed of ACN allowed to obtain excellent peak efficiencies, good resolution and high sensitivity thanks to the existence of stacking phenomena during CE separation [20,55]. This strategy is very adapted in our project.

1.3 Preliminary results

As mentioned before in chapter II, 50/50 ACN/plasma (v/v) in the presence of 1.0 % of NaCl (w/v) were the optimal conditions to analyze imatinib which was not the case for lapatinib ditosylate. In addition, a large peak of protein was detected just after lapatinib peak, affecting both identification and quantification.

From these results, we could conclude that the plasma matrix adversely affected the analytical performance and there is a need to eliminate this effect by optimizing extraction steps. Therefore, it was mandatory to search another strategy in order to pre-concentrate all the four TKIs from human plasma. SALLE appeared to be a promising applicable method for extracting hydrophobic compounds from high saline biological samples as described above.

Our first concern was to determine at which concentration of salt and water/ACN ratio, a two phases separation occurs. According to the work of M. Tabatat [16], several water-miscible polar solvents were examined for salting-out in the presence 4 mol/l (nearly 23.5%, m/v) of NaCl. It was observed that the water-miscible polar solvents, acetone, ACN, 1,4-dioxane, tetrahydrofuran, 1-propanol and 2-propanol, were easily separated from aqueous solutions. Also, the volumes of the organic phases recovered after salting-out were smaller than their initial volumes. In addition, the upper phase-separated organic solvents contain significant amount of water and chloride. The concentration of chloride in the organic phase increases with the increase in % of water (w/w) in the organic phase as shown in [table 3](#). This means that the upper organic phase is not purely the organic solvent.

Table 3: Salting-out data for the phase-separation by sodium chloride ^[16]

Solvent	Volume/cm ³		Water in the organic phase		Chloride in the organic phase/10 ² mol/L
	Organic phase	Aqueous phase	%(w/w)	X (mole fraction)	
Acetone	3.11	6.99	17.3	0.390	9.62
Acetonitrile	4.17	6.11	10.3	0.208	2.49
1,4 Dioxane	2.04	8.16	9.55	0.340	2.06
Tetrahydrofuran	4.66	5.65	5.99	0.203	0.162
1-Propanol	5.27	4.97	18.4	0.430	16.4
2-Propanol	5.21	4.95	24.2	0.516	28.2

These data were very important for our research. The first concern about the above data, is the use of a high concentration of salt to cause two phases separation by salting-out effect. As ACN is the most efficient organic solvent to precipitate proteins. In addition, ACN stacking obtained when using CE technique. Accordingly, three different mixtures of ACN/water with ratios of 40/60, 50/50 and 60/40 (v/v) were prepared. For each ratio, different amounts of NaCl salt (m/v) were added to obtain a final concentration ranging from 0.5 to 10 % (m/v). In order to visualize the separation between the two phases, methyl red indicator solution was added and mainly solubilized in the organic phase. It was found that 40/60, 50/50 and 60/40 ACN/water (v/v) mixtures required respectively the presence of 5, 5 and 2 % NaCl (m/v) to obtain two immiscible phases (Fig. 2).

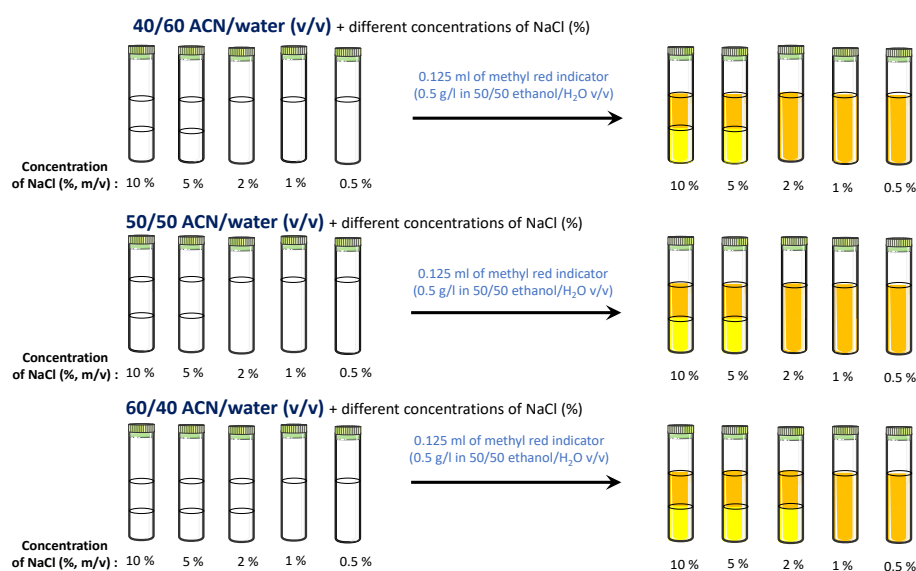
**Figure 2:** Testing different mixture of ACN/water (v/v) at different concentration of salt (m/v)

Fig. 3 below represent a real picture taken with 50/50 (v/v) ACN/water and 10 % (m/v) of NaCl salt).



Figure 3: picture of a mixture of 50/50 (v/v) ACN/water and 10 % (m/v) of NaCl salt. Methyl red indicator solution was added and was mainly solubilized in organic phase.

Furthermore, according to the work of Polson [59], ratios of 40/60, 50/50 and 60/40, ACN/plasma (v/v) induced the precipitation of 3.6, 88.7 and 91.6 % of plasma proteins respectively. Therefore, the ratio of ACN was kept to be more than 50 % (m/v) of the initial sample volume to have both an efficient PP and to decrease the amount of NaCl needed to obtain two phases separation. Moreover, different ratios of ACN/water at 60/40, 70/30, 75/25, 80/20 % (v/v) were prepared with fixed concentration of NaCl salt at 2 % (m/v) and with the four TKIs at a concentration of 5 $\mu\text{g}/\text{mL}$ each. Then, the upper phase extract of each ratio was analysed by CZE-UV. From 60/40 to 80/20 (v/v) ratio, a decrease by nearly 1.5 in terms of height of peak of analytes was observed. This was attributed to the fact that a higher percentage of acetonitrile induced a larger volume of extraction (upper phase) resulting in a significant dilution of the sample.

As best compromise, the SALLE methodology was further developed for the 4 TKIs with a ratio of 60/40 (v/v) ACN/plasma in the presence of 2 % (m/v) NaCl to have an efficient plasma deproteinization, a moderate dilution of TKIs and a good separation of the two phases. In addition, the fact that the analytes will be extracted in the upper phase which is mostly ACN, will help to on-line concentrate the analytes by stacking phenomena. In section II, the upper phase extract (containing TKIs) was successfully and directly injected to CE coupled to a UV detection. This was the subject of a scientific paper accepted in journal of chromatography A.

References of section I

- [1] B.H. Chang, Y.C. Bae, Salting-out in the aqueous single-protein solution: the effect of shape factor., *Biophys. Chem.* 104 (2003) 523–33.
- [2] Y.Q. Tang, N. Weng, Salting-out assisted liquid-liquid extraction for bioanalysis, *Bioanalysis.* 5 (2013) 1583–1598.
- [3] P.K. Grover, R.L. Ryall, Critical appraisal of salting-out and its implications for chemical and biological sciences, *Chem. Rev.* 105 (2005) 1–10.
- [4] Y. Marcus, Effect of ions on the structure of water: Structure making and breaking, *Chem. Rev.* 109 (2009) 1346–1370.
- [5] A.A. Zavitsas, Some opinions of an innocent bystander regarding the Hofmeister series, *Curr. Opin. Colloid Interface Sci.* 23 (2016) 72–81.
- [6] C.E. Matkovich, G.D. Christian, Salting-Out of Acetone from Water-Basis of a New Solvent Extraction System, *Anal. Chem.* 45 (1973) 1915–1921.
- [7] Samuel Glasstone, *Text-book of physical chemistry*, 11th ed., 1898.
- [8] J. Zhang, H. Wu, E. Kim, T.A. El-Shourbagy, Salting-out assisted liquid/liquid extraction with acetonitrile: A new high throughput sample preparation technique for good laboratory practice bioanalysis using liquid chromatography-mass spectrometry, *Biomed. Chromatogr.* 23 (2009) 419–425.
- [9] F. Myasein, E. Kim, J. Zhang, H. Wu, T.A. El-Shourbagy, Rapid, simultaneous determination of lopinavir and ritonavir in human plasma by stacking protein precipitations and salting-out assisted liquid/liquid extraction, and ultrafast LC-MS/MS, *Anal. Chim. Acta.* 651 (2009) 112–116.
- [10] A.M. Rustum, N.E. Hoffman, Determination of cyclophosphamide in whole blood and plasma by reversed-phase high-performance liquid chromatography, *J. Chromatogr. B Biomed. Sci. Appl.* 422 (1987) 125–134.
- [11] T. Li, L. Zhang, L. Tong, Q. Liao, High-throughput salting-out-assisted homogeneous liquid-liquid extraction with acetonitrile for determination of baicalin in rat plasma with high-performance

- liquid chromatography, *Biomed. Chromatogr.* 28 (2014) 648–653.
- [12] N.H. Chung, M. Tabata, Salting-out phase separation of the mixture of 2-propanol and water for selective extraction of cobalt(II) in the presence of manganese(II), nickel(II), and copper(II), *Hydrometallurgy*. 73 (2004) 81–89.
- [13] Y. Nagaosa, M. Taniguchi, J. Miura, Hydrophobic salt-induced phase-separation and extraction for sample preparation in chromatographic determination of heavy metal ions as dibenzylthiocarbamates, *Anal. Chim. Acta.* 356 (1997) 135–140.
- [14] T.F. Jenkins, P.H. Miyares, Nonevaporative Preconcentration Technique for Volatile and Semivolatile Solutes In Certain Polar Solvents, *Anal. Chem.* 63 (1991) 1341–1343.
- [15] D.C. Leggett, T.F. Jenkins, P.H. Miyares, Salting-Out Solvent Extraction for Preconcentration of Neutral Polar Organic Solutes from Water, *Anal. Chem.* 62 (1990) 1355–1356.
- [16] M. Tabata, M. Kumamoto, J. Nishimoto, Chemical Properties of Water-Miscible Solvents Separated by Salting-out and Their Application to Solvent Extraction., *Anal. Sci.* 10 (2007) 383–388.
- [17] M.G. Horning, E.A. Boucher, M. Stafford, E.C. Horning, A rapid procedure for the isolation of drugs and drug metabolites from plasma, *Clin. Chim. Acta.* 37 (1972) 381–386.
- [18] M.G. Horning, P. Gregory, J. Nowlin, M. Stafford, K. Lertratanangkoon, C. Butler, W.G. Stillwell, R.M. Hill, Isolation of drugs and drug metabolites from biological fluids by use of salt-solvent pairs., *Clin. Chem.* 20 (1974) 282–287.
- [19] G.G. Chen, G. Turecki, O.A. Mamer, A novel liquid-liquid extraction and stable isotope dilution NCI-GC-MS method for quantitation of agmatine in postmortem brain cortex, *J. Mass Spectrom.* 45 (2010) 560–565.
- [20] T.S.K. So, C.W. Huie, Salting-out solvent extraction for the off-line preconcentration of benzalkonium chloride in capillary electrophoresis, *Electrophoresis.* 22 (2001) 2143–2149.
- [21] Q. Li, C.W. Huie, Coupling of acetonitrile deproteinization and salting-out extraction with acetonitrile stacking for biological sample clean-up and enrichment of hydrophobic compounds (porphyrins) in capillary electrophoresis, *Electrophoresis.* 27 (2006) 4219–4229.

- [22] A.M. Rustum, Determination of cadralazine in human whole blood using reversed-phase high-performance liquid chromatography: utilizing a salting-out extraction procedure, *J. Chromatogr. B Biomed. Sci. Appl.* 489 (1989) 345–352.
- [23] A.M. Rustum, Determination of diltiazem in human whole blood and plasma by high-performance liquid chromatography using a polymeric reversed-phase column and utilizing a salting-out extraction procedure, *J. Chromatogr. B Biomed. Sci. Appl.* 490 (1989) 365–375.
- [24] A.M. Rustum, Estimation of Cyclosporin-A in whole blood by simple and rapid reversed-phase HPLC utilizing a salting-out extraction procedure, *J. Chromatogr. Sci.* 28 (1990) 594–598.
- [25] M. Cociglio, R. Alric, O. Bouvier, Performance analysis of a reversed-phase liquid chromatographic assay of lamotrigine in plasma using solvent-demixing extraction, *J. Chromatogr. B Biomed. Sci. Appl.* 572 (1991) 269–276.
- [26] R. Alric, M. Cociglio, J.P. Blayac, R. Puech, Performance evaluation of a reversed-phase, high-performance liquid chromatographic assay of valproic acid involving a “solvent demixing” extraction procedure and precolumn derivatisation, *J. Chromatogr. B Biomed. Sci. Appl.* 224 (1981) 289–299.
- [27] H. Wang, X. Zhou, Y. Zhang, H. Chen, G. Li, Y. Xu, Q. Zhao, W. Song, H. Jin, L. Ding, Dynamic microwave-assisted extraction coupled with salting-out liquid-liquid extraction for determination of steroid hormones in fish tissues, *J. Agric. Food Chem.* 60 (2012) 10343–10351.
- [28] S. Song, E.N. Ediage, A. Wu, S. De Saeger, Development and application of salting-out assisted liquid/liquid extraction for multi-mycotoxin biomarkers analysis in pig urine with high performance liquid chromatography/tandem mass spectrometry, *J. Chromatogr. A.* 1292 (2013) 111–120.
- [29] D. Moreno-González, A.M. García-Campaña, Salting-out assisted liquid–liquid extraction coupled to ultra-high performance liquid chromatography–tandem mass spectrometry for the determination of tetracycline residues in infant foods, *Food Chem.* 221 (2017) 1763–1769.
- [30] S. Akram, B. Sultana, M.R. Asi, M. Mushtaq, Salting-out-assisted liquid–liquid extraction and reverse-phase high-performance liquid chromatographic monitoring of thiacloprid in fruits and vegetables, *Sep. Sci. Technol.* 53 (2018) 1563–1571.

- [31] R. Tabaraki, E. Heidarizadi, Spectrophotometric determination of phenol and chlorophenols by salting out assisted liquid-liquid extraction combined with dispersive liquid-liquid microextraction, *Spectrochim. Acta - Part A Mol. Biomol. Spectrosc.* 215 (2019) 405–409.
- [32] A. Nemeškalová, M. Bursová, D. Sýkora, M. Kuchař, R. Čabala, T. Hložek, Salting out assisted liquid-liquid extraction for liquid chromatography tandem-mass spectrometry determination of amphetamine-like stimulants in meconium, *J. Pharm. Biomed. Anal.* 172 (2019) 42–49.
- [33] A. Diuzheva, J. Balogh, Y. Studenyak, Z. Cziáky, J. Jekő, A salting-out assisted liquid-liquid microextraction procedure for determination of cysteine followed by spectrophotometric detection, *Talanta.* 194 (2019) 446–451.
- [34] M. Rashidipour, R. Heydari, A. Maleki, E. Mohammadi, B. Davari, Salt-assisted liquid–liquid extraction coupled with reversed-phase dispersive liquid–liquid microextraction for sensitive HPLC determination of paraquat in environmental and food samples, *J. Food Meas. Charact.* 13 (2019) 269–276.
- [35] Y. qin Wei, M. man Sun, H. yan Fang, Dienzyme-assisted salting-out extraction of flavonoids from the seeds of *Cuscuta chinensis* Lam., *Ind. Crops Prod.* 127 (2019) 232–236.
- [36] C. Tejada-Casado, F.J. Lara, A.M. García-Campaña, M. del Olmo-Iruela, Ultra-high performance liquid chromatography with fluorescence detection following salting-out assisted liquid–liquid extraction for the analysis of benzimidazole residues in farm fish samples, *J. Chromatogr. A.* 1543 (2018) 58–66.
- [37] M. Hassannejad, K. Alizadeh, M. Nemat, Determination of 17- β -Estradiol in water samples using salting-out assisted liquid-liquid extraction followed by hplc and experimental design for optimization, *Anal. Bioanal. Chem. Res.* 6 (2019) 353–363.
- [38] J.M.F. De Almeida, E.M.F. Silva, L.M. Veríssimo, N.S. Fernandes, Salting-out assisted liquid-liquid extraction method combined with GC-MS for the determination of topiramate in aqueous solutions: development and application of the methodology, *Sep. Sci. Technol.* (2019) 1–10. doi: 10.1080/01496395.2019.1624570.
- [39] T. Gezahegn, B. Tegegne, F. Zewge, B.S. Chandravanshi, Salting-out assisted liquid–liquid extraction for the determination of ciprofloxacin residues in water samples by high performance liquid

- chromatography–diode array detector, *BMC Chem.* 13 (2019) 28.
- [40] M. Hernández-Mesa, C. Cruces-Blanco, A.M. García-Campaña, Simple and rapid determination of 5-nitroimidazoles and metabolites in fish roe samples by salting-out assisted liquid-liquid extraction and UHPLC-MS/MS, *Food Chem.* 252 (2018) 294–302.
- [41] H. Wu, J. Zhang, K. Norem, T.A. El-Shourbagy, Simultaneous determination of a hydrophobic drug candidate and its metabolite in human plasma with salting-out assisted liquid/liquid extraction using a mass spectrometry friendly salt, *J. Pharm. Biomed. Anal.* 48 (2008) 1243–1248.
- [42] J. Zhang, F. Myasein, R. Rodila, H. Wu, T.A. El-Shourbagy, High-throughput salting-out assisted liquid/liquid extraction and ultrafast LC for same-day delivery of first-in-human bioanalytical data, *Bioanalysis.* 1 (2009) 715–719.
- [43] J. Zhang, R. Rodila, E. Gage, M. Hautman, L. Fan, L.L. King, H. Wu, T.A. El-Shourbagy, High-throughput salting-out assisted liquid/liquid extraction with acetonitrile for the simultaneous determination of simvastatin and simvastatin acid in human plasma with liquid chromatography, *Anal. Chim. Acta.* 661 (2010) 167–172.
- [44] G.B. Frankforter, L. Cohen, Equilibria in the systems, water, acetone and inorganic salts, *J. Am. Chem. Soc.* 36 (1914) 1103–1134.
- [45] B. Wang, T. Ezejias, H. Feng, H. Blaschek, Sugaring-out: A novel phase separation and extraction system, *Chem. Eng. Sci.* 63 (2008) 2595–2600.
- [46] W.H. Tsai, H.Y. Chuang, H.H. Chen, Y.W. Wu, S.H. Cheng, T.C. Huang, Application of sugaring-out extraction for the determination of sulfonamides in honey by high-performance liquid chromatography with fluorescence detection, *J. Chromatogr. A.* 1217 (2010) 7812–7815.
- [47] J. Zhang, F. Myasein, H. Wu, T.A. El-Shourbagy, Sugaring-out assisted liquid/liquid extraction with acetonitrile for bioanalysis using liquid chromatography–mass spectrometry, *Microchem. J.* 108 (2013) 198–202.
- [48] X. Tu, F. Sun, S. Wu, W. Liu, Z. Gao, S. Huang, W. Chen, Comparison of salting-out and sugaring-out liquid–liquid extraction methods for the partition of 10-hydroxy-2-decenoic acid in royal jelly and their co-extracted protein content, *J. Chromatogr. B Anal. Technol. Biomed. Life Sci.* 1073 (2018)

90–95.

- [49] K.A. Alireza Pourhossein, Salt-Assisted Liquid-Liquid Extraction followed by High Performance Liquid Chromatography for Determination of Carvedilol in Human Plasma, *J. Reports Pharm. Sci. (J. Rep. Pharm. Sci.)*. 7 (2018) 79–87.
- [50] M.L. Bastos, G.E. Kananen, R.M. Young, J.R. Monforte, I. Sunshine, Detection of basic organic drugs and their metabolites in urine., *Clin. Chem.* 16 (1970) 931–940.
- [51] M. Cociglio, D. Hillaire-Buys, H. Peyrière, R. Alric, Performance analysis of a rapid HPLC determination with the solvent demixing extraction of hiv antiproteases and efavirenz in plasma, *J. Chromatogr. Sci.* 41 (2003) 80–86.
- [52] P.G. Wang, J.S. Wei, G. Kim, M. Chang, T. El-Shourbagy, Validation and application of a high-performance liquid chromatography-tandem mass spectrometric method for simultaneous quantification of lopinavir and ritonavir in human plasma using semi-automated 96-well liquid-liquid extraction, *J. Chromatogr. A.* 1130 (2006) 302–307.
- [53] E.G. Yanes, D.P. Lovett, High-throughput bioanalytical method for analysis of synthetic cannabinoid metabolites in urine using salting-out sample preparation and LC–MS/MS, *J. Chromatogr. B.* 909 (2012) 42–50.
- [54] F.J. Zhao, H. Tang, Q.H. Zhang, J. Yang, A.K. Davey, J. ping Wang, Salting-out homogeneous liquid-liquid extraction approach applied in sample pre-processing for the quantitative determination of entecavir in human plasma by LC-MS, *J. Chromatogr. B Anal. Technol. Biomed. Life Sci.* 881–882 (2012) 119–125.
- [55] M. Wang, Z. Cai, L. Xu, Coupling of acetonitrile deproteinization and salting-out extraction with acetonitrile stacking in chiral capillary electrophoresis for the determination of warfarin enantiomers, *J. Chromatogr. A.* 1218 (2011) 4045–4051.
- [56] S. Magiera, A. Kolanowska, J. Baranowski, Salting-out assisted extraction method coupled with hydrophilic interaction liquid chromatography for determination of selected β -blockers and their metabolites in human urine, *J. Chromatogr. B Anal. Technol. Biomed. Life Sci.* 1022 (2016) 93–101.
- [57] D. Jain, R. Athawale, A. Bajaj, S. Shrikhande, Double-salting out assisted liquid-liquid extraction

- (SALLE) HPLC method for estimation of temozolomide from biological samples, *J. Chromatogr. B Anal. Technol. Biomed. Life Sci.* 970 (2014) 86–94.
- [58] C. Polson, P. Sarkar, B. Incledon, V. Raguvaran, R. Grant, Optimization of protein precipitation based upon effectiveness of protein removal and ionization effect in liquid chromatography–tandem mass spectrometry, *J. Chromatogr. B.* 785 (2003) 263–275.
- [59] C. Polson, P. Sarkar, B. Incledon, V. Raguvaran, R. Grant, Optimization of protein precipitation based upon effectiveness of protein removal and ionization effect in liquid chromatography–tandem mass spectrometry., *J. Chromatogr. B. Analyt. Technol. Biomed. Life Sci.* 785 (2003) 263–75.

Section II (published paper)

Coupling of salting-out assisted liquid-liquid extraction with on-line stacking for the analysis of tyrosine kinase inhibitors in human plasma by capillary zone electrophoresis

Omar S. Ahmed¹, Yoann Ladner¹, Jérôme Montels¹, Laurent Philibert², Catherine Perrin¹

¹ Institut des Biomolécules Max Mousseron (IBMM), UMR 5247-CNRS-UM-ENSCM, Montpellier, France.

² Institut régional du Cancer de Montpellier (ICM), Département de Pharmacie et Pharmacologie, Montpellier, France.

Research article published in

Journal of chromatography A

J. Chromatogr. A. 1579 (2018) 121–128.

Abbreviations

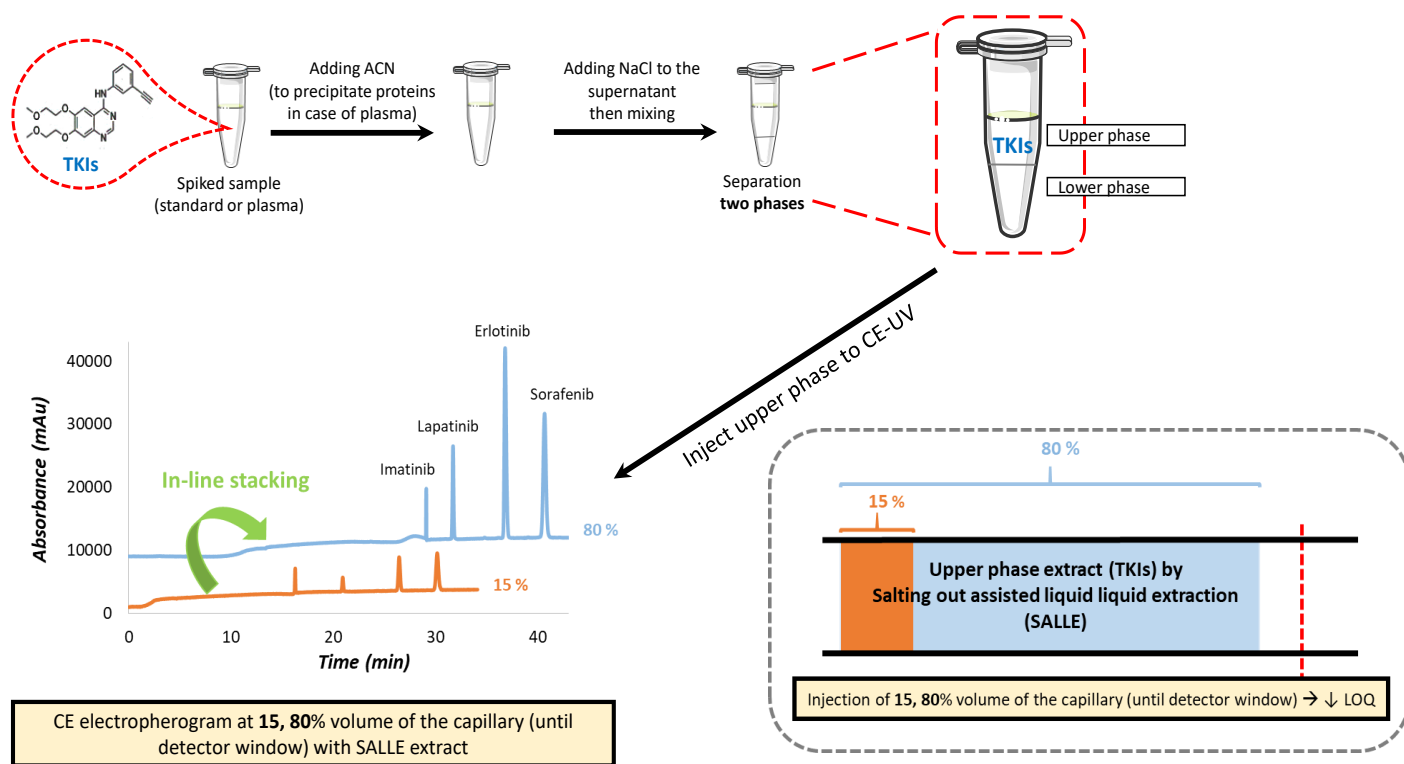
Background electrolyte (BGE), Capillary electrophoresis (CE), Ionic strength (IS), Liquid-liquid extraction (LLE), Therapeutic drug monitoring (TDM), Salting-out assisted liquid-liquid extraction (SALLE).

Keywords: Capillary electrophoresis, Salting-out assisted liquid-liquid extraction (SALLE), On-line CE stacking, Tyrosine Kinase Inhibitor (TKI).

Highlights

- Extraction of tyrosine kinase inhibitors by salting-out liquid–liquid extraction.
- Analysis of tyrosine kinase inhibitors by capillary electrophoresis technique.
- On-line concentration by acetonitrile stacking at high sample volume injected.

Graphical abstract



Abstract

Developing an easy to use, cheap and fast analytical methodology is highly demanded for clinical practices, such as therapeutic drug monitoring (TDM). The present work deals with the development of an analytical methodology for the analysis of four basic anticancer drugs, namely tyrosine kinase inhibitors (TKIs), in human plasma by combining salting-out assisted liquid-liquid extraction (SALLE) with capillary electrophoresis (CE). This SALLE-CE methodology makes a full use of the advantages of both techniques by combining extraction, on-line concentration and separation in a simple way. First, plasma samples containing TKIs are mixed with acetonitrile (ACN) in appropriate volumes to precipitate proteins. After vortexing and centrifugation, sodium chloride (NaCl) is added to the plasma-ACN mixture to induce a two phases separation. TKIs are efficiently extracted (60–100% extraction efficiency) in the upper (mostly organic) phase which is directly analyzed by capillary electrophoresis (CE) coupled to UV detection. The high content of ACN in the upper phase allows the stacking of the analytes in the capillary (on-line stacking) during analysis. For the first time thanks to this electrophoretic process, the injected sample volume can be as large as 80% of the capillary volume (till the detector window). Good linearity was obtained for each TKI in the concentration range 60–2000 ng/ml with correlation coefficient (r^2) between 0.997 and 0.999. LOD and LOQ in human plasma with such large injected volume were determined from 16 to 280 ng/ml and from 62 to 900 ng/ml respectively depending on the TKI. Recoveries for the four TKIs ranged from 60 to 100%. The repeatability of the SALLE-CE methodology for the analysis of TKIs in human plasma was evaluated with injected sample volume equal to 80% of the capillary volume till detector window. Relative standard deviations (RSDs) of less than 1.24 and 2.84% on migration times and corrected peak areas respectively were obtained at the LOQ. The sensitivity was enhanced by 61 to 265 folds confirming the applicability of the proposed methodology for the assay of TKIs in patients' plasma.

1. Introduction

Sample preparation techniques such as liquid–liquid extraction (LLE) and solid-phase extraction (SPE) are frequently used prior to capillary electrophoresis (CE) for the determination of drugs in biological fluids (urine, plasma and serum) [1–4]. These techniques aim to reduce interferences due to endogenous compounds (proteins, salts . . .) and to concentrate the analytes of interest. However, several drawbacks are often reported such as multi-step time consuming procedures, the use of large amounts of sample/organic solvents and extra operational costs for waste treatment. In the last decade, liquid phase microextraction (LPME) techniques have been developed using the potentialities of miniaturized systems for sample preparation allowing easy to implement, highly selective and high-speed analyses with minimal solvent consumption [1,5–7]. Recently, new sample treatments based on salting-out assisted liquid–liquid extraction (SALLE) were proposed for the determination of analytes in various sample matrices (water, food, human urine and plasma . . .) [8–11]. SALLE is a homogeneous liquid–liquid extraction (LLE) method in which the addition of salts (e.g. NaCl) into a sample solution composed of a miscible mixture of water and an organic solvent (such as ACN or acetone) induces a two phases separation (organic phase from bulk aqueous phase) [9]. SALLE appears to be well suited for the determination of drugs in biological samples as it allows deproteinization and extraction of analytes in the same procedure. Some applications of SALLE coupled to chromatographic systems were developed for the determination of molecules of interest in environmental and biological samples [12–14]. However, there are only few reports concerning its use prior to CE analysis. Huie et al. [10] developed an off-line pre-concentration methodology based on SALLE for the determination of benzalkonium chloride in pharmaceutical products by CE. Xu et al. [11] used SALLE to extract warfarin enantiomers in human urine. The fact that the extracted solution was mainly composed of acetonitrile allowed to obtain excellent peak efficiencies, good resolution and high sensitivity thanks to the existence of stacking by ACN-salt mixture during the electrophoretic process [7,15,16]. Acetonitrile stacking in the presence of salt makes it possible to inject large volumes of samples (more than 50% of the capillary volume) without peak broadening allowing to improve the sensitivity of the analysis. Surprisingly, the performance of the SALLE-CE methodology was only evaluated with small injected sample volume (less than 10% of the capillary volume). There are no report concerning the coupling of SALLE methodology (acetonitrile deproteinization and extraction) with on-line CE stacking of large sample volumes for the determination of drugs in biological fluids. In the present work, the feasibility and advantages of coupling SALLE methodology with CE in terms of sample volume injected are demonstrated. The applicability of the proposed method was tested with four basic anticancer drugs, namely Tyrosine Kinase Inhibitors (TKIs), in human plasma. These TKIs are imatinib mesylate, lapatinib

ditosylate, sorafenib and erlotinib hydrochloride. These basic molecules are extensively used for the treatment of malignant tumors such as chronic myeloid leukemia, lung cancer and breast cancer [17–19]. First, SALLE experimental conditions were optimized to maximize analytes extraction and on-line CE stacking. SALLE was then used to eliminate proteins and to extract TKIs from human plasma samples. Then, the extracted solutions were directly analyzed by CE coupled with UV detection. For the first time, an injected volume up to 80% of the capillary volume till detector window was successfully achieved with an excellent separation of analytes and a significant enhancement of the sensitivity of analysis. The usefulness of this approach in terms of on-line sample stacking, electrophoretic separation and sensitivity was established.

2. Experimental

2.1. Chemicals and reagents

All reagents were of analytical grade and used as received without further purification. Acetonitrile (ACN, purity $\geq 99.9\%$) was from Honeywell Riedel de Haen (Seelze, Germany). γ -amino caproic acid (purity $\geq 99\%$) was from Acros organics (Geel, Belgium). Sodium chloride (NaCl, purity $\geq 99.5\%$), sodium hydroxide (purity $\geq 99\%$), citric acid (purity $\geq 99\%$), imatinib mesylate (purity $\geq 98\%$), plasma from human for reconstitution were purchased from Sigma Aldrich (Saint-Quentin-Fallavie, France). Sorafenib (purity $\geq 99\%$), erlotinib hydrochloride (purity $\geq 99\%$) and lapatinib ditosylate (purity $\geq 99\%$) were purchased from Molekula (Munich, Germany).

2.2. Apparatus and software

All CE separations were carried out using a Beckman P/ACEMDQ instrument (Fullerton, USA) equipped with a UV detection system. Data were acquired by 32 Karat software (Version 8.0, Beck man Coulter). Uncoated fused-silica capillaries (50 μ m ID) were obtained from Polymicro Technologies (Phoenix, USA). Two lengths of capillary were used for the experiments, 50 and 30 cm (40 and 20 cm effective lengths to the detector respectively).

2.3. CE methods

New capillaries were pre-conditioned with 1.0 M NaOH for 3.0 min under 20 psi followed by distilled water for 3.0 min under 20 psi. Then, the capillary was flushed with the background electrolyte (BGE) for 5.0 min under 20 psi. Hydrodynamic injections of the samples were varied between 0.4 to 0.5 psi and injection times were varied between 20 to 94 seconds (s) to obtain injection volumes comprised between 30–313 nl. All separations were carried out with an applied voltage of 15 kV. The capillary was thermostated at 25 °C. UV detection was performed at 254 nm. Corrected areas were calculated by dividing each TKIs area by its corresponding migration time.

2.4. Preparation of background electrolyte and stock sample solutions

The background electrolyte (BGE) was chosen based on previous study (not published results) and was a mixture of citric acid (1800 mM) and -amino caproic acid (137 mM) of pH 2.0 and ionic strength (I) 150 mM. BGE composition with the desired I and pH was calculated with the software "Peakmaster" 5.3 (Prague, Czech Republic, <https://web.natur.cuni.cz/~gas/>). Aqueous stock solutions of imatinib mesylate were prepared at a concentration of 100 mg/l. Stock solutions of erlotinib hydrochloride, sorafenib and lapatinib ditosylate were prepared in dimethyl sulfoxide (DMSO) solvent due to their low solubility in water. All stock samples were stored frozen at -20 °C. All other solutions were stored in refrigerator at 4 °C.

2.5. Standard solutions

- Individual TKI standard solution: relevant volumes (depending on desired concentration) of distilled water and appropriate TKI stock solution were mixed in an eppendorf centrifuge tube.
- Standard mixed solution of the four TKIs: relevant volumes (depending on desired concentration) of distilled water and the four TKI stock solutions were mixed in an eppendorf centrifuge tube.

2.6. Optimized SALLE procedure of standard sample solutions

To each standard solution (2000 l), 3000 l of ACN were added in an eppendorf to have a ratio of 60/40 ACN/standard solution (v/v). After vortexing for 1 min, 0.1 g of NaCl (2% NaCl (m/v)) was added to the mixture. The solution was then vortexed for 1.0 min and were left to stand for 3.0 min A separation into two phases, lower (mostly aqueous) and upper (mostly organic) occurred. 80 nl of the organic phase was injected and analyzed by CE coupled to UV detection.

2.7. Optimized SALLE procedure from human plasma spiked with TKIs

Briefly, human plasma samples were placed in an eppendorf centrifuge tube and spiked with appropriate volumes of imatinib mesylate, erlotinib hydrochloride, sorafenib and lapatinib ditosylate stock solutions. Then, the spiked plasma was mixed during 1 h at room temperature. 3000 l of ACN was added to have a ratio of 60/40 ACN/plasma (v/v). The addition of acetonitrile induced protein precipitation. A dilution factor of 2.5 was obtained for imatinib mesylate and of 1.5 for the other three TKIs. The supernatant was separated from the precipitated proteins after the mixture was vortexed for 1 min and centrifuged for 5 min (11,000 rpm, 4 °C). Then, 0.1 g of NaCl was added to the mixture (2% NaCl (m/v)). The solution was then shaken for 1.0 min and left to stand for 3.0 min A separation into two phases, aqueous and organic occurred. Total analysis time (from SALLE extraction to CE analysis) was 65 min.

2.8. SALLE procedure for human plasma spiked with TKIs with organic phase evaporation

The same procedure as described in 2.7 for the preparation of plasma sample spiked with the 4 TKIs except, after the addition of salt and obtaining the two phases (organic and aqueous phases). After applying the procedure described in 2.7, 200 μ l of the upper organic phase was transferred to a centrifuge tube and evaporated on a dry bath at 80 °C for 1 h. After evaporation, the centrifuge tube was left to cool down, then 200 l of ACN solvent was added to the residue, mixed for 1 min and left to stand for 2 min. Total analysis time (from SALLE extraction to CE analysis) was 128 min.

2.9. Sample stacking mechanisms

The actual mechanism behind electrophoretic stacking in the presence of acetonitrile and salt with large injected sample volume (up to 80% of the capillary volume till detector window) is complex. The simplest mechanism that may first describe the occurring stacking phenomenon is field-amplified sample stacking (FASS). Generally, FASS is based on the electrophoretic migration of ions through a low-conductivity solution to a high-conductivity solution. This makes ions to slow down dramatically at the boundary of the two solutions due to the difference in field strengths between them. However, the presence of salt in the SALLE (mostly acetonitrile) extract involves more complex phenomena. According to the work of Shihabi [16], the mechanism behind stacking by acetonitrile–salt mixture is not very clear but it may be similar to that of transient isotachopheresis (t-ITP). Due to the low conductivity of acetonitrile, salt ions act as leading ions, moving rapidly in the sample region (upper phase extract of SALLE, mostly ACN, in this study) until they are slowed down at the interface of the BGE. This produces a very sharp band of analyte ions which are stacked between high field strength sample zone (ACN) and the leading ion at the BGE interface.

3. Results and discussion

The proposed methodology was developed to simultaneously eliminate plasma endogenous compounds such as proteins and salts, and extract TKIs to an organic phase prior to their analysis by CE in a simple, cheap and rapid way. TKIs have to be extracted in an organic phase to allow on-line CE stacking improving electrophoretic analysis performance. The use of SALLE technique allows to answer to these objectives. First, it is well known that the addition of ACN in the sample causes the precipitation of plasma proteins. Moreover, the addition of sufficient amount of NaCl in a sample solution composed of a mixture of ACN and water induces a two phases separation (mostly organic and mostly aqueous phases) [10]. Preliminary studies were realized to determine the optimal percentage of acetonitrile for protein precipitation as well as the optimal concentration of salt needed to cause the two phases separation. At first, four different mixture of ACN/water with ratios of 40/60, 50/50 or 60/40 and 70/30 (v/v) were prepared. For each ratio,

different amounts of NaCl salt (m/v) ranging from 0.5 to 10% (m/v). In order to visualize the separation between two phases, methyl red indicator solution was added and was solubilized in organic phase. It was found that 40/60, 50/50, 60/40 and 70/30 ACN/water (v/v) mixtures required respectively the presence of 7.5, 5, 2 and 2% NaCl (m/v) to get two immiscible phases. Furthermore, according to the work of Polson [20], ratios of 40/60, 50/50 or 60/40 and 70/30 (v/v) ACN/plasma induced the precipitation of 3.6, 88.7, 91.6 and 92.1% of plasma proteins respectively. Therefore, two ratios of 60/40 and 70/30 of ACN/water (v/v) with 2% (m/v) NaCl were chosen to have both an efficient protein precipitation and to decrease the amount of NaCl needed to obtain a two phases separation. Moreover, different ratios of ACN/water at 60/40, 70/30, 75/25, 80/20% (v/v) were prepared with fixed concentration of NaCl salt at 2% (m/v) and with the four TKIs at a concentration of 5 g/ml each. Then, the upper phase extract of each ratio was injected to CE-UV. From 60/40 to 80/20 (%/%) ratio, a decrease by nearly 1.5 in terms of height of peak of analytes was observed. This is attributed to the fact that a higher percentage of acetonitrile induced a large volume of extraction (upper phase) resulting in a significant dilution of the sample. As best compromise, the SALLE methodology was further developed for the 4 TKIs with a ratio of 60/40 (v/v) ACN/plasma in the presence of 2% (m/v) NaCl to have an efficient plasma deproteinization, a moderate dilution of TKIs and a good separation of the two phases.

3.1. Extraction of TKIs with SALLE methodology

The structures of the 4 TKIs selected as model compounds to evaluate the performance of SALLE method are given in Fig. 1.

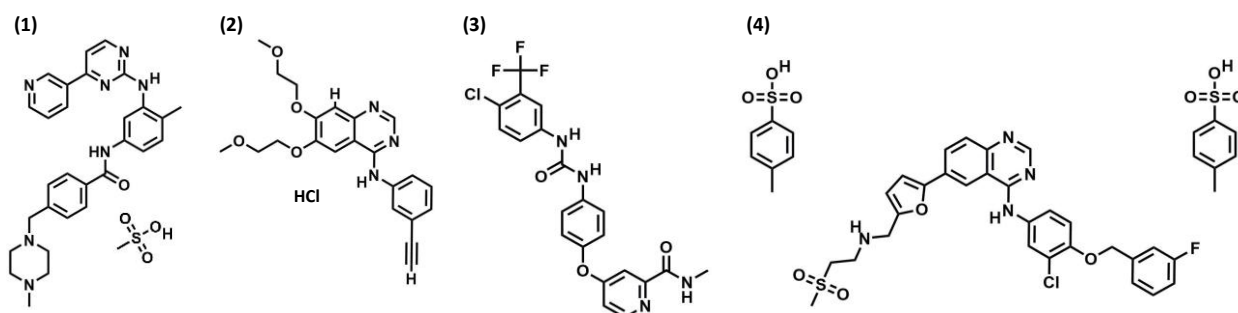


Figure 1: Molecular structures of the studied Tyrosine Kinase Inhibitors (TKIs). (1) imatinib mesylate, (2) erlotinib hydrochloride, (3) sorafenib and (4) lapatinib ditosylate.

The upper (mostly organic) and lower (mostly aqueous) phases were analyzed separately by CE as shown in Fig. 2. Because all the four compounds are basic, an acidic BGE was used as separation medium with a positive separation voltage of +15 kV. This BGE was a mixture of α -amino caproic acid and citric acid at a pH of 2.0 and an ionic strength of 150 mM. The total capillary length was 50 cm and the injected sample

volume was 60 nl (corresponding to 7.5% of the capillary volume till the detector window). The analysis of the upper phase gave symmetric and efficient peaks for TKIs showing the ability of the SALLE methodology to extract TKIs from the aqueous sample. The migration times of imatinib mesylate, lapatinib ditosylate, erlotinib hydrochloride and sorafenib in the upper (ACN) phase were 43, 62, 74 and 83 min respectively. The extraction efficiencies (%) were approximately estimated (calculations based on analytes corrected peak areas in both phases) at 60, 100, 98.0 and 100% for imatinib mesylate, lapatinib ditosylate, erlotinib hydrochloride and sorafenib respectively. As the SALLE extraction method is realized at about pH 7.0, erlotinib hydrochloride and sorafenib had no charge in accordance to their pKa values (2.66 and 5.18 respectively) and were easily extracted in ACN. Imatinib mesylate and lapatinib ditosylate were totally or partially positively charged during the extraction step according to their pKa values (1.52, 2.56, 3.73 and 8.07 for imatinib mesylate and 7.2 for lapatinib ditosylate). Both of them should be weakly extracted due to their ionization state, this result showed that SALLE methodology didn't work as a classical LLE methodology [21].

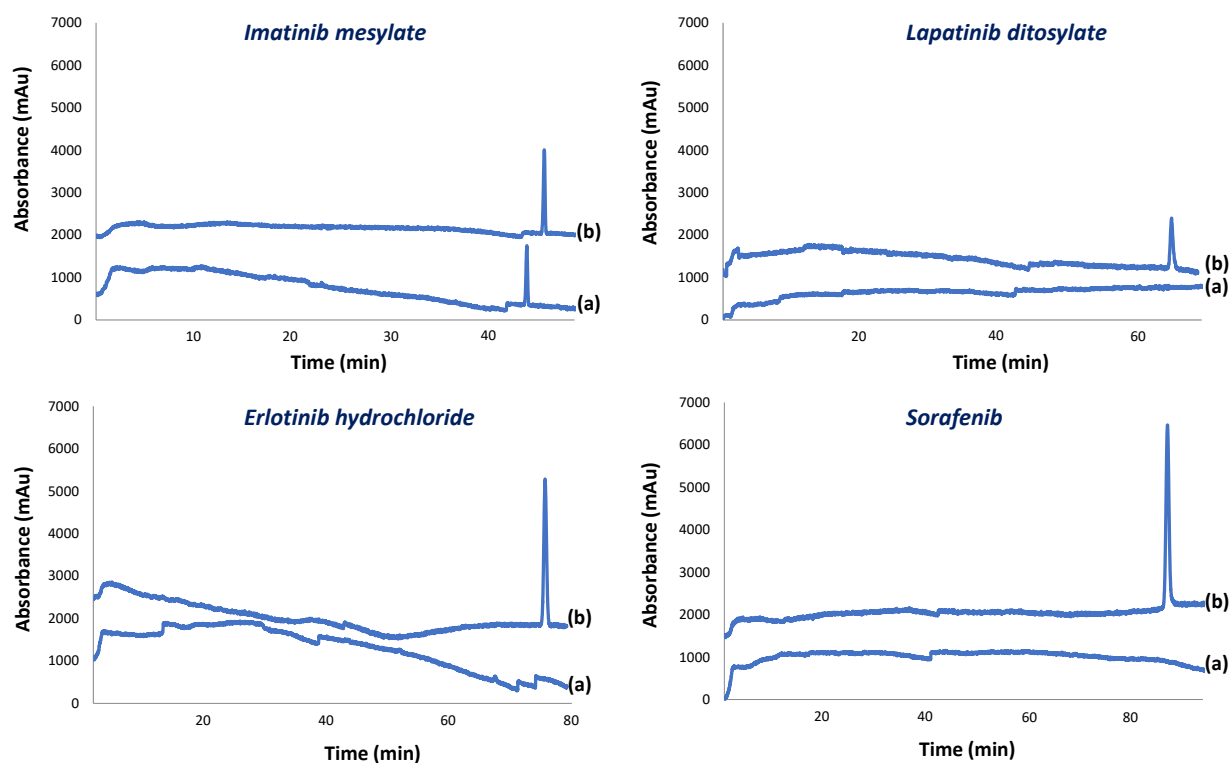


Figure 2: Analysis of imatinib mesylate, lapatinib ditosylate, erlotinib hydrochloride and sorafenib in (a) lower (mostly aqueous) phase and (b) upper (mostly ACN) phase obtained by SALLE methodology. Analysis conditions: silica capillary 50 μm i.d., total length 50 cm, effective length 40 cm. BGE: citric acid – ϵ -aminocaproic acid buffer I 150 mM pH 2.0. Temperature: 25°C. Separation voltage: 15 kV. Sample injection volume: 60 nl (corresponding to 7.5% of the capillary volume till the detector window). Detection: 254 nm.

Additional experiments were realized showing that a mixture of 6 ml ACN with 4 ml of water in the presence of 2% (m/v) of NaCl gave lower and upper phases of 3 and 7 ml, respectively. This result confirmed that the upper phase does not only contain pure organic solvent (ACN solvent). The upper phase in which the TKIs concentration is a mixture of a high amount of ACN and a low amount of water [10]. The extraction efficiency (%) of imatinib mesylate could be increased by controlling the ionization of imatinib mesylate. This was achieved by adding 10 μ l of NaOH (1.0 M) in the aqueous phase increasing the pH to 12.0. In this case, the extraction efficiency of imatinib mesylate was increased to 84.1% (results not shown). The SALLE procedure was also tested at different concentration of NaCl to test its impact on the extraction efficiency of the four TKIs. The concentration of salt was varied between 2 to 10% (m/v). The upper (mostly organic) and lower (mostly aqueous) phases were analyzed separately by CE. No significant difference in terms of corrected peak area of analytes was observed (result not shown). Therefore, the standard sample solutions were prepared at 2% NaCl (m/v).

3.2. CE separation of TKIs

A standard solution containing the four TKIs was prepared by the SALLE methodology as described in 2.5. The two phases were analyzed by CE under the same electrophoretic conditions (see 3.1). Fig. 3A confirms the ability of the proposed method to separate the four TKIs by capillary zone electrophoresis thanks to their difference in charge and size. Symmetric and efficient peaks were obtained for the four TKIs. However, the analysis time was too long (100 min).

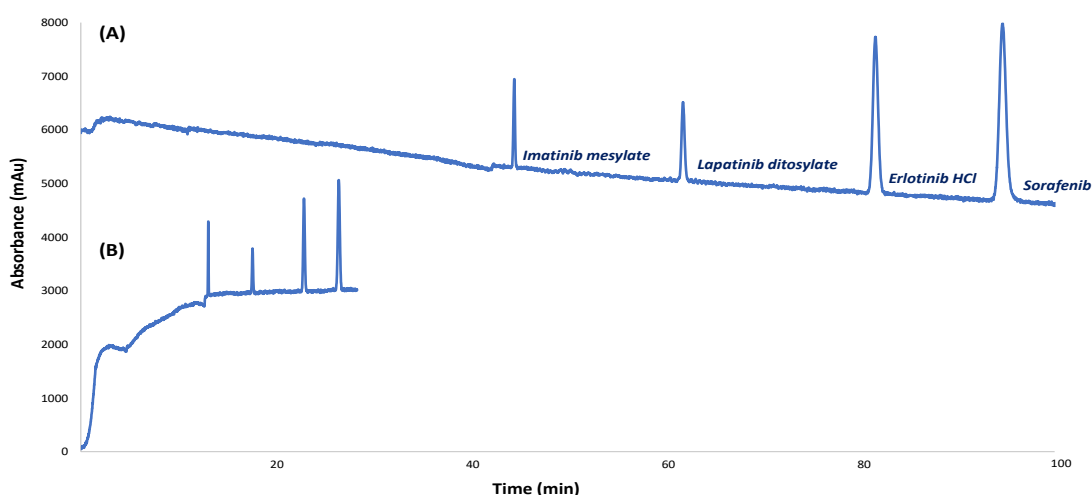


Figure 3: Electropherogram of 4 TKIs obtained by SALLE methodology with a total capillary length of (A) 50 cm (effective length 40 cm) and (B) 30 cm (effective length 20 cm). Analysis conditions: BGE: citric acid – ϵ -aminocaproic acid buffer I 150 mM pH 2.0. Temperature: 25°C. Separation voltage: 15 kV. Sample injection volume till the detector window: 7.5 %. Detection: 254 nm.

So, the total capillary length was reduced from 50 to 30 cm. The separation voltage was kept at 15 kV, resulting in an increased electrical field of separation from 300 to 500 V/cm. The percentage of injected volume till the detector window was also kept constant at 7.5% involving a decreased injected volume from 60 to 30 nL. Fig. 3B shows the separation of TKIs in less than 30 min with symmetric and efficient peaks.

3.3. On-line CE stacking of TKIs

An important but often unappreciated characteristics of the SALLE method is that the analytes which are extracted in the upper (mostly organic) phase can be concentrated inside the CE capillary thanks to on-line acetonitrile stacking phenomenon [7,15]. To evaluate the efficiency of on-line CE stacking, the injected sample volume was varied from 10 to 313 nL (corresponding to 2.5–80% of the capillary volume till the detector window) by varying hydrodynamic injection pressure and injection time (see part 2.3). Whatever the injected volume, an efficient separation of the 4 TKIs was observed (Fig. 4). An increase in analysis time was observed when the sample injected volume increased. Indeed, when the sample zone (containing high percentage of acetonitrile) becomes longer, the conductance of the whole fluid in the capillary becomes lower, which decreases the electric field intensity of both the sample zone and the BGE. In addition, the pH of the BGE being equal to 2.0, the electroosmotic mobility is very low (negligible) ($eof = 3.14 \times 10^{-5} \text{ cm}^2/\text{V}/\text{s}$) compared to the average effective mobilities of the TKIs ($eff \approx 5 \times 10^{-4} \text{ cm}^2/\text{V}/\text{s}$).

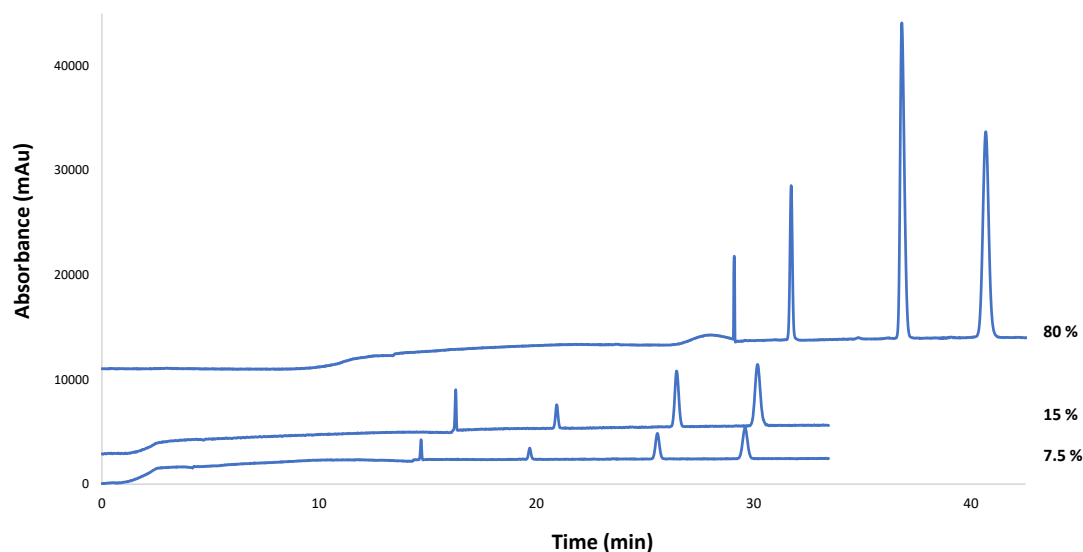


Figure 4: Effect of sample injected volume (7.5, 15 and 80 % of effective capillary volume) on the separation of TKIs. Analysis conditions: silica capillary 50 μm i.d., total length 30 cm, effective length 20 cm. BGE: citric acid – ϵ -aminocaproic acid buffer I 1 150 mM pH 2.0. Temperature: 25°C. Separation voltage: 15 kV. Sample injection volumes are expressed in percentage of injected volume till the detector window. Detection: 254 nm.

As a result, the mobility of analytes being predominantly based on their effective mobilities, the migration times of TKIs were extended when the sample injected volume increased [11]. The analytes corrected peak areas (Fig. 5) and heights increased linearly with the sample injected volume confirming the existence of on-line acetonitrile stacking phenomenon inside the capillary.

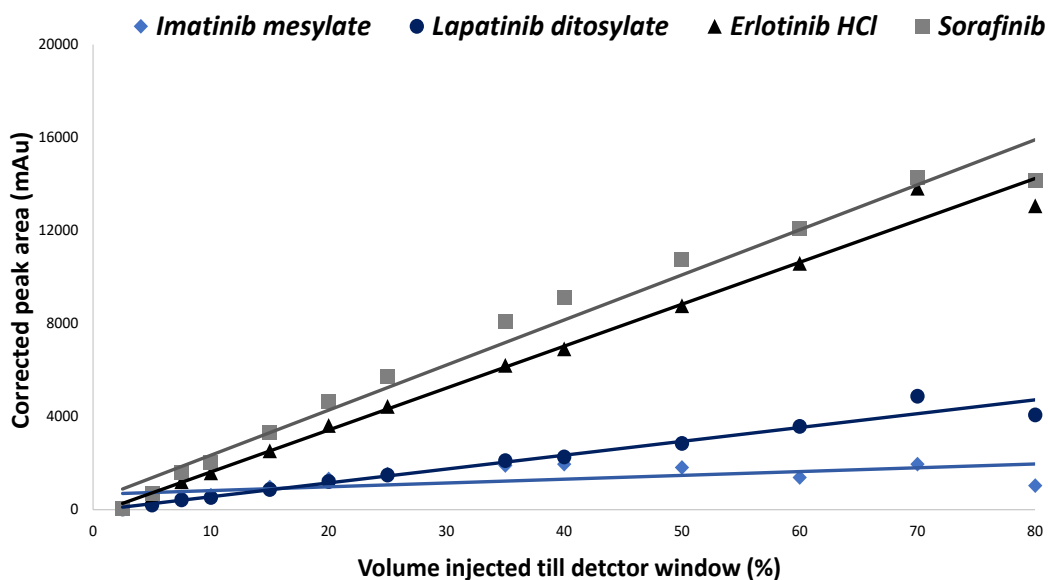


Figure 5: Effect of injected sample volume (from 7.5 to 80 % of effective capillary volume) on the analyte corrected peak areas. Analysis conditions: silica capillary 50 μm i.d., total length 30 cm, effective length 20 cm. BGE: citric acid – ϵ -aminocaproic acid buffer I 150 mM pH 2.0. Temperature: 25°C. Separation voltage: 15 kV. Sample injection volumes are expressed in percentage of injected volume till the detector window. Detection: 254 nm.

Evaluation of the sensitivity enhancement factor (SEF) of the proposed methodology compared to conventional CZE was performed. For this, a comparison of peak heights of analytes obtained for injected volumes equal to 80% and 2.5% (considered as conventional CZE mode) of the capillary volume till the detector window was done at the LOD. LOD of imatinib mesylate, lapatinib ditosylate, erlotinib hydrochloride and sorafenib were estimated at 3355, 7979, 4250 and 3750 ng/ml respectively for an injected volume equal to 2.5% of the capillary volume till the detector window (10 nl). For an injected volume equal to 80% of the capillary volume till the detector window (313 nl), LOD of imatinib mesylate, lapatinib ditosylate, erlotinib hydrochloride and sorafenib were estimated at 55, 35, 16 and 26 ng/ml respectively. The SEF was then equal to 61, 227, 265, and 144 folds for imatinib mesylate, lapatinib ditosylate, erlotinib hydrochloride and sorafenib respectively when increasing from 10 to 313 nl the injected volume.

3.4. Analysis of human plasma spiked with TKIs

The developed SALLE methodology was used to extract the four TKIs from human plasma. Human plasma was spiked with the four TKIs (see 2.6). The addition of ACN and NaCl in plasma in appropriate amounts

to get a ratio of 60/40 (v/v) ACN/plasma with 2% added NaCl (m/v) allowed to precipitate plasma proteins and to obtain two immiscible phases allowing the extraction of TKIs from human plasma. Fig. 6 shows the electropherogram obtained from human plasma with a total capillary length of 30 cm, a sample injection volume of 30 nl (corresponding to 7.5% of the capillary volume till the detector window) and a separation voltage of 15 kV. In comparison, a standard sample solution containing the four TKIs was analyzed following the same procedure as human plasma. Similar electrophoretic profiles in terms of migration times, peak areas and resolutions were obtained. These results show that the plasma sample matrix did not affect both the efficiency of the extraction of TKIs by SALLE method (similar extracted amount) and their analysis by CE (similar electrophoretic mobilities) for low injected volume (30 nl).

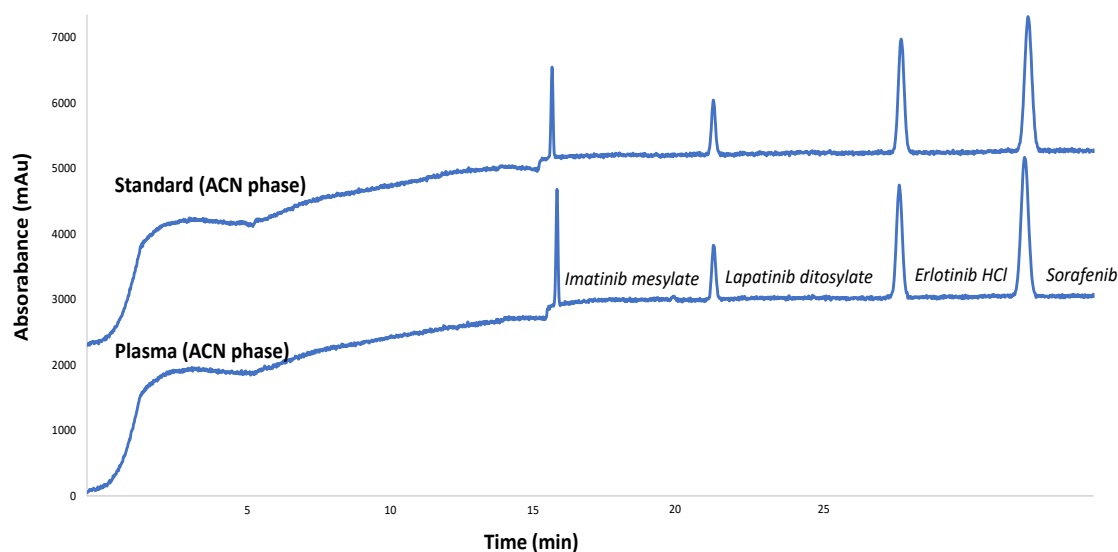


Figure 6: Electropherogram of 4 TKIs obtained from standard and human plasma samples using SALLE methodology. Analysis conditions: silica capillary 50 μm i.d., total length 30 cm, effective length 20 cm. BGE: citric acid – ϵ -aminocaproic acid buffer I 150 mM pH 2.0. Temperature: 25°C. Separation voltage: 15 kV. Sample injection volume: 30 nl (corresponding to 7.5% of the capillary volume till the detector window). Detection: 254 nm.

Injection of blank sample (plasma sample prepared as mentioned in part 2.7 without adding TKIs) showed no interfering peaks of endogenous proteins at the migration time of analytes (Fig. 7.A), demonstrating the specificity of the method. Fig. 7.B shows the electropherogram obtained from human plasma under the same analytical conditions but with a sample injected volume of 313 nl (corresponding to 80% of the capillary volume till the detector window). In comparison with the results obtained for the standard sample, different electrophoretic profiles in terms of migration times, peak shapes and resolutions were obtained for the 4 TKIs, especially sorafenib. This may be related to a matrix effect between plasma samples and standard solutions, in particular regarding the salt content. Indeed, the ionic strength of the

organic phase extract from plasma sample will be higher than the organic phase extract from standard solution which may be attributed to the difference in matrix composition between the two extracts. This resulted in reduced stacking phenomenon in the capillary. This effect is only noticed at large sample volume injected, i.e. 80%, where the separation length is reduced till the detector window. In order to ameliorate this result, an extra step was added after the SALLE procedure. This step consisted to evaporate a 200 nl volume of the upper (organic) phase, and to reconstitute the residue with 200 nl of ACN (for details see 2.8). The idea was mainly to remove the excess of salt found in the organic extract of plasma, by replacing it by pure ACN (salt is poorly soluble in pure ACN). This should improve the stacking of the 4 TKIs when analyzed by CE. Fig. 7.C shows a great amelioration in terms of migration times, peak shapes and resolutions of the 4 TKIs which is very similar to the one obtained with standard sample solution.

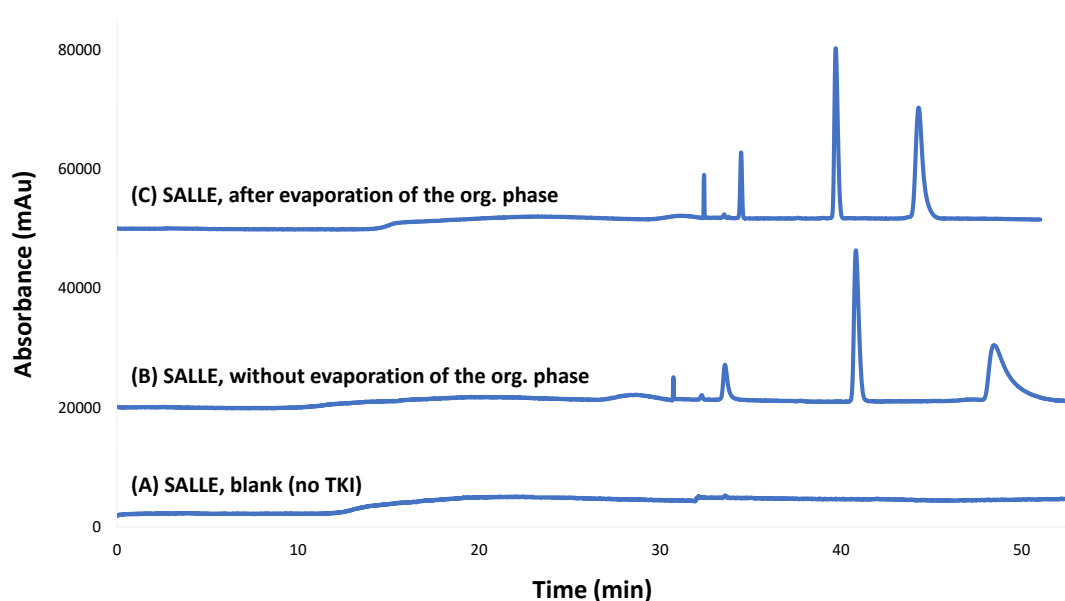


Figure 7: Electropherograms of (A) blank sample (no TKIs) and of the 4 TKIs obtained from human plasma samples using SALLE methodology (B) without, (C) with the evaporation of the organic extract. Analysis conditions: silica capillary 50 μm i.d., total length 30, effective length 20 cm. BGE: citric acid – ϵ -aminocaproic acid buffer I 150 mM pH 2.0. Temperature: 25°C. Separation voltage: 15 kV. Sample injection volume: 313 nl (corresponding to 80% of the capillary volume till the detector window). Detection: 254 nm.

Corrected peak areas obtained for the different analytes with and without evaporation of the organic phase were compared. They were found to be statistically equivalent. An increase observed in peak heights after evaporation (Fig. 7.C), is to be attributed to the partial removal of salt after evaporation step inducing better stacking. However, this extra evaporation step induced significant longer analysis times (one hour extra). Consequently, performances of the proposed SALLE-CE methodology were evaluated on plasma sample without evaporation of the organic phase. For a sample injected volume equal to 80% of

the capillary volume till the detector window (313 nl), LOQ of imatinib mesylate, lapatinib ditosylate, erlotinib hydrochloride and sorafenib were determined at 380, 900, 62 and 350 ng/ml respectively. These LOQ values are much lower than plasma levels observed for patients treated by TKIs, which are estimated at 1000, 1740, 1200 and 1440 ng/ml for imatinib mesylate, lapatinib ditosylate, erlotinib hydrochloride and sorafenib respectively [22–24]. Relative standard deviations (RSD) of less than 1.24 and 2.84% on migration times and corrected peak areas respectively were observed at the LOQ with 6 repeats showing the good repeatability of the CE methodology. LOD of imatinib mesylate, lapatinib ditosylate, erlotinib hydrochloride and sorafenib were determined at 160, 280, 16 and 100 ng/ml respectively. Good linearity of calibration lines was obtained for each TKI in the concentration range 60–2000 ng/ml with correlation coefficient (r^2) between 0.997 and 0.999. These values are summarized in Table 1. They confirm the applicability of the proposed methodology for dosing the TKIs in patients' plasma.

Table 1: Summary of SALLE-CE-UV quantitative results achieved on plasma samples with injected sample volume equal to 80 % of the capillary volume till detector window.

SALLE-CE-UV performance parameters	Imatinib mesylate	Lapatinib ditosylate	Erlotinib hydrochloride	Sorafenib
<i>SALLE extraction efficiency (%)</i>	60.6	100	98	100
<i>Sensitivity enhancement factor</i>	61	227	265	144
<i>Linearity (ng/ml)</i>	380-2000	900-2000	60-2000	350-2000
<i>Correlation coefficient (r^2)</i>	0.997	0.999	0.999	0.998
<i>LOD (ng/ml)</i>	160	280	16	100
<i>LOQ (ng/ml)</i>	380	900	62	350
<i>% RSD^a (corrected peak area)</i>	2.84	2.50	1.4	1.95
<i>% RSD^a (migration time)</i>	1.24	0.55	0.56	1.12

^a Calculated for 6 successive runs of LOQ levels

4. Conclusion

In this study, a SALLE-CE-UV method was proposed for the analysis of basic drugs in human plasma. SALLE has the advantages to eliminate simultaneously proteins, salts and to extract the molecules of interest from the sample matrix. The extracted solution (containing mostly ACN as solvent) could be injected up to 80 % of the capillary volume till the detector window due to the existence of on-line acetonitrile stacking phenomenon inside the capillary. This approach was successfully applied to human plasma spiked with 4 TKIs. The developed SALLE-CE methodology offers a number of features including high separation ability between analytes, easy operational procedure, low consumption of organic solvent, environmental benignity and applicability to high salinity matrix. Further research will be done to optimize the SALLE procedure for human plasma and to apply SALLE-CE-UV for the therapeutic drug monitoring of TKIs.

Acknowledgments:

This work was supported by a PhD grant from Misr University for science and technology (MUST), 6th October City, Egypt. The authors would like to thank Prof. Joseph Joachim the coordinator of the collaboration between MUST University and the University of Montpellier.

References

- [1] S. Pedersen-Bjergaard, K.E. Rasmussen, Liquid-phase microextraction and capillary electrophoresis of acidic drugs, *Electrophoresis* 21 (2000) 579-585.
- [2] R. Ramautar, G.W. Somsen, G.J. de Jong, Developments in coupled solid-phase extraction-capillary electrophoresis 2011-2013, *Electrophoresis* 35 (2014) 128-137.
- [3] R. Ramautar, G.W. Somsen, G.J. de Jong, Developments in coupled solid-phase extraction-capillary electrophoresis 2013-2015, *Electrophoresis* 37 (2016) 35-44.
- [4] L.I. Andersson, Molecular imprinting for drug bioanalysis: a review on the application of imprinted polymers to solid-phase extraction and binding assay, *J. Chromatogr. B: Biomed. Sci. Appl.* 739 (2000) 163-173.
- [5] A. Sarafraz-Yazdi, A. Amiri, Liquid-phase microextraction, *TrAC Trends Anal. Chem.* 29 (2010) 1-14.
- [6] S. Pedersen-Bjergaard, K.E. Rasmussen, Liquid-liquid-liquid microextraction for sample preparation of biological fluids prior to capillary electrophoresis, *Anal. Chem.* 71 (1999) 2650-2656.
- [7] J. Sun, J. Feng, L. Shi, L. Liu, H. He, Y. Fan, S. Hu, S. Liu, Study of the mechanism of acetonitrile stacking and its application for directly combining liquid-phase microextraction with micellar electrokinetic chromatography, *J. Chromatogr. A* 1461 (2016) 161-170.
- [8] D. Moreno-González, A.M. García-Campana, ~ Salting-out assisted liquid-liquid extraction coupled to ultra-high performance liquid chromatography-tandem mass spectrometry for the determination of tetracycline residues in infant foods, *Food Chem.* 221 (2017) 1763-1769.
- [9] Y.Q. Tang, N. Weng, Salting-out assisted liquid-liquid extraction for bioanalysis, *Bioanalysis* 5 (2013) 1583-1598.
- [10] T.S.K. So, C.W. Huie, Salting-out solvent extraction for the off-line preconcentration of benzalkonium chloride in capillary electrophoresis, *Electrophoresis* 22 (2001) 2143-2149.
- [11] M. Wang, Z. Cai, L. Xu, Coupling of acetonitrile deproteinization and salting-out extraction with acetonitrile stacking in chiral capillary electrophoresis for the determination of warfarin

- enantiomers, *J. Chromatogr. A* 1218 (2011) 4045–4051.
- [12] Y. Wen, J. Li, F. Yang, W. Zhang, W. Li, C. Liao, L. Chen, Salting-out assisted liquid–liquid extraction with the aid of experimental design for determination of benzimidazole fungicides in high salinity samples by high-performance liquid chromatography, *Talanta* 106 (2013) 119–126.
- [13] J. Liu, M. Jiang, G. Li, L. Xu, M. Xie, Miniaturized salting-out liquid–liquid extraction of sulfonamides from different matrices, *Anal. Chim. Acta* 679 (2010) 74–80.
- [14] J. Zhang, R. Rodila, E. Gage, M. Hautman, L. Fan, L.L. King, H. Wu, T.A. El-Shourbagy, High-throughput salting-out assisted liquid/liquid extraction with acetonitrile for the simultaneous determination of simvastatin and simvastatin acid in human plasma with liquid chromatography, *Anal. Chim. Acta.* 661 (2010) 167–172.
- [15] F. Kitagawa, K. Otsuka, Recent applications of on-line sample preconcentration techniques in capillary electrophoresis, *J. Chromatogr. A* 1335 (2014) 43–60.
- [16] Z.K. Shihabi, Organic solvent high-field amplified stacking for basic compounds in capillary electrophoresis, *J. Chromatogr. A* 1066 (2005) 205–210.
- [17] A. Arora, E.M. Scholar, Role of tyrosine kinase inhibitors in cancer therapy, *J. Pharmacol. Exp. Ther.* 315 (2005) 971–979.
- [18] E. Pirro, S. De Francia, F. De Martino, S. Racca, F. Di Carlo, C. Fava, S. Ulisciani, G. Rege Cambrin, G. Saglio, A new HPLC-UV validated method for therapeutic drug monitoring of tyrosine kinase inhibitors in leukemic patients, *J. Chromatogr. Sci.* 49 (2011) 753–757.
- [19] H. Gharwan, H. Groninger, Kinase inhibitors and monoclonal antibodies in oncology: clinical implications, *Nat. Rev. Clin. Oncol.* 13 (2016) 209–227.
- [20] C. Polson, P. Sarkar, B. Incedon, V. Raguvaran, R. Grant, Optimization of protein precipitation based upon effectiveness of protein removal and ionization effect in liquid chromatography–tandem mass spectrometry, *J. Chromatogr. B* 785 (2003) 263–275.
- [21] F.F. Cantwell, M. Losier, Liquid–liquid extraction, Chapter 11, *Compr. Anal. Chem.* 37 (2002) 297–340.

- [22] N.A.G. Lankheet, L.M. Knapen, J.H.M. Schellens, J.H. Beijnen, N. Steeghs, A.D.R. Huitema, Plasma concentrations of tyrosine kinase inhibitors imatinib, erlotinib, and sunitinib in routine clinical outpatient cancer care, *Ther. Drug Monit.* 36 (2014) 326–334.
- [23] H. Akaza, T. Tsukamoto, M. Murai, K. Nakajima, S. Naito, Phase II study to investigate the efficacy, safety, and pharmacokinetics of sorafenib in Japanese patients with advanced renal cell carcinoma, *Jpn. J. Clin. Oncol.* 37 (2007) 755–762.
- [24] B. Thiessen, C. Stewart, M. Tsao, S. Kamel-Reid, P. Schaiquevich, W. Mason, J. Easaw, K. Belanger, P. Forsyth, L. McIntosh, E. Eisenhauer, A phase I/II trial of GW572016 (lapatinib) in recurrent glioblastoma multiforme: clinical outcomes, pharmacokinetics and molecular correlation, *Cancer Chemother. Pharmacol.* 65 (2010) 353–361.

Section III

III.1 Comparison of both methodologies developed in chapter II and chapter III for the extraction and quantification of the four TKIs:

At first, performances of conventional PP by ACN (method I) developed in chapter II and SALLE technique (developed in this chapter, method II) coupled both to CE-UV analytical method were compared for the quantification of imatinib from human plasma and were resumed in [table 1](#). The maximum injected sample volume was of 156 nl (corresponding to 40% of the capillary volume till the detector window) for developed CE-UV using PP by ACN (method I) while, it was 313 nl (corresponding to 80% of the capillary volume till the detector window) for SALLE-CE-UV (method II). Both methods were specific as confirmed by the analysis of blank samples (as shown before). Peak heights and peak areas of imatinib obtained for injected sample volumes equal to 80% (method II) and 40% (method I) of the capillary volume till the detector window were evaluated. A sensitivity enhancement factor (SEF) of 1.6 in term of peak area was obtained for method II compared to method I. The recovery (%) of both methods was also compared. For method II, the recovery (%) was 60.0% compared to 90.3% for method I. LOQs of imatinib mesylate was determined to be equal to 191 and 380 ng/mL for method I and II respectively. LODs of imatinib mesylate was determined to be equal to 48 and 160 ng/mL respectively. The reason why method I based on PP by ACN extraction is more sensitive than method II based on SALLE methodology, is related to the partitioning of imatinib between the two phases after SALLE extraction. 60% of imatinib is extracted in the upper mostly organic phase while, 40% is lost in the lower mostly aqueous phase. Relative standard deviations (RSD) of less than 1.68 % and 2.85 % in migration times and corrected peak areas was observed for both methods at the LOQ (n = 6). Good linearity of calibration curve was obtained for both method with r^2 of 0.997.

Table 1: Comparison between method I based on PP by ACN and method II based on SALLE for the analysis of imatinib mesylate.

Performance parameters	Method I	Method II
Recovery (%)	90.3	60.0
Linearity (ng/mL)	191-5000	380-2000
Correlation coefficient (r^2)	0.997	0.997
LOD (ng/mL)	48	160
LOQ (ng/mL)	191	380
% RSD ^a (corrected peak area)	2.60	2.84
% RSD ^a (migration time)	1.68	1.24
Total analysis time (min)	26	43

^a Calculated for 6 successive runs of LOQ level

SALLE gave cleaner upper phase extract of plasma compared to PP by ACN, which is very clear when comparing two electropherograms obtained by both methods (I and II) as shown in Fig. 1. In contrast, the total analysis time concerning SALLE procedure is longer by 17 minutes as additional steps are needed including addition of salting-out agent and mixing/standing time after adding the salt.

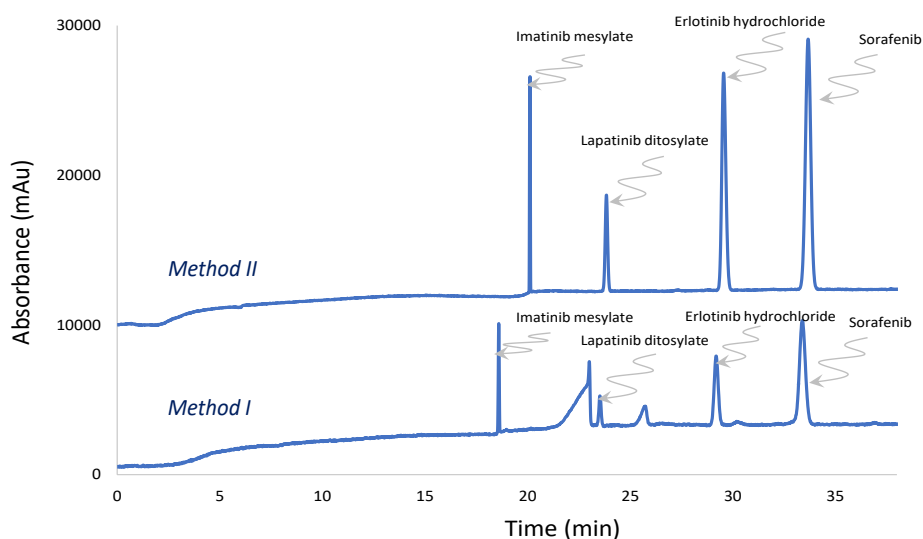


Figure 1: Electropherograms by method I and method II of the 4 TKIs obtained from human plasma samples. Analysis conditions: silica capillary i.d. 50 μ m, total length 30 cm, effective length 20 cm. BGE: citric acid– ϵ -amino caproic acid buffer / 150 mM pH 2.0. Temperature: 25°C. Separation voltage: 15 kV. Sample injection volume for method I

was 156 nl (corresponding to 40% of the capillary volume till the detector window). For method II was 313nl (corresponding to 80% of the capillary volume till the detector window). Detection: 254nm.

Evaluation of the sensitivity enhancement factor (SEF) of the SALLE methodology compared to conventional ACN precipitation was also performed for the three other TKIs (lapatinib ditosylate, erlotinib hydrochloride and sorafenib). A SEF of 7.6, 7.2 were obtained for method II for lapatinib ditosylate, 6.8, 6.8 for erlotinib hydrochloride and 3.7, 3.0 for sorafenib in term of peak heights and peak areas respectively compared to method I. Also, the estimated LOQs of lapatinib ditosylate, erlotinib hydrochloride and sorafenib by method I were estimated at 2400, 625 and 441 ng/mL respectively for an injected volume equal to 40% of the capillary volume till the detector window. While, the measured LOQs of lapatinib ditosylate, erlotinib hydrochloride and sorafenib by method II were at 900, 62 and 350 ng/mL respectively for an injected volume equal to 80% of the capillary volume till the detector window. Also as mentioned in chapter II, the estimated LOQ of lapatinib ditosylate did not arrive to its plasma level (1740 ng/mL). This makes it more advantageous to use method II with SALLE extraction technique in order to quantify the four TKIs. All these values proved that method II is more sensitive than method I for the extraction and quantification of the four TKIs.

Section IV

As mentioned in section II of this chapter, TKIs corrected peak areas and heights increased with the sample injected volume confirming the existence of on-line ACN stacking phenomenon inside the capillary as shown in Fig. 1.A. However, this increase was not linear for imatinib mesylate. Fig. 1.B shows that the increase in imatinib peak area was linear for injected volumes representing up to 25% of the capillary effective volume. For greater injected volumes, the increase of imatinib peak area becomes random. The reason may be related to the formation of various boundaries (dispersion of sample zone) as described in chapter II. Thus, different electrophoretic zones are formed which develop in long injection plugs related to the large sample volume injected (see chapter II). Unfortunately, there is no theoretical model that can describe this kind of behavior inside the capillary when organic solvent is present in the sample matrix with salt. Herein, in this section, the analytical conditions concerning imatinib analysis was changed and optimized to avoid such behavior for large injected sample volume injected.

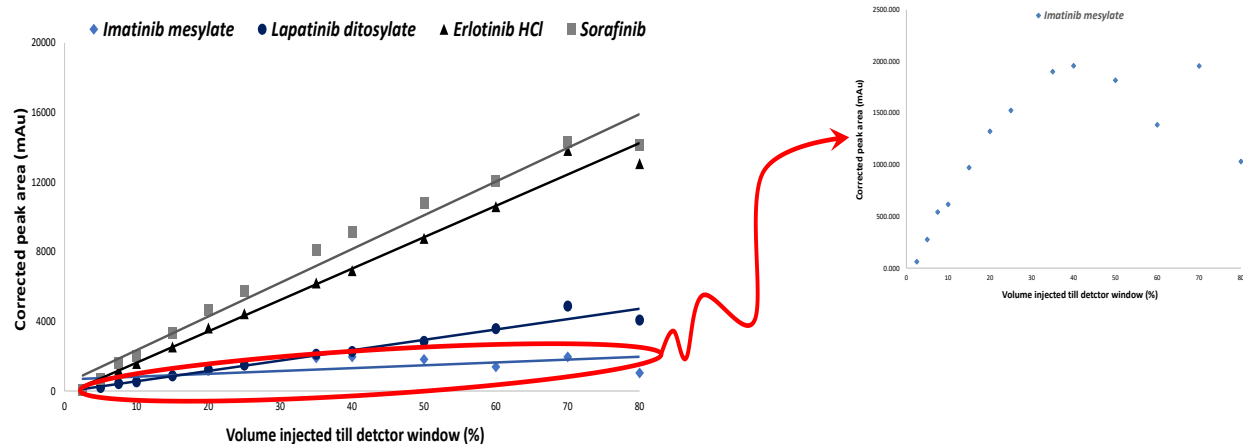


Figure 1: (A) effect of injected sample volume (from 7.5–80 % of effective capillary volume) on the analyte corrected peak areas. Analysis conditions: silica capillary 50 m i.d., total length 30 cm, effective length 20 cm. BGE: citric acid/6-aminocaproic acid buffer I 150 mM pH 2.0. Temperature: 25 °C. Separation voltage: 15 kV. Sample injection volumes are expressed in percentage of injected volume till the detector window. Detection: 254 nm. (B) zoom in on the curve of imatinib mesylate.

IV.1 Experimental:

IV.1.1 Materials and methods

- *Electrophoretic conditions*

As in section II (published paper) of this chapter except 1/ two lengths of the capillary 50 and 30 cm were used (40 and 20 cm effective length to the detector). 2/ hydrodynamic injections of the samples were varied between 0.4 to 1.8 psi and injection times were varied between 20 to 87 seconds (s) to obtain injection volumes comprised between 20-395 nl (equivalent to 2.5 to 50% of the capillary effective length) for 50 cm capillary. In addition, hydrodynamic injection of the sample was at 0.6 psi and injection time was at 33 seconds (s) to obtain injection volume of 78.31 nl (equivalent 20% of the capillary effective length) for 30 cm capillary.

- *Spectrophotometric trials*

Beckman coulter spectrophotometer DU-640 (P/ACE system MDQ) with Single beam. The DU Series 600s operates in the wavelength range of 190 to 1100 nm. The wavelength was at 254 nm.

IV.1.2 Preparation of BGE and stock solutions:

The BGE was a mixture of citric acid and ϵ -amino caproic acid. BGE composition with the desired I and pH was calculated using the software "Peakmaster" 5.3. Citric acid (100 mM) and ϵ -amino caproic acid (163 mM) were mixed together to obtain pH 4.0 and I 150 mM.

IV.1.3 Preparation of the standard imatinib solutions

- Imatinib standard solution: relevant volumes (depending on the desired concentration) of distilled water and appropriate imatinib stock solution were mixed in an eppendorf centrifuge tube.
- Imatinib standard solution for spectrophotometric measurements: relevant volumes of BGE (I 150 mM) at pH 2.0 or 4.0 and appropriate imatinib stock solution were mixed in an eppendorf centrifuge tube to obtain a final concentration of 10 $\mu\text{g}/\text{mL}$.

IV.1.4 Optimized SALLE procedure of imatinib standard solution

To imatinib standard solution (2000 μL), 3000 μL of ACN were added in an eppendorf to have a ratio of 60/40 ACN/standard solution (v/v). After vortexing for 1 min, 0.1 g of NaCl (2% NaCl (m/v)) was added to the mixture. The solution was then vortexed for 1.0 min and were left to stand for 3.0 min. A separation into two phases, lower (mostly aqueous) and upper (mostly organic) occurred. 80 nL of the organic phase was injected and analyzed by CE coupled to UV detection.

IV.1.5 Optimized SALLE procedure from human plasma spiked with imatinib mesylate

Briefly, human plasma were placed in an eppendorf centrifuge tube and spiked with appropriate volume of imatinib mesylate stock solution. Then, the spiked plasma was mixed during 1 h at room temperature. 3000 μ L of ACN was added to have a ratio of 60/40 ACN/plasma (v/v). The addition of ACN induced protein precipitation. The supernatant was separated from the precipitated proteins after the mixture was vortexed for 1 min and centrifuged for 5 min (11,000 rpm, 4 °C). Then, 0.1 g of NaCl was added to the mixture (2% NaCl (m/v)). The solution was then shaken for 1.0 min and left to stand for 3.0 min. A separation into two phases, lower mostly aqueous and upper mostly organic phase occurred.

IV.2 Results and discussion

The pH of the BGE was changed to 4.0 to see if the same effect will be observed as at pH 2.0. Fig 2.A shows the peak of imatinib obtained at pH 4.0 with injected sample volume equal to 7.5% of the capillary effective volume after injecting the upper mostly organic phase obtained by SALLE. The peak was symmetric in shape as the one obtained at pH 2.0. Comparison of this peak with the peak obtained at pH 2.0 (Fig. 2.B) shows a difference in both imatinib peak height and peak area by a factor of 1.67x and of 1.54x respectively.

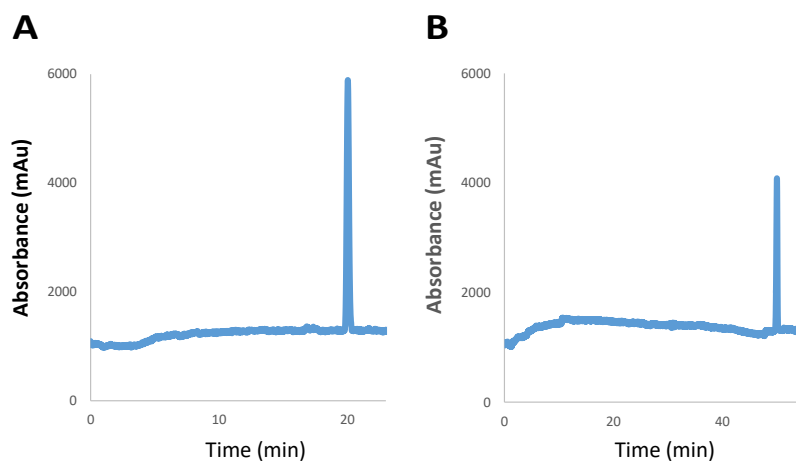


Figure 2: Electropherograms of imatinib mesylate obtained by SALLE methodology with a total capillary length of 50 cm (effective length 40 cm). Analysis conditions, BGE: citric acid/ ϵ -aminocaproic acid buffer I 150 mM pH (A) 4.0 and (B) 2.0. Temperature: 25 °C. Separation voltage: 15 kV. Sample injection volume: 7.5% of the capillary effective length. [imatinib] = 5.0 μ g/mL. Detection: 254 nm.

This observation suggests reduced dispersion during the electrophoretic process for imatinib at pH 4.0. It was supposed that the molar absorptivity of imatinib could change with the change in pH of the BGE. Two imatinib standard solutions were prepared (see point IV.1.1). However, the ϵ was 26865.7 $M^{-1}cm^{-1}$ at pH 2.0 and was 24906.2 $M^{-1}cm^{-1}$ at pH 4.0 showing no significant difference between the two pH.

The injected sample volume was then varied from 9.5 to 157 nl (equivalent to 2.5 to 40% of the capillary effective volume) by varying hydrodynamic injection pressure and time (see [part IV.1.1](#)). For injected volumes greater than 40% of the capillary effective volume, imatinib peak is detected with kind of a negative peak. This negative peak was related to system zones (system eigen zones) as shown in [Fig. 3](#). As the volume of the sample increased, the distance between imatinib peak and system zones decreased, impairing imatinib peak efficiency. The system zones or system eigen zones were described by B. Gaš [1]. He mentioned that when a sample is injected to CZE, the analyte creates a disturbance in the concentration of the BGE. The system retains a kind of memory for this inhomogeneity, which is propagated with time and leads to so-called system zones (or system eigen zones) migrating in an electric field with a certain eigen mobility. This phenomenon could be the reason for the negative zone obtained in [Fig. 3](#).

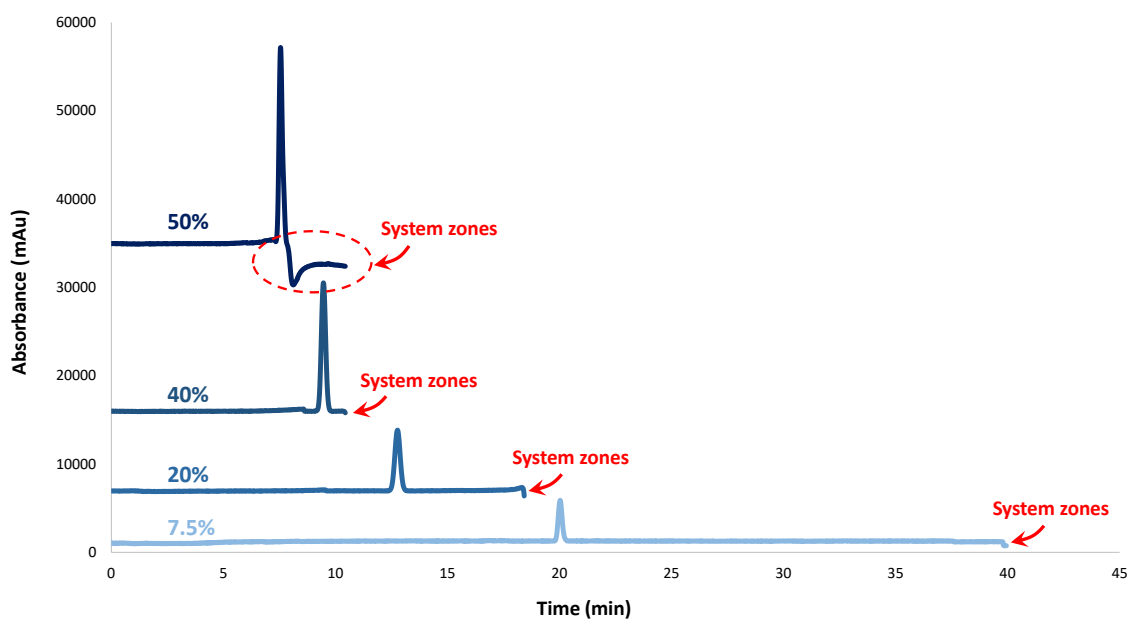


Figure 3: Effect of sample injected volume (7.5, 20, 40 and 50% of effective capillary volume) on imatinib analysis. Analysis conditions: silica capillary 50 μ m i.d., total length 50 cm, effective length 40 cm. BGE: citric acid/6-aminocaproic acid buffer I 150 mM, pH 4.0. Temperature: 25 °C. Separation voltage: 15 kV. Sample injection volumes are expressed in percentage of injected volume of the capillary effective length. Detection: 254 nm.

The next step was to choose the optimal injected sample volume, which is repeatable, far from eigen zones and sufficient to give the required LOQ of imatinib. [Fig. 4.A](#) shows the linear relation obtained when increasing the sample volume injected from 2.5 to 40% of the capillary effective length on imatinib corrected peak areas. The correlation coefficient (r^2) was 0.993. Repeating sample injection at 40% gave a RSD% of more than 3.6%. However, it is not necessary to inject such volume to achieve a LOQ sufficient for the TDM of imatinib. It was found that a sample volume injected of 20% gave an estimated LOQ of 400

ng/mL with a RSD% of less than 2.0%. Tracing the same line but for a sample volume injected from 2.5 to 20% gave better r^2 of 0.998 as shown in Fig. 4.B. So, for the rest of CE trials, imatinib will be analyzed at pH 4.0 with a sample injected volume of 20% of the capillary effective length.

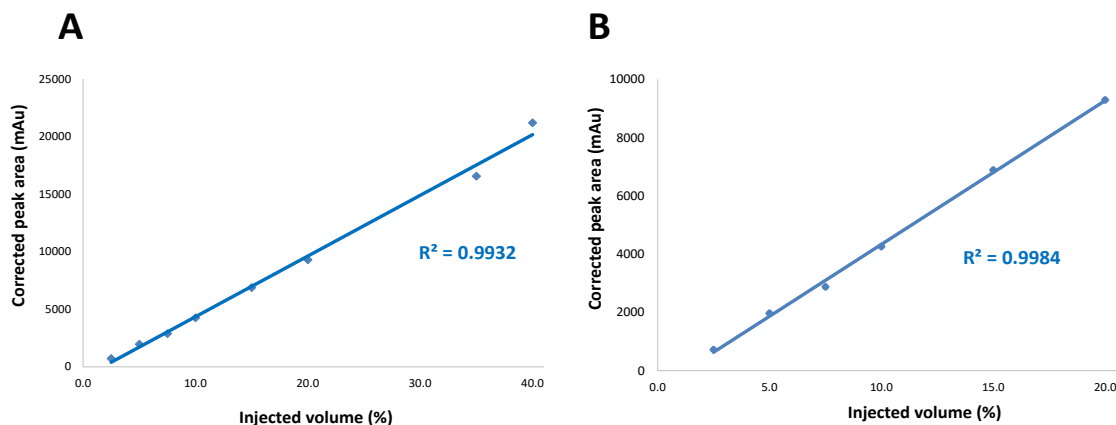


Figure 4: Effect of injected sample volume from (A) 2.5 to 40% and from (B) 2.5 to 20% of the capillary effective length on imatinib corrected peak areas. Analysis conditions: silica capillary 50 μm i.d., total length 50 cm, effective length 40 cm. BGE: citric acid/6-aminocaproic acid buffer I 150 mM pH 4.0. Temperature: 25 $^{\circ}\text{C}$. Separation voltage: 15 kV. Sample injection volumes are expressed in percentage of injected volume till the detector window. Detection: 254 nm.

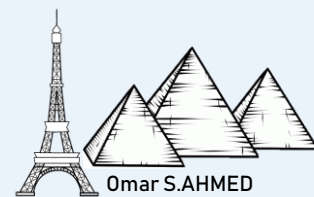
References of section IV

- [1] B. Gaš, E. Kenndler, System zones in capillary zone electrophoresis, *Electrophoresis*. 25 (2004) 3901–3912.

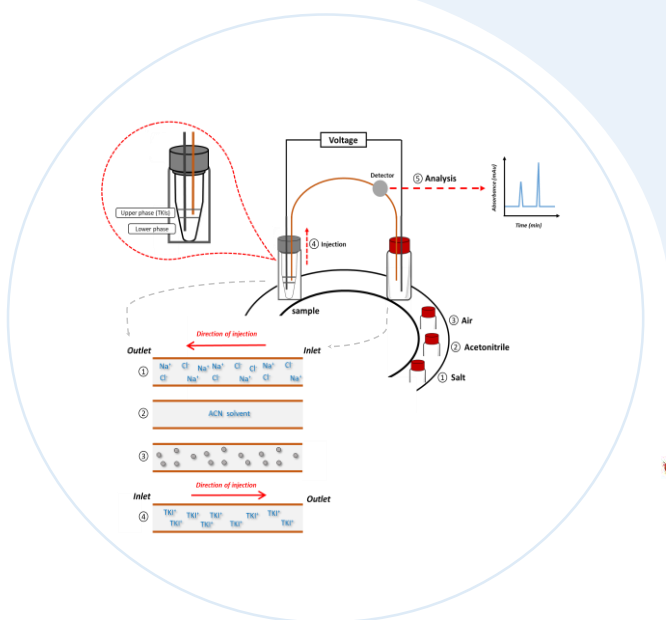
General conclusion of the chapter

In this chapter, the use of the salting-out effect in analytical chemistry was demonstrated. The salting-out effect can be used to create a phase separation between water-miscible organic solvents and water by simply increasing the concentration of salt. SALLE is an advantageous sample preparation technique, which was used when developing analytical methodologies aimed to quantify different compounds. In the context of our project, a new SALLE-CE-UV methodology was developed for the extraction and the analysis of four TKIs namely imatinib mesylate, lapatinib ditosylate, erlotinib hydrochloride and sorafenib in human plasma. SALLE has the advantages to eliminate simultaneously proteins, salts and to extract the TKIs from the plasma matrix giving cleaner upper phase extract. TKIs were efficiently extracted (60–100% extraction efficiency) in the upper phase which was analyzed by CE coupled to UV detection. The fact that the extracted upper phase solution was mainly composed of ACN allowed to obtain excellent peak efficiencies, good resolution and high sensitivity thanks to the existence of stacking phenomena during CE separation. The injected sample volume can be up to 80% of the capillary volume (till the detector window). The performance of SALLE-CE-UV methodology was evaluated in terms of extraction efficiency, LOQ and LOD of the four selected TKIs. This performance was sufficient for the analysis of the four TKIs in term of the required LOQ obtained. These LOQ values are much lower than mean plasma levels observed for patients treated by TKIs, which are estimated at 1000, 1740, 1200 and 1440 ng/mL for imatinib mesylate, lapatinib ditosylate, erlotinib hydrochloride and sorafenib respectively. This method SALLE-CE-UV (method II) was better than the first method (method I) developed in chapter II. Moreover, imatinib mesylate was successfully analyzed at pH 4.0 by CE-UV after SALLE extraction. The modified pH of the BGE enabled to obtain a linear relation between increased sample volume injected and imatinib peak area to avoid the random increase in imatinib peak area at pH 2.0. In the next chapter, the first demonstration of a fully automated SALLE by CE for the analysis of TKIs is presented.

Chapter IV



Automation of the SALLE-CE methodology



This chapter is the subject of:

- 📄 **A scientific paper:** *A fully automated on-line salting-out assisted liquid-liquid extraction capillary electrophoresis methodology: Application to tyrosine kinase inhibitors in human plasma.* Accepted in Talanta. (2019) 120391.
- 🗣️ **An oral presentation:** *A fully automated salting-out assisted liquid-liquid extraction (A-SALLE) procedure coupled with on-line stacking for the analysis by capillary electrophoresis: application to tyrosine kinase inhibitors (TKIs) in human plasma.* 45th HPLC conference- June 2019, Milan, Italy.



Preface

Recently, sample pretreatment and analysis are moving towards the development of fully automated analytical methodologies in particular for bioanalysis. The techniques used are very diverse and range from using commercially available machines to homemade devices coupled to separation and detection techniques.

In this chapter, we will discuss the next step of our work, which was to automate the SALLE-CE-UV methodology previously developed for the analysis of the three selected TKIs. Automation of analytical methodology allows to decrease human errors related to manual sample preparation and to decrease the general analysis cost per sample. In this context, our idea was to automate the optimal analytical conditions determined before for the analysis of the three TKIs by SALLE-CE-UV without making any modifications of the CE machine. The first section of this chapter, relate most of the literature reviews that deal with full automation of CE analytical methodologies including flow system analysis, robots and interfaces used to couple flow system with CE. Section II reports a scientific paper accepted in *Talanta* journal describing the automation of the SALLE-CE-UV methodology to analyze three TKIs (erlotinib hydrochloride, lapatinib ditosylate and sorafenib) in human plasma at pH 2.0. This includes preliminary results, optimization steps and its application to human plasma spiked with the three TKIs. Supplementary results supporting our work are given at the end of the section II.

Section I

I.1 Literature review on automation of sample extraction and analysis

As mentioned before, sample pretreatment steps are the most time-consuming and error-prone parts of the whole analytical procedure. Manual sample pretreatment is labor intensive, expensive, besides, variations in results obtained from run-to-run. In addition, the human errors caused by handling when dealing with manual preparation and the need to rerun samples manually which are time consuming and could adversely affect the analytical results.

Over the past years, sample preparation and analysis are moving towards the development of a fully automated analytical techniques that allow the extraction, the injection, the separation, the detection, and the quantification in a single and continuous stages. One or more of these stages may be online (outside the capillary in case of CE) or inline (inside the CE capillary). Other strategies dealt with the use of robots or the use of a homemade devices to achieve specific targets the could simplify of sample preparation procedures in an automated way. Most of the methods published in literature reviews report the coupling of flow systems with separation systems (e.g. HPLC, CE) and detection techniques such as UV, fluorescence, MS, etc.

In this section, a brief overview of the current trends in the automation of sample preparation techniques based on different strategies is discussed.

I.1.1 Automated extraction and analysis strategies based on flow analysis

I.1.1.1 Flow injection analysis (FIA)

FIA system could be used to integrate both extraction and analysis. FIA is the generic name for all analytical techniques that are based on the introduction, processing and detection of liquid samples in a flowing media. It was first developed by J. Růžička, E.H. Hansen [1] in 1980, where the analytes and reagents are injected into a constant carrier flow (laminar flow), mixed there reproducibly and finally sent towards the detector using the same carrier flow. FIA instrument was set up at the beginning of the process and the reaction as well as the detection was carried out in a fast-automated way. FIA offers many advantages including time saving, improvement of the precision over manual operations involved in sample preparation and reduction in analysis costs due to reduced sample and reagent consumption. Fig. 1 shows the simplest FIA instrument where the sample or reagent are injected using a two ways valve, mixed in the coil then, injected into the detector (UV/VIS detector in this case).

Many applications mentioned FIA for the analysis of pharmaceuticals. M.S. Bloomfield [2] developed a sensitive and a rapid assay for degradant 4-aminophenol in paracetamol drug and tablet formulation, by FIA hyphenated to UV-Vis detection. P. Viñas and al [3] developed an analytical method for the determination of cysteine, N-acetylcysteine, penicillamine, 2-mercaptopropionylglycine and thiouracil in pharmaceuticals using FIA coupled to chemiluminescence detection. Procedures are based on the inhibition by these drugs of the chemiluminescence generated in the copper-catalysed oxidation of luminol by hydrogen peroxide. N.A. Mohamed [4] developed an online determination of some selective α_1 -blockers by FIA with micelle-enhanced fluorescence detection. The idea is based on based on enhancement of the native fluorescence of the studied drugs in the presence of sodium dodecyl sulfate (SDS). The proposed FIA method had the advantages of simplicity, sensitivity, speed, accuracy and the use of environmentally safe reagents. Other applications of FIA techniques are found in biotechnology [5,6], proteomics [7], environmental analysis [8] and food analysis [9].

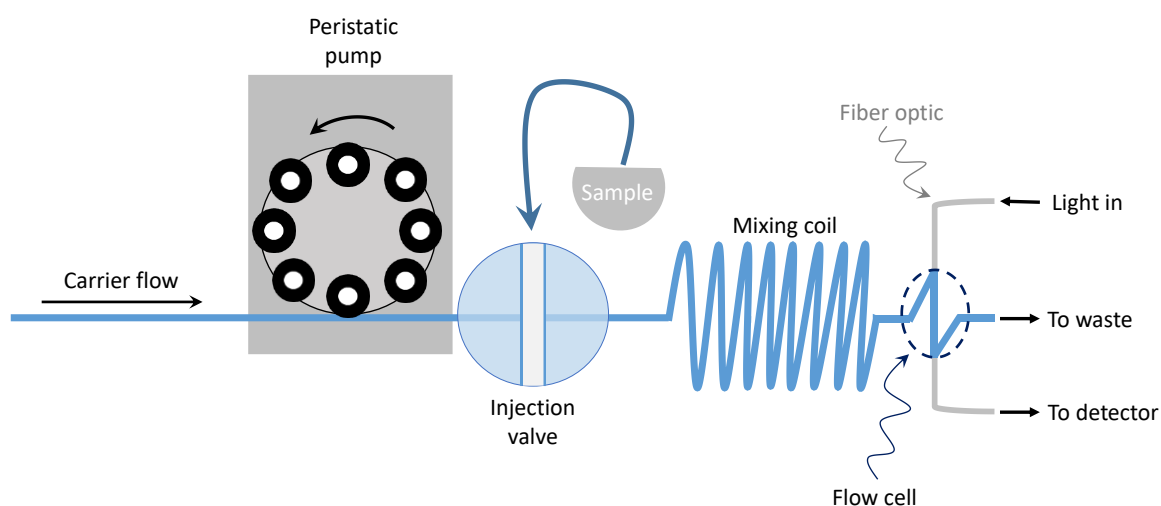


Figure 1: Schema of FIA

1.1.1.2 Sequential injection analysis (SIA)

SIA which is a novel variation of FIA using flow programming and flow reversal controlled by a computer. The flow is not continuous compared to FIA. Advantages of SIA over FIA are 1/small volume of reagents used, 2/less waste generated, 3/can be used to monitor environmental and industrial processes and 4/instrumentation was miniaturized to what is called "lab on a valve" with less waste generation [10]. The main key of SIA is the six-way valve which allows the computer to inject whether the sample or reagent to flow (as shown in Figure 2). The syringe pump can draw liquids including sample, carrier buffer

or reagents accessed by the three-way valve and inject the liquids into the holding coil. Both sample and reagents are withdrawn and mixed inside the holding coil (stopping flow for a while). Then, the flow is inversed and the liquids are sent to port 2 (flow cell). Flow, reaction time and number of reagents used, are optimized depending on the objective of analysis and the products to be analyzed. Dialysis [11], SPE [12,13] or LLE [14], can be incorporated without difficulty into such flow systems. However, the resolution of separations concerning HPLC and CE analysis cannot be achieved directly by employing these flow systems as different configuration parameters have to be considered (e.g. constant flow generated by peristaltic pump and hydrodynamic injection of the sample in case of CE). In such situations, interfaces connect the automated flow system to a separation system where the analytes are separated and detected (examples will be discussed in point 1.1.1.6). The separation and detection in this case, are carried out in the connected separation system. SIA and FIA has been adapted as a tool for the automation of pharmaceutical analysis. R. Segarra Guerrero et al. [15] developed a fluorimetric determination of captopril by FIA. M.C. Sanfeliu Alonso et al. [16] developed a new FIA-chemiluminescence method for the determination of iproniazid phosphate an antidepressant drug. Another application involved [17] quantitative determination of ciprofloxacin and norfloxacin antibiotics complexed with iron(III) in sulfuric acid media using SIA-spectrophotometric measurement.

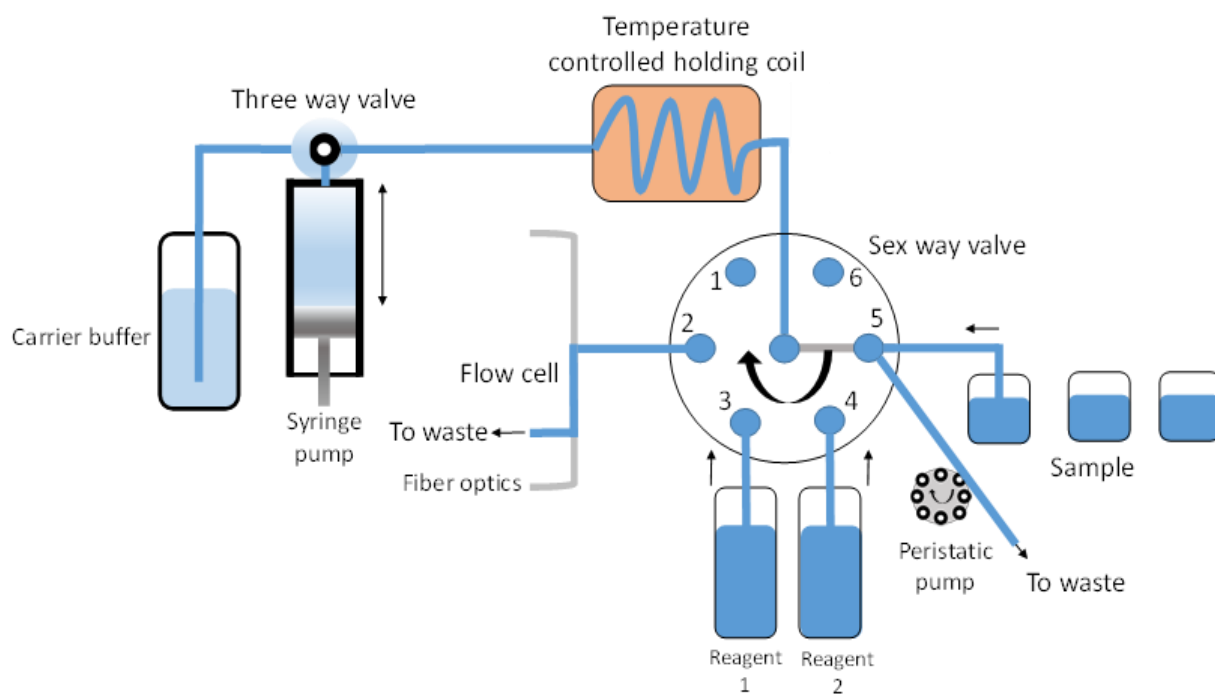


Figure 2: Hardware of SIA

1.1.1.3 Stepwise injection analysis (SWIA)

SWIA is a variant of SIA (without a holding coil), in which a general scheme of chemical analysis, regardless of methods, can be represented as a set of sequential cycles [18]. In turn, these cycles include a certain sequence of operations (steps or stages). These stages are portion sampling, sample pretreatment, the addition of reagent solutions to sample solutions, intermixing of the solutions with the help of gas stream until the equilibrium of the system will be gained, thermostating (if necessary), analytical signal measuring (Fig. 3).

Applications of SWIA extend to many fields. K. Medinskaia and her group [19] developed a fully automated effervescence assisted DLLME based on a SWIA for the determination of antipyrine in saliva samples. I. Timofeeva and his group [20] developed SWIA for potentiometric determination of caffeine in saliva using SDME.

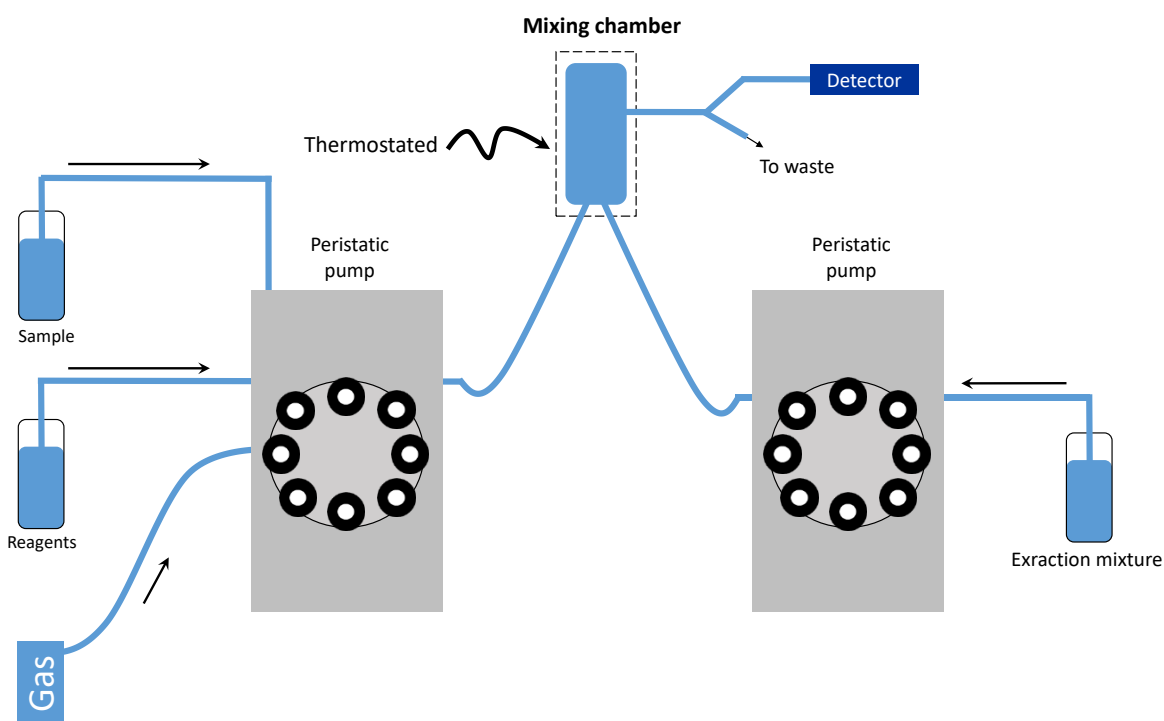


Figure 3: Schema of SWIA

I.1.1.4 Strategies for the hyphenation of LLE to FIA and SIA

A classical liquid–liquid flow injection system is characterized by three main components: a phase segmenter, an extraction coil and a phase separator. After the introduction of an aqueous sample, either in a continuous process or in a well-defined volume, into an aqueous stream (which acts as reagent and as carrier stream) solutions, homogenization occurs and a reaction zone is formed. This zone is directed towards the segmenter [21]. In the segmenter, the two streams of aqueous and organic immiscible phases are put into contact and a single flow of alternate reproducible zones of both phases is generated (Fig. 4). Subsequently, in the extraction coil, the mass transfer in between both phases takes place. The two phases multiple interfaces created by the segmentation process. Finally, in the phase separator, the small aqueous and organic phase segments are continuously split into individual streams, being the one that contains the analyte directed towards the detector for measurement. The two phases separation and segmentation are very important for the extraction efficiency and repeatability of the analytical results. Another example is the work of T. Blanco [22] who developed a LLE in FIA using an open-phase separator with a solenoid valves for the spectrophotometric determination of copper in plant digests. The open tube enclosed by computer-controlled solenoid valves was installed vertically to promote fast phase separation by differences in density. The solenoid valves were used to introduce the reacted sample zone into the tube, to select a precise volume of the extracted complex to be detected and to pass the remaining solution to waste. A preconcentration factor of 10 was attained, corresponding to the aqueous to organic phase volume ratio and with a small solvent volume 700 μL per determination.

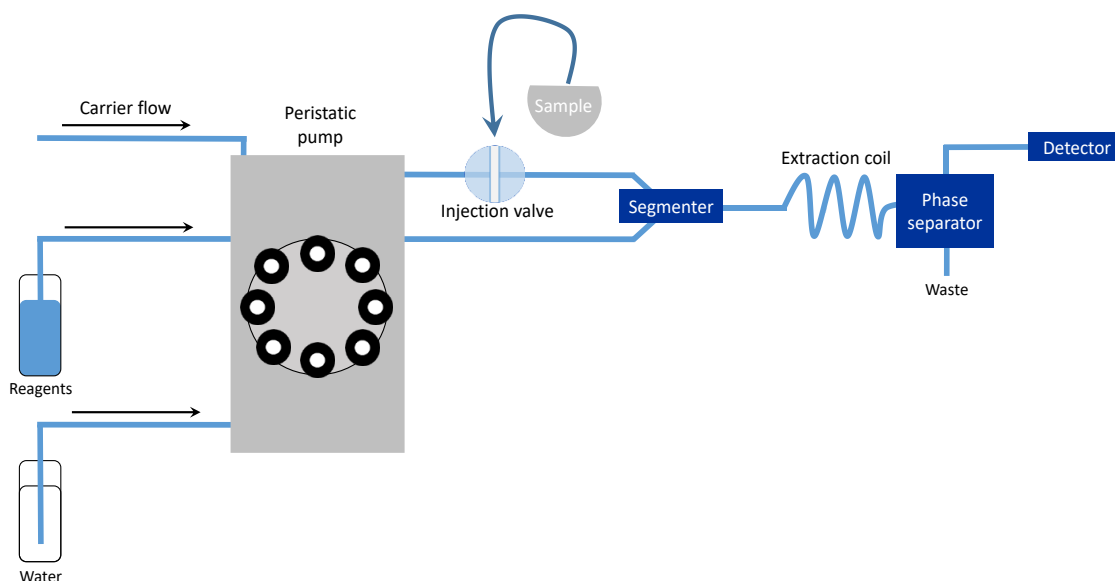


Figure 4: Typical LLE flow analysis system manifold using FIA

I.1.1.5 Strategies for the hyphenation of SPE to FIA and SIA

N. Kasthurikrishnan et al. [23] was the first to use SPE in FIA. By incorporating a SPE column in the system flow, analytes can be collected, pre-concentrated and separated prior to detection. FIA and SIA coupled to on-line sample pretreatment offer many advantages such as 1/ high sample throughput, 2/ decrease of reagent consumption and wastes and 3/ ability to couple these systems to different detection modes. The diagram of the FIA–SPE automated system is illustrated in Fig. 5. It is constructed by combination of a peristaltic pump, a SPE column and the detector. The injection valve plays the most important role as it controls the pre-concentration mode (sample and carrier are loaded to the column) or the elution mode where the eluent is injected, followed by detection.

Many applications involved the use of SIA and FIA with SPE or LLE extraction systems coupled to separation and detection techniques. A.Tolokán et al. [24] developed an automated quantification method of levodopa and carbidopa in plasma by HPLC coupled to electrochemical detection using an on-line FIA sample pretreatment unit. After PP of the plasma samples with perchloric acid, the catecholamines were extracted from the supernatant by adsorption on a small column filled with alumina. The extraction and redissolution were automatically performed in FIA coupled to the HPLC system. Another example is Z.Legnerová et al. [25] who developed an on-line SPE for simultaneous determination of ascorbic acid and rutin trihydrate by SIA in combined pharmaceutical formulation. Other applications extended to food analysis [13,26–28] and environmental applications [29,30].

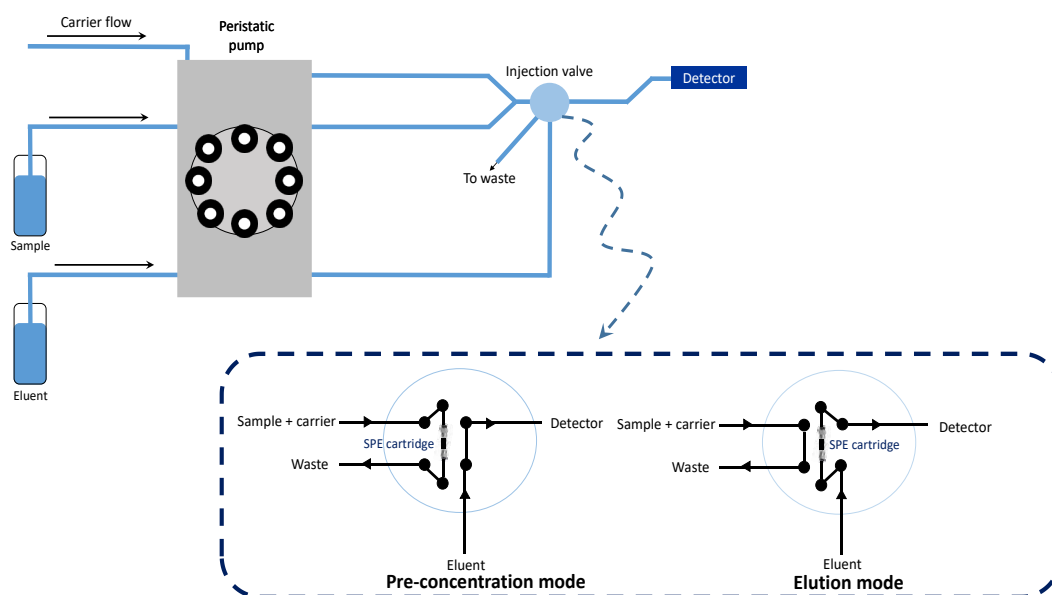


Figure 5: Typical solid phase extraction flow analysis system manifold using FIA

1.1.1.6 Coupling of FIA, SIA and SWIA with CE

The first on-line interfaces between a flow system and a CE system have already been demonstrated. The first interfaces were reported in 1997 by the groups of Karlberg and Fang [31]. In the following years, these interfaces have been applied to a wide variety of applications. S. Kulka [32] used an interface connecting the SIA with the CE unit which consisted of two T-pieces (see Fig. 6.A, red circle), where the capillary was inserted in one T-piece and a platinum electrode in the other. Z.L. Fang [33] developed another type of interface by using a horizontal splitting device (Fig. 6.B), which was applied to chiral separations. In both approaches, FIA was used for sample delivery and injecting the BGE. The sample introduction had to be performed by electrokinetic (EK) injection, as hydrodynamic (HD) injection proved to be difficult due to the constant flow generated by continuously working with peristaltic pumps. Another application dealt with the use of SWIA coupled to CE by using the same horizontal splitting device as shown in figure 6.C (red circle) [34]. In this work, multi-commutated SWIA was used for the determination of ascorbic acid in medicinal plants and food samples by CZE coupled to UV detection. Also, an electrokinetic injection was used to inject the sample for the same reason as mentioned above.

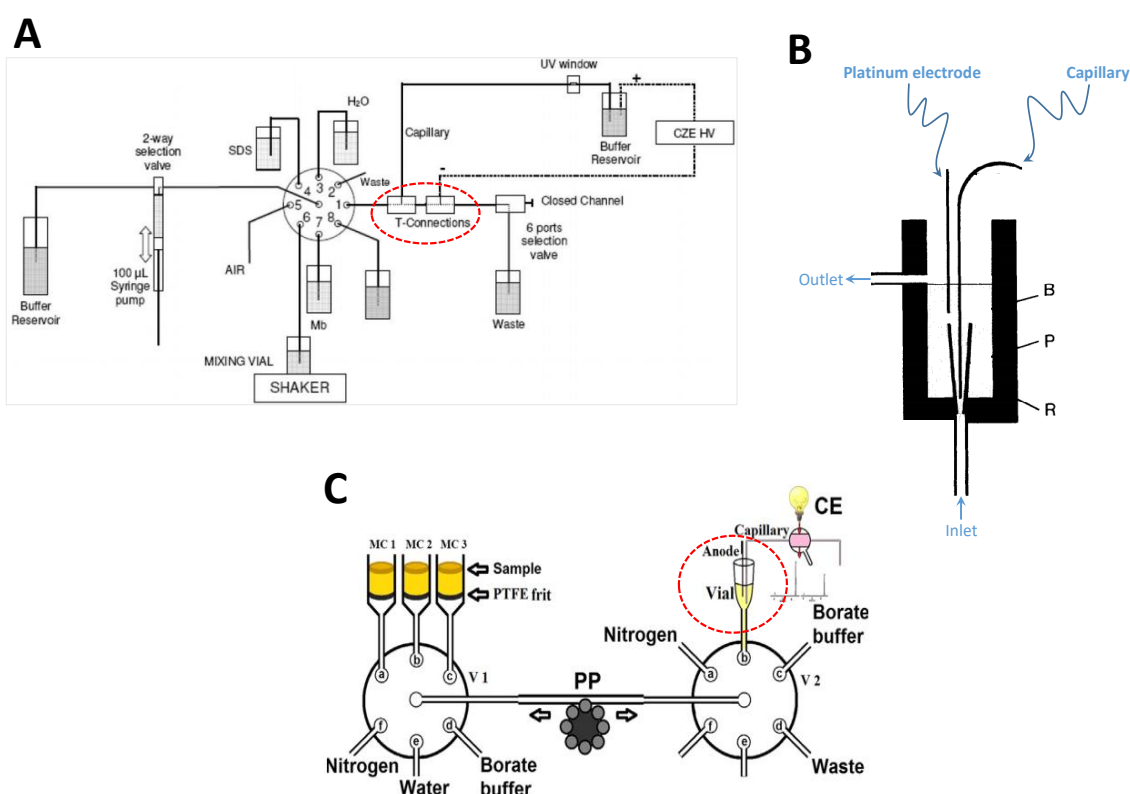


Figure 6: Different interfaces used to couple FIA, SIA and SWIA with CE.

1.1.2 Other strategies based on the use of robots and homemade devices

1.1.2.1 Robots

Robots in general are used to mimic the sample preparation scheme done by a technician. Their speed may be less than that of a technician, but, they are capable of achieving different operations such as liquid dispenser, automatic vortex mixer, barcode reader, centrifuge, SPE, tube dispenser, evaporation station, etc [35]. Nowadays, robots are widely used in life science automation due to their advantages, such as reducing manpower, ensuring uniformity, reducing risks to human operators, eliminating sample contamination and so on [36]. Fig. 7 shows some commercially available robots which differ in shape, price, protocol to apply and separation technique or detection mode used. Human-like dual-arm robots (shown in Fig. 7 at the right) draw much attraction in designing an automated sample preparation and measurement processes, because they can work in a very similar way to a human due to a structural similarity [37].



Figure 7: Some commercially available robots used for sample preparation

The integration of robots in analytical systems such as LC-MS is a challenging task since analytical systems are usually closed systems without any interfaces for automated sample delivery [38]. B. Streele [39] developed a determination of nifedipine and dehydronifedipine in human plasma by LC-MS. He used a SPE cartridges where the extraction of analytes was performed automatically by means of a sample processor equipped with a robotic arm. Also the work of Binnian Wei [40] who developed a high-

throughput robotic sample preparation system and LC-MS/MS for measuring urinary anatabine, anabasine, nicotine and major nicotine metabolites.

Also, sample preparation by robots was also coupled to CE analysis. The use of a robotic interface for sample treatment requires of an electronic interface and software to synchronize the movement of the robotic interface with the movement of autosampler [41]. B.M. Simonet [42] developed a FIA-CZE-UV methodology for the determination of myo-inositol phosphates in food samples. The FIA system was automatically coupled to CE equipment via a mechanical robotic arm. Also the work of C. Mardones [43] who developed a FIA-MEKC-UV methodology for the determination of chlorophenol in human urine by the use of a mechanical robotic arm. The use of robots in sample preparation is still growing and not yet universal. This may be related to the elevated price or the difficulty to switch from one protocol to another with the need to program every step.

I.1.2.2 Homemade devices

E. Fornells [44] developed an automated on-line extract evaporation procedure coupled to HPLC analysis in order to remove the organic solvent from sample extracts to increase the performance of reversed phase HPLC analysis. The online evaporation occurs inside a microfluidic channel confined with a hydrophobic gas-permeable membrane. Then, the sample is reconstituted and analyzed in milk samples by HPLC-UV and HPLC-MS/MS. Another example is the work of W. Liu [45] who developed a homemade SPME fiber coupled with GC-MS for trace analysis of antiestrogens (tamoxifen, cis- and trans-clomiphene) in biological matrices. Also, F. Maya [46] who developed a fully automated DLLME with integrated spectrophotometric detection inside a syringe (Lab in a Syringe concept). The organic droplets released during extraction accumulated at the head of the syringe, where two optical fibers are placed on both sides of the syringe, facing each other and enabling the in situ quantification of the extracted compounds as shown in Fig. 8. The proposed methodology has been characterized by the extraction of rhodamine B, which is suspected to be carcinogenic.

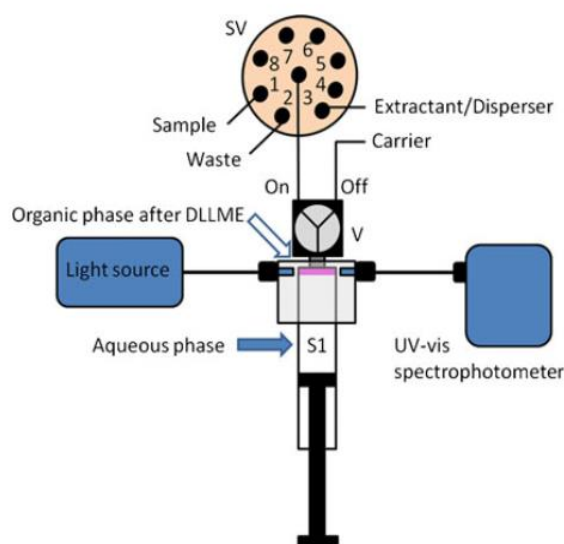


Figure 8: Schema representation of the developed system for in-syringe analysis [46]

Also, P. Kuban [47] who developed an on-line dialysis performed in a FIA system integrated with a CE system via a homemade specially designed interface for determination of small anions.

It was observed that these reported methods describe diverse sample preparation techniques based on homemade individuals' ideas. While all of the above-mentioned methods provide powerful analytical techniques with excellent performances, most of these, required sophisticated homemade modifications at the level of the instrumentation for analysis. This is not suitable for routine analysis like in our case the TDM of TKIs.

In the next section, a fully automated SALLE-CE-UV was developed for the analysis of TKIs without any modifications to the existing commercially available CE machine. The steps taken to optimize this methodology were discussed. This section represents a scientific paper accepted in *Talanta* journal.

References of section I

- [1] J. Růžička, E.H. Hansen, Flow injection analysis. principles, applications and trends, *Anal. Chim. Acta.* 114 (1980) 19–44.
- [2] M.S. Bloomfield, A sensitive and rapid assay for 4-aminophenol in paracetamol drug and tablet formulation, by flow injection analysis with spectrophotometric detection, *Talanta.* 58 (2002) 1301–1310.

-
- [3] P. Viñas, I.L. Garcia, J.A.M. Gil, Determination of thiol-containing drugs by chemiluminescence-flow injection analysis, *J. Pharm. Biomed. Anal.* 11 (1993) 15–20.
- [4] N.A. Mohamed, S. Ahmed, S.A. El Zohny, Rapid and sensitive online determination of some selective α 1-blockers by flow injection analysis with micelle-enhanced fluorescence detection, *J. Fluoresc.* 23 (2013) 1301–1311.
- [5] P.J. Keay, Y. Wang, Applications of flow injection analysis to analytical biotechnology, *Trends Biotechnol.* 15 (1997) 76–81.
- [6] R.D. Schmid, W. Künnecke, Flow injection analysis (FIA) based on enzymes or antibodies - applications in the life sciences, *J. Biotechnol.* 14 (1990) 3–31.
- [7] P. Akhtar, C.O. Too, G.G. Wallace, Detection of amino acids at conducting electroactive polymer modified electrodes using flow injection analysis. Part II. Use of microelectrodes, *Anal. Chim. Acta.* 339 (1997) 211–223.
- [8] K. Cammann, Flow injection analysis with electrochemical detection, *Fresenius J. Anal. Chem.* 329 (2004) 691–697.
- [9] M. Valcarcel, F. Lazaro, M.D. Luque de Castro, Individual and Simultaneous Determination of Ethanol and Acetaldehyde in Wines by Flow Injection Analysis and Immobilized Enzymes, *Anal. Chem.* 59 (1987) 1859–1863.
- [10] P. Chocholouš, P. Solich, D. Šatínský, An overview of sequential injection chromatography, *Anal. Chim. Acta.* 600 (2007) 129–135.
- [11] K. Dai, A.G. Vlessidis, N.P. Evmiridis, Dialysis membrane sampler for on-line flow injection analysis/chemiluminescence-detection of peroxynitrite in biological samples, *Talanta.* 59 (2003) 55–65.
- [12] M.F. El-Shahat, N. Burham, S.M.A. Azeem, Flow injection analysis-solid phase extraction (FIA-SPE) method for preconcentration and determination of trace amounts of penicillins using methylene

- blue grafted polyurethane foam, *J. Hazard. Mater.* 177 (2010) 1054–1060.
- [13] F.N. Arslan, H. Kara, Fully Automated Three-Dimensional Column-Switching SPE-FIA-HPLC System for the Characterization of Lipids by a Single Injection: Part I. Instrumental Design and Chemometric Approach to Assess the Effect of Experimental Settings on the Response of ELSD, *JAOCS, J. Am. Oil Chem. Soc.* 93 (2016) 11–26.
- [14] F. Cañete, A. Ríos, M.D. Luque de Castro, M. Valcárcel, Liquid—Liquid Extraction in Continuous Flow Systems Without Phase Separation, *Anal. Chem.* 60 (1988) 2354–2357.
- [15] R. Segarra Guerrero, S. Sagrado Vives, J. Martínez Calatayud, Fluorimetric determination of captopril by flow injection analysis, *Top. Catal.* 43 (1991) 176–180.
- [16] M.C. Sanfeliu Alonso, L. Lahuerta Zamora, J. Martínez Calatayud, Flow-injection with chemiluminescence detection for the determination of iproniazid, *Anal. Chim. Acta.* 437 (2001) 225–231.
- [17] F.E.O. Suliman, S.M. Sultan, Sequential injection technique employed for stoichiometric studies, optimization and quantitative determination of some fluoroquinolone antibiotics complexed with iron(III) in sulfuric acid media, *Talanta.* 43 (1996) 559–568.
- [18] A. V. Mozhukhin, A.L. Moskvina, L.N. Moskvina, Stepwise injection analysis as a new method of flow analysis, *J. Anal. Chem.* 62 (2007) 475–478.
- [19] K. Medinskaia, C. Vakh, D. Aseeva, V. Andruch, L. Moskvina, A. Bulatov, A fully automated effervescence assisted dispersive liquid-liquid microextraction based on a stepwise injection system. Determination of antipyrine in saliva samples, *Anal. Chim. Acta.* 902 (2016) 129–134.
- [20] I. Timofeeva, K. Medinskaia, L. Nikolaeva, D. Kirsanov, A. Bulatov, Stepwise injection potentiometric determination of caffeine in saliva using single-drop microextraction combined with solvent exchange, *Talanta.* 150 (2016) 655–660.
- [21] C.I.C. Silvestre, J.L.M. Santos, J.L.F.C. Lima, E.A.G. Zagatto, Liquid-liquid extraction in flow

- analysis: A critical review, *Anal. Chim. Acta.* 652 (2009) 54–65.
- [22] T. Blanco, N. Maniasso, M.F. Giné, A.O. Jacintho, Liquid-liquid extraction in flow injection analysis using an open-phase separator for the spectrophotometric determination of copper in plant digests, *Analyst.* 123 (1998) 191–193.
- [23] N. Kasthurikrishnan, J.A. Koropchak, Flow Injection Donnan Dialysis Preconcentration of Trace Metal Cations for Inductively Coupled Plasma Atomic Emission Spectrometry, *Anal. Chem.* 65 (1993) 857–862.
- [24] A. Tolokán, I. Klebovich, K. Balogh-Nemes, G. Horvai, Automated determination of levodopa and carbidopa in plasma by high-performance liquid chromatography-electrochemical detection using an on-line flow injection analysis sample pretreatment unit, *J. Chromatogr. B Biomed. Appl.* 698 (1997) 201–207.
- [25] Z. Legnerová, D. Šatínský, P. Solich, Using on-line solid phase extraction for simultaneous determination of ascorbic acid and rutin trihydrate by sequential injection analysis, *Anal. Chim. Acta.* 497 (2003) 165–174.
- [26] J. Riber, C. De La Fuente, M.D. Vazquez, M.L. Tascón, P. Sánchez Batanero, Electrochemical study of antioxidants at a polypyrrole electrode modified by a nickel phthalocyanine complex. Application to their HPLC separation and to their FIA system detections, *Talanta.* 52 (2000) 241–252.
- [27] A.W. Jaworski, C.Y. Lee, Fractionation and HPLC Determination of Grape Phenolics, *J. Agric. Food Chem.* 35 (1987) 257–259.
- [28] J. Vichapong, R. Burakham, S. Srijaranai, K. Grudpan, Sequential injection-bead injection-lab-on-valve coupled to high-performance liquid chromatography for online renewable micro-solid-phase extraction of carbamate residues in food and environmental samples, *J. Sep. Sci.* 34 (2011) 1574–1581.

- [29] R.B.R. Mesquita, A.O.S.S. Rangel, A review on sequential injection methods for water analysis, *Anal. Chim. Acta.* 648 (2009) 7–22.
- [30] D. Šatínský, J. Huclová, P. Solich, R. Karlíček, Reversed-phase porous silica rods, an alternative approach to high-performance liquid chromatographic separation using the sequential injection chromatography technique, *J. Chromatogr. A.* 1015 (2003) 239–244.
- [31] H.-W. Chen, Z.-L. Fang, Combination of flow injection with capillary electrophoresis. Part 3. On-line sorption column preconcentration capillary electrophoresis system, *Anal. Chim. Acta.* 355 (1997) 135–143.
- [32] S. Kulka, G. Quintás, B. Lendl, Automated sample preparation and analysis using a sequential-injection- capillary electrophoresis (SI-CE) interface, *Analyst.* 131 (2006) 739–744.
- [33] Z.L. Fang, Z.S. Liu, Q. Shen, Combination of flow injection with capillary electrophoresis. Part I. The basic system, *Anal. Chim. Acta.* 346 (1997) 135–143.
- [34] M.T. Falkova, A. V. Bulatov, M.O. Pushina, A.A. Ekimov, G.M. Alekseeva, L.N. Moskvin, Multicommutated stepwise injection determination of ascorbic acid in medicinal plants and food samples by capillary zone electrophoresis ultraviolet detection, *Talanta.* 133 (2015) 82–87.
- [35] J.R. Strimaitis, Robots in the laboratory: Part II. An overview, *J. Chem. Educ.* 67 (1990) A20.
- [36] R. Bogue, Robots in the laboratory: A review of applications, *Ind. Rob.* 39 (2012) 113–119.
- [37] H. Fleischer, R.R. Drews, J. Janson, B.R. Chinna Patlolla, X. Chu, M. Klos, K. Thurow, Application of a Dual-Arm Robot in Complex Sample Preparation and Measurement Processes, *J. Lab. Autom.* 21 (2016) 671–681.
- [38] L.H. Cohen, Surrendering to the robot army: Why we resist automation in drug discovery and development, *Bioanalysis.* 4 (2012) 985–987.
- [39] B. Streel, C. Zimmer, R. Sibenaler, A. Ceccato, Simultaneous determination of nifedipine and dehydronifedipine in human plasma by liquid chromatography/tandem mass spectrometry, *J.*

- Chromatogr. B Biomed. Appl. 720 (1998) 119–128.
- [40] B. Wei, J. Feng, I.J. Rehmani, S. Miller, J.E. McGuffey, B.C. Blount, L. Wang, A high-throughput robotic sample preparation system and HPLC-MS/MS for measuring urinary anatabine, anabasine, nicotine and major nicotine metabolites., *Clin. Chim. Acta.* 436 (2014) 290–7.
- [41] M. Valcárcel, M. Gallego, A. Ríos, Coupling continuous flow systems to instruments based on discrete sample introduction, *Fresenius. J. Anal. Chem.* 362 (1998) 58–66.
- [42] B.M. Simonet, A. Ríos, F. Grases, M. Valcárcel, Determination of myo-inositol phosphates in food samples by flow injection-capillary zone electrophoresis, *Electrophoresis.* 24 (2003) 2092–2098.
- [43] C. Mardones, A. Ríos, M. Valcárcel, Determination of chlorophenols in human urine based on the integration of on-line automated clean-up and preconcentration unit with micellar electrokinetic chromatography, *Electrophoresis.* 20 (1999) 2922–2929.
- [44] E. Fornells, E.F. Hilder, R.A. Shellie, M.C. Breadmore, On-line solvent exchange system: Automation from extraction to analysis, *Anal. Chim. Acta.* 1047 (2019) 231–237.
- [45] W. Liu, L. Zhang, S. Chen, H. Duan, X. Chen, Z. Wei, G. Chen, A method by homemade OH/TSO-PMHS fibre solid-phase microextraction coupling with gas chromatography-mass spectrometry for analysis of antiestrogens in biological matrices, *Anal. Chim. Acta.* 631 (2009) 47–53.
- [46] F. Maya, B. Horstkotte, J.M. Estela, V. Cerdà, Lab in a syringe: Fully automated dispersive liquid-liquid microextraction with integrated spectrophotometric detection, *Anal. Bioanal. Chem.* 404 (2012) 909–917.
- [47] P. Kuban, B. Karlberg, On-Line Dialysis Coupled to a Capillary Electrophoresis System for Determination of Small Anions, *Anal. Chem.* 69 (1997) 1169–1173.

Section II

A fully automated on-line salting-out assisted liquid-liquid extraction capillary electrophoresis methodology: Application to tyrosine kinase inhibitors in human plasma

Omar S. Ahmed^{1,3}, Yoann Ladner¹, Junyi Xia¹, Jérôme Montels¹, Laurent Philibert², Catherine Perrin¹

¹Institut des Biomolécules Max Mousseron (IBMM), UMR 5247-CNRS-UM-ENSCM, Montpellier, France.

²Institut régional du Cancer de Montpellier (ICM), Département de Pharmacie et Pharmacologie, Montpellier, France.

³Department of Analytical Chemistry, Faculty of Pharmacy, Misr University of Science and Technology (MUST). Al-Motamayez District, 6th of October City, P.O.Box: 77, Egypt.

Research article accepted in

Talanta

Talanta. (2019) 120391.

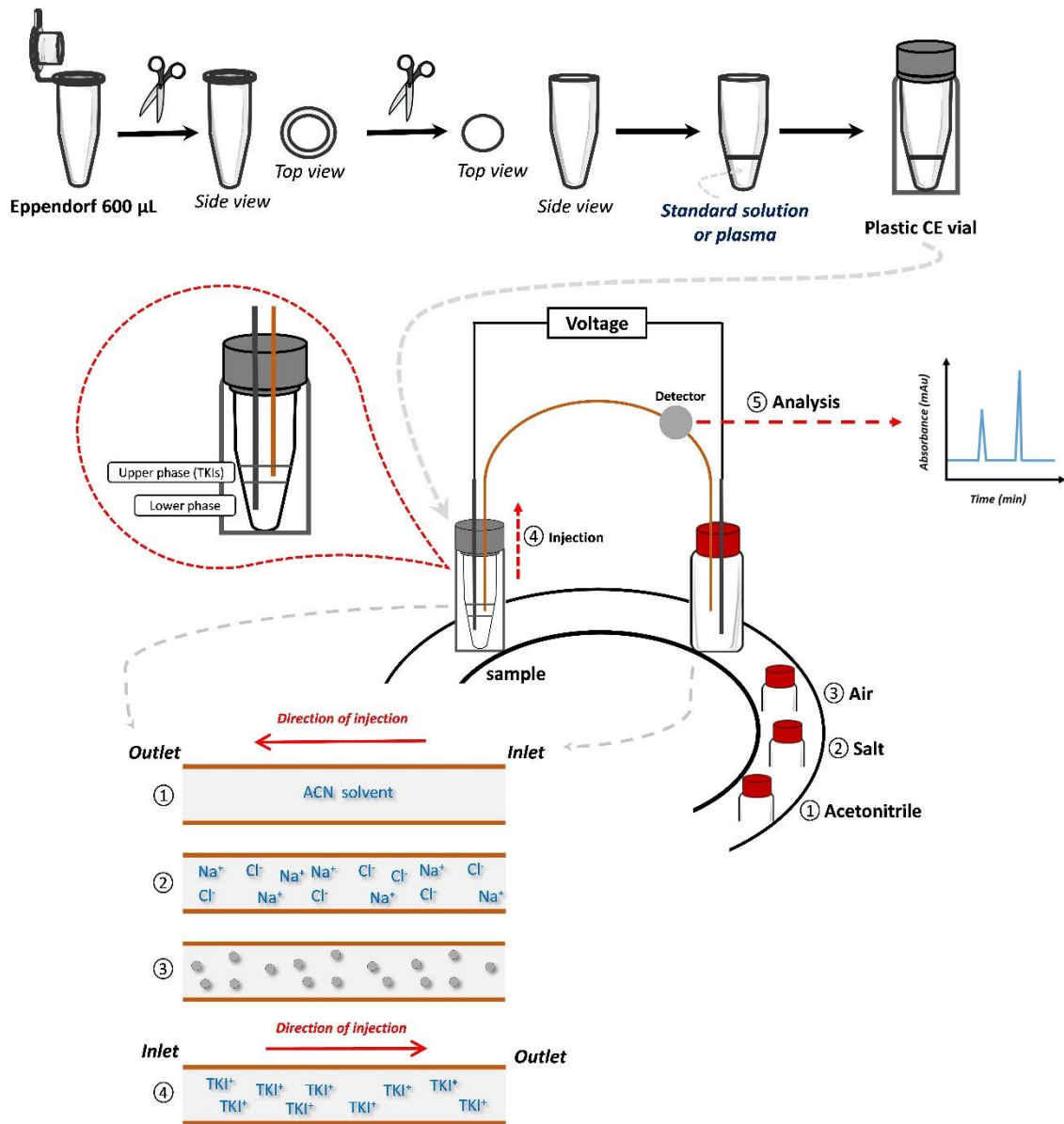
Keywords:

Automated sample preparation, desalting, in-line CE stacking, protein precipitation, tyrosine kinase inhibitors (TKIs), salting-out assisted liquid-liquid extraction (SALLE).

Highlights:

- Automated salting-out assisted liquid-liquid extraction coupled with CE-UV analysis (A-SALLE-CE-UV)
- Injected sample volume up to 70% of the capillary effective length
- In-line stacking
- A-SALLE-CE-UV analysis of tyrosine kinase inhibitors in human plasma samples

Graphical abstract



Abstract

A fully automated analytical methodology combining salting-out assisted liquid-liquid extraction (SALLE) and capillary electrophoresis (CE) for the analysis of three Tyrosine Kinase Inhibitors (TKIs) in plasma samples is proposed. The automated methodology, called A-SALLE-CE-UV, makes full use of the advantages of both techniques by combining desalting, protein precipitation, automated liquid-liquid extraction, in-line CE stacking and electrophoretic separation of analytes in plasma samples in a fully integrated way. At first, the capillary is used to deliver appropriate micro-volumes of extraction agent solutions (acetonitrile, salt) in the plasma sample. ACN and salting-out agent (NaCl) solutions are added by pressure from outlet vials into the sample vial (inlet) containing human plasma sample spiked with the three tested TKIs. After addition of both ACN and NaCl solutions, mixing is achieved by generating air bubbles leading to a two phases separation and extraction of TKIs in the upper mostly organic phase (ACN). The upper phase containing the TKIs is then injected and analyzed by CE-UV. Due to the presence of ACN, the analytes are stacked in-line and successfully separated in the same capillary. The results obtained in terms of limit of detection (LOD), limit of quantification (LOQ), sensitivity enhancement factor (SEF), repeatability and linearity demonstrate the applicability of the proposed method for possible therapeutic drug monitoring (TDM) of TKIs.

1. Introduction

Capillary electrophoresis (CE) is a separation technique extensively used for the analysis of a wide range of drugs in biological matrices such as plasma [1]. However, the presence of interfering compounds (e.g. protein, salts) in the sample can affect the analytical performances of CE methodologies causing peak broadening, baseline distortion and a lack of specificity [2]. Therefore, sample preparation techniques such as liquid–liquid extraction (LLE) and solid-phase extraction (SPE) are frequently used prior to CE analysis to remove proteins, desalt, concentrate the analytes of interest and obtain efficient electrophoretic peaks [3,4]. However, these methods are based on the use of complex, long procedure and expensive sample preparation protocols (multi-steps) which are not suitable for routine analysis. In the last decade, several improvements of extraction techniques have been reported to address these problems, such as the development of solid phase microextraction (SPME) and liquid phase microextraction (LPME) techniques [5,6]. More recently, new LLE technique based on salting-out assisted liquid–liquid extraction appeared to be well suited for the determination of drugs in plasma samples as it allows desalting, deproteinization and extraction of analytes in the same procedure [7]. SALLE is based on the addition of salts (e.g. sodium chloride (NaCl)) into a sample solution composed of a miscible mixture of water and an organic solvent (such as acetonitrile (ACN)), inducing a two phases separation (organic phase from bulk aqueous phase) [8]. SALLE can be easily coupled with CE technique (SALLE-CE-UV) since the high content of ACN in the upper phase allows the in-line CE stacking of the analytes in the capillary even for injected sample volumes exceeding 80% of the capillary volume till the detector window. Excellent peak efficiencies, good resolution and high sensitivity were obtained with SALLE-CE-UV methodology for the analysis of drugs in plasma [7].

Since a few years, analytical strategies tend towards automation and on-line combination of sample preparation procedures with separation systems such as liquid chromatography (LC), gas chromatography (GC) and CE [9–11]. Indeed, automation offers many advantages including lab efficiency, reduced human errors and lower operating cost per sample. Many works dealt with the automation of LPME techniques including single drop microextraction [12,13], dispersive liquid-liquid microextraction [9,14–17] and hollow fiber-based microextraction [18–20]. However, only two reports mention the automation of SALLE. The first one is based on the oxidation of diclofenac with potassium ferricyanide in an alkaline medium, was followed by the separation of the ACN phase from the homogeneous sample solution, the simultaneous extraction of the derivative and in-line organic-phase detection by an optical probe [21]. The second work is based on the aspiration of 1-octylamine, urine sample solution containing tetracycline

and salting-out agent solution (NaCl) into a mixing chamber of a flow system followed by air bubbles mixing, resulting in isotropic solution formation [11]. After phase separation, the micellar 1-octylamine phase containing analyte is mixed with methanol and analysed by a LC-UV. Both methods require special technical modifications of analytical materials and the use of additional instruments such as external syringe or peristaltic pumps, multi-port selection valves and cone-shaped glass. This include homemade modifications, which are difficult to realize, making them not suitable for routine analysis.

Herein, we describe the first demonstration of a fully automated SALLE capillary electrophoresis (CE)-UV methodology, called A-SALLE-CE-UV. The applicability of the proposed A-SALLE-CE-UV methodology was evaluated for the analysis of 3 tyrosine kinase inhibitors (TKIs) namely lapatinib ditosylate, erlotinib hydrochloride and sorafenib in human plasma samples as proof-of-concept analytes. These basic molecules are extensively used for the treatment of malignant tumors such as renal cell carcinoma, lung cancer and breast cancer [22–24]. Different factors including the effects of filling schemes of the sample vial by several solutions (ACN, salt), time/volume of mixing using air bubbles and the type of salting-out agents on the performance of A-SALLE-CE-UV methodology were optimized. Several analytical performances such as the limit of detection (LOD), the limit of quantification (LOQ), sensitivity enhancement factor (SEF), repeatability, and linearity were determined.

2. Experimental:

2.1. Chemicals and reagents:

All reagents were of analytical grade and used as received without further purification. Acetonitrile (ACN, purity $\geq 99.9\%$) was from Honeywell Riedel de Haen (Seelze, Germany). 6-amino caproic acid (purity $\geq 99\%$) was from Acros organics (Geel, Belgium). Ammonium acetate (purity $\geq 99\%$), potassium chloride (KCl, purity $\geq 99\%$), sodium chloride (NaCl, purity $\geq 99.5\%$), sodium hydroxide (NaOH, purity $\geq 99\%$), citric acid (purity $\geq 99\%$), dimethylsulfoxide (DMSO) were purchased from Sigma Aldrich (Saint-Quentin-Fallavie, France). Sorafenib (purity $\geq 99\%$), erlotinib hydrochloride (purity $\geq 99\%$) and lapatinib ditosylate (purity $\geq 99\%$) were purchased from Molekula (Munich, Germany).

2.2. Apparatus and CE software:

All CE separations were carried out using a Beckman P/ACE-MDQ instrument (Fullerton, USA) equipped with a UV detection system. 600 μL eppendorf tubes (Thermoscientific, Pittsburgh, USA) used as mixing chamber between plasma sample, ACN and NaCl stock solution. The eppendorf containing the solutions was placed in a plastic 2 ml vial (P/ACETM MDQ, reference number 970657, France) covered with plastic cap (P/ACETM MDQ, reference number 144656, grey, France). The cap and the crown of the eppendorf

tube was cut to be adjusted in the CE plastic vial (see [Figure 1S in supplementary information](#)). 2 ml glass vials (P/ACETM MDQ, reference number 358807, France) covered with vial caps (P/ACETM MDQ, reference number 144648, red, France) were filled with other solutions. Data were acquired by 32 Karat software (Version 8.0, Beckman Coulter, Fullerton, USA). Uncoated fused-silica capillaries (50 μm ID) were obtained from Polymicro Technologies (Phoenix, USA). The length of the capillary was 31 cm (21 cm effective length to the detector).

2.3. Preparation of background electrolyte and stock solutions:

The background electrolyte (BGE) was chosen based on our previous studies [7,25] and was a mixture of citric acid (1800 mM) and 6-amino caproic acid (137 mM) at pH 2.0 and ionic strength (IS) 150 mM. BGE composition with the desired IS and pH was calculated with the software "Peakmaster" 5.3 (Prague, Czech Republic, <https://web.natur.cuni.cz/~gas/>). Stock solutions of erlotinib hydrochloride, sorafenib and lapatinib ditosylate were prepared in DMSO solvent at the concentration of 1.0 g/L due to their low solubility in water. NaCl, ammonium acetate and KCl solutions were prepared at a concentration of 25% (m/v) in water. All stock samples were stored frozen at -20°C . All other solutions were stored in refrigerator at 4°C .

2.4. Samples preparation

- Standard sample solution: relevant volumes of distilled water and the three TKIs stock solutions were mixed in an eppendorf tube of 600 μL to obtain a final volume of 80 μL . Then, the eppendorf tube containing the standard solution was placed in the CE plastic vials.
- Plasma sample solution: relevant volumes of plasma solution and the three TKIs stock solutions were mixed in an eppendorf tube of 600 μL to obtain a final volume of 80 μL . Then, the spiked plasma was mixed during 1 hour at room temperature. Then, the eppendorf tube containing the spiked plasma solution was placed in the CE plastic vials.

2.5. The A-SALLE-CE-UV procedure:

New capillaries were pre-conditioned with 1.0 M NaOH for 3.0 min under 20 psi followed by distilled water for 3.0 min under 20 psi. Then, the capillary was flushed with BGE for 5.0 min under 20 psi. The A-SALLE-CE-UV procedure ([Fig. 1](#)) consisted of a commercially available CE apparatus, a silica capillary and a 600 μL tube containing the standard or the plasma sample placed in a plastic vial (mixing chamber). At first, the capillary was used as a tool to deliver 150 μL of ACN and 20 μL of NaCl from outlet vials to the inlet vial holding the 600 μL tube filled with 80 μL of sample containing TKIs (60 psi pressure, reverse mode) were applied (see [video 1 in the supplementary information](#)). This was followed by a mixing step using air

bubbles at 90 psi during 5.0 minutes (see video 2 in the supplementary information) leading to two phases separation and extraction of TKIs in the upper phase. The capillary was rinsed with water (60 psi during 2.0 minutes) between each addition of liquids (sample, NaCl solution and ACN) in the 600 μ L tube and dried with air (30 psi during 1.0 minutes), to start each filling of the sample vial from a cleaned and empty capillary. This rinsing procedure was optimized to ensure that NaCl solution doesn't get in contact with ACN to avoid any precipitation of NaCl inside the capillary. Then, the upper phase containing TKIs was hydrodynamically injected (forward mode) in the capillary at 0.8 psi during 94 seconds to obtain an injection volume equivalent to 287 nL (70% of the capillary effective length). All separations were carried out with an applied voltage of 15 kV. The capillary was thermostated at 25°C. The capillary usage life was between 45 to 50 analysis. UV detection was performed at 254 nm. The detailed A-SALLE-CE-UV methodology is mentioned in Table 15 in supplementary information. Corrected peak areas were calculated by dividing each peak area by its corresponding migration time.

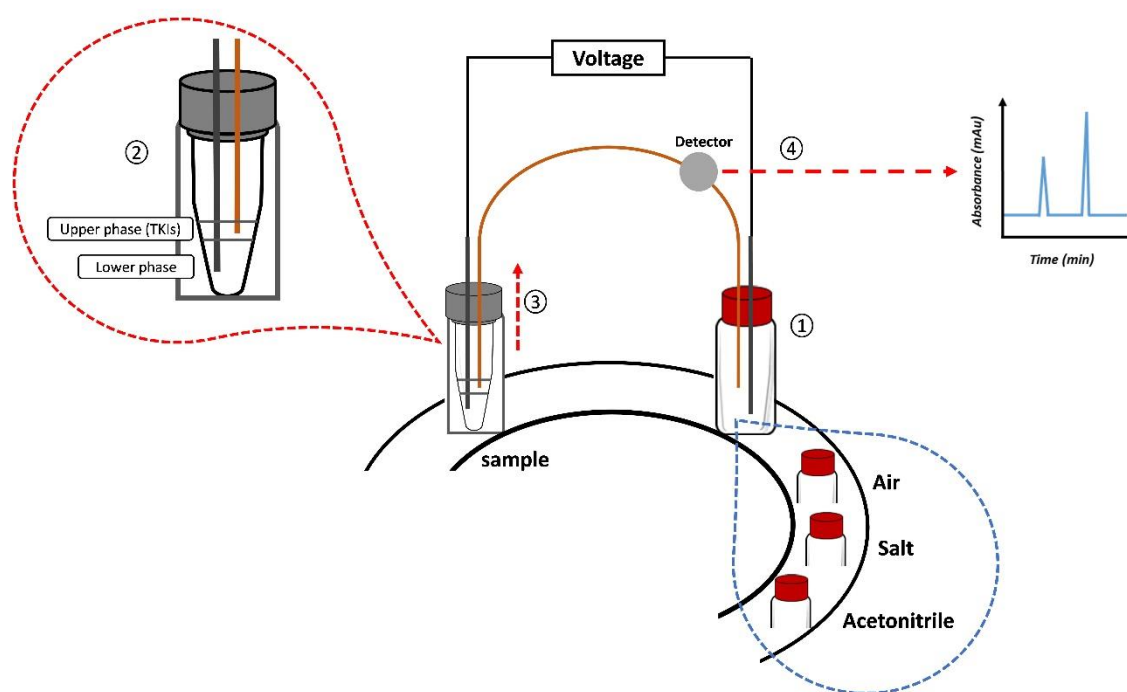


Figure 1: A-SALLE-CE-UV procedure. Step (1) delivering of appropriate micro-volumes of solutions (ACN and NaCl stock solution) from outlet side to the inlet side (sample vial) by hydrodynamic injection in inverse mode. Followed by mixing by air bubbles injected from an empty vial (hydrodynamic injection in inverse mode). Step (2) after mixing, separation into 2 phases (upper mostly organic phase from bulk mostly aqueous phase) occurred. Step (3) hydrodynamic injection of the upper mostly organic phase (hydrodynamic injection, forward mode). Step (4) Separation and detection of the three TKIs by CE-UV.

3. Results and discussion

Automation and on-line combination of sample preparation with analytical separation techniques fit perfectly with the criteria required for analytical methods dedicated to routine analysis such as therapeutic drug monitoring (TDM): simple, fast and cost-effective. TDM of TKIs is required to evaluate the relation between dose and efficacy/toxicity of TKIs. As mentioned before, SALLE applies the salting out effect to separate water-miscible organic solvent such as ACN from aqueous/biological sample. The separation will result in two phases: upper mostly organic and lower mostly aqueous. SALLE-CE-UV methodology offers a number of features for the analysis of TKIs in human plasma including high separation ability between TKIs, applicability to saline sample matrix, easy operational procedure, low consumption of organic solvent, and environmental benignity.

3.1. Preliminary Trials

According to our previous work [7], SALLE methodology based on a ratio of 60/40 (v/v) ACN/sample in the presence of 2% (m/v) of NaCl gives the best compromise to obtain an efficient plasma protein precipitation, a good separation of the two phases and a moderate dilution of the samples. Moreover, a BGE composed of a mixture of 6-amino caproic acid and citric acid at pH of 2.0 with ionic strength (IS) of 150 mM allows an efficient electrophoretic separation of the TKIs. Therefore, these SALLE-CE-UV conditions were used for the automation of the overall procedure of the A-SALLE-CE-UV methodology. The first experimental investigations were realized to check if it was possible to 1/ obtain a two phases separation, 2/ successfully extract the TKIs in the upper (mostly CAN) phase and 3/ separate the TKIs in an automated manner. Three TKIs (Fig. 2) were chosen as proof-of-concept analytes.

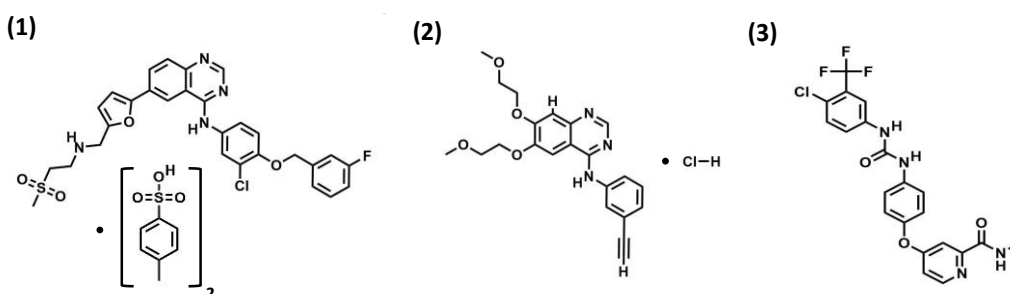


Figure 2: Molecular structures of (1) lapatinib ditosylate, (2) erlotinib hydrochloride and (3) sorafenib.

The length of the capillary was adjusted to be immersed only in the upper phase (mostly organic) of the sample after SALLE extraction. The adjustment of the capillary length passed through several steps. At first, two samples were prepared by SALLE (manually) and by A-SALLE. In order to visualize properly the two phases separation, methyl red indicator was added (Fig. 2S, supplementary results). Estimated heights

of the upper phase of both manually and automatically prepared samples was verified to be the same. Accordingly, the length of the capillary inlet was optimized and measured to be immersed only in the upper phase ($L_{\text{tot}} = 31$ cm, $L_{\text{eff}} = 21$ cm). Both ends of the capillary were set at the same level to avoid siphoning effect that would affect the robustness of the proposed methodology. The filling scheme of the sample vial with the different extraction solutions (ACN, salt stock solution) allowing to automate the extraction procedure can be resumed as following: ACN/NaCl/air. ACN and NaCl stock solution were successively added from outlet vials (hydrodynamic injection, reverse mode) to the sample vial containing 160 μL of TKIs at 5 $\mu\text{g}/\text{mL}$ at 80 psi during 8.5 min (300 μL) and at 80 psi during 3.5 min (40 μL) respectively. The final volume was fixed at 500 μL for preliminary trials. Mixing of the different solutions was done by generating air bubbles from an empty outlet vial at 80 psi during 5 min. After this step, a two phases separation was observed in the inlet vial confirming the possibility to automate SALLE technique. The upper mostly organic phase was then injected. An electrophoretic separation between the 3 TKIs was obtained. Maximum upper phase injected volume was 10% of the capillary effective length (Fig. 3).

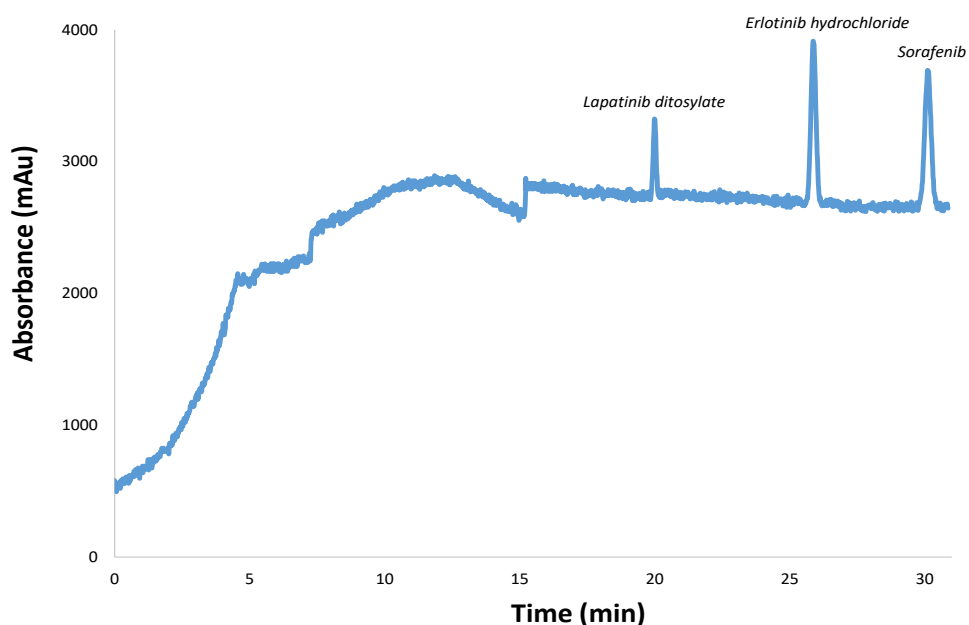


Figure 3: Electropherogram of the 3 TKIs obtained from blank sample (no TKIs) and human plasma samples using A-SALLE-CE-UV procedure. Analysis conditions: silica capillary 50 μm i.d., total length 31 cm, effective length 21 cm. BGE: citric acid – ϵ -aminocaproic acid buffer IS 150 mM pH 2.0. Temperature: 25°C. Separation voltage: 15 kV. Sample injection volume: 39 nl (corresponding to 10% of the capillary effective length). Detection: 254 nm.

This was less than what was obtained by manual preparation (80 % of the capillary effective length for SALLE-CE-UV methodology [7]). This could be attributed to the difference in composition of the obtained upper phases by automated and by manual methodologies in terms of ACN, NaCl and water. Moreover,

extraction efficiencies (%) and sensitivity enhancement factors (SEF) of the 3 TKIs obtained by A-SALLE-CE-UV methodology were four and ten times less than those obtained by manual SALLE-CE-UV methodology (98 – 100 % for extraction efficiencies, 144-265 for SEF), respectively. This lack of performance was mainly attributed to an insufficient mixing of ACN, NaCl and sample solutions in the inlet vial affecting both extraction efficiency (%) and sensitivity. However, similar electrophoretic profiles were obtained from A-SALLE-CE-UV and manual methodology in terms of migration times. Good repeatability ($n = 3$) were obtained for the 3 TKIs with RSD of less than 0.7% and of less than 3.6% for migration times and corrected peak areas respectively, confirming the feasibility of combining SALLE preparation procedure with CE separation in an automated manner. Nevertheless, further optimizations were required to improve the efficiency of the A-SALLE-CE-UV methodology.

3.2. Optimization of the mixing efficiency of standard sample solution with ACN and NaCl

The first step in the optimization of the automated extraction procedure was to adjust both filling pressure and time to obtain accurate volumes of both ACN/NaCl solution to the standard sample contained in a 600 μL tube (mixing chamber). Five different pressures ranging from 5 to 80 psi were evaluated with a fixed filling time of 6 min. The mean added volume ($n=3$) of ACN or NaCl (V_x) to the sample was calculated based on mass differences ($V_x \text{ (ml)} = (m_{\text{filled}} - m_{\text{empty}})/\rho$), where m_{filled} is the mass (g) of the 600 μL eppendorf tube filled with ACN solvent or NaCl solution, m_{empty} is the mass (g) of the empty 600 μL eppendorf tube and ρ is the density of the ACN solvent (0.79) or aqueous NaCl solution (1). The mean volumes of both ACN and NaCl increased linearly (correlation coefficient (r^2) higher than 0.999) from 4 to 317 μL with good repeatability (RSD < 1.53 %, $n = 3$) for the different tested pressures (Fig. 4A and B). Hydrodynamic pressure of 60 psi was chosen as the optimal pressure as it gave the best compromise between low RSD (less than 0.63 %, $n=3$) and rapidity of filling the vials. The same procedure was repeated varying the filling time from 1 to 8 minutes with fixed 60 psi pressure. Mean volumes of both ACN and NaCl increased linearly from 8 to 293 nL ($r^2 > 0.999$) for the different filling times (Fig. 4C and D) with high repeatability (RSD < 0.63 %, $n = 3$) whatever the injection time applied.

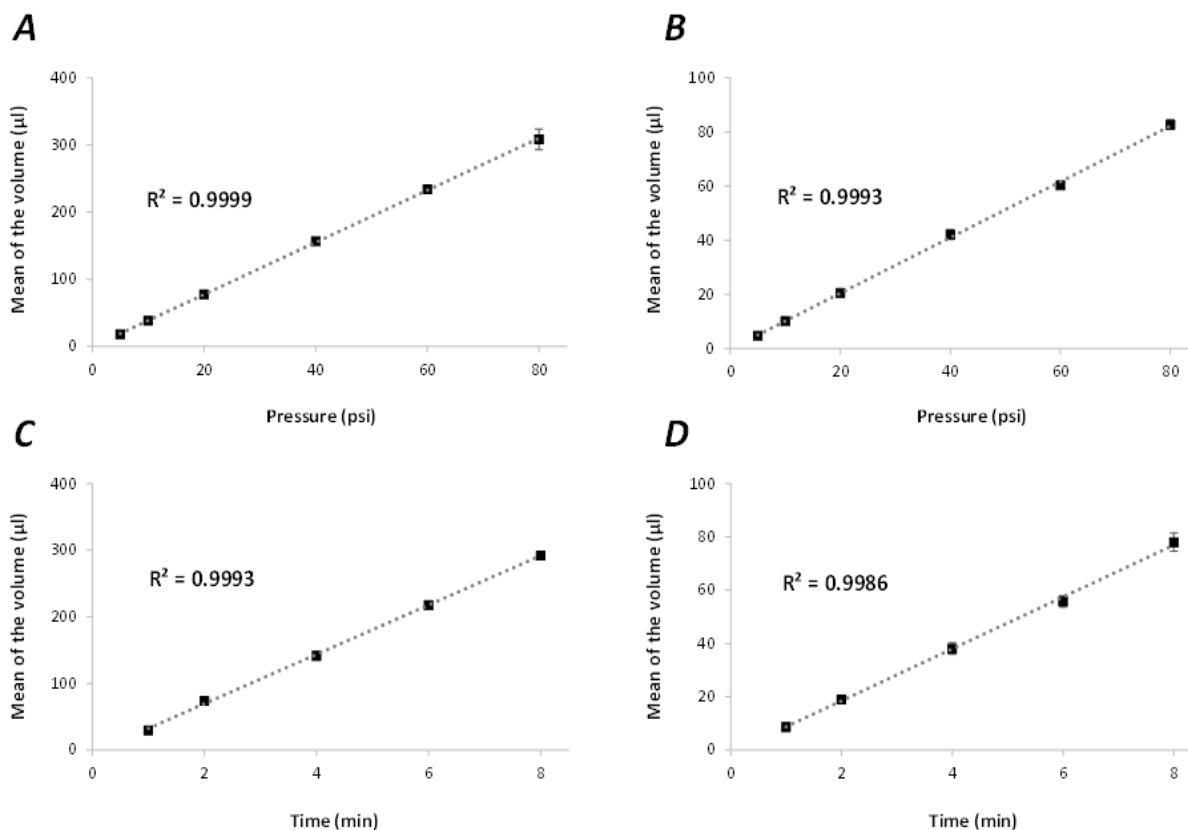


Figure 4: Effect of increasing the hydrodynamic pressure during 6 minutes on the volume obtained of (A) ACN and (B) NaCl. Effect of increasing the time at 60 psi on the volume obtained of (C) ACN and (D) NaCl.

The second step to ameliorate the mixing efficiency was to decrease the sample, ACN and NaCl volumes introduced in the 600 μL eppendorf tube. Indeed, more than 83 % (500 μL) of the 600 μL eppendorf tube was filled with solutions. Consequently, a loss of solutions and a lack of mixing efficiency could occur during the mixing step with air bubbles affecting the repeatability and the performance of the A-SALLE-CE-UV methodology. Moreover, decreasing the solution volumes helps to reduce the time needed to fill the inlet vial. Therefore, the volumes of sample, ACN and NaCl were divided by a factor of 2 and the total volume was fixed at 250 μL. NaCl and ACN were added to the standard samples at 60 psi during 2.4 (20 μL) and 4.0 minutes (150 μL), respectively. The pressure applied for the mixing by air bubbles was increased to 90 psi during 5 min without risk of loss of sample. Improvements in the injected sample volume (up to 40%), SEF (up to 125) and extraction efficiencies (up to 45%) for the 3 TKIs were observed confirming the benefit of decreasing ACN, NaCl and sample volumes besides increasing the air pressure used for mixing.

The third step in the optimization of the extraction procedure, was to modify the filling scheme of the sample vial by ACN and NaCl. Instead of adding the entire volume of these solutions to the standard sample at once as previously described, NaCl and ACN solutions were added to the sample in 2 steps each to obtain total added volumes of 20 and 150 μL , respectively. So, 75 μL of ACN and 10 μL of NaCl were successively added to the standard sample solution at 60 psi during 2.0 minutes and at 60 psi during 1.2 minutes, respectively. Mixing by air bubbles at 90 psi during 2.0 minutes was performed after the first addition of ACN and salt, and repeated after the next addition of ACN. After the second NaCl solution addition, a final mixing was realized at 90 psi during 5.0 minutes after addition all solutions ($V_{\text{total}} = 250 \mu\text{L}$). The filling scheme of sample vial can be resumed as following: ACN/NaCl/air/ACN/air/NaCl/air. The injected volume of the upper phase could be successfully increased to 287 nl (corresponding to 70% of the capillary effective length) without peak broadening due to in-line acetonitrile CE stacking increasing the sensitivity of the A-SALLE-CE-UV methodology (Fig. 5).

Moreover, TKIs were efficiently extracted (60–62% of extraction efficiency) in the upper phase. The injection was repeated three times. RSD ranging from 0.85 to 1.12 % for migration times and from 1.40 to 2.40 % for peak areas were obtained. SEF factors of 94.1, 134.1 and 196.3 were obtained for lapatinib, erlotinib and sorafenib, respectively. All results indicate an improvement of the analytical performances of the proposed A-SALLE-CE-UV methodology due to better mixing efficiency. However, the values obtained in term of extraction efficiency (%) and SEF were about 1.6 times less important than with SALLE-CE-UV (98 – 100 % for extraction efficiencies, 144-265 for SEF factors). The mixing generated by a stirrer and a centrifugator in the case of manual SALLE-CE-UV is more efficient than with air bubbles for A-SALLE-CE-UV. Other developments (time and pressure of mixing, volume and shape of the mixing chamber) were realized without technical modifications at the level of the commercially available CE apparatus but didn't give significant improvements. Even though, the performances of the proposed A-SALLE-CE-UV methodology are sufficient to quantify TKIs in human plasma (see 3.4). Consequently, these conditions were defined as being the optimal A-SALLE-CE-UV procedure (see section 2.5; Table 1S in supplementary information) and were applied in the rest of this study.

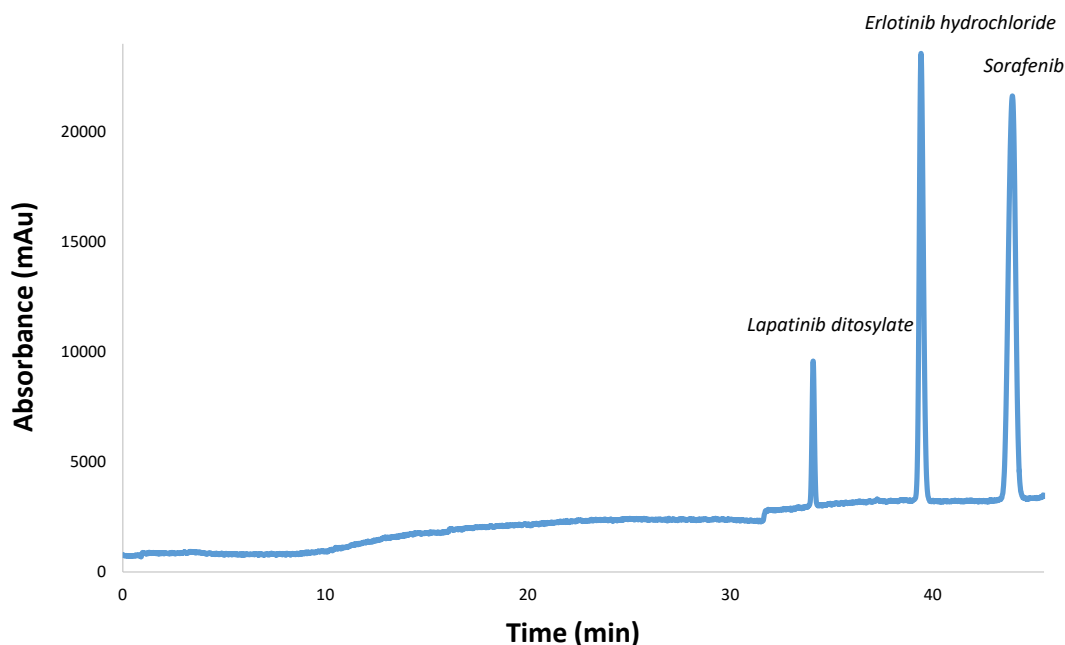


Figure 5: Analysis of lapatinib ditosylate, erlotinib hydrochloride and sorafenib after injecting upper phase (mostly ACN) obtained by A-SALLE-CE-UV methodology. Analysis conditions: silica capillary 50 μm i.d., total length 31 cm, effective length 21 cm. BGE: citric acid – ϵ -aminocaproic acid buffer IS 150 mM pH 2.0. Temperature: 25°C. Separation voltage: 15 kV. Sample injection volume: 287 nL (corresponding to 70% of the capillary effective length). Detection: 254 nm.

3.3. Effect of the type of the salting-out agent

Different salts were studied with the aim to choose the optimal salting-out agent. NaCl, potassium chloride (KCl) and ammonium acetate were tested because these salting-out agents gave the best extraction efficiencies in many works [25,26]. It was found that corrected peak area values were 1.3 times more important with KCl than for the two other salts (NaCl and ammonium acetate) suggesting better extraction efficiencies (Fig. 6A). However, KCl led to the reduction of peak efficiencies compared to the other two salting-out agents (Fig. 6B). As KCl is more soluble in a 100% ACN phase (≈ 24 mg/L) than for the two other salts (≈ 3 mg/L), the amount of salt in the upper phase obtained with KCl was probably higher than that of NaCl and ammonium acetate. The presence of salt in the upper phase allows to extract more easily the 3 TKIs due to better solubility. However, the presence of salts in the injected sample, affects the performance of in-line acetonitrile stacking [27]. NaCl and ammonium acetate nearly lead to the same performance in terms of corrected peak areas of TKIs but, NaCl gave the most efficient peaks. Better repeatability ($n=3$) for corrected peak areas was obtained with NaCl with values of less than 2.5

%. Therefore, NaCl was chosen as the salting out agent for the A-SALLE-CE-UV as it gives the best compromise between extraction efficiency, repeatability and peak efficiency.

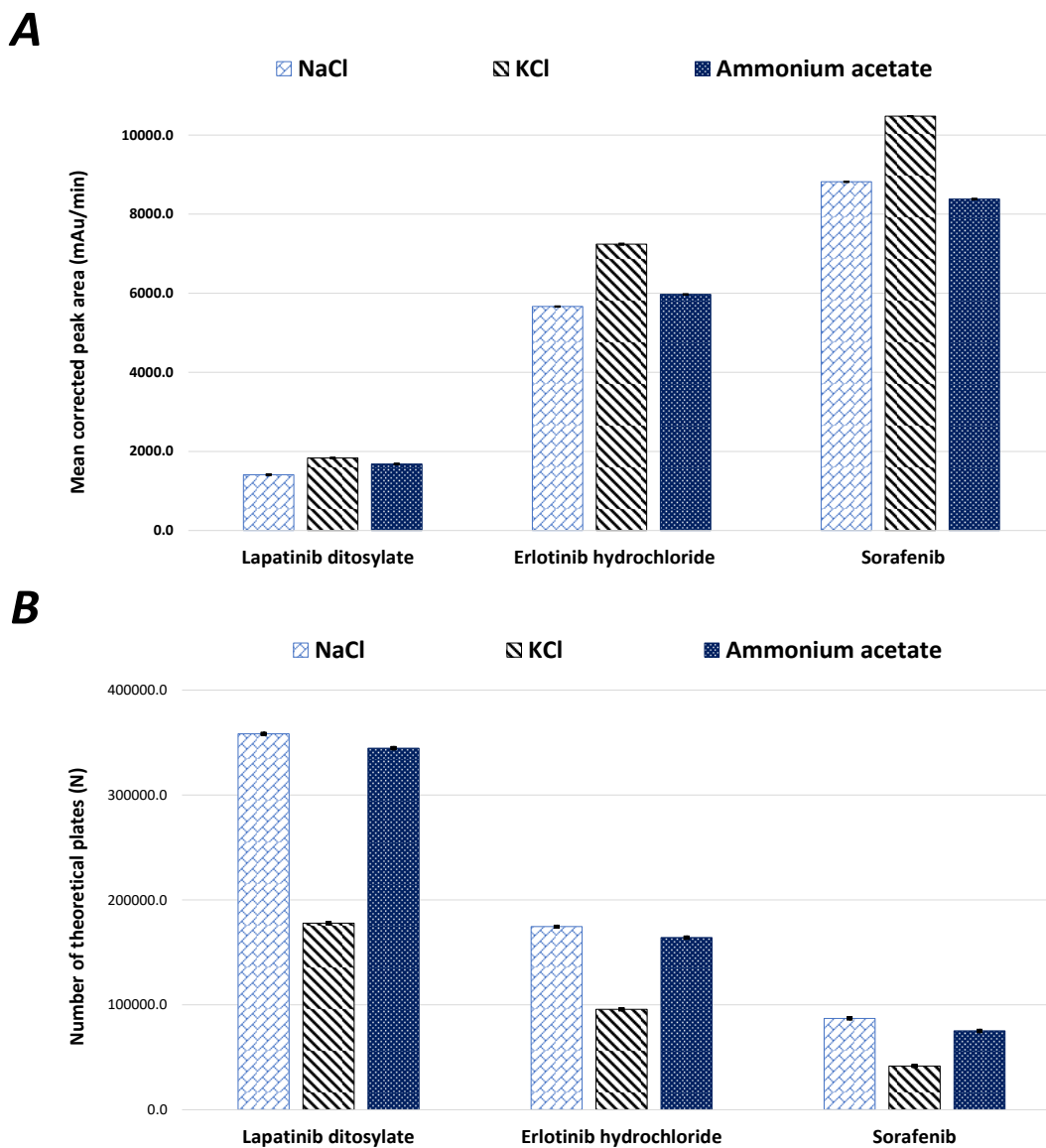


Figure 6: Effect of the type of salting-out agent on (A) the corrected peak area and (B) the number of theoretical plates (N) of the 3 TKIs.

3.4. Analysis of human plasma spiked with TKIs:

The performance of the proposed A-SALLE-CE-UV methodology was evaluated on plasma sample spiked with the three TKIs. The pH of the BGE was 2.0 and the ionic strength 150 mM. Protein precipitation was observed in the sample vial after the addition of ACN. Fig. 7 shows the electropherograms obtained for blank plasma (no TKIs) and TKIs plasma sample (injected volume equal to 70% of the capillary effective length). No interfering peaks of endogenous proteins were observed at the migration time of the TKIs

demonstrating the specificity of the proposed methodology. The maximum injected sample volume without peak broadening was similar to that obtained with a standard sample solution (287 nl corresponding to 70% of the capillary effective length). This result indicates that the in-line stacking performances were similar for standard and plasma solutions and confirmed the robustness of the proposed methodology.

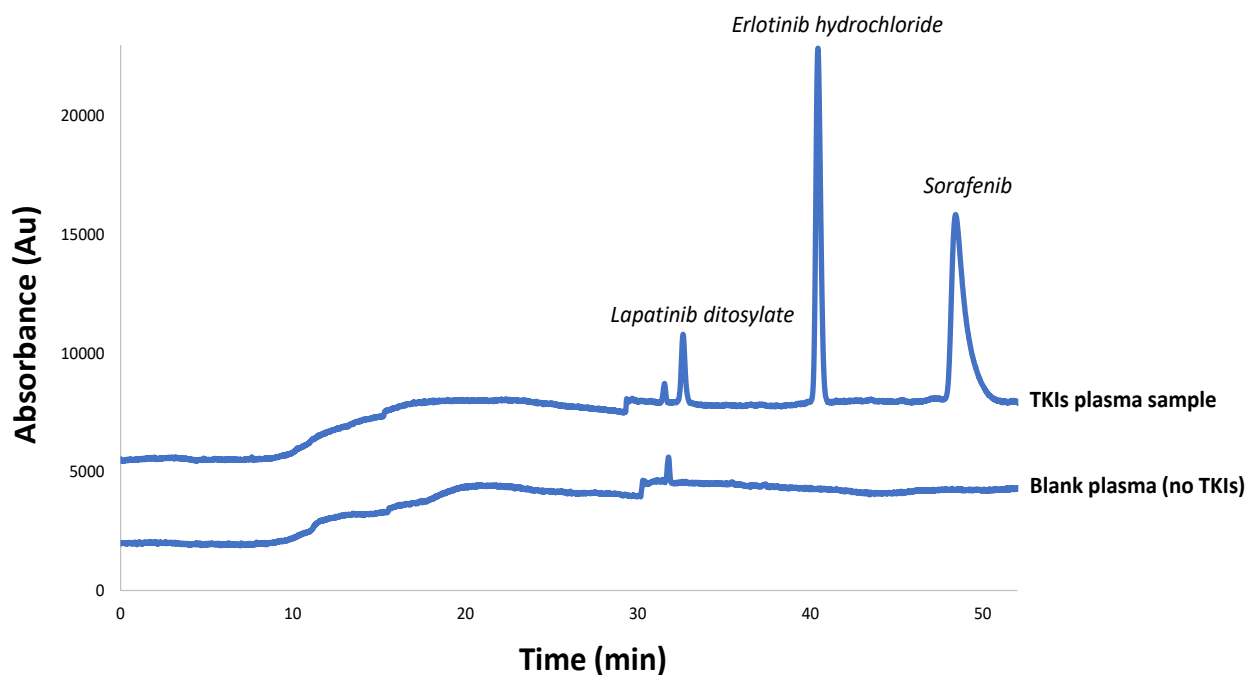


Figure 7: Electropherograms of the 3 TKIs obtained from blank plasma sample (no TKIs) and human plasma samples spiked with the three TKIs using A-SALLE-CE-UV procedure. Analysis conditions: silica capillary 50 μm i.d., total length 31 cm, effective length 21 cm. BGE: citric acid – ϵ -aminocaproic acid buffer IS 150 mM pH 2.0. Temperature: 25°C. Separation voltage: 15 kV. Sample injection volume: 287 nl (corresponding to 70% of the capillary effective length). Detection: 254 nm.

The analytical performances of the developed methodology were evaluated and are summarized in [table 1](#). LOQ of lapatinib, erlotinib and sorafenib were determined at 1260, 200 and 640 ng/ml respectively. These LOQ values were slightly higher than that obtained by manual sample preparation since the type of mixing was different. However, these values are still lower than mean plasma levels observed for patients treated by TKIs, which are estimated at 1570, 1200 and 1440 ng/ml for lapatinib, erlotinib and sorafenib respectively [28–30]. Good repeatability was obtained at the LOQ levels ($n = 6$) in term of migration time ($\text{RSD} < 2.88\%$) and corrected peak areas ($\text{RSD} < 2.73\%$). Good linearity of the calibration curve from 200 to 5000 ng/ml was obtained with r^2 higher than 0.995. Moreover, several advantages are offered by the proposed A-SALLE methodology. The small volume of the sample used (80 μL compared to 2.0 mL of plasma for manual SALLE methodology) which will be more convenient for the patient's quality of life i.e.

less blood sample collected. The reduction in the volume of organic solvent used (about 20x less) compared to manual methodology which will effectively lower the cost and toxicity of analysis per sample. In addition, automation makes analyses easier to realize minimizing manual labor and human error. All these results confirm the possibility to automate SALLE by CE without the need to make any modification at the level of the commercially available CE machine. Moreover, the applicability of the proposed A-SALLE-CEUV for the routine analysis of these three TKIs was successfully tested against plasma sample spiked with the three TKIs.

Table 1: Summary of A-SALLE-CE-UV quantitative results achieved on plasma samples with injected sample volume equal to 70 % of the capillary effective length.

A-SALLE-CE-UV performance parameters	Lapatinib ditosylate	Erlotinib hydrochloride	Sorafenib
Extraction efficiency (%)	62	62	60
Specificity	Confirmed	Confirmed	Confirmed
Linearity (ng/ml)	1360-5000	200-5000	640-5000
Correlation coefficient (r^2)	0.996	0.998	0.995
LOD (ng/ml)	1100	80	200
LOQ (ng/ml)	1360	200	640
% RSD^a (corrected peak area)	2.19	2.73	2.67
% RSD^a (migration time)	2.88	1.40	2.03

^a Calculated for 6 successive runs at the LOQ levels

4. Conclusion

A novel automated salting-out assisted liquid-liquid microextraction approach for plasma sample before CE analysis was developed. The capillary was used as a tool to deliver appropriate microvolumes of ACN and NaCl to the inlet vial containing the plasma sample. This was followed by mixing using air bubbles leading to a two phases separation and extraction of the TKIs in the upper phase. NaCl was chosen as the salting out agent as it gives the best compromise between high extraction and peaks efficiency. The ASALLE-CE-UV methodology has the advantages to eliminate simultaneously biological proteins, salts and to extract the molecules of interest from the sample matrix. This new approach, A-SALLE-CE-UV, was successfully applied for the analysis of 3 TKIs in plasma samples. The extracted solution (upper phase, mostly ACN solvent) could be injected up to 70% of the capillary effective length due to the existence of in-line acetonitrile stacking phenomenon inside the capillary. Thus, it can be considered as a rapid, simple, cheap, convenient and well suited for possible TDM of TKIs and for further applications concerning the use of SALLE. This A-SALLE-CE-UV methodology does not require to make any technical modifications at the level of the commercially available CE apparatus.

Acknowledgments

This work was supported by a PhD grant from Misr University for science and technology (MUST), 6th October City, Egypt. The authors would like to thank Prof. Joseph Joachim and Prof. Emmanuel Cornillot the coordinators of the collaboration between MUST University and the University of Montpellier. The authors would like also to thank Mr Khaled El-toukhy chancellor, chairman of trustees in MUST university, Pr Mohamed Mostafa, the vice president of MUST university and Dr Yasmin El kashef, the responsible of foreign affairs in MUST university for their support.

References

- [1] C.M. Boone, J.C.M. Waterval, H. Lingeman, K. Ensing, W.J.M. Underberg, Capillary electrophoresis as a versatile tool for the bioanalysis of drugs - A review, *J. Pharm. Biomed. Anal.* 20 (1999) 831–863.
- [2] J.R. Veraart, H. Lingeman, U.A.T. Brinkman, Coupling of biological sample handling and CE, *J. Chromatogr. A.* 856 (1999) 483–514.
- [3] D.K. Lloyd, Chapter 7 Sample preparation for capillary electrophoresis, *Prog. Pharm. Biomed. Anal.* 2 (1996) 309–326.
- [4] A.N. Anthemidis, K.I.G. Ioannou, Recent developments in homogeneous and dispersive liquid-liquid extraction for inorganic elements determination. A review, *Talanta.* 80 (2009) 413–421.
- [5] S. Risticvic, D. Vuckovic, H.L. Lord, J. Pawliszyn, Solid-phase microextraction, *Compr. Sampl. Sample Prep.* 2 (2012) 419–460.
- [6] A. Sarafraz-Yazdi, A. Amiri, Liquid-phase microextraction, *TrAC - Trends Anal. Chem.* 29 (2010) 1–14.
- [7] O.S. Ahmed, Y. Ladner, J. Montels, L. Philibert, C. Perrin, Coupling of salting-out assisted liquid-liquid extraction with on-line stacking for the analysis of tyrosine kinase inhibitors in human plasma by capillary zone electrophoresis, *J. Chromatogr. A.* 1579 (2018) 121–128.
- [8] J. Liu, M. Jiang, G. Li, L. Xu, M. Xie, Miniaturized salting-out liquid-liquid extraction of sulfonamides from different matrices, *Anal. Chim. Acta.* 679 (2010) 74–80.
- [9] L. Guo, S. Tan, X. Li, H.K. Lee, Fast automated dual-syringe based dispersive liquid-liquid microextraction coupled with gas chromatography-mass spectrometry for the determination of polycyclic aromatic hydrocarbons in environmental water samples, *J. Chromatogr. A.* 1438 (2016) 1–9.
- [10] S. Clavijo, J. Avivar, R. Suárez, V. Cerdà, Analytical strategies for coupling separation and flow-injection techniques, *TrAC Trends Anal. Chem.* 67 (2015) 26–33.
- [11] A. Lezov, C. Vakh, A. Pochivalov, A. Bulatov, S. Lebedinets, L. Moskvina, K. Cherkashina, An automated salting-out assisted liquid-liquid microextraction approach using 1-octylamine: On-line separation of tetracycline in urine samples followed by HPLC-UV determination, *Talanta.* 184 (2018) 122–127.
- [12] A.N. Anthemidis, I.S.I. Adam, Development of on-line single-drop micro-extraction sequential injection system for electrothermal atomic absorption spectrometric determination of trace metals, *Anal. Chim. Acta.* 632 (2009) 216–220.

- [13] I. Timofeeva, K. Medinskaia, L. Nikolaeva, D. Kirsanov, A. Bulatov, Stepwise injection potentiometric determination of caffeine in saliva using single-drop microextraction combined with solvent exchange, *Talanta*. 150 (2016) 655–660.
- [14] I. Timofeeva, S. Timofeev, L. Moskvina, A. Bulatov, A dispersive liquid-liquid microextraction using a switchable polarity dispersive solvent. Automated HPLC-FLD determination of ofloxacin in chicken meat, *Anal. Chim. Acta*. 949 (2017) 35–42.
- [15] A. Bulatov, K. Medinskaia, D. Aseeva, S. Garmonov, L. Moskvina, Determination of antipyrine in saliva using the dispersive liquid-liquid microextraction based on a stepwise injection system, *Talanta*. 133 (2015) 66–70.
- [16] M.L.M.F.S. Saraiva, F.R.P. Rocha, P.C.A.G. Pinto, S.P.F. Costa, M.A.S. Brasil, C.F. Nascimento, Exploitation of pulsed flows for on-line dispersive liquid-liquid microextraction: Spectrophotometric determination of formaldehyde in milk, *Talanta*. 144 (2015) 1189–1194.
- [17] F. Maya, B. Horstkotte, J.M. Estela, V. Cerdà, Lab in a syringe: fully automated dispersive liquid-liquid microextraction with integrated spectrophotometric detection, *Anal. Bioanal. Chem.* 404 (2012) 909–917.
- [18] A. Esrafilov, Y. Yamini, M. Ghambarian, B. Ebrahimpour, Automated preconcentration and analysis of organic compounds by on-line hollow fiber liquid-phase microextraction-high performance liquid chromatography, *J. Chromatogr. A*. 1262 (2012) 27–33.
- [19] Y.Y. Chao, Y.M. Tu, Z.X. Jian, H.W. Wang, Y.L. Huang, Direct determination of chlorophenols in water samples through ultrasound-assisted hollow fiber liquid-liquid-liquid microextraction on-line coupled with high-performance liquid chromatography, *J. Chromatogr. A*. 1271 (2013) 41–49.
- [20] A. Nazari-pour, Y. Yamini, B. Ebrahimpour, J. Fasihi, Automated hollow-fiber liquid-phase microextraction followed by liquid chromatography with mass spectrometry for the determination of benzodiazepine drugs in biological samples, *J. Sep. Sci.* 39 (2016) 2595–2603.
- [21] A. Pochivalov, C. Vakh, V. Andruch, L. Moskvina, A. Bulatov, Automated alkaline-induced salting-out homogeneous liquid-liquid extraction coupled with in-line organic-phase detection by an optical probe for the determination of diclofenac, *Talanta*. 169 (2017) 156–162.
- [22] J. Baselga, I. Bradbury, H. Eidtmann, S. Di Cosimo, E. De Azambuja, C. Aura, H. Gómez, P. Dinh, K. Fauria, V. Van Dooren, G. Aktan, A. Goldhirsch, T.W. Chang, Z. Horváth, M. Coccia-Portugal, J. Domont, L.M. Tseng, G. Kunz, J.H. Sohn, V. Semiglazov, G. Lerzo, M. Palacova, V. Probachai, L. Pusztai, M. Untch, R.D. Gelber, M. Piccart-Gebhart, Lapatinib with trastuzumab for HER2-positive early breast cancer (NeoALTTO): A randomised, open-label, multicentre, phase 3 trial, *Lancet*. 379

- (2012) 633–640.
- [23] M.S. Tsao, A. Sakurada, J.-C. Cutz, C.-Q. Zhu, S. Kamel-Reid, J. Squire, I. Lorimer, T. Zhang, N. Liu, M. Daneshmand, P. Marrano, G. da Cunha Santos, A. Lagarde, F. Richardson, L. Seymour, M. Whitehead, K. Ding, J. Pater, F.A. Shepherd, Erlotinib in Lung Cancer — Molecular and Clinical Predictors of Outcome, *N. Engl. J. Med.* 353 (2005) 133–144.
- [24] B. Escudier, T. Eisen, W.M. Stadler, C. Szczylik, S. Oudard, M. Siebels, S. Negrier, C. Chevreau, E. Solska, A.A. Desai, F. Rolland, T. Demkow, T.E. Hutson, M. Gore, S. Freeman, B. Schwartz, M. Shan, R. Simantov, R.M. Bukowski, Sorafenib in Advanced Clear-Cell Renal-Cell Carcinoma, *N. Engl. J. Med.* 356 (2007) 125–134.
- [25] O.S. Ahmed, M. Malý, Y. Ladner, L. Philibert, P. Dubský, C. Perrin, Influence of salt and acetonitrile on the capillary zone electrophoresis analysis of imatinib in plasma samples, *Electrophoresis*. (2019). doi:10.1002/elps.201900188.
- [26] A.M. Hyde, S.L. Zultanski, J.H. Waldman, Y.-L. Zhong, M. Shevlin, F. Peng, General Principles and Strategies for Salting-Out Informed by the Hofmeister Series, *Org. Process Res. Dev.* 21 (2017) 1355–1370.
- [27] I.M. Valente, L.M. Gonçalves, J.A. Rodrigues, Another glimpse over the salting-out assisted liquid–liquid extraction in acetonitrile/water mixtures, *J. Chromatogr. A.* 1308 (2013) 58–62.
- [28] S. ZK, Sample stacking by acetonitrile-salt mixtures., *J. Capillary Electrophor.* 2 (1995) 267–271.
- [29] N.A.G. Lankheet, L.M. Knapen, J.H.M. Schellens, J.H. Beijnen, N. Steeghs, A.D.R. Huitema, Plasma concentrations of tyrosine kinase inhibitors imatinib, erlotinib, and sunitinib in routine clinical outpatient cancer care, *Ther. Drug Monit.* 36 (2014) 326–334.
- [30] H. Akaza, T. Tsukamoto, M. Murai, K. Nakajima, S. Naito, Phase II study to investigate the efficacy, safety, and pharmacokinetics of sorafenib in Japanese patients with advanced renal cell carcinoma, *Jpn. J. Clin. Oncol.* 37 (2007) 755–762.
- [31] B. Thiessen, C. Stewart, M. Tsao, S. Kamel-Reid, P. Schaiquevich, W. Mason, J. Easaw, K. Belanger, P. Forsyth, L. McIntosh, E. Eisenhauer, A phase I/II trial of GW572016 (lapatinib) in recurrent glioblastoma multiforme: Clinical outcomes, pharmacokinetics and molecular correlation, *Cancer Chemother. Pharmacol.* 65 (2010) 353–361.

Supplementary results

In this part, supplementary figures are given concerning the A-SALLE-CE-UV methodology. In addition to a detailed description of the steps involved in this methodology.

Figure 1: Schema of adjusting an eppendorf (Thermoscientific, Pittsburgh, USA) of 600 μL to be placed in a plastic CE vial.

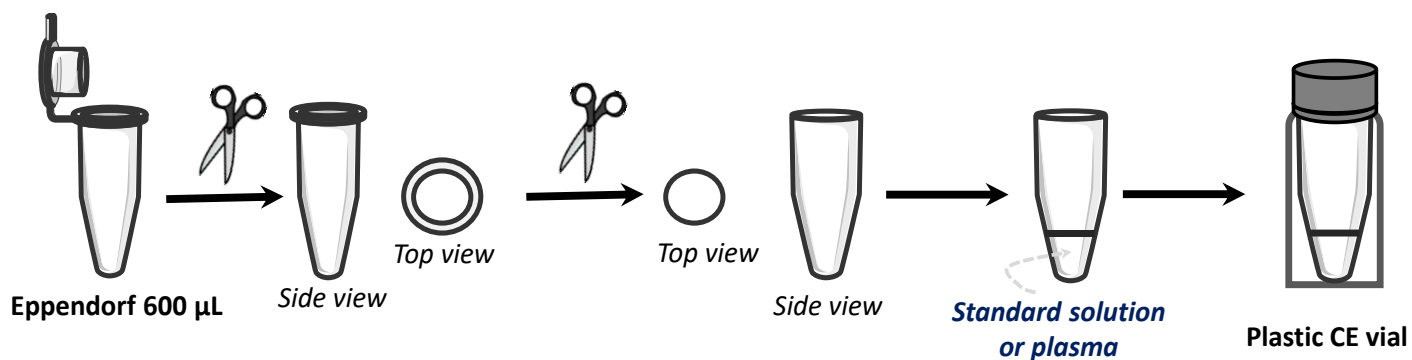


Figure 2: Two phases separation after applying A-SALLE procedure visually verified by the addition of 2 μL methyl red indicator.

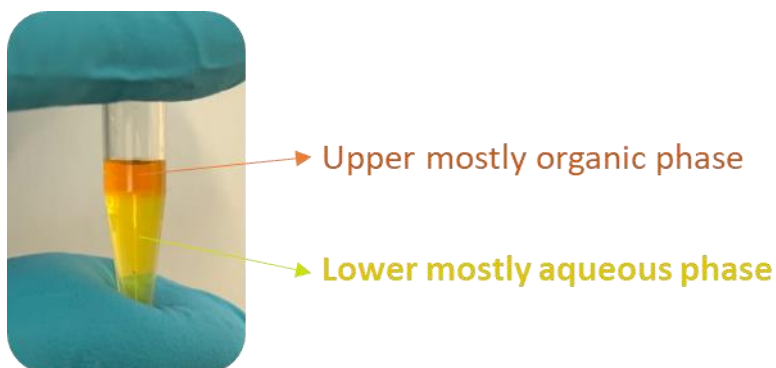


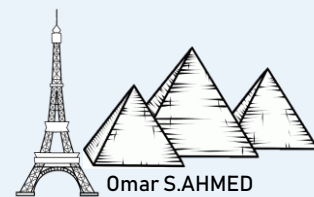
Table 1: The detailed steps of the A-SALLE-CE-UV methodology.

<i>No.</i>	<i>Procedure</i>	<i>Description of the step</i>
1	Conditioning of new capillaries	pre-conditioning with 1.0 M NaOH for 3.0 min under 20 psi
2		pre-conditioning with distilled water for 3.0 min under 20 psi
3	Evacuating the capillary by air	Injecting air from an empty vial at 30 psi during 1.0 min
4	Adding acetonitrile solvent	Injecting acetonitrile solvent to the sample vial at 60 psi during 2.0 minutes
5	Wash	Wash the capillary with distilled water at 60 psi during 2.0 minutes then evacuate the capillary by injecting air at 30 psi during 1.0 min
6	Adding salt	Injecting NaCl salt t to the sample vial at 60 psi during 1.20 minutes
7	Wash	Wash the capillary with distilled water at 60 psi during 2.0 minutes then evacuate the capillary by injecting air at 30 psi during 1.0 min
8	Mixing by air	Mixing by injecting air from an empty vial at 90 psi during 2.0 minutes
9	Adding acetonitrile solvent	Injecting acetonitrile solvent to the sample vial at 60 psi during 2.0 minutes
10	Wash	Wash the capillary with distilled water at 60 psi during 2.0 minutes then evacuate the capillary by injecting air at 30 psi during 1.0 min
11	Mixing by air	Mixing by injecting air from an empty vial at 90 psi during 2.0 minutes
12	Adding salt	Injecting NaCl salt t to the sample vial at 60 psi during 1.20 minutes
13	Wash	Wash the capillary with distilled water at 60 psi during 2.0 minutes then evacuate the capillary by injecting air at 30 psi during 1.0 min
14	Mixing by air	Mixing by injecting air from an empty vial at 90 psi during 5.0 minutes
15	Wait	Wait 5 minutes for the separation into 2 phases occurs
16	Wash	Wash the capillary with distilled water at 60 psi during 2.0 minutes then evacuate the capillary by injecting air at 30 psi during 1.0 min
17	Wash with the BGE	Wash the capillary with the BGE at 60 psi during 5.0 minutes
18	Inject the sample	Inject the sample at 0.8 psi during 94 seconds (equivalent to 70% of the capillary length till detector window)
19	Analysis	Analysis of the sample at 15 kV

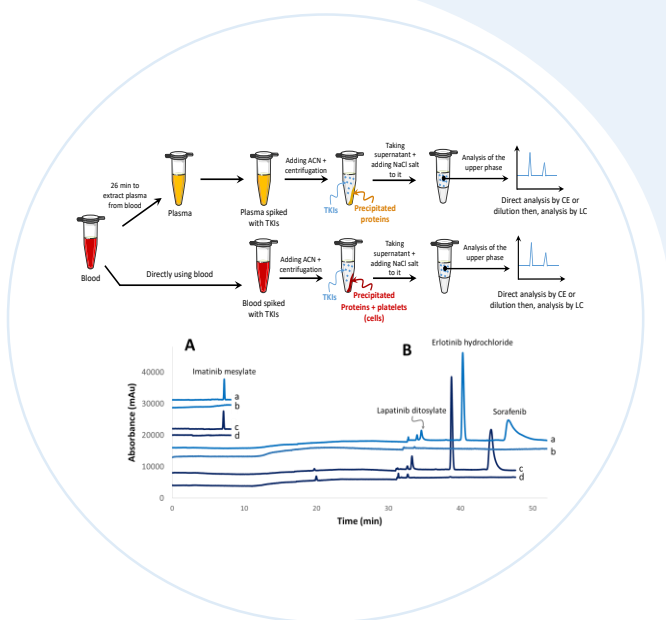
General conclusion of the chapter

In this chapter, the first demonstration of a new automated salting-out assisted liquid-liquid extraction (A-SALLE) approach coupled to CE-UV was developed. The A-SALLE-CE-UV was successfully optimized and applied to the analysis of 3 TKIs namely lapatinib ditosylate, erlotinib hydrochloride and sorafenib in human plasma. This methodology has the advantages to eliminate in one automated step biological proteins, salts and to extract the TKIs from plasma matrix. The performances of the A-SALLE-CE-UV methodology was slightly lower than those obtained with the manual SALLE-CE-UV methodology in terms of extraction efficiency, LOQ and LOD of the 3 TKIs. This could be related to the difference in mixing efficiency by air bubbles for the A-SALLE and by stirrer for manual SALLE giving two different upper phase composition. Even though, the performance of the A-SALLE-CE-UV was sufficient for the analysis of the 3 TKIs in term of the required LOQ. The developed methodology needs no modifications to the existing commercially available CE machine. This automated methodology has not been yet applied to imatinib mesylate as further optimization steps are needed to have a stable current at pH 4.0. Further research needs to be done to optimize the A-SALLE procedure and to apply A-SALLE-CE-UV on real patients' plasma samples. Amelioration of the analytical performances of the A-SALLE-CE-UV to reach those of SALLE-CE-UV in terms of extraction efficiency (%), LOQ and LOD of the tested TKIs. In the next chapter, SALLE was successfully applied for the direct extraction of the four TKIs from human blood for the objective to simplify more the extraction procedure.

Chapter V



Application of SALLE for the direct extraction of TKIs from blood



This chapter is the subject of:

- 📄 **A poster:** *Use of salting-out assisted liquid-liquid Extraction (SALLE) for the analysis of tyrosine kinase inhibitors (TKIs) in human blood by capillary electrophoresis (CE) and liquid chromatography (LC).* 45th HPLC conference- June 2019, Milan, Italy.
- 📄 **A scientific paper:** *Direct salting-out assisted liquid-liquid extraction (SALLE) from human blood: application for the analysis of tyrosine kinase inhibitors.* Submitted to Microchemical journal.



Preface

Herein, the first demonstration of SALLE for the direct extraction of the four selected TKIs from human blood is discussed. The upper extract was successfully injected to CE and LC coupled both to UV detection. A comparison between performances of both methodologies is made.

This work will be submitted shortly as a scientific article.

Direct salting-out assisted liquid-liquid extraction (SALLE) from human blood: application for the analysis of tyrosine kinase inhibitors

Omar S. Ahmed^{1,3}, Yoann Ladner¹, Céline Bousquet¹, Jérôme Montels¹, Laurent Philibert², Catherine Perrin¹

¹Institut des Biomolécules Max Mousseron (IBMM), UMR 5247-CNRS-UM-ENSCM, Montpellier, France.

²Institut régional du Cancer de Montpellier (ICM), Département de Pharmacie et Pharmacologie, Montpellier, France.

³Department of Analytical Chemistry, Faculty of Pharmacy, Misr University of Science and Technology (MUST). Al-Motamayez District, 6th of October City, P.O.Box: 77, Egypt.

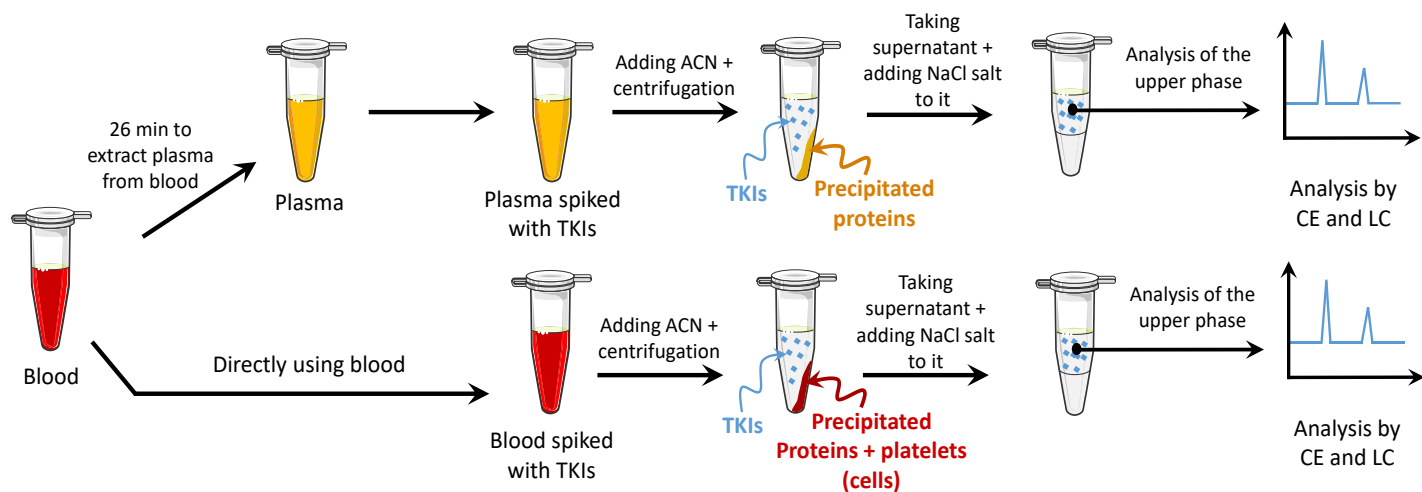
Research article submitted to

Microchemical journal

Keywords:

Sample preparation, blood samples, desalting, in-line CE stacking, protein precipitation, salting-out assisted liquid-liquid extraction (SALLE), tyrosine kinase inhibitors (TKIs)

Graphical abstract



Abstract

The application of salting-out assisted liquid-liquid extraction (SALLE) is proposed for the first time for the extraction of drugs directly from whole blood samples. The SALLE technique was successfully coupled to capillary electrophoresis (CE) or liquid chromatography (LC) with UV detection both. Four anticancer drugs namely tyrosine kinase inhibitors (TKIs) were selected as proof-of-concept analytes. First, blood samples containing TKIs are mixed with acetonitrile (ACN) in appropriate volumes to precipitate proteins. After vortexing and centrifugation, sodium chloride (NaCl) was added to the blood-ACN mixture to induce a two phases separation. TKIs are efficiently extracted (60–100% extraction efficiency) in the upper mostly organic phase which is directly analyzed by CE-UV or after simple dilution by LC-UV. These SALLE-CE-UV and SALLE-LC-UV methodologies offers many advantages by combining fast extraction procedure from whole blood samples and separation efficiency in a simple cost effective way. Performances of both methodologies were evaluated in terms of extraction efficiency, LOQ, LOD, specificity, repeatability, total analysis time and cost per analysis.

1. Introduction

Bioanalysis has evolved considerably over the past 10 years with the development of simple and fast analytical methods for the quantitative measurement of a drug and/or its metabolites in biological fluids (blood, plasma, serum, urine or tissue extracts) [1]. Drug quantification in biological fluids is a key point to understand the time course of drug action or pharmacokinetics [2]. Analytical strategies tend towards on-line combination of sample preparation procedures with separation systems such as liquid chromatography (LC), gas chromatography (GC) and capillary electrophoresis (CE) [3] specially for routine analysis applications. Sample preparation is a crucial step in bioanalysis due to the presence of many endogenous compounds such as proteins and salts that could adversely affect the quality of analytical results obtained. So, solid phase extraction (SPE), liquid–liquid extraction (LLE) and protein precipitation (PP) are commonly used as sample preparation techniques to extract many analytes from the biological matrices [4] due to their simplicity and versatility. However, some drawbacks are encountered with PP and LLE such as a lack of selectivity, difficulty with handling large volume samples and insufficient purification [5–7]. In addition, possible interaction with the sorbent, and laborious time consuming procedure can be encountered with SPE [5].

Preferred matrices for most of the developed analytical methodologies are plasma and urine [8–11]. Uncommonly, whole blood samples were used for assay purposes due to highly complex composition, high viscosity and the need to choose an appropriate anticoagulant that don't interfere with the assay [12]. Therefore, more labor-intensive treatment is needed to extract targeted analytes from blood. Normally, a combination of PP with LLE [13,14] or SPE [15] is used to extract analytes from whole blood samples. The extract is then, evaporated and reconstituted in a suitable solvent to be analyzed by LC coupled to UV detection or to tandem mass (MS) detection. More recently, whole blood samples were used in forensic analysis using the same type of sample pretreatment procedure followed LC-MS [12] and CE-UV [16] analysis. Although the high recovery and sensitivity obtained, the sample preparation protocol requires sophisticated, time-consuming and manually intensive sample pre-concentration/clean-up strategies.

For these reasons, a salting-out assisted liquid liquid extraction (SALLE) method was developed for the direct extraction of drugs from human blood without the need to apply any complicated procedures. SALLE is a homogeneous LLE technique in which the addition of salts into a sample solution composed of a miscible mixture of water and an organic solvent causes two phases separation (upper mostly organic and lower mostly aqueous phases) [17,18]. SALLE has the advantages to eliminate simultaneously

proteins, salts and to extract the molecules of interest from the blood sample matrix in the upper phase in a simple way. The extract was then, analyzed by capillary zone electrophoresis (CZE) or LC coupled to UV detection. Four anticancer drugs namely tyrosine kinase inhibitors (TKIs), were used as proof-of-concept analytes. These TKIs are imatinib mesylate, erlotinib hydrochloride, lapatinib ditosylate and sorafenib. To the best of our knowledge, SALLE has never been applied for the extraction of therapeutic molecules directly from blood samples. The ability of SALLE extraction methodology to extract TKIs from human blood was evaluated. Then, a comparison between the analytical performances of both methodologies (SALLE-LC-UV and SALLE-CE-UV) was done in terms of extraction efficiency, LOQ, LOD, specificity, repeatability, total analysis time and the cost per analysis.

2. Experimental

2.1. Chemicals and reagents

All reagents were of analytical grade and used as received without further purification. ACN (purity $\geq 99.9\%$) was from Honeywell Riedel de Haen (Seelze, Germany). 6-amino caproic acid (purity $\geq 99\%$) was from Acros organics (Geel, Belgium). Sodium chloride (NaCl, purity $\geq 99.5\%$), sodium hydroxide (purity $\geq 99\%$), citric acid (purity $\geq 99\%$), imatinib mesylate (purity $\geq 98\%$), potassium dihydrogen phosphate (KH_2PO_4 , purity $\geq 99\%$), disodium hydrogen phosphate dodecahydrate ($\text{Na}_2\text{HPO}_4 \cdot 12\text{H}_2\text{O}$, purity $\geq 99\%$), ammonium acetate (purity $\geq 99\%$), plasma from human for reconstitution were purchased from Sigma Aldrich (Saint-Quentin-Fallavie, France). Sorafenib (purity $\geq 99\%$), erlotinib hydrochloride (purity $\geq 99\%$) and lapatinib ditosylate (purity $\geq 99\%$) were purchased from Molekula (Munich, Germany). Human blood with potassium EDTA as anticoagulant was collected by biological specialties from healthy volunteers. Distilled water was used for the preparation of solutions.

2.2. Analytical conditions

2.2.1. Electrophoretic conditions

All CE separations were carried out using a Beckman P/ACEMDQ instrument (Fullerton, USA) equipped with a UV detection system. Data were acquired by 32 Karat software (Version 8.0, Beckman Coulter). Uncoated fused-silica capillaries (50 μm internal diameter) were obtained from Polymicro Technologies (Phoenix, USA). The total length of the capillary was 30 cm (20 cm effective length to the detector). New capillaries were pre-conditioned with 1.0 M NaOH for 3.0 min under 20 psi followed by distilled water for 3.0 min under 20 psi. Then, the capillary was flushed with the background electrolyte (BGE) for 5.0 min under 20 psi. Hydrodynamic injections of the samples were varied between 0.4 to 0.5 psi and injection times were varied between 60 to 94 seconds (s) to obtain injection volumes comprised between 78–313

nl (equivalent to 20 to 80% of the capillary effective length). All separations were carried out with an applied voltage of 15 kV. The capillary was thermostated at 25 °C. UV detection was performed at 254 nm. Corrected areas were calculated by dividing each TKIs area by its corresponding migration time.

2.2.2. Chromatographic conditions

LC separations were carried out using a Dionex UltiMate 3000 instrument (ThermoFischer, USA) equipped with a UV detection system, a pump chromatographic system, an autosampler (in case of isocratic elution), manual injector (in case of gradient elution) and an oven to control the temperature of the column. Data were acquired by Chromeleon software (Version 8.0, ThermoFischer Scientific). Injected sample volume of 20 µL. Two columns were used: C18 column (Agilent, USA) 100 mm* 2.1 mm*5.0 µm and Altima phenyl column (Grace, USA) 250 mm*4.6 mm*5.0 µm. The detection was fixed at 254 nm. The separations were done with a flow rate of 1.5 mL/min (for isocratic elution) to 2.0 mL/min (for gradient elution). The temperature was maintained at 25 °C. The mobile phase used for isocratic elution was a mixture of ACN/phosphate buffer, 5.0 mM at pH 7.0, 70/30 % (v/v). The mobile phase used for gradient elution was a mixture of mobile phase A (100% ACN) and mobile phase B (20 mM ammonium acetate solubilized in distilled water). The mobile phase gradient is displayed in [Table 1](#).

Table 1: Mobile phase composition

Time (min)	A (%)	B (%)	Flow rate (mL/min)
<i>Analysis</i>			
0	50	50	2.0
1.0	95	5	2.0
3.0	95	5	2.0
3.5	50	50	2.0
<i>Conditioning</i>			
3.6	50	50	1.5
4.5	50	50	1.5

2.3. Preparation of CE background electrolyte, HPLC mobile phases and sample stock solutions:

- The background electrolyte (BGE) was chosen based on our previous study [17] and was a mixture of citric acid and ε-amino caproic acid. BGE composition with the desired *I* and pH was calculated using the software “Peakmaster” 5.3: 1/ pH 2.0 and *I* 150 mM (citric acid (1800 mM) and ε-amino caproic acid (137 mM)), 2/ pH 4.0 and *I* 50 mM (citric acid (37 mM) and ε-amino caproic acid (55 mM)).

- Preparation of phosphate buffer at 5.0 mM: dissolve 1.361 g of potassium dihydrogen phosphate in distilled water and dilute to 100 mL with the same solvent. Adjust the pH at 7.0 using a 35 g/L solution of disodium hydrogen phosphate dodecahydrate. Final concentration obtained at 100 mM. Then, the phosphate buffer was diluted to 5.0 mM with distilled water.
- Preparation of ACN/phosphate buffer at pH 7.0, 70/30 (v/v): 700 mL of ACN and 300 mL of phosphate buffer (5.0 mM) were mixed to obtain a final volume of 1.0 L.
- Preparation of ammonium acetate solution at 20 mM: dissolve 0.771 g of ammonium acetate in distilled water and dilute to 500 mL with distilled water to obtain a final concentration of 20 mM.
- Aqueous stock solutions of imatinib mesylate were prepared at a concentration of 100 mg/L in water.
- Stock solutions of erlotinib hydrochloride, sorafenib and lapatinib ditosylate were prepared in DMSO solvent at the concentration of 1.0 g/L due to their low solubility in water.

All stock samples were stored frozen at -20°C . All other solutions were stored in refrigerator at 4°C .

2.4. Preparation of standard sample solutions:

- Standard mixed solution of the three TKIs (lapatinib ditosylate, erlotinib hydrochloride and sorafenib): relevant volumes (depending on desired concentration) of distilled water and the three TKI stock solutions were mixed in an eppendorf centrifuge tube.
- Standard imatinib mesylate solution: relevant volume (depending on desired concentration) of distilled water and imatinib mesylate stock solution were mixed in an eppendorf centrifuge tube.

2.5. Optimized SALLE procedure of standard sample solutions

To each standard solution (800 μl), 1200 μl of ACN were added in an eppendorf to have a ratio of 60/40 ACN/standard solution (v/v). After vortexing for 1.0 min, 0.1 g of NaCl was added to the mixture to obtain a final concentration of 2.0% NaCl (m/v). The solution was then vortexed for 1.0 min and were left to stand for 3.0 min. A separation into two phases, lower (mostly aqueous) and upper (mostly organic) phase occurred. Then:

- *For CE analysis*, 78-313 nl of the organic phase (equivalent to 78-80% of the capillary effective length) was directly injected and analyzed by CE with on-line UV detection.
- *For LC analysis*, 200 μl of the upper phase was diluted by a factor of 3 with distilled water. Then, 20 μl of the diluted organic phase was injected and analyzed by LC with UV detection.

The same exact procedure was used for the preparation of standard blank solution except distilled water was used instead of the standard sample solution.

2.6. Optimized SALLE procedure from human blood and human plasma spiked with TKIs

Briefly, 800 μ l human blood or human plasma was placed in an eppendorf centrifuge tube and spiked with appropriate volumes of imatinib mesylate, erlotinib hydrochloride, sorafenib and lapatinib ditosylate stock solutions. Then, the spiked plasma or blood was mixed during 1 h at room temperature. 1200 μ l of ACN was added to obtain a ratio of 60/40 ACN/plasma (v/v). The addition of ACN induced protein precipitation. The supernatant was separated from the precipitated proteins after the mixture was vortexed for 1 min and centrifuged for 5 min (11,000 rpm, 4 °C). Then, 0.1 g of NaCl was added to the mixture to obtain a final concentration of 2.0% NaCl (m/v). The solution was then, shaken for 1.0 min and left to stand for 3.0 min. A separation into two phases, lower mostly aqueous and upper mostly organic phases occurred. Then:

- *For CE analysis*, 78 to 313 nl of the organic phase (equivalent to 20-80% of the capillary effective length) was directly injected and analyzed by CE-UV.
- *For LC analysis*, 200 μ l of the upper phase was diluted by a factor of 3 with distilled water. Then, 20 μ l of the diluted organic phase was injected and analyzed by LC coupled to UV detection.

Blank solutions of both plasma and blood samples were prepared by the same procedure but, without TKIs added. Instead, distilled water was used.

3. Results and discussion

Four TKIs were selected for our study namely imatinib mesylate, lapatinib ditosylate, erlotinib hydrochloride and sorafenib. These drugs are basic, slightly soluble in water. Their structures are shown in Fig. 1.

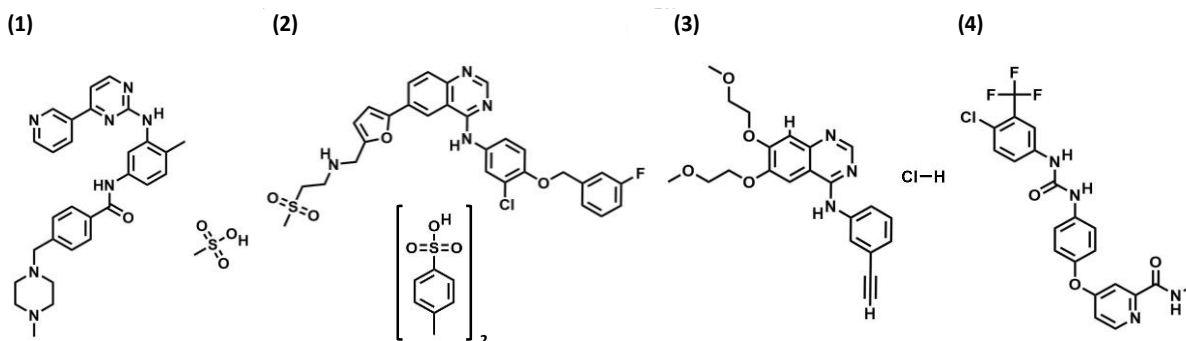


Figure 1: Structures of the four selected TKIs. (1) imatinib mesylate, (2) lapatinib ditosylate, (3) erlotinib hydrochloride and (4) sorafenib.

TKIs are oral anticancer drugs characterized by a broad inter-individual variability for their therapeutic and toxic effects, which requires applying therapeutic drug monitoring (TDM) [19]. TDM is the clinical practice of measuring specific drugs at designated intervals to maintain a constant concentration in a patient's bloodstream at the active range, thereby optimizing individual dosage regimens [20]. Therefore, simpler sample preparation techniques and analytical methods would be beneficial to monitor TKIs concentration in cancer patients to achieve therapeutic outcome and treatment efficiency. In our previous work [17,21], SALLE methodology was developed for the extraction of TKIs in human plasma. The ratio 60/40 (v/v) ACN/plasma in the presence of 2.0% (m/v) NaCl was found to be the best compromise between an efficient plasma deproteinization, a moderate dilution of TKIs and a good separation between the two phases (Fig. 2). The extraction efficiencies (%) were approximately estimated at 60, 100, 98.0 and 100% for imatinib mesylate, lapatinib ditosylate, erlotinib hydrochloride and sorafenib respectively.

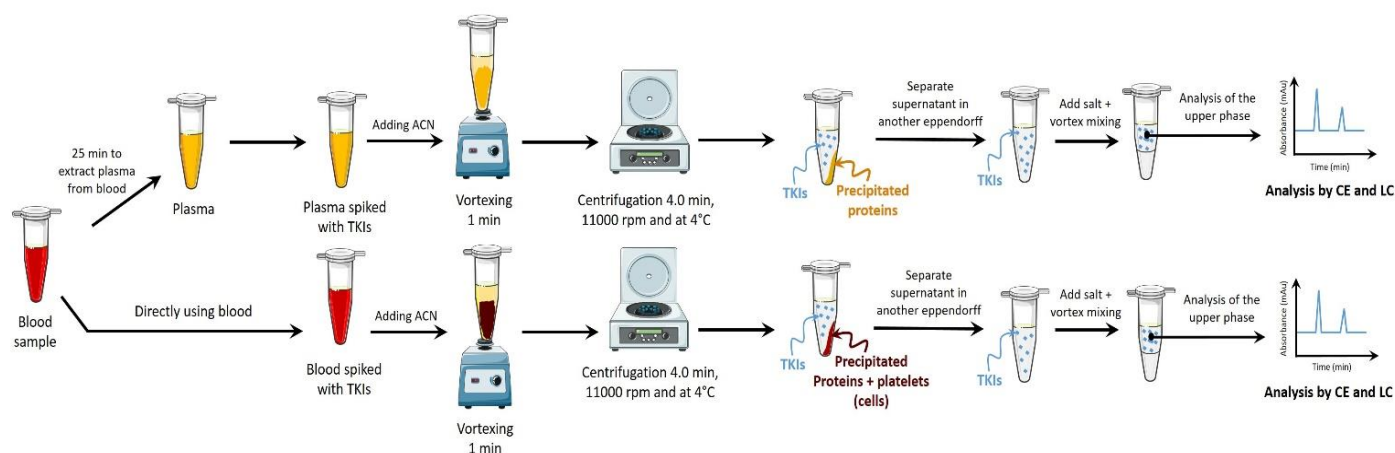


Figure 2: SALLE procedure of TKIs from human plasma and blood.

For blood samples, two centrifugation processes are normally needed to remove cells, platelets and to separate plasma from blood. This process needs at least 25 minutes per sample, which could be time consuming plus, the time needed for sample preparation. For this reason, developing an extraction method directly applicable on blood samples will be highly valuable.

3.1. Analysis of TKIs in biological samples by capillary electrophoresis (SALLE-CE-UV)

A SALLE-CE-UV methodology was previously developed for the analysis of TKIs in human plasma [17,21]. A positive separation voltage of +15 kV was applied. The total capillary length was 30 cm (effective length 20 cm). Some modifications were brought to the analytical conditions for imatinib so that each of the four selected TKIs was analysed under under optimal conditions. Better analytical performances are obtained for imatinib at pH 4.0, I 150 mM than pH 2.0 / 150 mM to avoid the sample zone dispersion observed at pH 2.0 specially when increasing the sample volume injected (results not shown) [17]. Under optimal conditions, the analysis of the upper mostly organic phase gave symmetric and efficient peaks for all TKIs showing the ability of the SALLE methodology to extract TKIs from the aqueous sample (Fig 3.A.a and B.a).

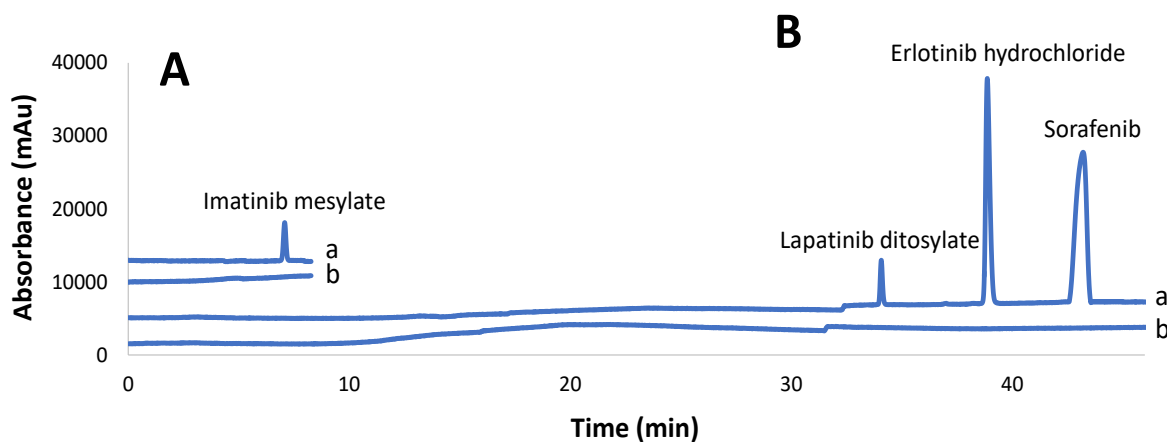


Figure 3: electropherograms of (A.a) imatinib mesylate, (B.a) lapatinib ditosylate, erlotinib hydrochloride and sorafenib, final concentration of 5.0 $\mu\text{g/ml}$ at pH (A) 4.0 and pH (B) 2.0 of the BGE. (A.b) and (B.b) represent the electropherograms obtained for blank standard samples (no TKIs). Analysis conditions: silica capillary 50 μm i.d., total length 30 cm, effective length 20 cm. BGE: citric acid – ϵ -aminocaproic acid buffer I 150 mM. Temperature: 25°C. Separation voltage: 15 kV. Sample injection volume: (A) 78.31 nL (corresponding to 20% of the capillary volume till the detector window) and (B) 313 nL (corresponding to 80% of the capillary volume till the detector window). Detection: 254 nm.

In addition, the upper phase extract was successfully loaded to the capillary exceeding 20 to 80% of the capillary effective length, increasing the sensitivity of the method. This was related to the nature of the upper phase extract (mostly ACN) leading to on-line stacking phenomena by transient isotachopheresis (t-ITP) followed by field amplified sample stacking (FASS). Fig 3.A.b and 3.B.b represent electropherograms of blank standard solutions. There is no effect of the composition of the upper phase extract on the analysis of the selected TKIs.

The same procedure was applied directly on plasma and blood samples spiked with TKIs. Fig 4.A.a and 4.A.c show electropherograms obtained for imatinib mesylate analyzed at pH 4.0 in plasma and blood respectively. Fig 4.B.a and 4.B.c show electropherograms obtained for the three other TKIs analyzed at pH 2.0 also in plasma and blood respectively.

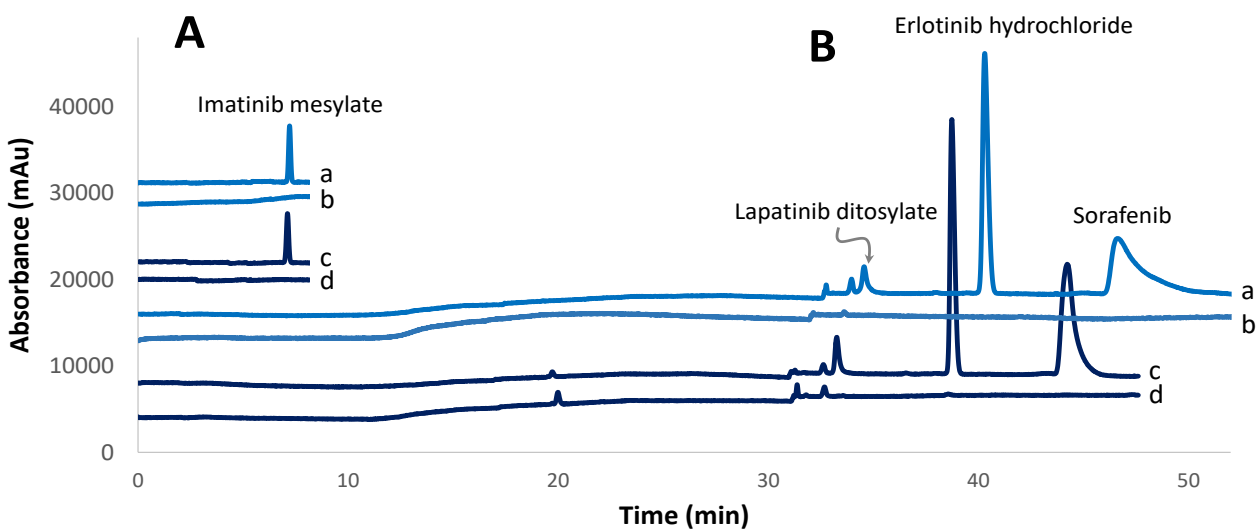


Figure 4: electropherograms of (A.a) and (A.c) imatinib mesylate, (B.a) and (B.c) lapatinib ditosylate, erlotinib hydrochloride and sorafenib, final concentration of 5.0 $\mu\text{g/ml}$ at pH (A) 4.0 and pH (B) 2.0 of the BGE in (A.a) plasma and (A.c) blood samples. (A.b), (A.d), (B.b) and (B.d) represent the electropherograms obtained for blood and plasma blank samples. Analysis conditions: as in figure 3.

The maximum sample volume injected of imatinib was 20% of the capillary effective length while, it was 80% of the capillary effective length in case of the three other TKIs. Electropherograms obtained from standard, plasma and blood samples showed similar electrophoretic profiles in terms of selectivity, peak areas and resolutions. The migration times in the case of imatinib mesylate were similar whatever the matrix. On the other hand, the three other TKIs were detected earlier in case of blood sample and sorafenib peak was more efficient compared to plasma sample. This could be related the slight difference in the upper phase composition in term of ACN, salt and water content between blood and plasma extract. This effect is less significant at pH 4.0 than pH 2.0. This could be related to the electro-osmotic flow (EOF). At pH 2.0, EOF is very low (negligible) ($\mu_{\text{eo}} = 3.14 \times 10^{-5} \text{ cm}^2/\text{V/s}$) compared to the average effective mobilities of the three TKIs ($\mu_{\text{eff}} \approx 5 \times 10^{-4} \text{ cm}^2/\text{V/s}$). Therefore, the contribution of EOF to the analysis time was negligible in this particular case. Therefore, any difference in the composition of the upper phase extract will affect both the stacking and the time of migration. On the other hand, the EOF at pH 4.0 was $1.03 \times 10^{-2} \text{ cm}^2/\text{V/s}$ and the effective mobility of imatinib mesylate was $9.95 \times 10^{-3} \text{ cm}^2/\text{V/s}$. Therefore, the EOF (at the same direction) will screen the slight difference in composition between the two extracts in term of migration time and efficiency of peak.

Fig 4.A.b, 4.A.d, 4.B.b and 4.B.d represent electropherograms of plasma and blood blank solutions. There was no interfering peaks of endogenous proteins at the migration time of analytes for both plasma

and blood samples. This demonstrates the specificity of the proposed SALLE method for the direct extraction from blood samples. All the above results confirmed the ability of SALLE-CE-UV to be used for the analysis of the selected TKIs in both plasma and whole blood samples.

3.2. Analysis of TKIs in biological sample by liquid chromatography (SALLE-LC-UV)

To demonstrate the utility of the SALLE methodology to be analyzed by different analytical methods, the extract were also analyzed by LC-UV (part 2.2.2). For imatinib mesylate, a C18 column with an isocratic elution using ACN/phosphate buffer (5.0 mM) at pH 7.0 (70/30 (v/v)) was used. When the same conditions were applied for the analysis of the three others TKIs, a co-elution between sorafenib and lapatinib was observed. Therefore, another strategy was developed by using phenyl column, which shows high selectivity for aromatic compounds. Gradient elution with ACN/ammonium acetate (20 mM) mobile phase was used (part 2.2.2) to separate the three TKIs. One difference in the SALLE procedure compared to that applied for CE analysis is the dilution by a factor 3 of the upper phase extract with water to avoid solute dispersion due to the high ACN content of the extract. The reason is to make the eluting force of the sample to be almost similar to that of the mobile phase used.

Fig. 5.A.a and B.a show the chromatograms obtained for the analysis of TKIs standard sample solutions. High peaks efficiency and high resolution were obtained besides short analysis times (about 3.5 minutes) showing the ability of SALLE to be coupled to LC-UV.

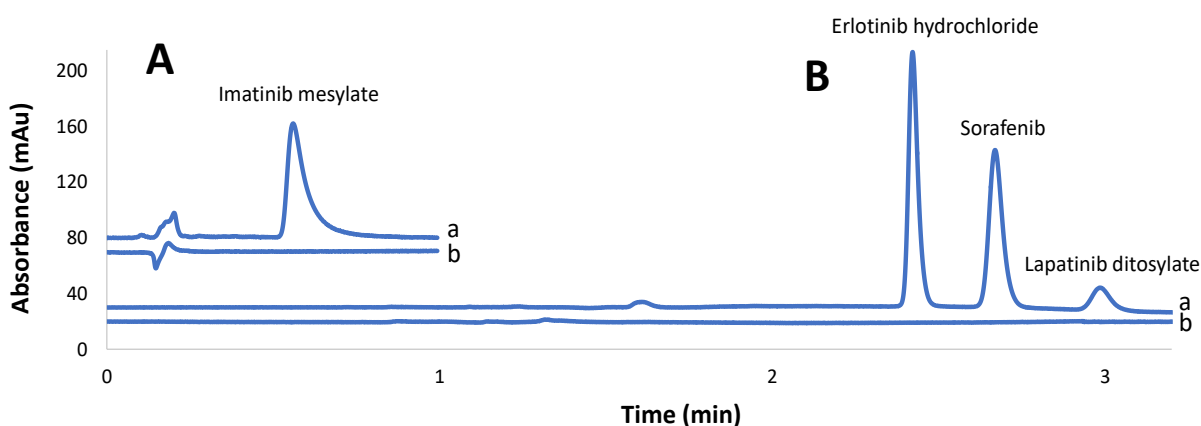


Figure 5: chromatograms of SALLE upper phase extract of TKIs standard solutions at concentration of 5.0 $\mu\text{g/ml}$. (A.a) analysis of imatinib mesylate standard solution using C18 column 100 mm*2.1 mm*5.0 μm , isocratic elution using ACN/phosphate buffer 5.0 mM at pH 7.0, 70/30 (v/v), flow rate 1.5 ml/min and detection at 256 nm. (B.a) analysis of the three others TKIs (erlotinib hydrochloride, sorafenib and lapatinib ditosylate) extracted also by SALLE using Altima phenyl column 250 mm*4.6 mm*5.0 μm , gradient elution using ACN/ammonium acetate (20 mM), flow rate 2.0 ml/min and detection at 256 nm. (A.b) and (B.b) represent the chromatograms obtained for blank standard samples (no TKIs) under the same conditions as standard solutions.

Fig 6.A.a and A.c show the analysis of imatinib mesylate in plasma and blood samples respectively with isocratic elution using ACN/phosphate buffer (5.0 mM) at pH 7.0 (70/30 (v/v)). Fig 6.B.a and B.c show the chromatograms of the other TKIs obtained in plasma and blood samples respectively with gradient elution using ACN/ammonium acetate (20 mM). Fig 6.A.a and 6.B.a represent the chromatograms obtained after SALLE extraction from plasma while, Fig 6.A.c and 6.B.c from blood samples. In comparison with Fig. 5.A.a and B.a, similar chromatographic profiles in terms of retention times, peak areas and resolutions were obtained for the selected TKIs between standard, plasma and blood sample solutions. Injection of blank sample solutions (blank sample solutions prepared according to point 2.6) showed no interfering peaks of endogenous proteins at the migration time of analytes (Fig 6.A.b, A.d, B.b and B.d), demonstrating the specificity of the proposed method for the direct extraction from blood samples and analysis by CE. All these results confirmed the ability of SALLE-LC-UV to be used for the analysis of TKIs in both plasma and whole blood samples. Moreover, these results also show that it is possible to directly analyze the blood without affecting the performance of the analysis. The total analysis time, the risk of the human error and the operating cost per sample will be all reduced.

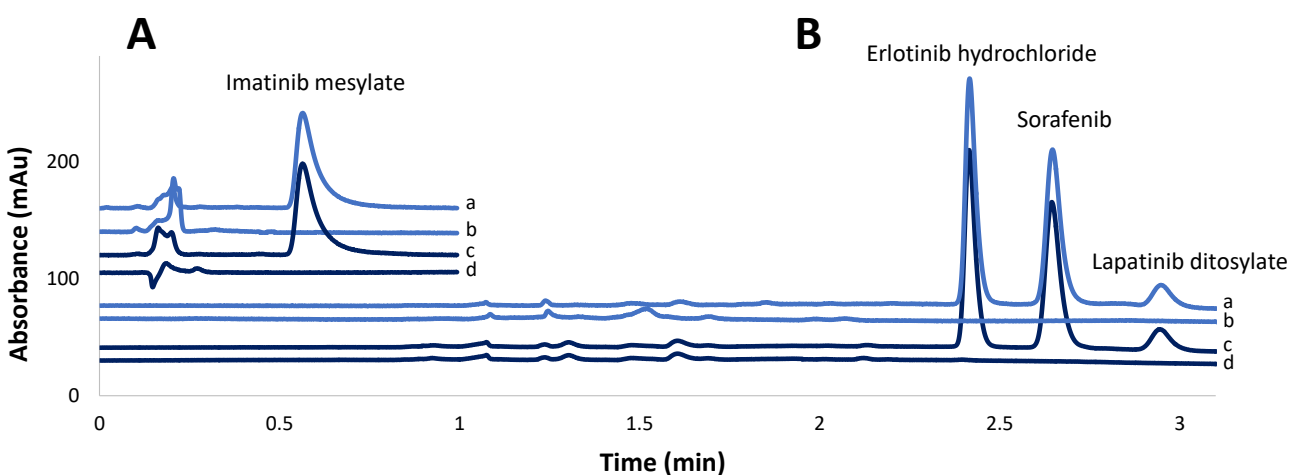


Figure 6: chromatograms of blank (no TKIs), blood and plasma samples spiked with TKIs (5.0 $\mu\text{g/ml}$). (A.a) and (A.c) represent analysis of imatinib in plasma and blood samples respectively. (B.a) and (b.c) represent analysis of the three others TKIs in also in plasma and blood samples respectively. (A.b), (A.d), (B.b) and (B.d) represent the chromatograms obtained for blood and plasma blank samples. Analysis conditions: as in figure 5.

3.3. Comparison between the performance of SALLE-CE-UV and SALLE-LC-UV methodologies

A comparison was done between both analytical methodologies in term of total analysis time, cost per sample and analytical performances obtained from blood samples spiked with selected TKIs (table 2). The total analysis time was much faster for the analysis by LC compared to CE. However, the operating cost is more expensive in term of column prices and consumption of organic solvents for LC than CE. Analytical

performances of both methodologies were evaluated. Relative standard deviations (RSD) of less than 1.48 and 3.38% on migration times and corrected peak areas respectively were observed at the LOQ with 6 repeats showing the good repeatability of both methodologies. For both method, LOQ of imatinib mesylate, erlotinib hydrochloride, lapatinib ditosylate and sorafenib were ranging from 315-560, 60-75, 600-750 and 81-500 ng/ml respectively. These LOQ values were much lower than plasma levels observed for patients treated by TKIs, which are estimated at 1000, 1740, 1200 and 1440 ng/ml for imatinib mesylate, lapatinib ditosylate, erlotinib hydrochloride and sorafenib respectively [22–24] proving the applicability of SALLE to extract TKIs from human blood and the utility of the extract to be analyzed by different analytical techniques.

Table 2: Summary of SALLE-LC-UV and SALLE-CE-UV quantitative results achieved on blood samples.

SALLE-LC-UV/SALLE-CE-UV Parameters	Imatinib mesylate	Erlotinib hydrochloride	Lapatinib ditosylate	Sorafenib
Extraction efficiency (%)	60.6	98	100	100
	60.6	98	100	100
LOD (ng/ml)	157.5	30	300	40
	224.0	35	350	330
LOQ (ng/ml)	315	60	600	81
	560	75	750	500
% RSD ^a (peak area, corrected peak area) (min)	2.17	2.84	2.25	1.79
	1.55	3.18	3.38	2.06
% RSD ^a (retention time, migration time) (min)	1.48	0.07	0.15	0.08
	0.83	0.78	0.80	2.33
Specificity	Confirmed	Confirmed	Confirmed	Confirmed
Total analysis time (min)	16	17	18	17.5
	20	51	45	64.5
Cost of LC-UV/CE-UV machines (€)	81,000			
	82,000			

Cost of LC columns/CE capillary machines (€)	584.0 (c18) – 659.0 (Altima phenyl) 700.0 (roll of 50 m)
Cost of LC/CE qualification/year	6,000 4,000
Cost/one sample (€) (one complete analysis)	1.20 - 1.30 0.40
Cost/100 completed analysis (€)	120 - 130 40.0
Cost of mobile phase/ BGE prepared/day (€)	39.0 1.0 (pH 4.0) - 5.60 (pH 2.0)

^a Calculated for 6 successive runs at the LOQ levels

4. Conclusion

In this study, a SALLE technique was proposed for the first time for the extraction of drugs directly from human blood. This SALLE extraction method offered many advantages including extraction efficiency, deproteinization, low sample volume used, utility of extract to be analyzed by LC/CE techniques and separation efficiency in a simple cost-effective way. In addition, on-line concentration by stacking of analytes obtained in case of CE analysis even at high sample volume injected without the loss of efficacy. The extracted solution (mostly ACN) could be directly injected to CE-UV or by a simple dilution followed by injection to LC-UV. The developed SALLE-CE-UV and SALLE-LC-UV methodologies offers a number of features including high separation ability, easy operational sample preparation protocol (few steps) and applicability to high saline complex matrix (e.g. blood and plasma). These methodologies could be a valuable tool in clinical practice such as TDM for the immediate short term extraction and direct analysis after whole blood sample collection.

Acknowledgment

This work was supported by a PhD grant from Misr University for science and technology (MUST), 6th October City, Egypt. The authors would like to thank Prof. Laila Abdel Fattah, Prof. Joseph Joachim and Prof. Emmanuel Cornillot the coordinators of the collaboration between MUST University and the University of Montpellier. The authors would like also to thank Mr Khaled El-toukhy chancellor, chairman of trustees in MUST university, Pr Mohamed Mostafa, the vice president of MUST university and Dr Yasmin El kashef, the responsible of foreign affairs in MUST university for their support.

References

- [1] Y. He, Chiral analysis in drug discovery and development, *Innov. Pharm. Technol.* 1 (2010) 18–23.
- [2] C.A. James, M. Breda, S. Baratt, M. Casati, S. Grassi, B. Pellegatta, S. Sarati, E. Frigerio, Analysis of Drugs and Metabolites in Tissues and Other Solid Matrices, *Chromatographia.* 59 (2004) 149–156.
- [3] S. Clavijo, J. Avivar, R. Suárez, V. Cerdà, Analytical strategies for coupling separation and flow-injection techniques, *TrAC Trends Anal. Chem.* 67 (2015) 26–33.
- [4] N.Y. Ashri, M. Abdel-Rehim, Sample treatment based on extraction techniques in biological matrices, *Bioanalysis.* 3 (2011) 2003–2018.
- [5] M. Rawa-Adkonis, L. Wolska, A. Przyjazny, J. Namieśnik, Sources of errors associated with the determination of PAH and PCB analytes in water samples, *Anal. Lett.* 39 (2006) 2317–2331.
- [6] D.A. Wells, Bioanalytical applications: solid-phase extraction, in: *Encycl. Sep. Sci.*, Academic Press, 2000: pp. 2142–2146.
- [7] G. Vas, K. Nagy, K. Vekey, Biomedical sampling, in: *Med. Appl. Mass Spectrom.*, Elsevier, 2008: pp. 37–59.
- [8] H. Juan, Z. Zhiling, L. Huande, Simultaneous determination of fluoxetine, citalopram, paroxetine, venlafaxine in plasma by high performance liquid chromatography-electrospray ionization mass

- spectrometry (HPLC-MS/ESI), *J. Chromatogr. B Anal. Technol. Biomed. Life Sci.* 820 (2005) 33–39.
- [9] N.L. Rezk, R.D. Crutchley, A.D.M. Kashuba, Simultaneous quantification of emtricitabine and tenofovir in human plasma using high-performance liquid chromatography after solid phase extraction, *J. Chromatogr. B Anal. Technol. Biomed. Life Sci.* 822 (2005) 201–208.
- [10] C. Sottani, R. Turci, L. Perbellini, C. Minoia, Liquid–liquid extraction procedure for trace determination of cyclophosphamide in human urine by high-performance liquid chromatography tandem mass spectrometry, *Rapid Commun. Mass Spectrom.* 12 (1998) 1063–1068.
- [11] S. Souverain, S. Rudaz, J.L. Veuthey, Protein precipitation for the analysis of a drug cocktail in plasma by LC-ESI-MS, *J. Pharm. Biomed. Anal.* 35 (2004) 913–920.
- [12] R.A.R. Bowen, A.T. Remaley, Interferences from blood collection tube components on clinical chemistry assays, *Biochem. Medica.* 24 (2014) 31–44.
- [13] J.L. Bernal, M.J. del Nozal, V. Rosas, A. Villarino, Extraction of basic drugs from whole blood and determination by high performance liquid chromatography, *Chromatographia.* 38 (1994) 617–623.
- [14] D.S. Jain, G. Subbaiah, M. Sanyal, U.C. Pande, P. Shrivastav, Liquid chromatography-tandem mass spectrometry validated method for the estimation of indapamide in human whole blood, *J. Chromatogr. B Anal. Technol. Biomed. Life Sci.* 834 (2006) 149–154.
- [15] L. Kristoffersen, E.L. Øiestad, M.S. Opdal, M. Krogh, E. Lundanes, A.S. Christophersen, Simultaneous determination of 6 beta-blockers, 3 calcium-channel antagonists, 4 angiotensin-II antagonists and 1 antiarrhythmic drug in post-mortem whole blood by automated solid phase extraction and liquid chromatography mass spectrometry. Method developm, *J. Chromatogr. B Anal. Technol. Biomed. Life Sci.* 850 (2007) 147–160.
- [16] X. Cui, C. Ni, C. Liang, F. Gong, R. Wang, G. Chen, Y. Zhang, Screening and quantitation of forty-six

- drugs of abuse and toxic compounds in human whole blood by capillary electrophoresis: Application to forensic cases, *Microchem. J.* 144 (2019) 403–410.
- [17] O.S. Ahmed, Y. Ladner, J. Montels, L. Philibert, C. Perrin, Coupling of salting-out assisted liquid–liquid extraction with on-line stacking for the analysis of tyrosine kinase inhibitors in human plasma by capillary zone electrophoresis, *J. Chromatogr. A.* 1579 (2018) 121–128.
- [18] Y.Q. Tang, N. Weng, Salting-out assisted liquid-liquid extraction for bioanalysis, *Bioanalysis.* 5 (2013) 1583–1598.
- [19] P. Herviou, E. Thivat, D. Richard, L. Roche, J. Dohou, M. Pouget, A. Eschalier, X. Durando, N. Authier, Therapeutic drug monitoring and tyrosine kinase inhibitors, *Oncol. Lett.* 12 (2016) 1223–1232.
- [20] B.A. Wolf, Overview of therapeutic drug monitoring and biotechnologic drugs, *Ther. Drug Monit.* 18 (1996) 402–404.
- [21] O.S. Ahmed, M. Malý, Y. Ladner, L. Philibert, P. Dubský, C. Perrin, Influence of salt and acetonitrile on the capillary zone electrophoresis analysis of imatinib in plasma samples, *Electrophoresis.* (2019). doi:10.1002/elps.201900188.
- [22] N.A.G. Lankheet, L.M. Knapen, J.H.M. Schellens, J.H. Beijnen, N. Steeghs, A.D.R. Huitema, Plasma concentrations of tyrosine kinase inhibitors imatinib, erlotinib, and sunitinib in routine clinical outpatient cancer care., *Ther. Drug Monit.* 36 (2014) 326–34.
- [23] H. Akaza, T. Tsukamoto, M. Murai, K. Nakajima, S. Naito, Phase II study to investigate the efficacy, safety, and pharmacokinetics of sorafenib in Japanese patients with advanced renal cell carcinoma, *Jpn. J. Clin. Oncol.* 37 (2007) 755–762.
- [24] B. Thiessen, C. Stewart, M. Tsao, S. Kamel-Reid, P. Schaiquevich, W. Mason, J. Easaw, K. Belanger, P. Forsyth, L. McIntosh, E. Eisenhauer, A phase I/II trial of GW572016 (lapatinib) in recurrent

glioblastoma multiforme: Clinical outcomes, pharmacokinetics and molecular correlation, *Cancer Chemother. Pharmacol.* 65 (2010) 353–361.

General conclusion of the chapter

In this chapter, SALLE was successfully applied for the extraction of the four selected TKIs directly from human blood. The upper phase extract was successfully injected to LC or CE coupled both to UV detection. Interestingly, the developed methodologies offered many advantages high separation ability, easy to apply sample preparation protocol and applicability to high saline blood complex matrix. Both methodologies could be a valuable tool in clinical practice towards a short term extraction and a direct analysis directly after blood sample collection.

General conclusion and perspectives

The objective of this work was to develop a CE method for the TDM of patients treated by TKIs. At first, preliminary studies were done to understand the effect of salt, normally present in plasma samples, on the CE of TKIs. Imatinib mesylate was the first TKIs to start with. Different I and pH of the BGE were tested. Different peak splitting patterns of imatinib were observed experimentally and were consistent with computer simulation performed using Simul software. These simulations proved that imatinib peak splitting is a consequence of the presence of salt (sodium ion) in the sample with the formation of imatinib/sodium boundaries that develop to different extends and propagate with various velocities within the sample zone depending on I and pH of BGE. ACN solvent was added to the sample to eliminate plasma protein and to allow on-line stacking of imatinib increasing the sensitivity of the method. Also, the addition of ACN eliminated the peak splitting at pH 2, allowing for the analysis of imatinib in plasma samples with simplicity, low cost, easy operational procedure and low consumption of organic solvent. The performance of the developed analytical CE methodology in terms of linearity, LOQ, LOD, repeatability and specificity was adapted for TDM application. The LOQ obtained was much lower than mean plasma level observed for patients treated by imatinib mesylate (about 1000 ng/ml). This developed method was applied for the analysis of the three other TKIs, namely lapatinib ditosylate, erlotinib hydrochloride and sorafenib. Good separation between the four TKIs was obtained. However, the estimated LOQ for lapatinib ditosylate did not arrived to its plasma level which is 1740 ng/mL. Another strategy was tested in order to improve the analytical performance (extraction and CZE analysis) of the methodology for the four TKIs.

In the second experimental part, an analytical methodology for the analysis of TKIs in human plasma was established by combining SALLE extraction followed by CE analysis. SALLE has the advantages to eliminate simultaneously proteins, most salts and to extract TKIs from plasma. The extracted solution (containing mostly ACN) allowed for the first time to inject up to 80% of the capillary effective length due to the existence of on-line ACN stacking phenomenon inside the capillary. The developed SALLE-CE methodology offered a number of features including high separation ability of the analytes, easy operational procedure, low consumption of organic solvent, environmental benignity and applicability to high salinity matrix. The performance of the SALLE-CE-UV methodology was assessed in terms of linearity, LOQ, LOD, repeatability and specificity.

In the third experimental part, a fully automated analytical methodology combining SALLE and CE for the analysis of TKIs in plasma samples was achieved. The A-SALLE-CE-UV, makes full use of the advantages of both techniques by combining desalting, PP, automated LLE, in-line CE stacking and electrophoretic

General conclusion and perspectives

separation of TKIs in plasma samples in a fully integrated way. This methodology was performed without any modification of the commercially available CE machine. The capillary was used as a tool to deliver appropriate micro-volumes of ACN and NaCl to the inlet vial containing the plasma sample. This was followed by mixing using air bubbles leading to a two phases separation by salting-out and extraction of the TKIs in the upper phase. The performance of the A-SALLE in terms of LOQ of TKIs values were slightly higher than that obtained by manual SALLE since the type of mixing was different. The results obtained in terms of LOD, LOQ, SEF, repeatability and linearity were however sufficient and demonstrate the applicability of the proposed method for possible TDM of TKIs.

In the final experimental part, the developed SALLE technique was proposed for the first time for the extraction of TKIs directly from human blood. The upper phase extract was analyzed by LC/CE techniques coupled both to UV detection. The extracted solution (mostly ACN) could be directly injected to CE-UV or by a simple dilution step followed by injection to LC-UV. The developed SALLE-CE-UV and SALLE-LC-UV methodologies offered many advantages including high separation ability, easy operational sample preparation protocol (few steps) and applicability to high saline complex matrix (e.g. blood and plasma). These methodologies could be a valuable tool in clinical practice such as TDM of TKIs for the immediate extraction and direct analysis after patients' blood sample collection.

For prospective study, further optimization steps are required for the A-SALLE-CE-UV methodology to increase its performance in parallel to manual methodology. Also, to apply both methodologies to real cancer patient samples with complete method validation. Moreover, to try to apply A-SALLE methodology to blood samples. Furthermore, to try integrate the SALLE method into microchips (lab-on-chip) based on droplet-based microfluidics. The preliminary results showed the possibility to generate droplet (rich in ACN) based on SALLE method. Towards the analysis of one droplet of blood by integrated microfluidic device to smartphones based on SALLE method.

Title in English: Contribution of capillary electrophoresis for the therapeutic drug monitoring of patients treated by targeted cancer therapy: application to tyrosine kinase inhibitors

Tyrosine kinase inhibitors (TKIs) are a class of targeted therapy used in the treatment of many types of malignant diseases. The inter-patients pharmacokinetic variability of TKIs was reported which could affect the efficacy of treatment. Therapeutic drug monitoring (TDM) of TKIs was suggested in many studies as a tool to improve their efficacy and safety profile of the treatment. TDM of TKIs requires to develop analytical methods to measure their plasmatic concentration.

The objective of the present work was to evaluate the relevance of capillary electrophoresis (CE) method for the quantification of tyrosine kinase inhibitors (TKIs) in human plasma in the context of TDM. Four TKIs were selected for this study: imatinib mesylate, erlotinib hydrochloride, lapatinib ditosylate and sorafenib.

A fast, simple and cost effective CZE-UV methodology for the quantification of imatinib in plasma was first developed using simply ACN precipitation as sample preparation before analysis. A complete study was performed to understand the electrophoretic behavior of imatinib in the presence of salt (from plasma) and ACN in the sample matrix. Then, a thorough study was performed to optimize an easy to use and performing sample pretreatment methodology based on salting-out assisted liquid-liquid extraction (SALLE) for the four TKIs from human plasma. SALLE, which is based on adding high concentration of salt to two miscible liquids, allows to extract in one step TKIs from plasma in an ACN phase with high recovery. The extracted TKIs can then be directly injected for further CZE-UV analysis. The use of ACN as extraction solvent allows to inject up to 80% of the capillary effective volumes. This allows in-line sample concentration through electrophoretic stacking mechanisms. In the perspective of routine use, the SALLE-CZE-UV methodology was fully automated. The analytical performances obtained for the four TKIs are fully suitable with TDM requirements. Finally, the SALLE-CZE-UV was successfully applied for the extraction and analysis of the four TKIs directly from human blood. All the present developments prove that CE is a relevant technique to address many TDM issues.

Field: Bioanalytical chemistry

Keywords: capillary electrophoresis (CE), protein precipitation by acetonitrile (ACN), salt, salting-out liquid-liquid extraction (SALLE), tyrosine kinase inhibitors (TKIs), therapeutic drug monitoring (TDM)

Institute and address: Institut des Biomolécules Max Mousseron (IBMM) - Montpellier university - Faculty of Pharmacy - Building E, 15 avenue de Charles Flahault, Montpellier, 34090 France.

Titre en français: Apport de l'électrophorèse capillaire pour le suivi thérapeutique personnalisée des patients traités par thérapie ciblée: application aux inhibiteurs de la tyrosine kinase

Les inhibiteurs de la tyrosine kinase (ITK) constituent une classe de traitements ciblés utilisés dans le traitement de nombreux types de cancer. La variabilité pharmacocinétique des ITK entre patients a été rapportée, ce qui pourrait affecter l'efficacité du traitement. Le suivi thérapeutique personnalisé (STP) des ITK a été suggérée dans de nombreuses études comme un moyen d'améliorer leur efficacité et leur profil d'innocuité du traitement. TDM des ITK nécessite de développer des méthodes analytiques pour mesurer leur concentration plasmatique.

L'objectif de ce travail de thèse était d'évaluer l'apport de l'électrophorèse capillaire (EC) comme technique analytique pour la quantification des inhibiteurs de la tyrosine kinase (ITKs) présents dans des échantillons plasmatiques humains dans le contexte du STP. 4 ITKs ont été sélectionnés pour cette étude: mesylate d'imatinib, chlorhydrate d'erlotinib, ditosylate de lapatinib et sorafenib.

Tout d'abord, une méthode simple, rapide et peu coûteuse a été développée par électrophorèse capillaire de zone (CZE) avec détection UV. Cette méthode reposait sur l'utilisation d'une méthode de préparation d'échantillon par précipitation des protéines à l'ACN avant l'analyse par CZE-UV. Une étude approfondie a également été réalisée pour comprendre le comportement électrophorétique de l'imatinib en présence de sels et d'ACN dans l'échantillon plasmatique. Ensuite, une seconde étude a été réalisée pour optimiser une méthode de préparation d'échantillon simple, rapide et efficace basée sur le principe d'extraction liquide-liquide en présence de sel (SALLE). Cette méthode SALLE reposait sur l'ajout de sels en grande concentration dans deux solvants immiscibles permettant ainsi d'extraire en une seule étape les ITKs du plasma vers la phase ACN avec des rendements d'extraction élevés. Les extraits étaient ensuite analysés directement par CZE-UV. L'utilisation de l'ACN comme solvant d'extraction permettait d'injecter des volumes d'échantillon allant jusqu'à 80% du volume effectif du capillaire. Les ITKs étaient donc concentrés en tête du capillaire grâce à l'existence de mécanisme de preconcentration électrophorétiques. Dans la perspective d'une utilisation en routine, la méthodologie SALLE-CZE-UV a été entièrement automatisée. Les performances analytiques obtenues pour les quatre ITKs sont parfaitement adaptées aux exigences du STP. Enfin, la méthode SALLE-CZE-UV a été appliquée avec succès pour l'extraction et l'analyse des quatre ITKs directement à partir de sang humain. Tous les développements actuels prouvent que la CE est une technique pertinente pour résoudre de nombreux problèmes rencontrés dans le contexte du STP.

Domaine : Chimie bioanalytique

Mots-clés: électrophorèse capillaire (EC), précipitation des protéines par acetonitrile (ACN), salt, extraction liquide-liquide par ajout de sels (SALLE), inhibiteurs de tyrosine kinase (ITKs), suivi thérapeutique personnalisé (STP)

Institut et adresse: Institut des Biomolécules Max Mousseron (IBMM) – Université de Montpellier – Faculté de pharmacie – Bâtiment E, 15 avenue de Charles Flahault, Montpellier, 34090 France.
